Two *Petunia hybrida* ABCG Type Transporters:

Characterization of a Strigolactone Exporter

and of a

Transporter Involved in Allocation of Sterol-Derived Compounds Important for Herbivore Defense

Dissertation

zur

Erlangung der naturwissenschaftlichen Doktorwürde
(Dr. sc. nat.)

vorgelegt der

Mathematisch-naturwissenschaftlichen Fakultät

der

Universität Zürich

von

Schläpfer, Joëlle

von
Uerkheim AG

Promotionskomitee
Prof. Dr. Enrico Martinoia (Leitung der Dissertation)
Prof. Dr. Beat Keller
Dr. Uta Paszkowski
Dr. Didier Reinhardt

Zürich, 2014

Contents

Summary

Pleiotropic Drug Resistance (PDR) proteins belong to the family of ATP binding cassette (ABC) proteins that transport substrates across membranes against a concentration gradient by the use of ATP. PDR proteins have been described to play a role for example in phytohormone, heavy metal, and secondary metabolite transport. Despite this, the function of many PDR proteins remains unknown.

In this thesis, the characterization of two PDR proteins of *Petunia hybrida* (Petunia) involved in secondary metabolite transport is described. PDR1 is the first transporter characterized for the only recently identified plant hormones, the strigolactones. In Chapter 2, PDR1 is shown to regulate strigolactone exudation to the rhizosphere, which is the first step in establishment of a symbiosis between plant roots and arbscular mycorrhizal fungi. The lower mycorrhization levels observed in *pdr1* deficient plants are not due to an interference in the symbiotic interaction, as the morphology of the symbiotic fungal structures involved in nutrient exchange remains unchanged. Aboveground, PDR1 is shown to be involved in regulation of initial axillary bud outgrowth, in concert with other plant hormones such as auxins and cytokinins. In Chapter 3, polar localization of PDR1 is reported in the root tip and in cells through which strigolactones are exuded to the soil. Absence of *PDR1* causes gene expression changes and morphological alterations in the root tip. Transport experiments with a synthetic, radiolabelled strigolactone show accumulation of the phytohormone in the root tip of *pdr1* deficient plants. These results emphasize the importance of strigolactone export from this tissue. In Chapter 5, unpublished data is presented, pointing towards an involvement of strigolactone transport in other developmental processes. The phenotypes of Petunia and Arabidopsis (*Arabidopsis thaliana*) plants over-expressing PDR1 are characterized, and differences between the two species are analyzed.

In Chapter 4, the identification and characterization of a second PDR transporter of Petunia is described. *PDR2* is expressed in trichomes, which are epidermal protrusions of aerial plant organs that were shown to play a major role in plant pathogen and herbivore defense. *PDR2* silenced plants allow faster weight gain and an increased survival of larvae of a generalist herbivore. An untargeted metabolite analysis shows a significant reduction of sterol-derived compounds in trichomes of *PDR2* silenced plants. These petuniasterones and petuniolides have been reported to be potent insecticides. Thus, it can be concluded that PDR2 plays a role in Petunia defense against herbivores by influencing sterol contents of trichomes.

Both studies emphasize the value of transport process investigations of secondary metabolites. The characterization of PDR1 as strigolactone exporter is the first step towards understanding the transport mechanisms for this plant hormone. The study reveals approaches on how to identify other strigolactone transporters that are likely present in plants, and how to understand the interplay of strigolactones and PDR1 with other plant hormones as well as their transporters. The study on PDR2, the first plant protein that is involved in transport of molecules with a sterol structure, highlights the importance of ABC transporters in accumulating secondary metabolites in trichomes for plant defense.

Zusammenfassung

Pleiotropische Drogen-Resistenz (PDR) Proteine gehören zu der Familie der ATP-bindenden Kassette (ABC) Proteine, welche unter dem Verbrauch von ATP Substrate entgegen einem Konzentrationsgradienten über eine Membran transportieren. Es wurde gezeigt, dass PDR Proteine eine Funktion im Transport von Pflanzenhormonen, Schwermetallen, und Sekundärmetaboliten haben. Dennoch ist die Funktion von vielen PDR Proteinen noch unbekannt.

In dieser Dissertation werden zwei PDR Proteine von *Petunia hybrida* (Petunie) charakterisiert, die eine Rolle im Sekundärmetabolit-Transport spielen. Für die erst kürzlich beschriebenen Pflanzenhormone, die Strigolactone, wird PDR1 als erstes Transportprotein identifiziert. In Kapitel 2 dieser Arbeit wird gezeigt, dass PDR1 die Strigolacton-Exudation in die Rhizosphäre reguliert, welches den ersten Schritt für eine Symbiose zwischen Pflanzenwurzeln und arbuskulären Mykorrhizapilzen darstellt. Die niedrigere Mykorrhizierungsrate von *pdr1*-defizienten Pflanzen wird nicht durch eine Beeinträchtigung der symbiotischen Interaktion verursacht, da die Morphologie der symbiotischen Pilzstrukturen für den Nährstoffaustausch zwischen den Partnern unverändert ist. In oberirdischen Geweben ist PDR1 an der Regulation des initialen Wachstums von axillaren Knospen beteiligt, welches auch von anderen Pflanzenhormonen wie Auxine und Cytokinine beeinflusst wird. In Kapitel 3 wird die polare Lokalisation von PDR1 in Wurzelspitzen und in Zellen, durch die Strigolactone in den Boden abgegeben werden, gezeigt. Die Abwesenheit von *PDR1* führt zu veränderter Genexpression und zu morphologischen Veränderungen der Wurzelspitze. Transportexperimente mit einem synthetischen, radioaktiv markiertem Strigolacton zeigen eine Akkumulation des Phytohormons in der Wurzelspitze von *pdr1*-defizienten Pflanzen. Diese Resultate unterstreichen die Bedeutung des Exportes von Strigolactonen aus diesem Gewebe. In Kapitel 5 werden bisher unpublizierte Daten präsentiert, die

darauf hindeuten, dass Strigolacton-Transport auch in anderen Entwicklungsprozessen involviert ist. Die durch die Überexpression von PDR1 in Petunie und Arabidopsis (*Arabidopsis thaliana*) beobachteten Phänotypen werden analysiert sowie die Unterschiede zwischen beiden Spezies aufgezeigt.

In Kapitel 4 wird die Identifizierung und Charakterisierung eines zweiten PDR Transporters aus Petunie beschrieben. *PDR2* wird in Trichomen exprimiert, welche hervorstehende, epidermale Gebilde von oberirdischen Pflanzenorganen sind und eine wichtige Rolle in Pathogen- und Herbivorenabwehr spielen. Larven eines Generalisten legten auf *pdr2*-defizienten Blättern schneller an Gewicht zu und zeigten eine höhere Überlebensrate. Eine ungerichtete Metabolitenanalyse zeigt in *pdr2*-defizientem Gewebe eine signifikante Reduktion von Komponenten mit einer Sterol-Struktur. Diese Petuniensterone und Petuniolide sind als potente Insektizide beschrieben worden. Deshalb konnte man aus diesen Daten schliessen, dass PDR2 durch die Beeinflussung der Sterolmengen in Trichomen eine Rolle in der Herbivorenabwehr von Petunien spielt.

Beide Studien zeigen die Bedeutung der Transportprozesse von Sekundärmetaboliten. Die Charakterisierung von PDR1 als Strigolacton-Transporter ist ein erster Schritt, um die Transportprozesse dieser Pflanzenhormone zu verstehen. Die in dieser Studie verwendeten Methoden ermöglichen die Identifizierung weiterer Strigolacton-Transporter, die höchstwahrscheinlich in Pflanzen vorkommen, sowie die Untersuchung des Zusammenspiels von PDR1 mit anderen Pflanzenhormonen und deren Transportern. Die Arbeiten an PDR2, dem ersten Protein aus Pflanzen, welches Moleküle mit einer Sterolstruktur transportiert, verweisen auf die Bedeutung von ABC Transportern für die Akkumulation von Sekundärmetaboliten in Trichomen hinsichtlich der Abwehr von Herbivoren.

List of Abbreviations

ABA	Abscisic acid
ABC	ATP binding cassette
AMF	Arbuscular mycorrhizal fungi
At	*Arabidopsis thaliana*
BFA	Brefeldin A
CCD	Carotenoid cleavage dioxygenase
CTL-VI	Cotylimide VI
D	Dwarf
DAD	Decreased apical dominance
dag	Days after germination
FW	Fresh weight
GapDH	Glyceraldehyde-3-phosphate dehydrogenase
GR24	synthetic SL
HPC	Hypodermal passage cells
HTD	High tillering dwarf
JA	Jasmonic acid
MJA	Methyl jasmonate
MAX	More axillary growth
NBD	Nucleotide binding domain
Np	*Nicotiana plumbaginifolia*
Nt	*Nicotiana tabacum*
Os	*Oryza sativa*
PDR	Pleiotropic drug resistance
Ph	*Petunia hybrida*
PIN	Pin-formed
RMS	Ramosus
SA	Salicylic acid
SL	Strigolactone
TMD	Transmembrane domain
TUB	Tubulin

1 General Introduction

1.1 ABC proteins are involved in major transport processes

1.1.1 ABC transporters

ATP-binding cassette (ABC) proteins are present in all kingdoms, from bacteria to humans. Generally, they function as pumps that shuttle substrates across membranes against a concentration gradient using ATP as direct source of energy. However, some of the members act also either as channels or channel regulators (Theodoulou, 2000). ABC transporters constitute one of the largest protein families (Kang *et al.*, 2011), and they consist of one or several nucleotide binding domains (NBDs) and transmembrane domains (TMDs). Full-size transporters incorporate two domains each, whereas half-size transporters only incorporate one (Martinoia *et al.*, 2002). The NBDs contain a Walker A motif, an ABC signature, and a Walker B motif, and the two Walker motifs are responsible for ATP binding (Walker *et al.*, 1982). Walker A represents the most well conserved motif, whereas the other two are more variable (Martinoia *et al.*, 2002). The TMDs usually consist of four to six α-helices (Rea, 2007). It is generally assumed that two TMDs are needed for substrate transport across membranes, which implies either a homo- or heterodimerization of half-size transporters. In plants, ABC transporters are divided into nine subfamilies, termed ABCA - ABCI, according to the number and organization of the NBDs and TMDs (Kang *et al.*, 2011; Verrier *et al.*, 2008).

The Arabidopsis genome codes for 130 ABC transporters (Kang *et al.*, 2011), while other plants encode a similar or even higher number of these transporters (Rea, 2007). Plants contain a consistently larger number of ABC transporters relative to most other organisms, such as *Saccharomyces cerevisae* or humans, which encode 31 and 48 members, respectively (Prasad and Goffeau, 2012; Dean *et al.*, 2001). ABC

transporters have been described to be involved in the transport of lipids, terpenoids, ions, heavy metals, peptides, sugars, alkaloids, and glutathione conjugates (Theodoulou, 2000; Verrier *et al.*, 2008; Kang *et al.*, 2011). In plants, ABC proteins are also involved in transport of secondary metabolites. There are tens of thousands of secondary metabolites described, and this variety of substances may represent the reason why plant genomes incorporate many more ABC proteins than other kingdoms.

1.1.2 PDR proteins transport secondary metabolites and are involved in defense reactions

The subfamily G of ABC proteins is the largest subfamily described for ABC transporters. The family consists of both, half- and full-size members (WBCs and PDRs, respectively) that contain NBDs and TMDs in reverse order compared to ABC transporters of other subfamilies (*e.g.* the NBD being located at the N-terminus of the protein, Verrier *et al.* 2008). Pleiotropic drug resistance (PDR) proteins in particular contain four class-specific signatures (van den Brule and Smart, 2002). They have been identified in plants and fungi but are absent in mammals and prokaryotes (Kang *et al.*, 2011). PDRs were first identified in yeast, in which they confer resistance against multiple drugs (Theodoulou, 2000). To date, there are nine members described in yeast (Prasad and Goffeau, 2012), 15 members in *Arabidopsis thaliana* (van den Brule and Smart 2002), and 23 members in rice (Crouzet *et al.*, 2006). Plant PDR proteins are organized in five clusters (Crouzet *et al.* 2006).

In plants, PDR proteins have been shown to be involved in a variety of processes such as transport of heavy metals, hormones, and secondary metabolites (Kang *et al.* 2011). In addition, several PDR proteins have been shown to take part in response to abiotic and biotic stress. *A. thaliana* PDR8 (*At*PDR8) is involved in pathogen response and in cadmium resistance (Stein *et al.*, 2006; Kim *et al.*, 2007), while *Nicotiana tabacum* PDR3 (*Nt*PDR3) is iron-responsive (Ducos *et al.*, 2005), and *AtPDR9* is induced in response to iron deficiency: *At*PDR9-mediated exudation of coumarins allows iron solubilization and increased iron uptake (Fourcroy *et al.*, 2013). Furthermore, *At*PDR9 was shown to excrete auxinic compounds (Ruzicka *et al.*, 2010), and over-expression of *At*PDR9 conferred resistance against herbicides (Ito and Gray, 2006). Several Arabidopsis PDR proteins are involved in cuticle formation (Kang *et al.*, 2011). In *Oryza sativa,* PDR9 (*Os*PDR9) was suggested to play a role in abiotic stress due to its induction

upon treatment with heavy metals, salt, jasmonic acid (JA), and other stresses (Moons, 2003). Several rice PDRs are induced by plant hormone treatments, by redox perturbations or by treatment with acids. Ten out of 23 rice PDR members were induced by JA treatment, making JA a dominant regulator of PDR expression (Moons, 2008).

*At*PDR12 illustrates the broad function ABC transporters can exhibit, as this ABC transporter was shown to be involved in lead resistance (Lee *et al.*, 2005), abscisic acid (ABA) transport (Kang *et al.*, 2010c), and in response to the antifungal diterpene sclareol (Campbell *et al.*, 2003). Five *Lotus japonicus* PDRs out of 12 are homologues of *At*PDR12, and they exhibit induction upon plant nodulation (Sugiyama *et al.*, 2006). All four potato PDRs characterized to date were pathogen responsive (Ruocco *et al.*, 2011).

Similar to *AtPDR12*, *Spirodela polyrrhiza TUR2 (SpTUR2),* and *N. plumbaginifolia PDR1 (NpPDR1)* are among the earliest PDRs characterized in plants (Rea, 2007). All three genes belong to cluster I of PDR proteins (for an overview on PDR clusters, see Supplementary Figure 4.1, van den Brule and Smart, 2002; Crouzet *et al.*, 2006), and they are induced in response to pathogens. *Sp*TUR2 confers resistance against sclareol (van den Brule *et al.*, 2002). *Np*PDR1 is involved in pathogen resistance (Stukkens *et al.*, 2005; Bultreys *et al.*, 2009) in addition to sclareol transport (Jasinski *et al.*, 2001). Involvement of proteins in pathogen resistance requires gene expression in aboveground tissues. Especially trichomes (see 1.3.2) have been shown to play an important role in defense responses, as they store high concentrations of secondary metabolites that are central to protect plants from pathogen attack and herbivory (see 1.3.3). Expression data for the abovementioned genes is usually only available for full leaf samples, not distinguishing trichome or leaf localization. Still, spatial resolution exists for some of the Nicotiana proteins. *NtPDR1* and *NpPDR1*, for which promoter-GUS constructs are reported, are expressed in trichomes. Both genes play a role in pathogen response (Crouzet *et al.*, 2013; Stukkens *et al.*, 2005; Sasabe *et al.*, 2002). *NtPDR5* expression is induced in the leaf tissue – not in trichomes – by methyl jasmonate (MJA) treatment, as well as upon mechanical wounding, in response to pathogens and to the *solanaceae* specialist *Manduca sexta*. Indeed, *M. sexta* caterpillars developed faster on *NpPDR5* silenced plants than on wild type. Until now, *NtPDR5* is the only PDR protein that has been reported to be involved in herbivore defense. However, the substrate of the transporter remains unknown (Bienert *et al.* 2012).

1.2 Strigolactones are signaling compounds

1.2.1 Strigolactone-related genes

1.2.1.1 Strigolactone synthesis and structure

Strigolactones (SLs) are β-carotene derived sequiterpenoid lactones (Figure 1.1). The first step in their synthesis is catalyzed by the isomerase DWARF 27 (D27, see Table 1-1 for an overview on SL-related genes) that produces 9-cis-β-carotene in the plastid, which is the preferred substrate for the CAROTENOID CLEAVAGE DIOXIGENASE 7 (CCD7, Alder *et al.*, 2012). In the following step, CCD8 cleaves the carotenoid again, producing carlactone. This contains the butenolide group of SLs, coupled to a backbone structure via an enol ether bridge (Alder *et al.*, 2012; Umehara *et al.*, 2008; Gomez-Roldan *et al.*, 2008). Carlactone was shown to be a precursor for endogenous SLs (Seto *et al.*, 2014), and its usage in various assays results in similar phenotypes reported for the synthetic SL analogue GR24 (Alder *et al.*, 2012). In Arabidopsis, a cytosolic cytochrome P450 protein termed MORE AXILLARY GROWTH 1 (MAX1), was described to be involved in further steps of SL biosynthesis (Booker *et al.*, 2005), although its function is still unknown. MAX1 may catalyze the conversion of carlactone to 5-deoxystrigol, which is thought to be the precursor for the various SL molecules identified.

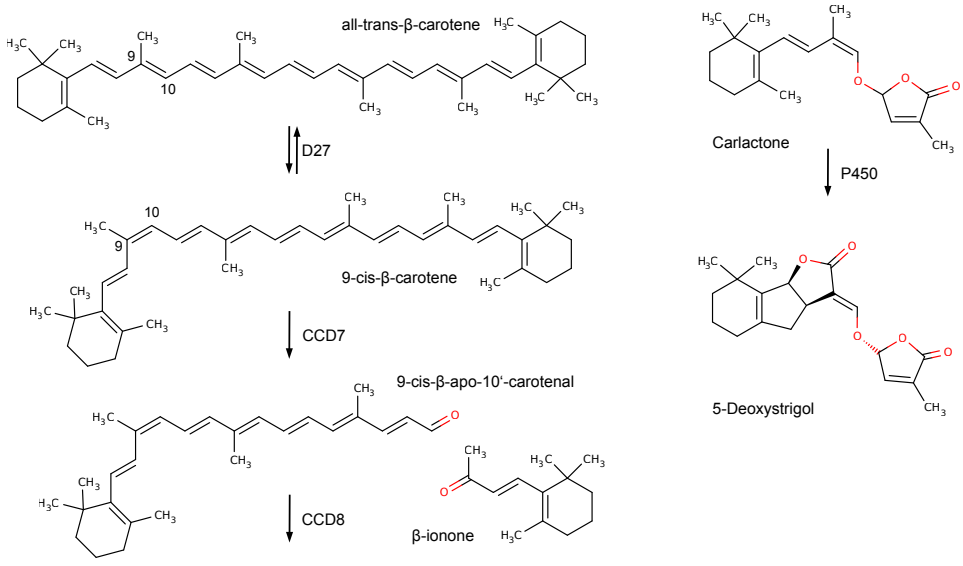

Figure 1.1: Strigolactone synthesis

Synthesis of a SL from a carotenoid precursor (Ruyter-Spira and Bouwmeester, 2012; Alder *et al.*, 2012).

Table 1-1: Genes involved in strigolactone synthesis and signaling

Names of proteins involved in SL metabolism and their function, as well as the names of the proteins in Petunia, Arabidopsis, rice, and pea. Abbreviations: DAD: DECREASED APICAL DOMINANCE, MAX: MORE AXILLARY GROWTH, BRC: BRANCHED, D: DWARF, HTD: HIGH TILLERING DWARF, FC: FINE CULM, TB: TEOSINTHE BRANCHED, RMS: RAMOSUS.

Protein	Function	Name Petunia	Arabidopsis	Rice	Pea
D27	Iron-containing isomerase			D27	
CCD7	Carotenoid cleavage dioxygenase	DAD3	MAX3	D17/HTD1	RMS5
CCD8	Carotenoid cleavage dioxygenase	DAD1	MAX4	D10	RMS1
Cyt P450	Cytochrome P450	*Ph*MAX1	MAX1		
F-box	Part of SCF complex	*Ph*MAX2a, *Ph*MAX2b	MAX2	D3	RMS4
DAD2	α/β hydrolase	DAD2	*At*D14	D14/D88/HTD2	
D53	ATPase, target protein			D53	
BRC	Transcription factor		BRC1, BRC2	FC1/*Os*TB1	PsPBRC1

SLs consist of a tricyclic structure that is linked to a methylbutenolide ring by a enol-ether bond (Figure 1.2). To date, more than 20 natural SLs have been described, differing mainly in modifications on the A and B ring, such as methyl, hydroxyl, keto, or epoxy substituents. Hydroxy-SLs can be further acetylated or conjugated to sugars as well as amino acids. SLs can be grouped in two classes, depending on the α- or β-orientation of the C-ring (see Figure 1.2, Xie *et al.*, 2013).

The ABC ring structure of 5-deoxystrigol is not substituted (see Figure 1.2), and this molecule is thus believed to be a precursor for the other SLs. Some SL molecules, such as 5-deoxystrigol or orobanchol, occur widely in monocotyledons and dicotyledons, others seem to be specific to a smaller group of plants. Most species seem to contain a mixture of several SLs, and the levels differ considerably within a single species (Xie and Yoneyama, 2010). For example in tobacco, 11 SLs were identified in root exudates (Xie *et al.*, 2013), and in several Fabaceae species, a mixture of two or more SLs in root exudates was observed (Yoneyama *et al.*, 2008). It was shown that the different SL structures have various effects on plant branching, hyphal branching, or parasite germination (see 1.2.2.1, 1.2.3.1, 1.2.3.4, Akiyama *et al.*, 2010; Cohen *et al.*, 2013). Substitutions of the ABC rings influence SL activity, whereas the D ring and the structure of the C - D bridge were shown to be essential for activity (Akiyama *et al.*, 2010). However, the bridge can be formed by other atoms if the 3D structure of the molecule is retained (Xie and Yoneyama, 2010). With this knowledge, synthetic SL analogues were generated, GR24 being among the first and it is still widely used in assays today. The extensive search for the bioactive parts of strigolactones lead to the discovery of

molecules that are active only in certain pathways, for example in branching control of the plant, but not in germination of parasites (Fukui *et al.*, 2013; Boyer *et al.*, 2013).

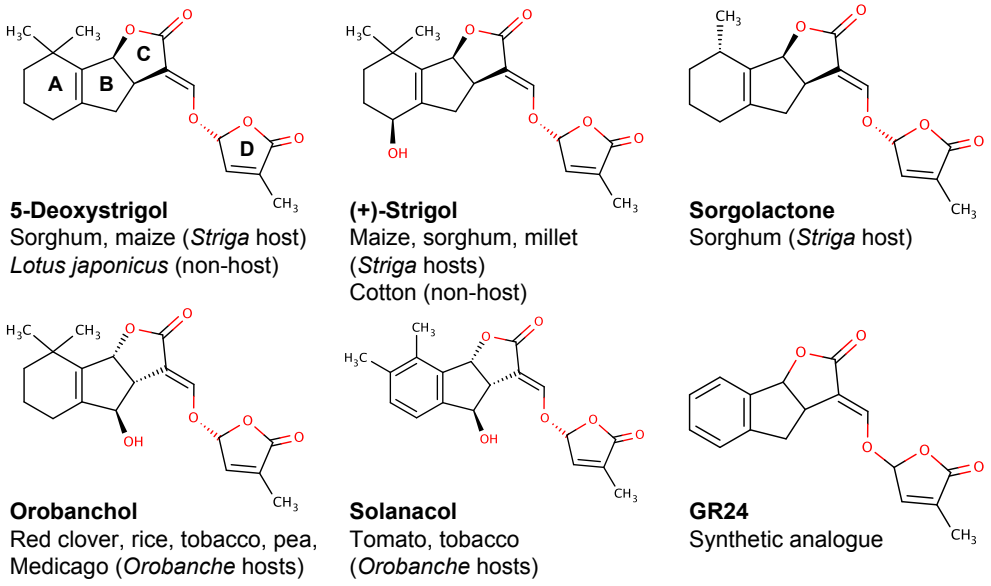

Figure 1.2: Strigolactone structures

Depicted are some of the most common SLs with their occurrence in plants. It is noted whether the plant species are hosts of *Striga* or *Orobanche* or not. To date, more than 20 natural SLs were identified, for which 5-deoxystrigol is believed to be the precursor. SLs group into strigol-like (α-orientation of C-ring, upper row), and orobanchol-like (β-orientation of the C-ring, lower row) molecules. GR24 is a synthetic SL analogue (Bouwmeester *et al.,* 2003; Humphrey and Beale, 2006; Yoneyama *et al.*, 2007; Kohlen *et al.*, 2012; Xie *et al.*, 2013).

1.2.1.2 Strigolactone sensing

Perception of SLs depends on several enzymes, among them are the α/β-hydrolase *At*D14/DAD2/D14, the F-box protein MAX2/*Ph*MAX2a/D3, and the ATPase D53. An overview of the genes involved in SL perception is given in Table 1-1, and the proposed mechanism is summarized in Figure 1.3. DECREASED APICAL DOMINANCE 2 (DAD2) was shown to hydrolyze GR24 to two products (Hamiaux *et al.*, 2012). The D-ring hydrolyzation product, 5-hydroxy-3-methylbutenolide (D-OH), remains bound to the hydrolase and enables the interaction with target proteins (Nakamura *et al.*, 2013). D-OH seems to be the bioactive form of SLs, as it has similar effects in assays as SLs or GR24. However, the interaction of D14 with target proteins did not take place upon addition of D-OH, indicating that the binding and hydrolyzation of SLs is necessary for the D14 function (Nakamura *et al.*, 2013). This model explains how structurally different SLs can induce similar responses in *e.g.* branching (see 1.2.2.1), but it does not explain how the different SLs can elicit variable responses as described for *e.g.* arbuscular mycorrhizal fungi (AMF) symbiosis formation (see 1.2.3).

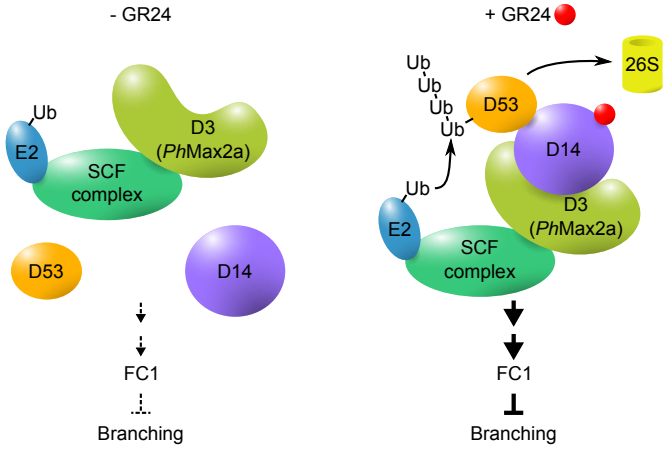

Figure 1.3: Strigolactone perception

The presence of GR24 enables the interaction of the SL receptor D14 with the F-box protein D3 that is part of an SCF complex. Binding of GR24 to D14 leads to binding of D53 to D14, to D53 ubiquitination, and degradation by the 26S proteasome. GR24 presence enables the activation of downstream targets and of FC1, which inhibits branching. In absence of GR24, FC1 is not activated and the plant is branching. Figure modified (Zhou *et. al*, 2013).

DAD2 was shown to bind *Ph*MAX2a in the presence of GR24 (Hamiaux *et al.*, 2012). MAX2 is part of a SCF complex (Stirnberg *et al.*, 2007). In rice, it was shown that the α/β-hydrolase-D3-SCF complex formation further triggers the interaction of D14 with D53. Upon binding, D53 is ubiquitinated and degraded by the proteasome. Thus, SL responsive genes are activated. Knockdown of *D53* in the background of *d3* or *d14* almost restores wild-type phenotypes, indicating that D53 acts downstream of D3 and D14, and that the accumulating D53 in *d3* or *d14* background is responsible for the observed phenotypes (Zhou *et al.*, 2013). A D53 homologue was identified in Arabidopsis: Unlike in rice, mutation of *suppressor of max2 1* (*smax1)* in the background of *max2* suppressed some but not all of the phenotypes caused by SL deficiency (Stanga *et al.*, 2013; Zhou *et al.*, 2013).

In *d53* mutants, expression levels of the transcription factor *FINE CULM 1 (FC1)* responsible for cell cycle control in dormant buds are reduced, indicating that SL signaling might involve FC1 (Jiang *et al.*, 2013). This transcription factor was first identified in maize as *TEOSINTHE BRANCHED 1* (*TB1)* and later in the monocotyledons maize and sorghum. The homologue *BRANCHED 1 (BRC1)* was described for Arabidopsis and pea (Janssen *et al.*, 2014). In pea, SL signaling via BRC1 was demonstrated with *brc1* mutant plants that are SL insensitive (Braun *et al.*, 2012). Transcription of the gene is increased by GR24 application and reduced by cytokinin addition, showing that BRC1 integrates signals of both pathways (Braun *et al.*, 2012). In monocotyledons, a

SL-independent TB1 branching inhibitory pathway seems to exist. In maize, *tb1/ccd8* double mutants showed a more prominent branching phenotype than *ccd8* mutant plants (Guan *et al.*, 2012); however, the authors did not measure SL levels in maize and thus cannot exclude the possibility that the weak *ccd8* phenotype results from residual SL production, as shown for other plants.

The aforementioned transcription factors integrate plant hormone signals and environmental input (Janssen *et al.*, 2014). Another output of SL signaling was identified by the interaction of D14 with the transcription factor SLR1, which is a gibberellic acid (GA) signaling repressor (Nakamura *et al.*, 2013). DELLA proteins were shown to be not only GA target proteins, but also to be involved in SL signaling. As the mechanism of SL perception seems to be almost identical to the GA perception model, it could be that SLs share interaction partners with the GA pathway, which would enable signal integration of both pathways (Nakamura *et al.*, 2013).

1.2.1.3 Strigolactone and SL-related genes in an evolutionary perspective

For plants and the moss *Physcomitrella patens*, SL synthesis and SL-related phenotypes are well described. It was shown that also in liverworts, the oldest Embryophytes, SLs have important functions such as stimulation of rhizoid elongation (Delaux *et al.*, 2012). A recent publication showed SL synthesis and exudation in liverworts and even in a Charophyte algae, which are a sister clade to the Embryophytes (Delaux *et al.*, 2012). The common ancestor of Embryophytes and Charophytes is a sister clade to the Chlorophytes. Although all three Viridiplantae clades have putative D27 homologues, the Chlorophytes seem to be mostly devoid of other SL-related genes. In agreement with this, bioassays showed SL presence in Charales but absence in Chlorophytes. The authors thus assume that SLs appeared in Charales (Delaux *et al.*, 2012).

D27 was first identified in rice (Alder *et al.*, 2012). The Arabidopsis ortholog *At*D27 was shown to act upstream of MAX1 (Waters *et al.*, 2012a), and due to its similar properties to *Os*D27, probably has the same function. Further, analysis of D27-like genes of plants, mosses, and algae showed presence of D27-like genes in all eukaryotes, but the clades containing the most similar sequences to *Os*D27 are plant specific (Waters *et al.*, 2012a; Challis *et al.*, 2013).

CCD7 and CCD8 have been identified in a number of species, among them are *MORE AXILLARY GROWTH 3* and *4 (MAX3, MAX4)* of Arabidopsis (Sorefan, 2003; Booker *et al.*,

2004), *DAD1* and *DAD3* of Petunia (Snowden *et al.*, 2005; Drummond *et al.*, 2009), *Solanum lycopersicum CCD7 and CCD8* (*SlCCD7, SlCCD8*) of tomato (Kohlen *et al.*, 2012; Vogel *et al.*, 2009), *D10* and *D17/High Tillering Dwarf 1* (*HTD1*) of rice (Zou *et al.*, 2006; Arite *et al.*, 2007), *RAMOSUS 1 and 5* (*RMS1, RMS5)* of pea (Sorefan, 2003; Ferguson and Beveridge, 2009), *Zea mays CCD8* (*ZmCCD8*) of maize (Guan *et al.*, 2012), *Dendranthema grandiflorum CCD8* (*DgCCD8*) of chrysanthemum (Liang *et al.*, 2010), *L. japonicus CCD7* (*LjCCD7*) of Lotus (Liu *et al.*, 2013), and *PpCCD8* of *P. patens* (Proust *et al.*, 2011).

In plants, CCD7 and CCD8 are generally assumed to work one after the other in the same pathway, and thus, mutation of one of the two genes should abolish the whole SL synthesis pathway. Indeed, for example in Arabidopsis, *max3/max4* double mutants do not show additive effects (Auldridge *et al.*, 2006), but for example in Petunia, *dad1/dad3* mutants are indeed additive (Drummond *et al.*, 2009). In favor of a parallel function is the fact that in *ccd8* mutants of Arabidopsis (Kohlen *et al.*, 2010) and *P. patens* (Proust *et al.*, 2011), minor amounts of SLs could still be identified. There is also some evidence for a CCD8-independent SL synthesis pathway, as CCD8 seems to be fully absent from liverworts and Charales; however, these organisms were reported to produce SLs (Delaux *et al.*, 2012).

MAX1 orthologues seem to be difficult to identify in other species than Arabidopsis, which is probably due to gene redundancy (Umehara *et al.*, 2010; Challis *et al.*, 2013). The importance of MAX1 is underlined by the fact that in rice, SL amounts are lower in cultivars having a natural depletion of a MAX1 orthologue relative to varieties that contain the endogenous copy (Cardoso *et al.*, 2014). In rice, there are five orthologues, of which two are regulated in a similar manner as SL biosynthetic genes (Umehara *et al.*, 2010). In addition, two rice cytochrome P450 rescued the *max1* phenotype in Arabidopsis (Cardoso *et al.*, 2014). Os01g0700900, identified in both the studies (Umehara *et al.*, 2010; Cardoso *et al.*, 2014), is therefore a good candidate for *Os*MAX1. In Petunia, the MAX1 orthologue *Ph*MAX1 was similarly shown to rescue *max1* phenotypes in Arabidopsis (Drummond *et al.*, 2012). To date, MAX1 orthologues were not identified in algae or mosses as *P. patens*, but MAX1 is present in *Selaginella moellendorffii*, a basal plant species. In monocotyledons, there are several MAX1 orthologues found. The low level of MAX1 conservation among plants can be interpreted as a potential involvement of MAX1 in SLs synthesis diversification (Challis *et al.*, 2013).

In contrast to MAX1, MAX2 seems to be well conserved among land plants (Challis *et al.*, 2013). It was identified in rice as D3 and in Petunia as *Ph*MAX2. Furthermore, MAX2 is also present in *P. patens* and probably in all other Embryophytes, but it is clearly absent from Chlorophytes (Challis *et al.*, 2013).

D14 and FC1 seem to be present only in Embryophytes through mosses (Delaux *et al.*, 2012). In *P. patens* and algae, several D14-like genes have been identified (Waters *et al.*, 2012b; Challis *et al.*, 2013). For an Arabidopsis D14-like protein, a role distinct from SL sensing was proposed (for a description of KAI2, see 1.2.2.3, Waters and Smith, 2013).

1.2.2 Strigolactones are plant hormones

1.2.2.1 Auxins, cytokinins, and strigolactones regulate axillary bud outgrowth

Auxins and cytokinins are well described players in the regulation of aboveground branching (for reviews, see Domagalska and Leyser, 2011; Müller and Leyser, 2011; Ongaro and Leyser, 2008). However, it was realized a long time ago that additional factors have to be involved, because for example auxin exhibits its inhibitory effect on bud outgrowth without actually being present in the bud (Booker, 2003). Later, a root-to-shoot transmissible signal was described that inhibits branching but was distinct from the established factors. Among those studies, Petunia *dad1* plants displaying an elevated branching phenotype were described (Napoli, 1996). Interstock graftings showed a phenotypic rescue of *dad1* tissue above, but not below, the wild-type interstock (Napoli, 1996), indicating that the inhibitory signal was mobile and delivered from the root to the shoot. Further, *CCD7* and *CCD8* were reported to be involved in the synthesis of the inhibitory signal (Sorefan, 2003). Based on the hypotheses that *CCD7* and *CCD8* are involved in synthesis of a carotenoid-derived compound, that *ccd8* plants show increased branching, and that there was no explanation for the presence of carotenoid-derived compounds in shoots, two groups performed experiments in rice, Arabidopsis, and pea that lead to the identification of SLs as plant hormones inhibiting branching (Umehara *et al.*, 2008; Gomez-Roldan *et al.*, 2008). Generally, plants with defective SL synthesis or perception exhibit increased branching phenotypes, whereas the synthesis mutants can be rescued by external SL application and the perception mutant cannot (Snowden and Napoli, 2003; Snowden *et al.*, 2005; Bainbridge *et al.*, 2005; Bennett *et al.*, 2006; Zou *et al.*, 2006; Sorefan, 2003; Drummond *et al.*, 2009; Stirnberg *et al.*, 2002; Stirnberg *et al.*, 2007).

The modes of bud outgrowth inhibition by SLs and their interaction with auxins and cytokinins are not fully resolved to date. Main sites of SL synthesis are roots, as shown by SL quantification, and by analysis of SL biosynthesis gene expression data (Bainbridge *et al.*, 2005; Arite *et al.*, 2007; Mashiguchi *et al.*, 2009). However, SL synthesis also takes place in shoot tissue, which is illustrated by the fact that a wild-type scion grafted on a SL-deficient stock displays wild-type branching (Bainbridge *et al.*, 2005). Interstock graftings of a wild-type interstock in between a SL mutant scion and stock resulted in a wild-type branching phenotype of the upper scion, illustrating the strictly shootwards transport of SLs (Snowden and Napoli, 2003; Napoli, 1996). Further, SL transport was reported to take place in the xylem (Kohlen *et al.*, 2010).

Currently, there are two models describing how branch outgrowth is inhibited by auxin (for reviews, see Müller and Leyser, 2011; Wang and Li, 2011). Auxin is synthesized in the shoot apical meristem (SAM) and is transported basipetally through xylem parenchyma cells. Among others, PIN1 protein levels at the plasma membrane regulate how much auxin can be transported. As auxin does not travel to the bud, the inhibitory signal of auxin could be transferred to the bud via a second messenger. In addition, auxin is synthesized in young leaves. For a bud to grow out, auxin needs to be exported from the bud into the main polar auxin transport stream, and vasculature formation needs to be established (for a review, see Domagalska and Leyser, 2011). This canalization of auxin is a developmental program that also depends on PIN1 (Balla *et al.*, 2011), and that can be regulated. For both, the second messenger and the canalization theory, there is experimental evidence (for reviews, see Dun *et al.*, 2009; Domagalska and Leyser, 2011). SLs could be involved in both pathways. High auxin levels increase SL synthesis (Hayward *et al.*, 2009; Zhang *et al.*, 2010) and suppress cytokinin synthesis, thus, both, SLs and cytokinins, could act as second messengers (Brewer *et al.*, 2009; Dun *et al.*, 2009). High SL amounts suppress PIN1 levels at the plasma membrane, reducing the auxin flux capacity (Shinohara *et al.*, 2013; Crawford *et al.*, 2010). Stems of SL synthesis mutant plants were shown to have elevated auxin transport capacity, enabling more auxin export from buds and thus, more branching (Bennett *et al.*, 2006; Agusti *et al.*, 2011). In turn, SL addition to stems lowers auxin transport capacity (Crawford *et al.*, 2010). In addition, it was shown that SL application to stem segments with one node does not suppress bud outgrowth, but application to stems with two nodes resulted in the outgrowth of only one bud. From this, the authors concluded that SL enhances

competition between buds by modulating PIN1 levels in the main stem and nodal tissue (Crawford *et al.*, 2010). This supports the canalization theory; however, as one model does not exclude the other, a combination of both mechanisms is probable.

Cytokinins are positive regulators of branching, promoting cell division and differentiation. They are synthesized mainly in roots, from which there are transported shootwards through the xylem, and into stem tissue (for reviews, see Müller and Leyser, 2011; Kudo *et al.*, 2010). Cytokinin levels are influenced by both, auxin and SLs. Auxin suppresses cytokinin synthesis and enhances its metabolism in nodal tissue, resulting in low cytokinin levels. Removal of the main auxin source by decapitation results in elevated cytokinin levels (Tanaka *et al.*, 2006). Cytokinin application to buds enhances transcription of the auxin transporters *PsPIN1* and *PsAUX1* (Kalousek *et al.*, 2010), enhancing auxin transport from buds and increasing the possibility for bud outgrowth. Cytokinins positively regulate auxin synthesis (Jones *et al.*, 2010), indicating that a feedback loop between the two pathways exists.

SL and cytokinin signaling also influence each other: In SL mutants, lower levels of xylem cytokinins are found, whereas local cytokinin synthesis in stem remains at wild-type levels (Foo *et al.*, 2007). The significance of this finding is still unclear, as the influence of the root-derived cytokinins on branching is still debated. Despite this, it was shown that SL mutant plants are more sensitive to exogenous cytokinin and that transcription of cytokinin biosynthetic genes was increased in SL mutants (Dun *et al.*, 2012; Janssen *et al.*, 2014; El-Showk *et al.*, 2013), indicating an antagonistic role of SLs and cytokinins in regulation of bud outgrowth. All hormonal signals mentioned above are probably integrated via BRC1/TB1/FC1 transcription factors to result in a decision for the bud, to grow out or not. SLs and cytokinins influence transcription factor levels directly, whereas auxin effects are probably indirect, via regulation of SL levels (Dun *et al.*, 2012; Aguilar-Martinez *et al.*, 2007; Braun *et al.*, 2012; Müller and Leyser, 2011).

Taken together, there are many cues that SLs, auxins, and cytokinins influence each other at various levels, either via synthesis or transport. As long as the amount and the transport of the different phytohormones is not resolved on a cellular level, it will remain difficult to understand how exactly the different signaling pathways interact to regulate branching.

Besides hormonal control of branching, environmental factors such as nutrient levels, temperature, or light are of similar importance (Waldie *et al.*, 2010). SLs as well as other hormones are also involved in mediating responses to those factors. SL synthesis is increased upon phosphate and nitrogen starvation, and elevated SL levels concur with inhibition of branching (Umehara *et al.*, 2010). Moreover, SL mutants were shown to play a role in red/far red light perception, and in photomorphogenesis (see also 1.2.2.3, Shen *et al.*, 2007).

1.2.2.2 Strigolactones regulate root morphology

After the identification of SLs as phytohormones regulating aboveground branching, the role of SLs in root morphology was soon identified. It seems that SLs first evolved a belowground function, before they became involved in symbiotic signaling or aboveground morphology (Delaux *et al.*, 2012). SLs are found in basal phytosynthetic Eukaryotes such as liverworts and *P. patens* (see 1.2.1.3), in which they have a role in rhizoid elongation and sensing of neighboring colonies (Delaux *et al.*, 2012; Proust *et al.*, 2011). In higher plants, SLs influence primary root length and number as well as length of lateral and adventitious roots in addition to root hair growth.

Almost 20 years ago, an inhibitory role of SLs in adventitious root formation was revealed (Napoli, 1996). Later, this function was described in Arabidopsis (Rasmussen *et al.*, 2012), pea (Rasmussen *et al.*, 2012), and in tomato (Kohlen *et al.*, 2012). In contrast to the inhibitory effect on adventitious roots, root hair length is increased upon GR24 application, and *max* mutants have shorter root hairs than wild type (Kapulnik *et al.*, 2010). SLs have been proposed to also promote primary root growth, by maintaining a high number of meristematic cells in the root tip (Ruyter-Spira *et al.*, 2011); however, the response of primary root growth to SLs seems to depend on many other factors such as phosphate and sucrose levels in the medium (Rasmussen *et al.*, 2013). Arabidopsis SL mutants showed increased lateral root density under phosphate sufficient conditions that could be partially rescued by GR24 application (Kapulnik *et al.*, 2010; Ruyter-Spira *et al.*, 2011). The opposite effect was observed under phosphate deficient conditions (Rasmussen *et al.*, 2013). In general, root morphology is heavily shaped by phosphate status of the plant: high phosphate levels promote main root growth and inhibit lateral root and root hair formation, whereas phosphate limiting conditions induce lateral growth of the plant to explore the rhizosphere for more nutrients. SL

synthesis is induced upon nutrient starvation, and SLs could therefore be involved in translation of nutrient status of the plant into morphological changes of the root.

Formation of root structures is modulated by a complex network of local hormone maxima and minima, by hormone transport, and by other environmental factors (Van Norman *et al.*, 2013). Adventitious root formation is inhibited by cytokinins and by SLs through two independent pathways, whereas the stimulatory effect of auxin on adventitious root formation can be abolished by SL addition, thus implicating SLs and auxin signal integration in the same pathway (Rasmussen *et al.*, 2012). The latter could be explained by a suppression of auxin levels by high SL levels. For example in tomato *ccd8* mutant plants, increased adventitious rooting correlated with higher auxin levels in lower parts of the stem (Kohlen *et al.*, 2012). Lateral root formation depends on the formation of local auxin maxima. The effects of SLs on lateral roots could be explained by modulation of auxin transport via SLs (Rasmussen *et al.*, 2013).

Root hair formation is induced by auxin, ethylene and SLs. SL signaling requires a functional ethylene pathway, and auxin signaling enhances root hair response to SLs (Kapulnik *et al.*, 2011). It is to date not resolved in which systems SLs act directly to influence plant morphology, and in which cases SLs modulate synthesis and/or transport of other hormones to modulate plant morphology more indirectly, or if SL action is a combination of both.

1.2.2.3 Strigolactones are involved in various metabolic processes

SLs are not only involved in above- and below-ground branching regulation, they have also been reported to play a role in other metabolic processes. Arabidopsis SL mutants show decreased stem diameter and a smaller cambium zone. GR24 application could increase cambium cell divisions to wild-type levels. Auxin has been shown to be a main promoter of secondary growth (Agusti *et al.*, 2011). Also in this case SLs seem to interplay with auxin, but the exact mode of interaction is not revealed to date (Agusti *et al.*, 2011).

In several species it was observed that SL mutants have a shorter stature than the wild type (Napoli, 1996; Kohlen *et al.*, 2012; Stirnberg *et al.*, 2002; Zou *et al.*, 2006; Liu *et al.*, 2013). In rice, branch removal resulted in almost wild-type growth (Zou *et al.*, 2006), indicating that the dwarfism is a result of high branching. An opposite result was obtained in pea, where removal of branches did not rescue plant height, but SL feeding

restored size while reducing branch length (de Saint Germain *et al.*, 2013). Internode cell length in pea was not changed in SL mutants compared to the corresponding wild type, indicating that overall cell number in SL mutant stems was lower (de Saint Germain *et al.*, 2013). In dark-grown rice seedlings, SLs were also found to inhibit cell division. SL mutant plants showed increased mesocotyl length and cell number, a phenotype that could be rescued by GR24 application (Hu *et al.*, 2010). In *d10* mutant seedlings, transcript levels of a negative regulator of branching were decreased, and mutants were shown to be more responsive to cytokinin application. SLs and cytokinins were shown to be antagonists in regulation of mesocotyl length (Hu *et al.*, 2013). SLs therefore inhibit cell division in this system, similar to inhibition of bud outgrowth, but different from the promotion of cambium activity.

Research in the past few years revealed that MAX2 is involved not only in SL signaling but also in other pathways. Originally, *MAX2* was identified as *ORE9*, a regulator of leaf senescence (Woo *et al.*, 2001). Mutant *max2* plants showed delayed senescence (Woo *et al.*, 2001), altered leaf shape, dwarfism, and increased branching (Stirnberg *et al.*, 2002). In addition, *max2* mutant plants were found to be hyposensitive to different light regimes, which was represented in an elongated hypocotyl, a reduced germination rate, and a smaller cotyledon angle (Shen *et al.*, 2007). These developmental defects were linked to altered GA, ABA, and auxin metabolism and sensitivity (Shen *et al.*, 2012). Another study linked the abovementioned *max2* phenotypes to the inhibition of light-induced genes in the absence of SLs. HY5 is such a light-responsive factor that is degraded by the E3 ligase COP1 in the nucleus during the night. During the day, COP1 is translocated from the nucleus to the cytosol, and HY5 is active. It was shown that the presence of SLs as well as cytosolic COP1, mimic the presence of light (Tsuchiya *et al.*, 2010). Further, it was shown that high light intensities increase transcription of *SlCCD7* resulting in increased SL quantities in tomato (Koltai *et al.*, 2011). Thus, SLs seem be positive regulators of light responses.

MAX2 was also identified in a screen for karrikin-responsive genes in Arabidopsis. Karrikins are germination-promoting compounds that were isolated from wildfire smoke (for a review, see Flematti *et al.*, 2013). SLs were described to play a role in germination of Arabidopsis seeds too, but only in high temperature conditions (Toh *et al.*, 2011). Karrikins and SLs are both butenolides and both signaling pathways include MAX2 (Nelson *et al.*, 2011). SL signaling requires D14, whereas for karrikin signaling,

a D14-like protein termed KAI2, was identified (Waters and Smith, 2013). These two receptors interact with MAX2 enabling modulation of responses. Branching for example is only influenced by D14, whereas germination responses and photomorphogenesis are regulated more by KAI2, with minor influence of D14 (Waters *et al.*, 2012b). Subsequently, the authors claimed that KAI2 and MAX2 responses to light are largely independent of HY5 (Waters and Smith, 2013), which is in contrast to the abovementioned study (Tsuchiya *et al.*, 2010) that investigated the effect of MAX2 on COP1 and HY5. Future studies should aim to understand the importance of the various players in these developmental processes.

Recently, a role of *MAX2* in abiotic stress was identified where Arabidopsis *max2* mutant plants were found to be less resistant to drought stress (Bu *et al.*, 2013). This was highlighted by reduced stomatal closure and a thinner cuticular layer. *MAX2* expression was found to be regulated by ABA, and MAX2 levels were found to regulate ABA signaling. However, other max genes were not found to be involved in the response, and SL was found not to be mandatory for the drought response of plants, implying that only MAX2, and not the SL pathway, is involved in abiotic stress response (Bu *et al.*, 2013). Contrasting this finding was a report in which SL application enhanced drought resistance in both, Arabidopsis wild type and in several *max* mutant plants. Subsequently however, an interplay between SL and the ABA pathway was noted (Ha *et al.*, 2013). Further studies are required to understand the precise role of SLs in abiotic stress responses.

Similar to MAX2, CCD7 and CCD8 have also been implicated in processes other than SL signaling, although to a lower extent. *CCD7*-deficient *L. japonicus* plants showed the typical SL-related phenotypes, in addition to delayed senescence, lower number of flowers, fruits, and seeds (Liu *et al.*, 2013). In contrast to other species, mycorrhization levels were only slightly reduced, but a defect in nodulation was observed. The phenotypic change of *ccd7* was thus a result of an enhanced investment in vegetative growth; which would imply that SLs promote reproductive growth (Liu *et al.*, 2013). In potato, a role of *CCD8* in tuber formation was proposed, since tubers and shoots grew out of *ccd8* mature tubers (Pasare *et al.*, 2013). *P. patens ccd8* lines are deficient of four of the six SLs identified. The mutant lines exhibited increased filament branching, and lost their ability to sense neighboring colonies. The authors thus propose that the SL exudation of *P. patens* is similar to quorum sensing of bacteria (Proust *et al.*, 2011).

1.2.3 Strigolactones are involved in arbuscular mycorrhizal symbiosis

1.2.3.1 The importance of arbuscular mycorrhizal symbiosis

Arbuscular mycorrhizal symbiosis is a mutual relationship between 74% of Angiosperm species and fungi of the order Glomeromycota (Brundrett, 2009). Fossils of Glomales-like fungi have been dated as 460 million years old (Redecker *et al.*, 2000), approximating the time when Bryophytes started to colonize land. Experiments showed that at least some Bryophytes are able to form an arbuscular mycorrhizal like symbiosis, rendering the common agreement that the association of plants with arbuscular mycorrhizal fungi (AMF) was particularly important in land colonization by photosynthetic Eukaryotes. Fungi deliver water and nutrients such as phosphorus and nitrogen to the plant, which in turn feeds the fungus with up to 20% of its photosynthetic products. Up to 80% of phosphate in a plant can be delivered by the fungus (Parniske, 2008). Nutrient exchange takes place in root cortex cells that contain highly branched hyphae, so-called arbuscules (arbusculum, greek: little tree), which are enclosed by a specialized part of the plant plasma membrane, termed periarbuscular membrane. Besides arbscular mycorrhizal symbiosis, other mycorrhizal symbiosis exist, such as ectomycorrhiza, where fungal structures reside outside of plant structures, or other endomycorrhizas that do not contain specialized structures such as arbuscules for nutrient exchange (Parniske, 2008; Gutjahr and Parniske, 2013; Parniske, 2000).

AMF enhance plant performance for example under altered climate conditions predicted for the future (Kivlin *et al.*, 2013). Additionally, AMF enhance plant performance under abiotic and biotic stress conditions (Pozo *et al.,* 2002, for reviews, see Ruiz-Lozano *et al.*, 2012; Singh *et al.*, 2011; Nadeem *et al.*, 2014). Most often, the mechanisms leading to a better performance are unknown, but the enhanced tolerance to the heavy metal arsenic (As) was proposed to result from increased expression of a fungal As efflux protein enabling the maintenance of low As levels in the plant (Gonzalez-Chavez *et al.*, 2011). The importance of such a protective role is highlighted by the fact that in crops, abiotic stress causes up to 50% yield loss. All cereals investigated so far retained the ability to form symbiosis with AMF, and yield is enhanced by AMF under non-optimal growth conditions (Singh *et al.*, 2011; Nadeem *et al.*, 2014). In recent agricultural practices, AMF are usually not included and thus, AMF-plant co-cultivation strategies have a great potential for future agricultural applications (Sawers *et al.*, 2008).

1.2.3.2 Induction and establishment of arbsucular mycorrhizal symbiosis on a morphological level

Plants typically induce arbuscular mycorrhizal symbiosis when phosphate or nitrate levels in the soil are low (Yoneyama *et al.*, 2007a; Yoneyama *et al.*, 2007b). Under such conditions, SL synthesis and export to the rhizosphere are significantly enhanced (Lopez-Raez *et al.*, 2008a; Yoneyama *et al.*, 2011). AMF are obligate symbionts, hence they rely on the symbiosis with a plant host to accomplish their lifecycle via spore production. Indeed, AMF spores germinate and grow only for a limited time depending on the amount of carbon stored in the spore. Further growth of the hyphae depends on the perception of SLs, which leads to a general enhancement of metabolic activity, to hyphal branching and a directed hyphal growth towards high SL concentrations (Akiyama *et al.*, 2005; Tamasloukht *et al.*, 2003; Besserer *et al.*, 2006).

AMF release myc factors that were recently identified as lipochitooligosaccharides (Maillet *et al.*, 2011), which are recognized by the plant. AMF first form an hyphopodium on the plant root surface, a mechanism dependent on plant cutin monomers (Murray *et al.*, 2013). Plants were shown to prepare for fungal entry by forming a prepenetration apparatus, a cytosolic column surrounded by ER and cytoskeleton, allowing the fungus to grow across cells without penetrating the plasma membrane (Genre *et al.*, 2005). During fungal penetration of a cell, many vesicles are formed below the hyphal tip, with Golgi, ER, and exocytotic markers present (Genre *et al.*, 2011). After crossing the epidermis, hyphae grow through unsuberized cells of the hypodermis, so-called hypodermal passage cells (HPCs). Because of their lack of cell wall, HPCs are sites of ion uptake from the soil, and they also serve as entry points for AMF (Sharda and Koide, 2008). Hyphae subsequently elongate intercellularly in the root cortex, and arbuscules, as well as other mycorrhiza-associated structures such as vesicles, are formed. The signal for arbuscule formation is currently unknown, but the process is again accompanied by major cytoskeleton, ER, and Golgi rearrangements (for reviews, see Parniske, 2008; Parniske, 2004; Gutjahr and Parniske, 2013; Harrison, 2012). Once a symbiosis with AMF is established, SL production is lowered (Lopez-Raez *et al.*, 2010).

Plants tightly control the extent of symbiosis with AMF by favoring fungi that deliver high amounts of nutrients (Kiers *et al.*, 2011), and arbuscules of fungi that do not deliver nutrients are abolished (Yang and Paszkowski, 2011). This was illustrated with

Medicago truncatula pt4 mutant plants that are deficient in a periarbuscular membrane localized phosphate transporter. These plants do not form AMF symbiosis under phosphate deficient conditions; however, the mutant could be rescued by nitrogen deficiency, illustrating that nitrogen supply by the fungus is favorable for the plant (Javot *et al.*, 2007). In turn, AMF establish higher levels of colonization when plants deliver high amounts of carbohydrates (Kiers *et al.*, 2011), and high carbohydrate levels increase nitrogen uptake by fungi (Fellbaum *et al.*, 2012). A recent field study showed that AMF not only elevate phosphate content in the shoot under low nutrient conditions, but that AMF function also to lower shoot phosphate increases after fertilization. This indicates that AMF could act as a nutrient buffer, maintaining phosphate and levels of other nutrients within a plants optimal range (Nazeri *et al.*, 2013).

1.2.3.3 Mechanistics of the arbuscular mycorrhizal symbiosis and the nodulation pathway

Symbiosis with AMF is very common among land plants, in contrast to the symbiosis with rhizobial bacteria that almost exclusively interact with members of the Fabaceae family. Both symbiosis share a part of their signaling pathway (Gutjahr et al., 2008; Parniske, 2008), and they have sets of genes that are co-regulated (Tromas *et al.*, 2012). As nodulation is only found in a limited set of plants, it is believed that this pathway evolved from mycorrhization. Both symbionts, nitrogen fixing bacteria and AMF, respectively, emit distinct lipochitooligosaccharides that are sensed by the host plant. Nod factor receptors are characterized in Medicago and Lotus, and receptors similar in structure are believed to exist for myc factors (for an overview of the SYM pathway, see Figure 1.4, Singh and Parniske, 2012). The receptor kinase SYMRK is required for both pathways (Singh and Parniske, 2012).

Early and late steps of mycorrhization, such as hyphopodia formation and cellular penetration, as well as nodulation, are accompanied by Ca^{2+} spiking of different frequencies (Navazio *et al.*, 2007; Gutjahr and Parniske, 2013; Ehrhardt *et al.*, 1996). The spiking occurs by fluctuations of the nuclear and cytosolic Ca^{2+} levels. The potassium transporters CASTOR and POLLUX (Imaizumi-Anraku *et al.*, 2005; Peiter *et al.*, 2007) located in the nuclear envelope likely regulate the flux of K^+ counterions, (Parniske, 2008) and an ATPase localized in the same membrane is involved in transporting Ca^{2+} ions into the nucleus (Singh and Parniske, 2012). Three nucleoporins are involved in calcium spiking too, but their role in the process is still

unknown (Kanamori *et al.*, 2006; Gutjahr and Parniske, 2013). The calcium spiking is sensed by the nuclear localized calcium calmodulin-dependent protein kinase CCaMK, which differentiates nodulation and mycorrhization responses by differential Ca^{2+} and calmodulin binding (Shimoda *et al.*, 2012). Upon binding, the kinase undergoes autophosphorylation and subsequently, phosphorylates its substrate CYCLOPS. Different transcription factors of the GRAS, ERF, and other families are activated by CCaMK (Singh and Parniske, 2012).

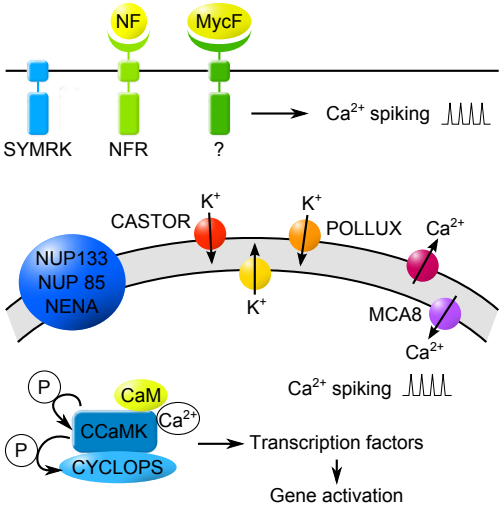

Figure 1.4: SYM pathway

Myc and Nod factors (MycF and NF, respectively) are bound by their receptors, the ones for Nod factors being already characterized (NFRs). The receptor kinase SYMRK is required for both pathways. Binding of both factors result in cytosolic calcium spiking. The presence of the potassium channels CASTOR and POLLUX is required for the spiking, they probably regulate the flux of potassium counterions. MCA8 is an ATPase, possibly involved in Ca^{2+} transport into the nucleus. The nuclear pore complex (NUPs) and some other genes are as well mandatory for the spiking. The calcium spiking activates a calmodulin calcium dependent protein kinase (CCaMK), its substrate CYCLOPS, and some transcription factors specific for both pathways. The calcium spiking and the CCaMK response seem to distinguish between nodulation and mycorrhization. Figure modified (Singh and Parniske, 2012).

After initiation of the symbiosis, other genes, among them transporters localized to the periarbuscular membrane, are required for sustained symbiotic interactions. Establishment and maintenance of rhizobial or mycorrhizal symbiosis seems to require expression of a tightly regulated set of genes in certain cells at a specific time points. Many more proteins and factors than the ones mentioned here are described to be involved, and the exact signaling pathways and interplay between these pathways is to date not fully resolved (for reviews, see Harrison, 2012; Gutjahr and Parniske, 2013).

Besides being of major importance for arbuscular mycorrhization initiation, SLs were shown to be important for nodulation in pea (Foo and Davies, 2011). Biosynthetic SL

mutants have significantly reduced nodule numbers compared to wild type. GR24 application elevated nodule numbers in both, *rms1* mutant and wild-type plants (Foo and Davies, 2011). The mechanism of how SLs influence nodulation is not resolved to date; however, there are some genes described that link arbscular mycorrhization, nodulation, and SLs. NODULATION SIGNALING PATHWAY 1 (NSP1) is a GRAS-type transcription factor that was described to be important for nodulation and arbuscular mycorrhization in Lotus (Takeda *et al.*, 2013). Medicago *nsp1* mutant plants have reduced *D27* expression levels and are devoid of SLs, indicating that NSP1 not only influences the SYM pathway but as well SL synthesis (Liu *et al.*, 2011). In addition to NSP1, NSP2 as well positively regulates *D27* expression. This protein is required for the production of didehydro-orobanchol in Medicago, but its exact function is not well understood (Gutjahr and Parniske, 2013; Liu *et al.*, 2011). Future experiments should aim to examine the interplay of NSP1 and NSP2 with SL production, nodulation, and mycorrhization.

1.2.3.4 Strigolactones induce germination of parasitic weeds

SL exudation by plants was first described in 1966, decades before the role of SLs in arbuscular mycorrhization was revealed (Cardoso *et al.*, 2011). SLs were first identified as germination stimulants of parasitic weeds of the genera *Striga, Orobanche*, and *Phelipanche*. The names of numerous SLs, such as strigol, orobanchol, and even the strigolactones themselves give credit to this function. Only later, it was realized that the foremost function of SLs was to attract AMF, and that the parasitic weeds took advantage of this system. Further, it was recognized that plants were mainly infected on soils with low nutrient levels. In such soils, plants exude SLs in search for AMF to enhance nutrient uptake, causing germination of the parasitic weeds. The weeds subsequently infect the roots, develop a plant body, and produce seeds (Lopez-Raez *et al.*, 2008b).

Infection of plants by parasitic weeds is mainly a problem in resource-limited agricultures. In sub-Saharan Africa, *Striga sp.* can cause yield losses up to 50% in cereals, and up to 70-100% in maize, sorghum and millet (Emechebe *et al.*, 2004). Broomrapes, including *Orobanche* and *Phelipanche sp*., cause similar levels of damage (Cardoso *et al.*, 2011); however, not all plants are infected by all kind of parasitic weeds (for some examples, see Figure 1.2). Cereals are a main target of *Striga sp.*, whereas Fabaceae and

Solanaceae are more susceptible to broomrapes. By characterizing which SLs are produced by the different families, in conjunction with germination assays involving SLs and parasitic seeds, it became clear that certain seeds only sense certain SLs (see 1.2.1.1, Mwakaboko and Zwanenburg, 2011; Cardoso *et al.*, 2011).

In agriculture, there exists considerable interest in lowering crop infection by parasitic weeds. One approach was to screen for commercial cultivars with lower SL exudation rates, maintaining low branching numbers. Such cultivars were identified in rice, the molecular mechanisms resulting in *S. hermontica* infection resistance are currently being investigated (Swarbrick *et al.*, 2008; Cissoko *et al.*, 2011; Jamil *et al.*, 2011). Another approach was to design SL analogues that inhibit branching, but do not induce *Striga sp.* germination (Fukui *et al.*, 2013; Cohen *et al.*, 2013; S., Ito *et al.*, 2011), or topically apply SLs to fields to induce parasite germination in absence of host plants (Lopez-Raez *et al.*, 2008b; Wigchert *et al.*, 1999). A future approach may involve the inoculation of host plants with AMF to increase plant nutrient levels and stress tolerance (see 1.2.3.1, 1.2.3.2), while retarding *Striga sp.* development (Cardoso *et al.*, 2011), as well as reducing SL exudation to the soil. This would result in overall reduction of parasitic seeds germination and increased crop yield.

1.3 Terpenes stored in trichomes are important for defense against herbivores

1.3.1 Biotic stress recognition and signaling

Plants are sessile organisms and are therefore unable to escape abiotic and biotic stress factors. Therefore, they have evolved a number of sophisticated mechanisms to cope with stresses. The distinction of tissue wounding by abiotic versus biotic factors is crucial for the plants to initiate appropriate responses, such as the production of defense compounds only when a response to herbivores is required. Herbivore presence is sensed by the detection of elicitors present in herbivore saliva, and by intrinsic herbivore-processed molecules. Alternatively, repetitive patterns of tissue wounding can induce a signaling cascade that initiates defense responses (Howe and Jander, 2008). Commonly, defense responses include the production of toxins and deterrents, the synthesis of protease inhibitors that prevent efficient nutrient uptake by the herbivore, and the release of volatiles that attract herbivore predators. Moreover, the fine-tuning of responses depends on the presence of generalist or specialist herbivores (Smith *et al.*, 2009), on the number of feeders present, and on the developmental stage of the plant and the herbivore.

Biotic stressors include not only macroorganisms, such as caterpillars, but also microorganisms, such as bacteria and fungi and even insect eggs. Generally, responses to microorganisms rely on salicylic acid (SA), whereas responses to herbivore attack induce JA dependent signaling pathways (Bodenhausen and Reymond, 2007). As a first step in herbivore defense, bioactive JA is synthesized and transported to other cells or tissues to induce a systemic defense response. In a second step, JA binds to the multicompound E3 ligase SCF^{COI1}, which ubiquitinates JAZ proteins and thus targets them for degradation. The absence of JAZ proteins releases transcriptional repressors from their DNA binding site and enables the transcription of JA-responsive genes in a third step. These gene products cause the various defense responses of the plant (Smith *et al.*, 2009).

1.3.2 Trichomes store large amounts of secondary metabolites

Trichomes are epidermal cells that protrude from surfaces of aerial plant parts. In angiosperms, a limited number of studies have been performed examining type and frequency of trichomes, but some plant families, among them Solanaceae, are described to be rich in trichomes (Tissier, 2012). Trichomes of tomato for example can be categorized into six types (Kang *et al.*, 2010b). A variety of shapes has been described, uni- or multicellular structures are found whereas both, the stalk and the top can be comprised of one or several cells. Non-glandular trichomes hinder movement of herbivores, they reduce irradiation and water loss from the plant surface (Howe and Jander, 2008), while glandular trichomes additionally include a bulbous head at the top of stalk cells (Schilmiller *et al.*, 2008), which is highly enriched in defense compounds. The glandular head is separated from the plant's environment by a cuticule layer only, and because of this fragile structure, trichome heads burst easily on contact with an herbivore releasing their toxic or deterrent content (Wagner, 1991).

The importance of glandular trichomes in herbivory is supported by several observations. For *Datura wrightii*, two different varieties, one with, another without trichomes was described; the latter being more susceptible to herbivores (van Dam and Hare, 1998; Hare, 2005). As mentioned before (1.3.1), herbivores often induce a JA response. Both, exposure to herbivores as well as JA application, can increase density of trichomes in plants (Boughton *et al.*, 2005; Traw, 2003). Further, several wild relatives of cultivated species show enhanced pest resistance due to a diverging trichome content (Bleeker *et al.*, 2012). Some of the trichome-stored compounds are harmful to the plant metabolism. In particular, leaf metabolism is largely disconnected from trichome metabolism, and the latter is usually constrained to specialized pathways for the synthesis of defense compounds. Precursors for these compounds, as well as energy-rich molecules, are imported from the leaf (Schilmiller *et al.*, 2008). Although the trichome metabolism is largely detached, lipophilic trichome compounds tend to diffuse back into the leaf. The mechanism maintaining a steep concentration gradient of secondary metabolites between the trichome and the leaf is currently unknown; however, one can imagine the involvement of ABC transporters, because they can shuttle substrates against a concentration gradient (see 1.1.1). In particular, it can be envisaged that PDR proteins are involved in this process, as they have been previously characterized in secondary metabolite transport (Kang *et al.* 2011).

1.3.3 Secondary metabolites are involved in plant defense

Secondary metabolites are believed to have evolved as a means of defense against abiotic and biotic stressors. The compounds may act as allelochemicals by hindering the growth of competitor plants, intoxicate feeders, or attract herbivore predators (Schilmiller *et al.*, 2008). Glandular trichomes store a wide variety of secondary metabolites belonging to different classes. Among them are terpenoids, phenylpropanoids, polyketides, fatty acid derivatives, and acyl sugars (Schilmiller *et al.*, 2008; Slocombe *et al.*, 2008; Wang *et al.*, 2001). For some of these compounds, it has been reported that the quantity varies substantially, depending on the season (Ambrosio *et al.*, 2008).

Many studies devoted to investigations of trichome metabolite contents, altered trichome structure or metabolite content, and their effects on herbivore resistance, have been performed in tomato. Commonly, wild tomato varieties are more resistant to herbivores than commercial cultivars (Besser *et al.*, 2009; Medeiros and Tingey, 2006; Kennedy, 2003). It was observed that the former mostly contain sesquiterpenes, whereas the latter are rich in monoterpenes (Besser *et al.*, 2009).Alteration of trichome types and metabolite content lead to increased susceptibility to herbivores (Kang *et al.*, 2010a; Kang *et al.*, 2010b), whereas incorporation of, for example, a sesquiterpene synthase from wild tomato to a commercial cultivar increased resistance markedly (Bleeker *et al.*, 2012). A linalool synthase was upregulated by JA treatment, emphasizing the link between herbivory and trichome metabolism (van Schie *et al.*, 2007). In transgenic *A. thaliana*, linalool and noralidol production increased resistance against apids (Kos *et al.*, 2012).

1.4 The role of sterols in plant defense

To defend against pathogens, plants have to be able to recognize foreign organisms (see 1.3.1). One of the molecules that elicits a defense response is ergosterol, a fungal sterol, which is a major compound of fungal membranes (see 1.4.3). The response of plants to ergosterol was investigated in several studies. The fact that ergosterol acts as an elicitor was discovered in tomato culture cells, where the addition of ergosterol lead to an elevation of the pH in the growth medium: Pre-treatment with ergosterol increased the cells resistance against the fungus from which ergosterol was extracted, indicating that ergosterol was the major elicitor of the fungus (Granado *et al.*, 1995). Similarly, a pH increase in the medium of ergosterol-treated *Beta vulgaris* leaf tissue was observed within a short time frame, likely due to an inhibition of the plasma membrane H^+-ATPase activity. After a couple of hours, the formation of hydrogen peroxide was induced. The addition of cholesterol, a mammalian sterol, induced both similar and some opposite effects compared to ergosterol, demonstrating that the ergosterol-response is specific for the fungal sterol (Rossard *et al.*, 2010). The abovementioned reactions to ergosterol occur also in tobacco culture cells. One study investigated the change in secondary metabolites upon ergosterol addition and found that synthesis of five bicyclic sesquiterpenes was upregulated (Tugizimana *et al.*, 2012).

Recently, plant sterols were described to play a role in pathogen infection. Inoculation of *A. thaliana* with pathogenic bacteria or fungi lead to an increase of stigmasterol, which is a plant sterol. Stigmasterol levels increased after the application of exogenous reactive oxygen, but this reaction was not linked to SA or JA dependent pathways. Elevation in stigmasterol levels increased *Pseudomonas syringae* multiplication in the apolast. Also, stigmasterol-defective plants were less susceptible to this pathogen than wild-type plants (Griebel and Zeier, 2010). Another study reported the same observation in Nicotiana, and in addition, could show that the susceptibility of the plant to bacteria and the enhanced bacterial growth in the apoplast are connected to enhanced nutrient transport to the apoplast. The authors speculate that increased stigmasterol levels alter the membrane composition, which leads to altered nutrient flows (Wang *et al.*, 2012).

1.4.1 Characteristics of sterols

Sterols are isoprenoid derived triterpenes found in all eukaryotes. On the one hand, they are incorporated into the lipid bilayer of membranes, where they regulate permeability, fluidity, protein sorting, and endocytosis (Schulz and Prinz, 2007). On the other hand, they are precursors for sterol-based hormones, for example ergosterol and testosterone in humans, or brassinosteroids in plants (Schaller, 2003; Maxfield and Menon, 2006). Animal membranes contain cholesterol, yeast ergosterol, and plants several phytosterols such as champesterol, sitosterol, or stigmasterol (see Table 1-2 for an overview on phytosterols).

Sterols are synthesized in the ER. Sterol concentrations are lowest at the site of synthesis and highest in the plasma membrane (1-10% cholesterol in ER and about 30% in the plasma membrane, Maxfield and Tabas, 2005), and because each membrane has a unique composition of lipids, it is assumed that the transport of sterols is tightly controlled. In addition to their presence in organelle membranes such as ER, Golgi, and vacuolar membrane, sterols are found in vesicles of the endosomal pathway, as well as in lipid particles of the cytosol. These compartments serve sterol sorting and storage (Maxfield and Menon, 2006).

Sterol transport is still not fully understood. It was shown to depend on ATP hydrolysis and it is partially Brefeldin A (BFA) dependent, a chemical that disrupts vesicle transport from the Golgi (Jacquier and Schneiter, 2012). It is generally accepted that there is a vesicular and a non-vesicular pathway: sterols can be incorporated into vesicles and transported between compartments; however, this mechanism would rapidly equilibrate sterol concentrations of the different compartments. Therefore, this pathway is assumed to be of minor importance (Schulz and Prinz, 2007). Non-vesicular transport is proposed to depend on lipid carrier proteins that have been described in mammals (Mesmin *et al.*, 2013) and in yeast (Schulz and Prinz, 2007). Sterols can diffuse into and out of membranes, and they can flip from one side of the bilayer to the other. Depending on membrane properties, this flipping may occur fast, within 10 ms to 1 min as in the ER, or much slower, as reported for the plasma membrane (Jacquier and Schneiter, 2012; Tarling *et al.*, 2013).

1.4.2 Sterol transport in humans

Human diet consists of cholesterol from meat, phytosterols from plants, and sterols from other sources. The sterols are incorporated into micelles in the intestinal lumen and are absorbed by enterocytes (Klett and Patel, 2003). In the cytosol, only cholesterol is esterified and further transported to other organs of the body, whereas other sterols are excreted from the liver into the bile. The excretion of sterols is conducted by two ABC transporters, ABCG5 and ABCG8, that form obligate heterodimers (Moitra *et al.*, 2011). Amino acid residues of both proteins are required to form the N-terminal NBD1 and the C-terminal NBD2. A Histidine residue in the H-loop of NBD2 was shown to be required for sterol transport, whereas alterations in NBD1 did not result in an abolishment of transport but in an alteration of substrate specificity (Wang *et al.*, 2011). ABCG5 and ABCG8 are expressed on the apical sides of hepatocyte plasma membranes and are believed to flip sterols from the inner side of the liver lipid bilayer to the outer side by the stepwise hydrolyzation of two ATP molecules. The exact mechanism of action is unknown to date (Tarling *et al.*, 2013). From the outer side, the sterols are incorporated into bile micelles or vesicles and are excreted. Mutations in either of the two transporters are the cause of the disease sitosterolemia or phytosterolemia (Wittenburg and Carey, 2002), which is characterized by the failure of cholesterol and phytosterol excretion from the liver to the bile. A common symptom of the disease is arthritis.

Of the 48 ABC proteins identified in humans, 20 members are characterized. They belong to the subfamilies ABCA, ABCB, ABCC, ABCD, and ABCG, and about half of them are involved in transport of lipids or compounds similar to lipids. Again about half of the lipid-related transporters are localized in intracellular membranes. The reported mutations emphasize the importance of the transporters in metabolism (for an overview on ABC proteins linked to disease, see Tarling *et al.*, 2013). Diseases such as arteriosclerosis are linked to alterations in cholesterol levels, but the exact role of sterols and other lipids in many diseases is not well understood yet (Klett and Patel, 2003).

1.4.3 Sterol transport in yeast

In *Saccharomyces cerevisae*, several transport pathways for sterols have been described. A protein complex was described as being potentially involved in bringing organelle membranes into close contact, although the specific membranes and the mode of action was not reported. This complex could possibly also enable the transfer of lipids between the membranes, and thus, the proteins part of the complex were termed lipid transfer proteins (Jacquier and Schneiter, 2012). ORP proteins were described first as lipid carrier proteins that take up a sterol, close their lid, and move through the cytosol to another membrane (Schulz and Prinz, 2007). Subsequent publications mention ORP proteins as candidates for lipid transfer proteins, because they have two membrane binding domains, enabling the interaction with two membranes simultaneously. However, the exact mechanism of action remains unclear. It is clear however, that these proteins play an important role in yeast sterol metabolism, because their mutation leads to altered sterol distribution, and a lack of all seven proteins is lethal for the organism (Jacquier and Schneiter, 2012).

Similar to the mammalian system, several membrane-bound ABC proteins have been described to be important for yeast sterol transport processes. The ABC transporters Aus1p and Pdr11p are expressed in the plasma membrane and are involved in the uptake of sterols from the environment, a process that only takes place under anaerobic conditions. These proteins catalyze mainly the movement of ergosterol. They are also involved in cholesterol and sitosterol transport from the plasma membrane to the ER, although the speed of phytosterol transport is lower. The exact mode of transport is not resolved to date (Li, 2004).

For the retrograde transport of sterols from the ER to the plasma membrane, another yeast PDR protein termed Pdr18p was described. The protein localizes to the plasma membrane. Ergosterol content in the plasma membrane of Pdr18 knockout lines was lower than in wild type, and ergosterol precursor levels were enhanced, indicating that Pdr18 is involved in the uptake of sterols into the plasma membrane (Cabrito *et al.*, 2011). Other yeast PDR proteins are described to be involved in lipid homeostasis (Jungwirth and Kuchler, 2006).

1.4.4 Sterol metabolism in plants

In plants, sterols are synthesized at the ER, similar to yeast and human (see 1.4.1, Schaller, 2003). This occurs mostly via the cytosolic mevalonate pathway of isoprenoid biosynthesis; however, when this pathway is not functional, the chloroplastic methyl-erythritol pathway can take over (Hemmerlin, 2003). In contrast to animals and fungi, plants contain a mixture of structural sterols. Some of the most abundant are sitosterol, stigmasterol, isofucosterol, and campesterol. The percentage of these sterols is genetically fixed and it varies between species (for some examples, see Table 1-2). However, upon infection, the ratio between the phytosterols may change (see 1.4).

Table 1-2: Phytosterol amounts

Relative amounts of selected structural sterols in *P. hybrida*, *N. tabacum*, and in *A. thaliana*. *P. hybrida* W138 percentages were calculated from g kg^{-1} fresh weight (FW) data (Schaller, 2004; Verhoef *et al.*, 2013; Schaeffer *et al.*, 2001).

	Isofucosterol	Sitosterol	Campesterol	24-Methylene cholesterol	Stigmasterol
Petunia W138	55%	36%	12%	9%	8%
Tobacco	0.3%	25%	16%	n.d.	44%
Arabidopsis	3%	64%	11%	11%	6%

The structural sterol campesterol is a precursor for the phytohormones of the brassinosteroid family (Schaller, 2004). It was shown that application of the most active brassinosteroid, brassinolide, to tobacco and rice induced resistance against bacterial and fungal pathogens. This seems to take place via an SA-independent pathway, since additive effects were observed when brassinolide and an elicitor of the SA-dependent response were supplied together (Nakashita *et al.*, 2003). Increased pathogen resistance upon application of brassinosteroids was further observed in other organisms, and it was suggested that this could be due to an interaction with ABA or ethylene (Bari and Jones, 2008). The brassinosteroid signaling pathway has become well resolved in the past few years, but the exact mechanism on how immunity against pathogens is required is still elusive (Choudhary *et al.*, 2012).

Knowledge about intra- and intercellular phytosterol transport in plants is scarce. However, it was shown that there is a BFA and cold sensitive transport from the ER to the plasma membrane (Moreau *et al.*, 1998). In Arabidopsis, sterol endocytosis to early endosomes was shown to be actin dependent and BFA sensitive (Grebe *et al.*, 2003). In regard to brassinosteroid transport, researchers seem to agree that there is no or little transport (Bishop and Yokota, 2001; Yang *et al.*, 2011) and thus, the necessity of a

transporter is not obvious. Lipid carrier proteins or PDR transporters that have a similar function as the ones described in yeast or human have not been identified to date.

1.4.5 Petuniasterones

Petuniasterones are ergostane-type sterols, bearing a ketone at the C3 of the backbone A ring (see Figure 1.5). These two properties, in addition to the species in which the molecules were discovered, gave the name to petuniasterones. Molecules of this class either bear a non-cyclic side chain similar to other sterols of plants, mammals, or yeast, or they incorporate an orthoester side chain. Various modifications at several positions of the backbone and side chain were described, such as acetylation, thiolation, epoxylation, methylation, ethylation, hydroxylation, or a combination of the mentioned (Elliger and Waiss, 1991). The side chain can undergo further modifications, such as an addition of pyridine rings (Elliger *et al.*, 1992) and the sterol backbone can for example be glycosylated (Shingu *et al.*, 1994).

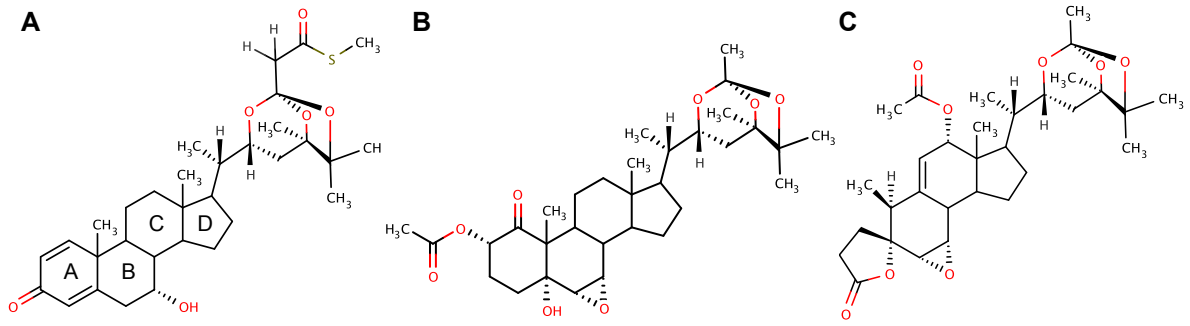

Figure 1.5: Petunia sterol structures

Structure of petuniasterone A **(A)**, petuniasterone O **(B)**, and petuniolide A **(C)**.

The class of petuniasterones was discovered and described first in the late 1980's and early 1990's by a group around C. A. Elliger and A. C. Waiss who investigated the toxicity of Petunia leaves. They extracted leaf material with solvents of different polarity and tested the obtained fractions for their toxicity on herbivores. Using HPLC and NMR analysis, the group identified the active substances to be sterol derivatives and they were termed petuniasterones.

Petuniasterones bearing an orthoester side chain were examined for their insecticidal activity compared to molecules having a regular ergostane side chain, with the latter being inactive towards insects (Elliger *et al.*, 1988). A modification that significantly enhances the toxicity of the compounds in the range of ten-fold or more is the

rearrangement of the A ring of the backbone, resulting in a lactone ring (compare A and B in Figure 1.5). Those molecules are termed petuniolides. For petuniolides, several modifications of the backbone and side chain have been described, similar to the ones of petuniasterones. Petuniasterone O (Figure 1.5 C) is proposed to be an intermediate of petuniasterones and petuniolides (Elliger *et al.*, 1989a).

Overall, approximately 60 Petunia sterols were described. Growth inhibition tests were performed with larvae of *Manduca sp.*, *Spodoptera sp.*, *Heliothis zea* and others. The strength of the effect was dependent on the insect species and of the age of the larvae (adult animals were usually less susceptible or not susceptible at all). In general, feeders that were highly specialized on a species other than Petunia were more susceptible than general feeders or than herbivores specialized for Petunia (Isman *et al.*, 1998). In addition, the compounds were tested on a crustacean, which was not susceptible (Elliger and Waiss, 1991). Other studies showed the poisonous effect of petuniasterones using *Biomphalaria glabrata*, a mollusk that is an intermediate host of schistosomes, causing bilharziasis (Moser *et al.*, 1999). Petuniolides C and D were shown to be weak ligands of the GABA receptor in rat brains. Similar to susceptible insects, feeding of the petuniolides to cockroaches induced disease symptoms. Cockroaches that have a mutated GABA receptor binding site showed elevated petuniolide resistance (Isman *et al.*, 1998).

One could imagine the use of petuniasterols or petuniolides as natural pesticides. In the last years, not many new natural insecticides have been developed, although this would be of interest for agriculture, as the acceptance of natural over synthetic pesticides is higher (Miresmailli and Isman, 2013). Toxicity of Petunia sterols is published as ED_{50}, which is the amount of chemical reducing growth of larvae to 50% of untreated controls (Elliger and Waiss, 1991). The most potent petuniolides have an ED_{50} of 3 parts per million (ppm). For pesticides, generally, the mean lethal concentration causing death of 50% of larvae (LD_{50}) is reported. In a study that tested natural oils on *S. littoralis* larvae, LC_{50} of 10 ppm were observed (Pavela, 2005). Thus, Petunia sterols can be regarded as potent insecticides.

1.5 Aim of the thesis

The goal of this thesis was to characterize two ABCG transporters of Petunia that were identified by T. Kretzschmar, a former PhD student of this laboratory. During his work T. Kretzschmar showed that *Petunia axillaris* PDR1 (PDR1) is very likely a strigolactone (SL) transporter, playing a role in SL excretion to the soil and in regulation of aboveground branching. However, direct evidence for SL transport by PDR1 as well as information on sites of SL transport on a cellular or tissue level were scarce. This thesis contains direct evidence for SL transport by PDR1, as well as detailed PDR1 polarity data in several cell types and localization studies at the cellular and tissue level. Furthermore, the role of SL transport in respect to other SL-dependent developmental processes is elucidated.

The second ABCG transporter identified by T. Kretzschmar was *Petunia hybrida* PDR2 (PDR2). He showed that PDR2 was expressed highly in trichomes, and that leaves of *PDR2*-silenced plants were more susceptible to herbivory. However, a more detailed characterization including cellular localization and the identification of potential substrates was required to learn more about the function of this ABC transporter. This thesis thus contains a characterization of PDR2 at the molecular and functional level. In addition, targeted and untargeted approaches were applied to identify potential PDR2 substrates, the latter in collaboration with L. Bigler (Department of Chemistry, University of Zürich).

2 A Petunia ABC protein controls strigolactone-dependent symbiotic signalling and branching

Tobias Kretzschmar[1], Wouter Kohlen[2*], Joelle Sasse[1*], Lorenzo Borghi[1], Markus Schlegel[1], Julien B. Bachelier[1], Didier Reinhardt[4], Ralph Bours[2], Harro J. Bouwmeester[2,3] & Enrico Martinoia[1]

[1]Institute of Plant Biology, University of Zurich, 8008 Zurich, Switzerland

[2]Laboratory of Plant Physiology, Wageningen University, 6700 AR Wageningen, The Netherlands

[3]Centre for Biosystems Genomics, P. O. Box 98, 6700 AB Wageningen, The Netherlands

[4]Department of Biology, University Fribourg, 1700 Fribourg, Switzerland

*These authors have contributed equally to this work

published in *nature* 2012; 483 (7389), 341-344

2.1 Abstract

Strigolactones were originally identified as germination stimulants of root-parasitic weeds[1] that pose a serious threat to resource-limited agriculture[2]. Primarily they are exuded from roots as signaling compounds involved in the initiation of arbuscular mycorrhiza[3], a mutual plant-fungal symbiosis with global impact on carbon and phosphate cycling[4]. Recently they were established as phytohormones that regulate plant shoot architecture by inhibiting the outgrowth of axillary buds[5,6]. Despite their importance, it is unknown how strigolactones are transported. ATP-binding cassette (ABC) transporters have functions in phytohormone translocation[7-9]. Here we show that the *Petunia hybrida* ABC transporter PhPDR1 plays a key role in regulating arbuscular mycorrhiza and axillary branch development by functioning as a cellular strigolactone exporter. *Phpdr1* mutants are defective in strigolactone exudation from roots, resulting in reduced symbiotic interactions. Aboveground, *phpdr1* exhibits an enhanced branching phenotype, suggestive of impaired strigolactone allocation. Over-expression of *PhPDR1* in Arabidopsis results in increased tolerance to high exogenous strigolactone concentrations, consistent with enhanced export from roots. PhPDR1 is the first known component in strigolactone transport, opening new routes for investigation and manipulation of strigolactone-dependent processes.

2.2 Main text

Strigolactones (SLs) are a new class of carotenoid-derived[10] phytohormones in land plants. Besides their role in shoot branching, SLs are exuded into the rhizosphere under P-limiting conditions[5] to act as growth stimulants of arbuscular mycorrhizal (AM) fungi[3]. To identify efflux carriers of AM-promoting factors such as SLs, we designed a degenerate primer approach (Supplementary fig. 2.2a) to isolate full-size ABCG/PDR transporters of *Petunia hybrida* abundant in phosphate-starved or mycorrhizal roots. The rationale to focus on ABCG/PDR-type transporters, with 15 members in *Arabidosis*[11], 23 in rice[11] and 23 putative members in tomato (Supplementary fig. 2.3a), was that they i) are plasma membrane proteins often found in roots[12]; ii) are implicated in belowground plant-microbe interactions[13,14]; iii) have affinities for compounds structurally related to SLs[8,9,15]. Of six primary candidates only *Petunia hybrida PDR1* (*PhPDR1*) displayed enhanced expression in roots subjected to either phosphate starvation (Fig 2.1a) or colonization by the AM fungus *Glomus intraradices* (Fig. 2.1b). Furthermore *PhPDR1* transcript levels increased in response to treatments with the synthetic SL analogue GR24 and the auxin analogue 1-naphthaleneacetic acid (NAA) (Fig. 2.1c). Auxin has been shown to up-regulate SL-biosynthetic genes[16] and to be involved in pre-symbiotic and early mycorrhizal events[17].

PhPDR1 is predicted to encode a full-size ABCG/PDR cluster I protein (GenBank accession: JQ280944, Supplementary fig. 2.2b-c, Supplementary fig. 2.3b). The closest *Arabidopsis thaliana* homologue, AtABCG40/AtPDR12, transports abscisic acid (ABA)[9]. However, as opposed to *AtABCG40*, *PhPDR1* is not regulated by ABA (Fig. 2.1c). A 1.8 kb upstream element of *PhPDR1* (JQ280944) was fused to the *GUS* reporter and stably transformed into the *Petunia* cultivar W115. Belowground *pPhPDR1::GUS* expression was pronounced in individual sub-epidermal cells of lateral roots (Fig 2.1d-e). These cells largely overlapped with hypodermal passage cells (HPC) (Fig. 2.1k-m) that are devoid of suberin and serve as cortical entry points for AM hyphae[18]. GUS staining was more prominent in roots grown under phosphate-deficient conditions (Fig. 2.1f) and in mycorrhizal roots, particularly in regions containing or flanking fully developed AM structures (Fig. 2.1g-h). These results suggested a role in AM during pre-symbiotic development and during intraradical colonization. Transient expression of a

GFP::gPhPDR1 fusion construct in *Arabidopsis* showed that PhPDR1 localizes to the plasma membrane (Fig. 2.1i-j), consistent with a role in secretion.

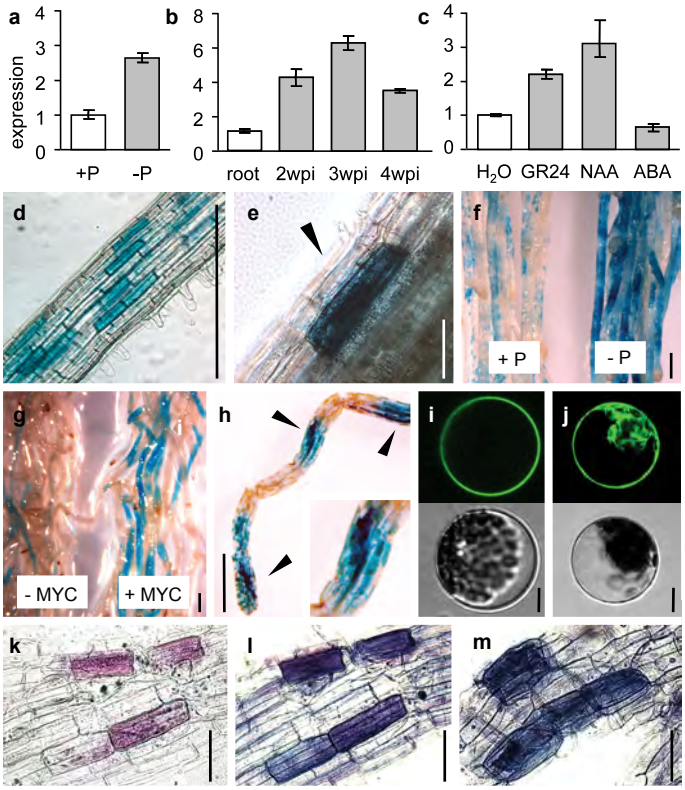

Figure 2.1: Belowground *PhPDR1* expression and PhPDR1 localization

a-c, qPCR for *PhPDR1* in W115 roots; in presence or absence of phosphate (P) **(a)**; 2-4 weeks post inoculation (wpi) with *G intraradices* **(b)**; in response to H2O, GR24, NAA, ABA **(c)**; means ± s.e.m. (N = 3). d-h, *pPhPDR1::GUS* signal in W115 roots without treatment (E: epidermal cell) **(d-e)**; under P-sufficient and P-deficient conditions **(f)**; in response to mycorrhization (+MYC = 8 wpi) **(g)**; in mycorrhized roots (8 wpi) co-stained with black ink (black arrows; mycorrhized sections) **(h)**. Scale bars = 1 mm (e: 0.1 mm). **i-j**, Transient *CaMV 35S::GFP-gPhPDR1* expression in *Arabidopsis* mesophyll protoplasts. GFP-gPhPDR1 signal and corresponding transmission image **(i)** and free GFP signal and transmission image **(j)**. Scale bar = 10 µm. k-m, *pPhPDR1::GUS* signal co-localization with trypan blue stained root hypodermal passage cells. Magenta GUS stained root section **(k)**; additional trypan blue stain of the same sample **(l)** and stained wild-type **(m)**. Scale bars = 0.1 mm.

For functional analysis we screened the transposon line W138 for insertional *pdr1* mutants. A PCR-based DNA library screen of 1,000 individuals led to the identification of a *dTph1* insertion in exon 4 of *PhPDR1* (Supplementary fig. 2.4a-d), together with a footprint allele causing a frameshift (Supplementary fig. 2.4e). Insertion of the *dTph1* in the coding region of a gene frequently results in a complete loss-of-function[19].

W138-*pdr1* was compared directly to W138 and crossed with W115 for further segregation analysis. Five homozygous *pdr1* mutant (W115xW138-*pdr1*) and wild-type lines (W115xW138) were derived from the F2 generation (Supplementary fig. 2.4d). Phenotypes co-segregated with the *PhDR1* mutation and transposon display analysis did not reveal other co-segregating *dTph1* insertions in the W115xW138

lines (Supplementary fig. 2.4f), suggesting that *dTph1* insertion in *PhPDR1* is responsible for the observed phenotypes. In addition, *PhPDR1* knock-down lines (*phpdr1*-RNAi), created in W115 by use of two independent RNAi constructs (Supplementary fig. 2.5a-b), exhibited similar phenotypes.

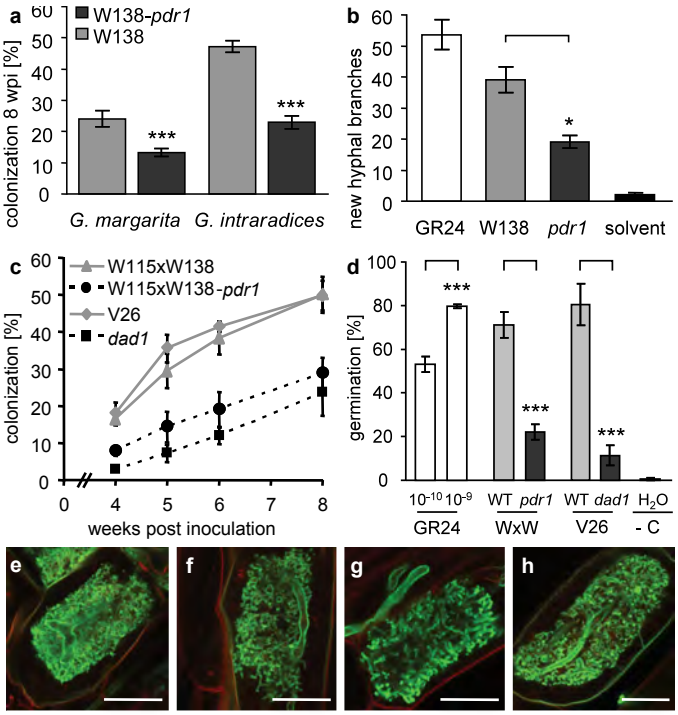

Figure 2.2: Belowground *phpdr1* phenotypes

a, AM colonization of W138 and W138-*pdr1* roots 8 wpi with two AM fungi, means ± s.e.m. (N > 20). **b,** *In vitro* branching response of *G. margarita* 24 h after GR24 application (N = 5), root exudates of W138 (N = 17), W138-*pdr1* (N = 36) or 10% acetone (solvent, N = 5), means ± s.e.m.. **c,** Kinetics of *G. intraradices* colonization of W115xW138 (N = 25), W115xW138-*pdr1* (N = 25), V26 (N = 5) *dad1* (N = 5), means ± s.e.m. ($p < 0.001$ for all time points between mutants and wild-types). **d,** *P. ramosa* germination induced by GR24 (N = 3), root exudates of W115xW138 (WxW WT, N = 10), W115xW138-*pdr1* (WxW *pdr1*, N = 10), V26 (N = 4), *dad1* (N = 4) or water (N = 4), means ± s.e.m.. **e-h,** *G. intraradices* intracellular AM morphology 4 wpi in W115xW138 **(e)**; W115xW138-*pdr1* **(f)**; V26 **(g)** and *dad1* **(h)**. Scale bars = 20 µm. * = $p < 0.05$; *** = $p < 0.001$ in all panels.

W138-*pdr1* displayed a significantly reduced ability to accommodate *Gigaspora margarita* and *G. intraradices* (Fig 2.2a), two distantly related AM fungi with different growth strategies[4]. This finding indicated that PhPDR1 functions as a transporter of a stimulatory molecule involved in symbiosis with diverse AM fungal species. Indeed, root exudates from W138-*pdr1* showed reduced activity to stimulate hyphal branching of *G. margarita* in an *in vitro* bioassay (Fig. 2.2b). As these results suggested an involvement of SLs, W115xW138-*pdr1* root exudates were assessed for their ability to stimulate germination of the root-parasitic weed *Phelipanche ramose* (Orobanchaceae). As control, root exudates of *dad1* in the *Petunia* cultivar V26 were used. *DAD1* encodes

Carotenoid Cleavage Dioxygenase 8 (*CCD8*)[20], an orthologue of the established SL-biosynthetic genes *RMS1*, *MAX4* and *D10* in pea, *Arabidopsis* and rice, respectively[5,6]. The germination rate of *P. ramosa* was significantly lower with root exudates of W115xW138-*pdr1* and *dad1* compared to exudates of the corresponding wild types, which induced germination to a similar extent as GR24 (Fig. 2.2d). Comparable results were obtained with *phpdr1*-RNAi lines (Supplementary figure 2.5c). When inoculated with *G. intraradices*, W115xW138-*pdr1* lines displayed similarly retarded colonization rates as W138-*pdr1* and *dad1* (Fig. 2.2c). Despite the delay in AM development, neither W115xW138-*pdr1* nor *dad1* displayed any morphological aberrations in intracellular mycorrhizal structures (Fig. 2.2e-h). Intraradical hyphae and arbuscules appeared normal, suggesting that the quantitative differences in colonization are due to a decreased number of hyphal penetrations and retarded intraradical expansion of AM fungal colonies, rather than to defects in intracellular fungal development. Thus, the phenotype of *dad1* and *phpdr1* was distinct from AM mutants such as *pam1*[21], *str1*[22] or SYM-pathway mutants[4] that commonly exhibit aberrant AM fungal structures.

Detailed analysis of W138 root exudates resulted in the identification of the SL orobanchol (Supplementary figure 2.6). Orobanchol levels in *phpdr1* root exudates were significantly reduced compared to wild-type plants (Fig. 2.3a), whereas the levels in root extracts were not affected (Fig. 2.3b), indicating that *phdr1* is not defective in SL biosynthesis. Orobanchol was detectable neither in root exudates nor in root extracts of *dad1* confirming its supposed defect in SL biosynthesis (Fig. 2.3a-b). The finding, that only extraradical orobanchol levels were affected in *phdr1*, indicated that PhPDR1 functions as an SL export carrier.

PhPDR1-dependent SL transport was further explored in a heterologous system by constitutive over-expression of a *GFP::gPhPDR1* fusion in *Arabidopsis* Col-0, resulting in *PhPDR1*-OE lines (Supplementary fig. 2.7a-b). *Arabidopsis* does not form AM and exudes only minute quantities of SLs[23]. When grown on GR24-containing medium, *PhPDR1*-OE lines proved more tolerant to the deleterious effects of high SL concentrations on root elongation[24] than the wild type (Fig. 3c, Supplementary fig. 2.7c). Direct SL exudation was assessed by quantifying the efflux of pre-loaded ^{3}H-GR24 from roots either incubated at 4 °C, to monitor passive diffusion, or at 23 °C, enabling transporter-mediated efflux. After a period of 1 h *PhPDR1*-OE roots incubated at 23 °C retained significantly less GR24 compared to controls at 4 °C (Fig. 2.3d, Supplementary fig. 2.7d).

In agreement with this observation, more GR24 was found in root exudates of *PhPDR1*-OE lines at 23 °C. No significant differences were found for root extracts or root exudates of wild-type or vector control lines in either condition (Fig. 2.3d). These results together with the observed GR24-resistance phenotype of *PhPDR1*-OE are best explained with PhPDR1 acting as an SL exporter.

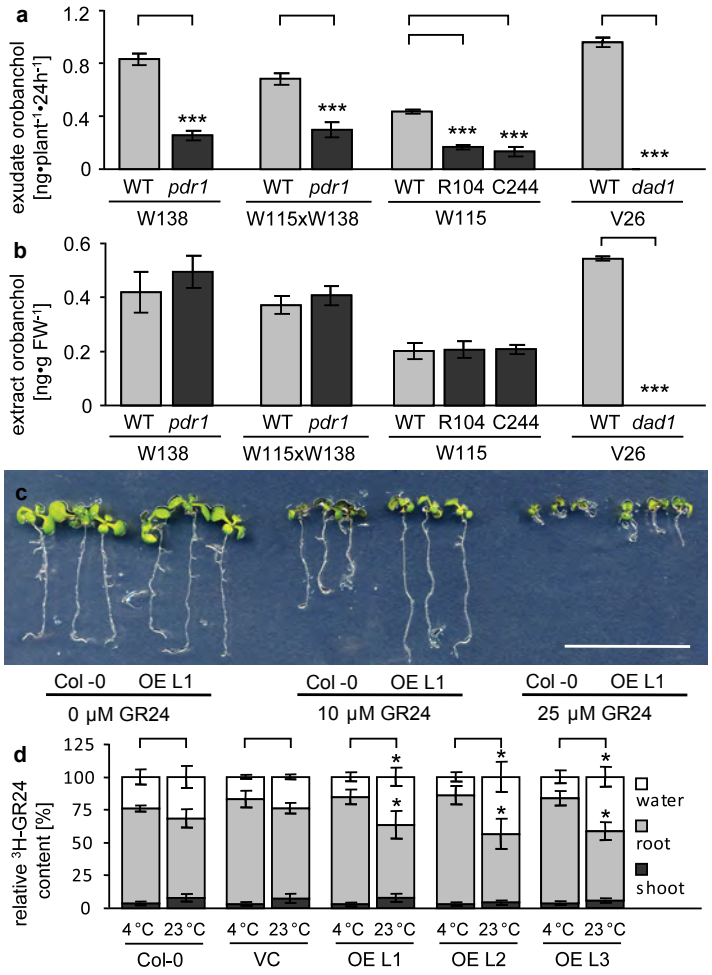

Figure 2.3: Orobanchol contents and PhPDR1-dependent GR24 tolerance and transport

a-b Orobanchol in the root exudates **(a)** and extracts **(b)** of *Phpdr1* lines, *dad1* and wild-types (N = 9), means ± s.e.m. **c,** Col-0 and *PhPDR1*-OE grown on 0, 10, and 25 µM GR24. Scale bar = 1 cm **d,** Export assay of ^{3}H-GR24 preloaded roots of Col-0, vector control (VC) and *PhPDR1*-OE lines (OE L1-3). Relative ^{3}H-GR24 in the medium (water), root and shoot, after 1 hour incubation at 4 °C and 23 °C; means ± s.e.m. (N = 8). * = $p < 0.05$; *** = $p < 0.001$ in all panels.

Taken together, our data suggest a role for PhPDR1 in SL secretion from HPC. We hypothesize that PhPDR1-mediated SL exudation under low phosphate conditions creates local rhizospheric gradients that guide AM hyphae to HPC, which are susceptible to hyphal penetration (Supplementary fig. 2.1), thereby initiating AM. The symbiotic phenotype of *phpdr1* and *dad1*, and the induction of *PhPDR1* in colonized root segments suggests that SLs may play an additional role in promoting sustained intercellular root

colonization, whereas intracellular stages (*e.g.* arbuscules) develop independently from SLs (Fig. 2.2e-h).

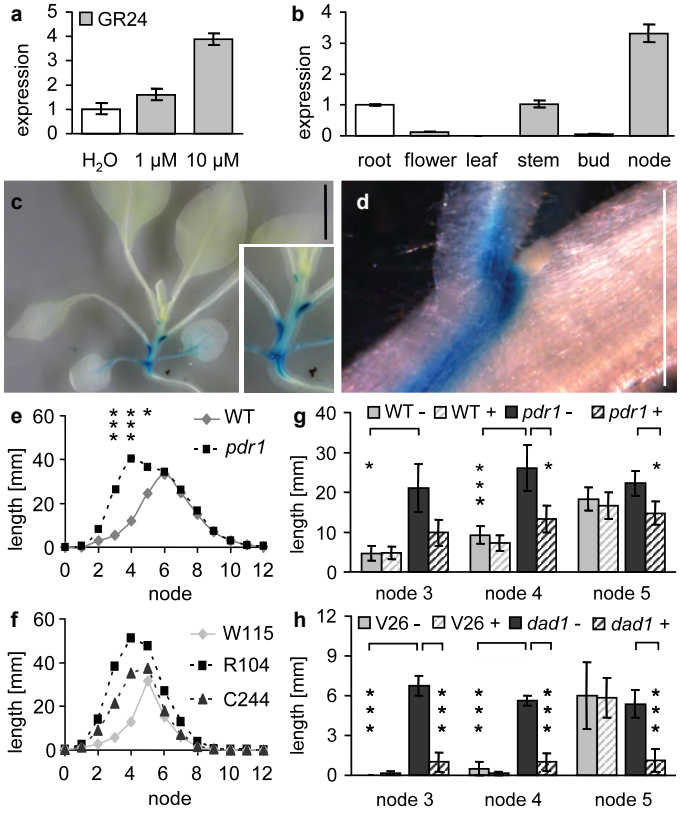

Figure 2.4: Aboveground *PhPDR1* expression and *phpdr1*-related branching phenotypes

a-b, qPCR for aboveground W115 GR24-treated tissue **(a)** and different organs **(b)**; means ± s.e.m. (N = 3). **c-d,** *pPhPDR1::GUS* in W115 at the four-leaf stage **(c)** and a node close-up **(d)** (white arrow: dormant axillary bud). Scale bars: b = 10 mm; d = 1 mm. **e-f**, Branch development 41 days post germination (dpg); means ± s.e.m.. Branch length for W115xW138 and W115xW138- *pdr1* (N = 110) **(e)** and for W115 and two *Phpdr1*-RNAi lines, R104 ($p < 0.001$ for node 3-4), and C244 ($p < 0.05$ for node 3) (N = 8) **(f)**. **g-h,** Effects of GR24 (striped) on branch development 34 dpg at node 3-5 for W115xW135 and W115xW138-*pdr1* (N = 24) **(g)**; V26 and *dad1* (N = 8) **(h)**; means ± s.e.m. * = $p < 0.05$; *** = $p < 0.001$ in all panels.

Recently it was demonstrated that SLs inhibit shoot branching[5,6]. Although some aspects of SL biosynthesis and signaling were unraveled[25], information about its mode of transport is scant. SLs are mobile within the xylem sap[23], but it is unknown how they are released from producing cells and whether directed cell-to-cell transport exists. SL biosynthesis is subject to direct negative feedback regulation[26]. Hence SL biosynthesis needs to be coordinated with export to prevent SL accumulation to levels that would restrict further production. Indeed, *PhPDR1* expression was found to be stimulated by exogenous application of GR24 (Fig. 2.1c and 2.4a), suggesting substrate-dependent induction, as previously observed for other *ABCG* subfamily[9,15] members.

Aboveground *PhPDR1* expression was largely confined to stem tissues, particularly the vasculature and nodal tissues adjacent to leaf axils (Fig. 2.4b, c). However, *PhPDR1*

expression was absent from dormant buds (Fig. 2.4d). This pattern is consistent with a function of PhPDR1 as an SL transporter. While SLs are xylem-mobile[23], a cellular transport system is required to deliver SL to dormant buds that are not yet connected to the xylem. This scenario is compatible with both current models for SL-dependent branching control[27]. According to the 'second messenger model', SLs are transported into the bud as a second messenger of auxin[28], hence cellular transport of SL in the axillary regions would be indispensable. In the 'auxin transport canalization-based model' SLs are thought to dampen polar auxin transport, resulting in the accumulation of auxin to levels that inhibit bud outgrowth[29]. SL could restrict auxin transport systemically and/or locally[27]. For both models local SL transport capacity near the axils would be in line with the inhibitory role of SL on branching. In W115xW138-*pdr1,* bud outgrowth was initiated sooner (Supplementary fig. 2.8a) and more vigorously than in the wild type, causing longer branches (Fig. 4e, Supplementary fig. 2.8e-h) at node three to five. This was also observed in *phpdr1*-RNAi lines (Fig. 2.4f). *Dad1* initiates branches from all nodes (Supplementary fig. 2.8d), and though branch elongation is retarded, it eventually produces full branches from every node[20,30]. At flowering time this results in a phenotype that is more pronounced than in any of the *phpdr1* mutants, which display final branch patterns that differ only marginally from the respective wild types (Supplementary fig. 2.8b-c, Supplementary table 2.1). Nevertheless the *phpdr1* branching phenotype appears SL-dependent and related to the *dad1* branching phenotype, as branch elongation in both mutants could be suppressed to near wild-type conditions by exogenous application of GR24 to the leaf axils (Fig. 2.4 g-h).

In conclusion, the identification of PhPDR1-mediated SL transport contributes to a more comprehensive view of SL modes of action. Understanding the underlying transport mechanisms is crucial for a holistic view of phytohormone function. SL transport has direct impact on phosphate-dependent control of AM levels and on control of shoot branching, where the integration of auxin and SL signaling seems partially achieved through reciprocal transport modulation. The mild branching phenotype of *phpdr1* relative to the SL biosynthetic mutant *dad1*[30] suggests that residual transport and/or locally produced SLs may compensate for defective SL transport in the shoot. However, AM development was affected to a similar degree in *phpdr1* and *dad1*, revealing that belowground SL transport and secretion relies primarily on PhPDR1.

2.3 Methods summary

All experiments with exception of transport assays were performed in accordance with established protocols. For transport, roots were pre-loaded with ^{3}H-GR24 for 2 h at 4 °C in dark, followed by quantification of ^{3}H-GR24 contents after 1 h incubation at 4 °C or 23 °C in light. Detailed methods and associated references can be found online as supplementary information.

2.4 Acknowledgements

We kindly thank: C. Gübeli for technical assistance; T. Gerats, S. Hörtensteiner, A. Osbourne, P. Schläpfer and C. Beveridge for comments. This study was funded by the Swiss National Foundation within the NCCR-Plant Survival, the project "ABC transporters involved in signaling" and by The Netherlands Organization for Scientific Research (NWO; VICI grant, 865.06.002 and Equipment grant, 834.08.001 to H.B.). H.B. was co-financed by the Centre for BioSystems Genomics (CBSG). E.M. would like to dedicate this work to U. Heber on occasion of his 80th birthday.

2.5 Author Contributions

T.K. wrote the manuscript, designed the project and carried out most of the experiments. W.K. and R.B. carried out the LC-MS/MS analysis and the *P. ramosa* biossays. J.S. performed qRT analysis and transport. J.S. and M.S. performed branching and GUS trials. L.B. analyzed *PhPDR1*-OE lines. J.B. sectioned material. D.R. investigated AM morphology. H.B. supervised the analytical part of the project. E.M. conceived and supervised the project. DR, EM, JS, WK and HB assisted in editing.

2.6 Reference List

1. Cook, C. E., Whichard, L. P., Turner, B., Wall, M. E. & Egley, G. H. Germination of Witchweed (Striga lutea Lour.): Isolation and Properties of a Potent Stimulant. *Science* 154, 1189-1190 (1966).
2. Yoder, J. I. & Scholes, J. D. Host plant resistance to parasitic weeds; recent progress and bottlenecks. *Current Opinion in Plant Biology* 13, 478-484 (2010).
3. Akiyama, K., Matsuzaki, K.-i. & Hayashi, H. Plant sesquiterpenes induce hyphal branching in arbuscular mycorrhizal fungi. *Nature* 435, 824-827 (2005).
4. Parniske, M. Arbuscular mycorrhiza: the mother of plant root endosymbioses. *Nat Rev Microbiol* 6, 763-775 (2008).
5. Umehara, M. *et al.* Inhibition of shoot branching by new terpenoid plant hormones. *Nature* 455, 195-200 (2008).
6. Gomez-Roldan, V. *et al.* Strigolactone inhibition of shoot branching. *Nature* 455, 189-194 (2008).
7. Petrasek, J. & Friml, J. Auxin transport routes in plant development. *Development* 136, 2675-2688 (2009).
8. Kuromori, T. *et al.* ABC transporter AtABCG25 is involved in abscisic acid transport and responses. *Proc Natl Acad Sci U S A* 107, 2361-2366 (2010).
9. Kang, J. *et al.* PDR-type ABC transporter mediates cellular uptake of the phytohormone abscisic acid. *Proc Natl Acad Sci U S A* 107, 2355-2360 (2010c).
10. Matusova, R. *et al.* The strigolactone germination stimulants of the plant-parasitic Striga and Orobanche spp. are derived from the carotenoid pathway. *Plant Physiol* 139, 920-934 (2005).
11. Verrier, P. J. *et al.* Plant ABC proteins--a unified nomenclature and updated inventory. *Trends Plant Sci* 13, 151-159 (2008).
12. Moons, A. Transcriptional profiling of the PDR gene family in rice roots in response to plant growth regulators, redox perturbations and weak organic acid stresses. *Planta* 229, 53-71 (2008).
13. Badri, D. V. *et al.* An ABC transporter mutation alters root exudation of phytochemicals that provoke an overhaul of natural soil microbiota. *Plant Physiol* 151, 2006-2017 (2009).
14. Sugiyama, A., Shitan, N. & Yazaki, K. Signaling from soybean roots to rhizobium: An ATP-binding cassette-type transporter mediates genistein secretion. *Plant Signal Behav* 3, 38-40 (2008).
15. Jasinski, M. *et al.* A plant plasma membrane ATP binding cassette-type transporter is involved in antifungal terpenoid secretion. *Plant Cell* 13, 1095-1107 (2001).
16. Hayward, A., Stirnberg, P., Beveridge, C. & Leyser, O. Interactions between auxin and strigolactone in shoot branching control. *Plant Physiol* 151, 400-412 (2009).
17. Hanlon, M. T. & Coenen, C. Genetic evidence for auxin involvement in arbuscular mycorrhiza initiation. *New Phytologist* 189, 701-709 (2011).
18. Sharda, J. N. & Koide, R. T. Can hypodermal passage cell distribution limit root penetration by mycorrhizal fungi? *New Phytologist* 180, 696-701 (2008).
19. Koes, R. *et al.* Targeted gene inactivation in petunia by PCR-based selection of transposon insertion mutants. *Proc Natl Acad Sci U S A* 92, 8149-8153 (1995).
20. Snowden, K. C. *et al.* The Decreased apical dominance1/Petunia hybrida CAROTENOID CLEAVAGE DIOXYGENASE8 gene affects branch production and plays a role in leaf senescence, root growth, and flower development. *Plant Cell* 17, 746-759 (2005).
21. Reddy D M R, S., Schorderet, M., Feller, U. & Reinhardt, D. A petunia mutant affected in intracellular accommodation and morphogenesis of arbuscular mycorrhizal fungi. *Plant J* 51, 739-750 (2007).
22. Zhang, Q., Blaylock, L. A. & Harrison, M. J. Two Medicago truncatula half-ABC transporters are essential for arbuscule development in arbuscular mycorrhizal symbiosis. *Plant Cell* 22, 1483-1497 (2010).
23. Kohlen, W. *et al.* Strigolactones are transported through the xylem and play a key role in shoot architectural response to phosphate deficiency in nonarbuscular mycorrhizal host Arabidopsis. *Plant Physiol* 155, 974-987 (2011).
24. Ruyter-Spira, C. *et al.* Physiological effects of the synthetic strigolactone analog GR24 on root system architecture in Arabidopsis: another belowground role for strigolactones? *Plant Physiol* 155, 721-734 (2011).

25. Beveridge, C. A. & Kyozuka, J. New genes in the strigolactone-related shoot branching pathway. *Curr Opin Plant Biol* 13, 34-39 (2010).

26. Mashiguchi, K. *et al.* Feedback-regulation of strigolactone biosynthetic genes and strigolactone-regulated genes in Arabidopsis. *Biosci Biotechnol Biochem* 73, 2460-2465 (2009).

27. Domagalska, M. A. & Leyser, O. Signal integration in the control of shoot branching. *Nat Rev Mol Cell Biol* 12, 211-221 (2011).

28. Brewer, P. B., Dun, E. A., Ferguson, B. J., Rameau, C. & Beveridge, C. A. Strigolactone Acts Downstream of Auxin to Regulate Bud Outgrowth in Pea and Arabidopsis. *Plant Physiol.* 150, 482-493 (2009).

29. Crawford, S. *et al.* Strigolactones enhance competition between shoot branches by dampening auxin transport. *Development* 137, 2905-2913 (2010).

30. Napoli, C. Highly Branched Phenotype of the Petunia dad1-1 Mutant Is Reversed by Grafting. *Plant Physiol* 111, 27-37 (1996).

2.7 Supplementary: Methods and Materials

1 Plant growth conditions: Petunia lines were grown at 16 h light, 60% relative humidity and 25 °C in soil (ED 73 Einheitserde, Einheitserde Werksverband e.V., Germany) or in clay granules (Oil Dry US Special, Damolin, Switzerland). Clay granules were supplemented once a week with half-strength Hoagland solution. For mycorrhization trials a mix of 40% [v/v] soil, 40% [v/v] clay granules, 10% [v/v] sand and 10% [v/v] mycorrhizal inoculum (AGRAUXINE, France) was used. Seeds were plated on medium containing 2.2 g L^{-1} MS (Duchefa, The Netherlands) and 15 g L^{-1} sucrose, supplemented with 9 g L^{-1} PHYTO AGAR (Duchefa, The Netherlands) at 16 h of light and 25 °C. For hormone treatment 14 d old W115 seedlings grown on plate were exposed for 24 h with final concentrations of 1 or 10 µM of the synthetic SL analog GR24 (Chiralix, The Netherlands), 10 µM abscisic acid (ABA) or 25 µM 1-naphthaleneacetic acid (NAA). For phosphate starvation 14 d old W115 seedlings were transferred to P-free plates for one week.

2 *PhPDR1* cloning strategy: *PDR*-specific 0.5 kb transcripts were amplified from W115 root cDNA five wpi with *G. intraradices* with: 5`-mgwatgactctdytkytkggacctcc and 5`-gyttcytytgncchcchgaaatwcc (5` region) or with: 5`-gggwaaracggwgtyagtggwgcw and 5`-ctcatnacaatdgcwgcwgctctwgc (3` region). Resulting 5` and 3` fragments were aligned and the deduced consensus primers 5`-tattgggacttgaaatttgtgccgatac and 5`-gctccactaacacccatcagagctgtc were used to amplify putative *PDR* fragments spanning 2.5 kb. 5` and 3` ends of *PhPDR1* were amplified using the SMART-RACE Amplification Kit (Clontech, Takara Bio Company, USA) with 5` RACE 5'-ctcgagtacattttctcggggaccttgg, nested 5` RACE 5'-ccatttcgtctccaacaatggtatcgg, 3` RACE 5'-gtcctcaagagtaggaagcatcactgcg and nested 3` RACE 5'-accgaggaccggcttgaactcttgagag.

To obtain the full length genomic sequence of *PhPDR1* a *Petunia axillaris* BAC library (kind gift of Chris Kuhlemeier, University of Bern) was screened with: 5'-tgccaatccttcatgatgtcagtgg and 5'-ccttctctctcctagacagctctgc. BACs were extracted from candidate clones via the Large Constuct Kit (Qiagen, Germany). Full length genomic *PhPDR1* was amplified from BAC with 5'-aattactagtatggagggtggtgaag and 5'-aattgcatgcctatcttttctggaaattaaatg cut with *Spe*I and *Sph*I and cloned into pUC18-GFP5sp[31]GFP5sp[1] via compatible *Nhe*I and *Sph*I restriction sites for GFP

localization studies[31]. For stable transformation the *CaMV 35S-GFP-gPhPDR1-terminator* cassette was cloned from pUC18-GFP5sp into pGreenII0179 vector[32] via the following strategy:

i) The *CaMV 35S* promoter from native pUC18-GFP5sp was cloned via *Xho*I and *Xma*I. ii) The terminator from the native pUC18-GFP5sp including the upstream *Sph*I site was cut with *Nhe*I and *Sac*I and inserted into *CaMV 35S*-pGreenII0179 via compatible *Xba*I and *Sac*I sites. iii) *GFP-gPhPDR1* was cut and cloned via *Xma*I and *Sph*1.

3 *PhPDR1* promoter GUS construct and GUS staining assay: A 1.8 kb *PhPDR1* promoter fragment was amplified using the Genome Walker Universal Kit (Clontech, Takara Bio Company, USA) with 5`-agttggaagtttctcaagtgcagccca and the nested 5`-ccctaaagagttcttcaccaccctccat. The fragment was cloned into the pGEM-T-Easy vector system (Promega, USA), reamplified with 5'-catgaagcttgcacccagaagaagattaggc and 5'-tcgatctagacacattaagaggaaagtaggtac and cloned into the pGPTV-Bar[33] vector system via *Hind*III and *Xba*I. Of the original T0 transformants eight lines were selected for further analysis. Segregating T1 individuals of all eight lines displayed comparable belowground and aboveground expression patterns at different developmental stages. Two of these lines were chosen for the in depth analysis presented in this work and all data presented was confirmed in both lines.

GUS-staining trials were performed as described previously[34]. After staining, samples were cleared for 24 h in 10% [w/v] KOH and stored in 70% [v/v] ethanol. For analysis of hypodermal passage cells, 5-bromo-6-chloro-3-indolyl β-D-glucuronide cyclohexylammonium salt was used for GUS staining and samples were cleared for 24 h in 10% [w/v] KOH before staining with trypan blue as described[18].

4 *PhPDR1* RNA interference constructs: Silencing of *PhPDR1*-specific transcripts was performed with the pKANNIBAL vector system[35]. Two constructs were designed, one targeting a highly variable region within the nucleotide binding domain 2 (NBD2) of *PhPDR1* (C-construct) and one targeting a part of the 3` end and the 3` UTR of *PhPDR1* (R-construct). The 148 bp C-fragment (ggaacgcaagcaaaaggggtgaggttattgaactat cttcgcttggaaagagctcttctgaaaaaggaaatgatgttcggcgaagtgcatcttccaggtcaatgtcctcaagagtaggaag catcactgcggctgatttgagcaagag) was amplified from W115 cDNA with 5'-cgatggatcctcgagggaacgcaa gcaaaaggg, containing *BamH*I and *Xho*I restriction sites and 5'-cgatatcgatggtaccctcttgctcaaatcagccgcagtga containing *Cla*I and *Kpn*I sites. The 411 bp R-fragment (gacattatatgactaattgcctcacaatttggagacatacaagacagacttgacacaaatg

agacagtggaacaattcatagagaatttctttgatttcaaacatgattttgtgggatatgttgctctcattcttgttgggatttctgtt cttttttctcttcatttttgcattttcaattaaaacatttaatttccagaaaagataggttggtccaggtatacacatgaaaagagcgtt tatcaagatatgtgtatattaggataataatataatctttctttttcctctttttttacttattgtggttttctcaagtttggaatagatag aaccaaaagtctgtactctgtatttaagaacaacttttgtacacattgttatgtattggagaagttatgagtatcttttg) was amplified with 5`cgatggatcctcgagacattatatggactaattgcc, containing *BamH*I and *Xho*I restriction sites and 5`cgatatcgatggtaccaaaagatactcataacttctcc containing *Cla*I and *Kpn*I sites. The resulting amplicons were cloned in sense and antisense direction in the two multiple cloning sites of pKANNIBAL. The pKANNIBAL RNAi cassette was excised from the vector backbone via *Not*I and transferred into the binary pGreenII0229 vector[32]. After stable transformation of W115 the extent of down-regulation was estimated via semi-quantitative PCR or RT-PCR.

5 Plant transformation: W115 was transformed as described[36]. Construct insertion was confirmed via PCR on genomic DNA with 5'-acggtccacatgccggtatatacgatg and 5'-gatggcatttgtaggagccaccttcc, targeting the *CaMV35S* promoter, or with 5'-gaattgatcagcgttggtgggaaagc and 5'-ggtaatgcgaggtacggtaggagttg, targeting the *GUS* gene.

Transient transformation of *Arabidopsis thaliana* Col-0 protoplasts was performed as described previously[31]. Arabidopsis plants were stably transformed as described[37]. T0 generation was selected for hygromycin resistance. Plants of the T1 generation were tested for hygromycin resistance and GFP expression.

6 Screening approach to identify transposon insertions in *PhPDR1:* A 3D-gDNA library (kind gift from Tom Gerats, Radboud University, Nijmegen) representing 10x10x10 (1,000) W138 individuals was screened for *dTph1* insertions in *PhPDR1* via a PCR-based method[38]. The entire genomic region of *PhPDR1* was scanned in contiguous steps covering less than 1 kb, using the *dTph1*-specific primer 5`-gaattcgctccgcccctg and a variety of ^{33}P-labeled gene-specific primers. The primer 5'-ccatttcgtctccaacaatggtatcgg yielded a positive result. Homozygosity PCRs were performed with the transposon flanking primers: 5'-tgccaatccttcatgatgtcagtgg and 5'-ccttctctctcctagacagctctgc. Homozygous *dTph1* insertion alleles were furthermore crossed into W115, the progeny selfed and the resulting offspring tested for homozygosity with the above mentioned primers. Transposon display analysis utilizing six W115xW138 and five W115xW138-*pdr1* lines was performed as described[39].

7 Mycorrhization trials: Subsets of mycorrhized roots were stained[40] and quantified for their level of colonization using the gridline intersect method[41]. Only the presence of clear intraradical structures such as coiled cortical hyphae, arbuscles and vesicles were scored as positively mycorrhized. A minimum of 200 intersecting root fragments per sample were investigated microscopically for intraradical AM structures. For trials involving W115xW1138 lines 5 individuals of 5 lines were analysed and the data presented as a pool of N = 25 (5 x 5). Double staining of colonized roots with propidium iodide and wheat germ agglutinin coupled to fluorescein isothiocyanate (WGA-FITC; Sigma-Aldrich) was performed as described[42].

8 Hyphal branching bioassays: Branching assays were performed as previously described[43] with pre-selected spores of *Gigaspora margarita* (AGRAUXINE, France). For production of the root exudates concentrate, *Petunia* lines were grown in clay granules and were transferred for 24 h to 0.1 L of a hydroponic solution containing 2 mM $CaCl_2$ and 2 mM KSO_4 and kept under constant aeration. The hydroponic solution was then run through a Sep-Pak Classic C18 Cartridge (Waters, Ireland) to adsorb hydrophobic root exudates. Exudates were eluted from the column using 2 ml of acetone and the eluent was dried over nitrogen. Dried exudates were re-dissolved in acetone and normalized according to root fresh weight (FW). Exudate equivalents of 10 mg root FW were used in each branching assay.

9 Transport assays and GR24 tolerance assays: Arabidopsis seeds of three independent *PhPDR1*-OE lines were surface-sterilized with 1% [v/v] bleach and 50% [v/v] ethanol and plated on media supplemented with 2.2 g L^{-1} MS, 1% [w/v] sucrose and 0, 10, or 25 µM GR24. After three days of stratification plants were moved to a 16 h light / 8 h dark regime and selected for GFP fluorescence after 3 days of growth. Root length was determined with the ImageJ 1.44 software (http://rsbweb.nih.gov/ij) after seven days and seedlings were moved to hygromycin-containing plates without sucrose to confirm the selection by GFP fluorescence.

For transport experiments, seeds were sterilized in the same way and plated on hygromycin-containing media. After three days of stratification and three days of growth, seedlings were checked for GFP fluorescence. After seven days, GFP- and hygromycin-positive plants were transferred to media supplemented with 2.2 g L^{-1} MS, 1% [w/v] sucrose and grown for another seven days. Three *PhPDR1*-OE lines, Col-0 and

a vector control line were incubated for 2 h in the dark at 4 °C with root tips submerged in 0.1% [w/v] Phyto agar (Duchefa Biochemie, The Netherlands) supplemented with 25 nM ^{3}H-GR24 (specific activity 40 Ci mmol^{-1}, American Radiolabeled Chemicals, USA). Subsequently, the plant roots were washed in ice-cold 1 mM $CaCl_2$ and incubated in 200 µl 0.1% Phyto agar. For each line, 50% of the plants were further kept for 1 h at 4 °C in the dark as diffusion control, the other 50% were shifted for 1 h to 23 °C to monitor transport. Subsequently, shoot, root and Phytoagar fractions were incubated for 30 min in 50 µl 24% [w/v] trichloroacetic acid at 23 °C. Tritium counts were determined in 3 ml Ultima Gold LSC cocktail (Perkin Elmer, USA) with Liquid Scintillation Analyzer Tri-Carb 2900TR (Packard BioScience, USA). Disintegrations per minute (dpm's) were computed into percentages for each fraction and normalized to tissue fresh weights.

10 RNA isolation, cDNA synthesis, semi-quantitative PCR and quantitative RT-PCR : RNA was isolated with the RNeasy Plant Mini Kit (Qiagen, Germany). Reverse transcription of RNA to cDNA was performed with the M-MLV reverse transcriptase (Promega, USA) and a polyT primer (Promega, USA).

PhPDR1 expression was quantified semi-quantitatively with 5'-gaaactgtggccgaaagg and 5'-gagttcaagccggtcct or 5`-aaatgctactacagtgcag and 5`-catataatgtccaggaaatggg. Tubulin 1 transcripts (*PhTUB*), partially amplified with 5`-cattggtcaagccggttattc and 5`-acccttgaagaccagtacagt served as housekeeping and loading control.

Samples were diluted 1:30, and 4 µl of the dilutions were added to each reaction well, serving as template for the reaction. Deionized water served as negative control for amplification. *PhPDR1* expression was quantified with 5'-cctgaggtttaccaaatggg and 5'-gatggtattggattggagca. *Glyceraldehyde 3-phosphate dehydrogenase* (*GapDH*) expression was quantified with 5'-gactggagaggtggaagagc and 5'-ccgttaagagctgggagaac. *GapDH* served as housekeeping gene for normalization because it was shown to be not regulated by hormonal treatments or mycorrhization (Didier Reinhardt, personal communication). Final primer concentrations of 50, 100, 200, and 300 nM were tested for cDNA amplification and melting behaviour in a range of 60 °C – 95 °C. Because no differences were recorded, the average concentration of 100 nM was chosen for further experiments. Primer efficiency was recorded with W115 root cDNA as template in a dilution range of 1:1 - 1:512, resulting in 94.42% for *PhPDR1* and 98.561% for *GapDH*. These values were taken into account in the calculations. Sybr Green PCR Master Mix (Applied Biosystems) was added to the samples to a final volume of 20 µl. For each

sample, three technical replicates were pipetted. RT-PCR was performed on a 7500 Fast Real-Time PCR System (Applied Biosystems) with the 7500 Software v2.0.4. The Quantitation-Comparative CT (ΔΔCT) was chosen as method[44], the PCR run was divided into three parts: 1. Hold stage (50 °C for 2 min, 95 °C for 10 min); 2. Cycling stage (95° C 15 s, 60 °C 1 min for 40 cycles); Melt Curve stage (95 °C 15 s, 60 °C to 95 °C 1 min, 95 °C 30 s, 60 °C 15 s). Relative differences were calculated as described[44,45]. Each experiment was performed for three biological replicates.

11 Isolation, identification and quantification of *Petunia* strigolactones: Plants were grown in a X-stream 20 aeroponic system (Nutriculture, UK) as previously described for *Medicago truncatula*[46]. From day eight until day twelve exudates were collected, pooled and root material sampled and stored at -80 °C for further analysis. *P. hybrida* root exudates and extracts were prepared and analyzed by ultra performance liquid chromatography coupled to tandem mass spectrometry (UPLC-MS/MS) as previously described for Arabidopsis[22]. Orobanchol was kindly provided by Koichi Yoneyama (Weed Science Center, Utsunomiya University, Japan). For trials involving W115xW1138 lines 3 individuals of 3 lines were analyzed and the data presented as a pool of N = 9 (3 x 3).

12 *Phelipanche ramosa* germination bioassay : Germination assays with *P. ramosa* seeds were conducted as reported previously[10]. Exudates were prepared as in **8**. GR24 at 1 and 0.1 nM and demineralised water were included as positive and negative controls. *P. ramosa* seeds were kindly provided by Maurizio Vurro (Istituto di Scienze delle Produzioni Alimentari, Italy). For trials involving W115xW1138 lines 2 individuals of 5 lines were analyzed and the data presented as a pool of N = 10 (5 x 2).

13 Trypan blue staining of hypodermal passage cells: Trypan blue stains of hypodermal passage cells in roots were performed as described[18].

14 Axillary branching trials: For a comparative analysis of lateral branch production in wild-type and *pdr1* backgrounds, plants were grown for 65 d in 0.55 L pots in soil as described in **1** and watered daily. Branch development was monitored at different time points in a binominal fashion (yes/no) in respect to the following parameters: bud length > 7 mm; full branch. Full branches were scored in accordance to a *Petunia* branch definition[47]. Furthermore branch length was scored as a continuous parameter. For trials involving W115xW1138 22 individuals of 5 lines were analyzed and the data

presented as a pool of N = 110 (5 x 22). For branch length trials in response to GR24 treatments three lines each of W115xW135, W115xW138-*pdr1*, V26, and *dad1* (kind gift of Kimberly Snowden, New Zealand Institute for Plant and Food Research Limited, Auckland) were grown on soil as described in **1**. From 25 - 40 dpg, plants were treated three times each week with 0 µM or 10 µM GR24 as described[6]. For trials involving W115xW1138 lines 8 individuals of 3 lines were analyzed and the data presented as a pool of N = 24 (3 x 8).

15 Statistical analyses: Depending on experimental set-ups and prerequisites Students t-tests, Fishers Exact tests or generalized linear models (GLM) with quasi-binominal error structures were applied using the "R" software (R Development Core Team 2009).

16 Bioinformatics: Analysis of DNA fragments and vector constructs was performed using VectorNTI (Invitrogen). Membrane topology of PhPDR1 was predicted using ConPredII (*bioinfo.si.hirosaki-u.ac.jp/~ConPred2/*). Phylogenetic analysis of PhPDR1 was performed using tools available at phylogeny.fr (www.phylogeny.fr). Alignments were performed with Multalin (***multalin****.toulouse.inra.fr/****multalin/***).

17 Robustness of data sets: All data sets presented were confirmed in at least two independent trials with similar set-ups and outcomes. For mycorrhization and branching trials individual pots were randomized to reduce positional effects and sample size was kept high to reduce background effects.

2.1 Supplementary: References

31. Meyer, A., Eskandari, S., Grallath, S. & Rentsch, D. AtGAT1, a high affinity transporter for γ-aminobutyric acid in *Arabidopsis thaliana*. *Journal of Biological Chemistry* 281 7197-7204 (2006).
32. Hellens, R. P., Edwards, E. A., Leyland, N. R., Bean, S. & Mullineaux, P. M. pGreen: a versatile and flexible binary Ti vector for Agrobacterium-mediated plant transformation. *Plant Mol Biol* 42, 819-832 (2000).
33. Becker, D., Kemper, E., Schell, J. & Masterson, R. New plant binary vectors with selectable markers located proximal to the left T-DNA border. *Plant Mol Biol* 20, 1195-1197 (1992).
34. Cervera, M. Histochemical and fluorometric assays for uidA (GUS) gene detection. *Transgenic Plants: Methods and Protocols* 286. 203-213 (2004).
35. Wesley, S. V. *et al.* Construct design for efficient, effective and high-throughput gene silencing in plants. *Plant J* 27, 581-590 (2001).
36. Lutke, W. K. Petunia (*Petunia hybrida*). *Methods Mol Biol* 344, 339-349 (2006).
37. Harrison, S. *et al.* A rapid and robust method of identifying transformed *Arabidopsis thaliana* seedlings following floral dip transformation. *Plant Methods* 2, 19 (2006).
38. Vandenbussche, M. & Gerats, T. TE-based mutagenesis systems in plants: a gene family approach. *Methods Mol Biol* 260, 115-127 (2004).
39. Van den Broeck, D. *et al.* Transposon Display identifies individual transposable elements in high copy number lines. *Plant J* 13, 121-129 (1998).
40. Vierheilig, H., Coughlan, A., Wyss, U. & Piche, Y. Ink and vinegar, a simple staining technique for arbuscular-mycorrhizal fungi. *Appl Environ Microbiol* 64, 5004-5007 (1998).
41. Giovannetti, M. & Mosse, B. An Evaluation of Techniques for Measuring Vesicular Arbuscular Mycorrhizal Infection in Roots. *New Phytologist* 84, 489-500.
42. Feddermann, N. *et al.* The PAM1 gene of petunia, required for intracellular accommodation and morphogenesis of arbuscular mycorrhizal fungi, encodes a homologue of VAPYRIN. *Plant J* 64, 470-481 (2010).
43. Nagahashi, G. & Douds, D. D. Rapid and sensitive bioassay to study signals between root exudates and arbuscular mycorrhizal fungi. *Biotechnology Techniques* 13, 893-897 (1999).
44. Livak, K. J. & Schmittgen, T. D. Analysis of relative gene expression data using real-time quantitative PCR and the 2(-Delta Delta C(T)) Method. *Methods* 25, 402-408 (2001).
45. Yuan, J. S., Reed, A., Chen, F. & Stewart, C. N. Statistical analysis of real-time PCR data. *BMC Bioinformatics* 7, 85 (2006).
46. Liu W. *et al.* Strigolactone biosynthesis requires the symbiotic GRAS-TYPE transcription NSP1 and NSP2. Plant Cell (2011) [epub ahead of print, doi: 10.1105/tpc.111.089771]
47. Snowden, K. C. & Napoli, C. A. A quantitative study of lateral branching in petunia. *Functional Plant Biology* 30, 987-994 (2003/01/01).

2.1 Supplementary: Figures

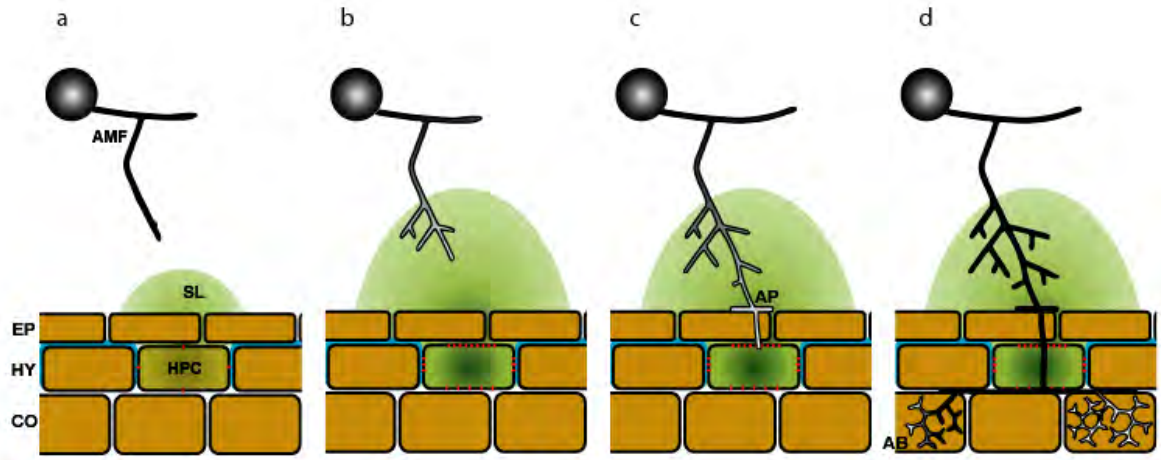

Supplementary Figure 2.1: Model for PhPDR1-dependent strigolactone (SL) exudation from hypodermal passage cells (HPC) and its effect on arbuscular mycorrhizal fungi (AMF)

Colonization rates of AMF reciprocally correlate with the phosphate status of the plant and it was suggested that differential exudation of SLs are partly responsible[1]. SL exudation has been demonstrated to be enhanced under low phosphate availability, when the plant benefits most from the symbiosis with AMF[2]. Extraradical AMF hyphal proliferation depends on SL perception within the rhizosphere that signals the vicinity of a susceptible mycotrophic root[3]. In absence of SLs AMF remain dormant and interaction is less likely to occur. Situated below the epidermis (EP), the hypodermis (HY) defines the outer boundary of the root cortex (CO). In plant species with a dimorphic hypodermis, hypodermal passage cells constitute single un-suberized cells in a matrix of suberized (blue layer) hypodermal cells[4]. In order to reach the cortex, where arbuscle formation and nutrient exchange takes place, AMF exclusively pass through HPCs[5]. a, Under phosphate sufficient conditions, SL production is low, which, in concomitance with low *PhPDR1* expression (red ellipses = PhPDR1), results in levels of SL exudation (green gradient) from HPCs that are not sufficient to activate AMF hyphal metabolism. b, Under phosphate deficient conditions SL biosynthesis and *PhPDR1* expression are up-regulated, resulting in increased SL exudation from HPCs. AMF metabolism is activated and vigorous hyphal branching and proliferation is induced. c, Guided by the SL gradient, AMF encounter the root surface, form appressoria (AP) in the proximity of HPCs and penetrate the epidermal layer. d, After successful cortical entry via penetration of HPCs, AMF can expand laterally and intracellularly within the cortex and form symbiotic structures such as arbuscles (AB).

References:

1. Balzergue, C., Puech-Pagès, V., Bécard, G. & Rochange, S. F. The regulation of arbuscular mycorrhizal symbiosis by phosphate in pea involves early and systemic signalling events. *Journal of Experimental Botany* 62(3), 1049-1060 (2011)

2. Lopez-Raez, J. A. *et al.* Tomato strigolactones are derived from carotenoids and their biosynthesis is promoted by phosphate starvation. *New Phytol* 178, 863-874 (2008a).

3. Akiyama, K., Matsuzaki, K.-i. & Hayashi, H. Plant sesquiterpenes induce hyphal branching in arbuscular mycorrhizal fungi. *Nature* 435, 824-827 (2005).

4 Enstone, D., Peterson, C. & Ma, F. in *Journal of Plant Growth Regulation* 335-351 (Springer New York, 2003).

5. Sharda, J. N. & Koide, R. T. Can hypodermal passage cell distribution limit root penetration by mycorrhizal fungi? *New Phytologist* 180, 696-701 (2008).

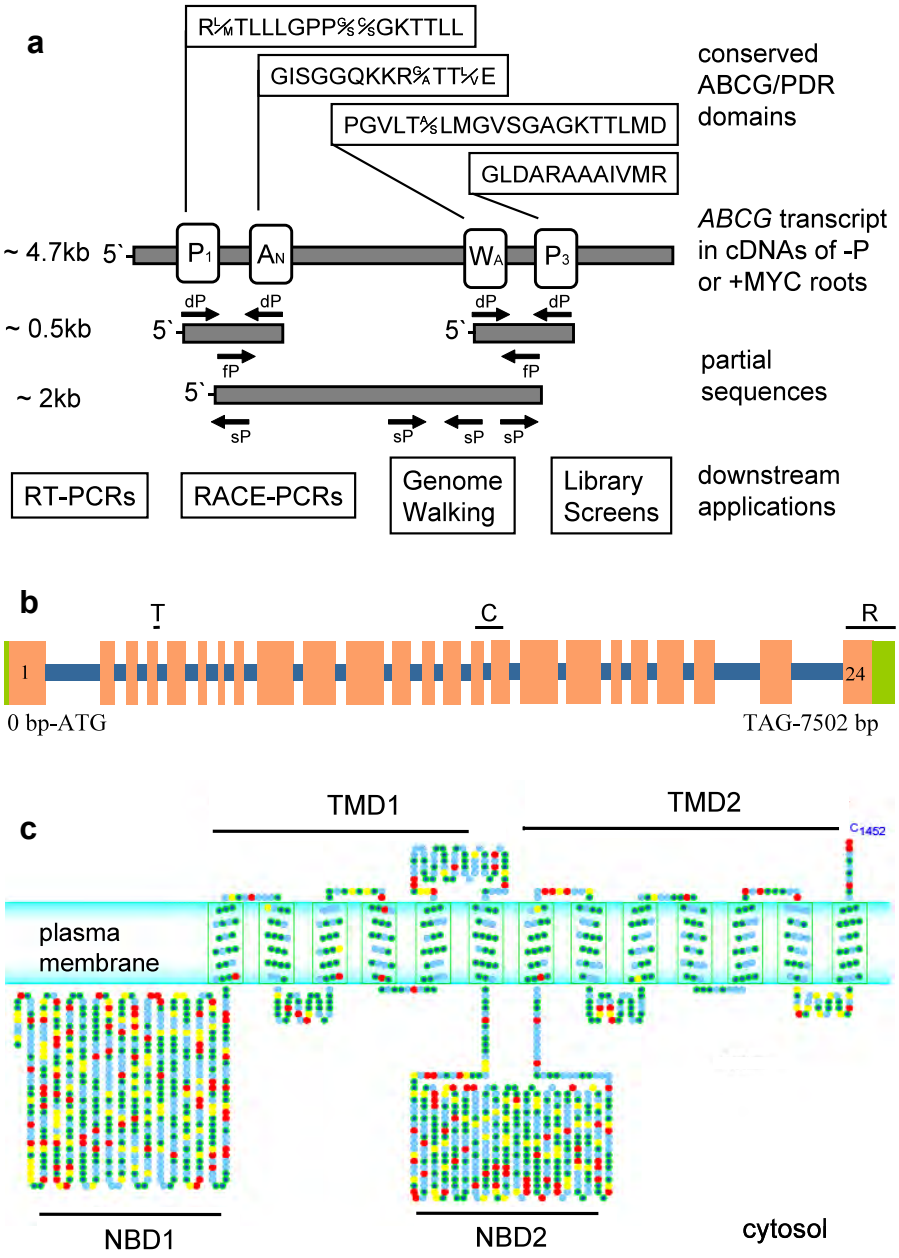

Supplementary Figure 2.2: Screening approach to identify *ABCG/PDR* candidate genes, genomic structure of *PhPDR1* and predicted protein topology of PhPDR1

a, Degenerate primer approach for amplification of ABCG/PDR candidate sequences from the cDNA of phosphate starved (-P) or 8 wpi *G. intraradices*-colonized (+MYC) roots of W115. Conserved ABCG/PDR domains were taken from Van den Brule *et al.*[1]. P1 = PDR signature 1, AN = N-terminal ABC signature, WA = Walker A motif, P3 = PDR signature 3, dP = degenerate primer, fP = subfamily specific primer, sP = sequence specific primer. **b,** Genomic structure of *PhPDR1* depicting exons (orange), introns (blue) and UTRs (green). T indicates *dTph1* insertion site. C and R indicate non-conserved target regions of RNA interference constructs. qRT primers were specific for C and R region. **c,** Putative transmembrane topology of PhPDR1, featuring a PDR-specific reverse orientation with an initial cytosolic nucleotide binding domain (NBD1) followed by a transmembrane domain (TMD1). TMD1 is followed by NBD2 and TMD2. Hydrophobic (green circles), hydrophilic (blue circles), positively charged (red circles) and negatively charged (yellow circles) residues are depicted.

References:

1. van den Brule, S. & Smart, C. C. The plant PDR family of ABC transporters. *Planta* 216, 95-9106 (2002).

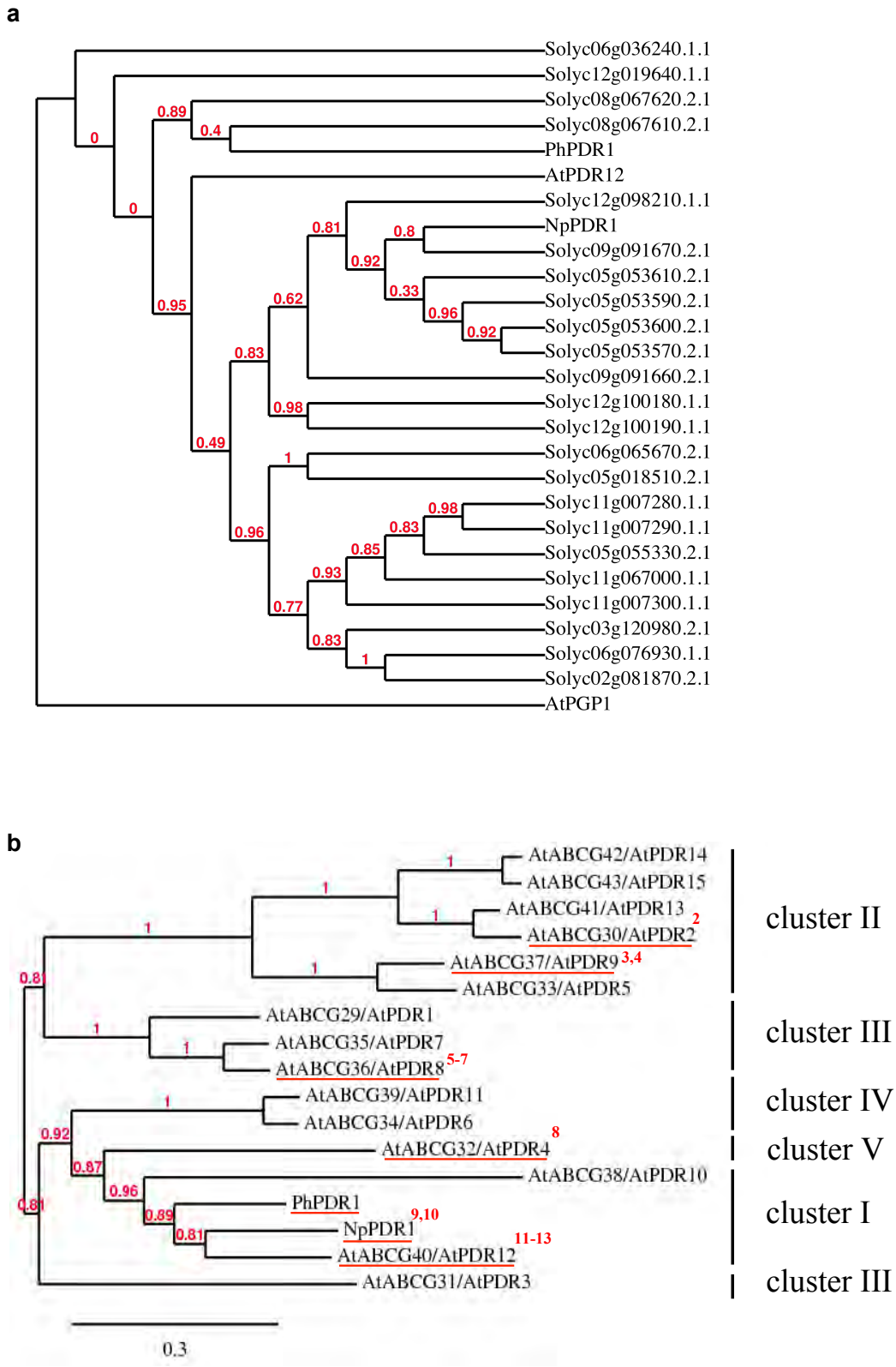

Supplementary Figure 2.3: Predicted ABCG/PDR family of *Solanum lycopersicum* (tomato) and phylogenetic position of PhPDR1 in relation to the Arabidopsis full size ABCG/PDR subfamily of ABC transporters

Legend on the following page

a, Maximum likelihood-based phylogenetic tree for putative Solanum lycopersicum full-size ABCG/PDR proteins based on a BLAST search on the http://mips.helmholtz-muenchen.de/plant/tomato/ database. The ABCG members AtABCG40/AtPDR12 (BK001011), NpPDR1 (CAC40990) and PhPDR1 (JQ280944) are included. The *Arabidopsis* auxin transporter AtABCB1/AtPGP1 (Q9ZR72) was used to root the tree. Numbers in red at branches indicate nonparametric bootstrap values. **b,** Maximum likelihood-based phylogenetic position of PhPDR1 in relation to the Arabidopsis full-size ABCG/PDR subfamily of ABC transporters and NpPDR1. Numbers in red at branches indicate nonparametric bootstrap values. PDR-specific clusters are indicated as previously defined[1]. Proteins underlined in red have been characterized on a functional level[2-13]. Accessions: AtPDR1 (BK001001), AtPDR2 (BK001000), AtPDR3 (BK001002), AtPDR4 (BK001003), AtPDR5 (BK001004), AtPDR6 (BK001005), AtPDR7 (BK001006), AtPDR8 (BK001007), AtPDR9 (BK001008), AtPDR10 (BK001009), AtPDR11 (BK001010), AtPDR12 (BK001011), AtPDR13 (BK001012), AtPDR14 (BK001013), AtPDR15 (BK001014), NpPDR1 (CAC40990), PhPDR1 (JQ280944)

References:

1. Crouzet, J., Trombik, T., Fraysse, A. S. & Boutry, M. Organization and function of the plant pleiotropic drug resistance ABC transporter family. *FEBS Lett* 580, 1123-1130 (2006).
2. Badri, D. V. *et al.* An ABC transporter mutation alters root exudation of phytochemicals that provoke an overhaul of natural soil microbiota. *Plant Physiol* 151, 2006-2017 (2009).
3. Ito, H. & Gray, W. M. A gain-of-function mutation in the Arabidopsis pleiotropic drug resistance transporter PDR9 confers resistance to auxinic herbicides. *Plant Physiol* 142, 63-74 (2006).
4. Ruzicka, K. *et al.* Arabidopsis PIS1 encodes the ABCG37 transporter of auxinic compounds including the auxin precursor indole-3-butyric acid. *Proc Natl Acad Sci U S A* 107, 10749-10753 (2010).
5. Kobae, Y. *et al.* Loss of AtPDR8, a plasma membrane ABC transporter of Arabidopsis thaliana, causes hypersensitive cell death upon pathogen infection. *Plant Cell Physiol* 47, 309-318 (2006).
6. Stein, M. *et al.* Arabidopsis PEN3/PDR8, an ATP binding cassette transporter, contributes to nonhost resistance to inappropriate pathogens that enter by direct penetration. *Plant Cell* 18, 731-746 (2006).
7. Kim, D.-Y., Bovet, L., Maeshima, M., Martinoia, E. & Lee, Y. The ABC transporter AtPDR8 is a cadmium extrusion pump conferring heavy metal resistance. *Plant J* 50, 207-218 (2007).
8. Bessire, M. *et al.* A Member of the PLEIOTROPIC DRUG RESISTANCE Family of ATP Binding Cassette Transporters Is Required for the Formation of a Functional Cuticle in Arabidopsis *The Plant Cell Online* 23 1958-1970 (2011).
9. Jasinski, M. *et al.* A plant plasma membrane ATP binding cassette-type transporter is involved in antifungal terpenoid secretion. *Plant Cell* 13, 1095-1107 (2001).
10. Stukkens, Y. *et al.* NpPDR1, a pleiotropic drug resistance-type ATP-binding cassette transporter from Nicotiana plumbaginifolia, plays a major role in plant pathogen defense. *Plant Physiol* 139, 341-352 (2005).
11. Campbell, E. J. *et al.* Pathogen-responsive expression of a putative ATP-binding cassette transporter gene conferring resistance to the diterpenoid sclareol is regulated by multiple defense signaling pathways in Arabidopsis. *Plant Physiol* 133, 1272-1284 (2003).
12. Lee, M., Lee, K., Lee, J., Noh, E. W. & Lee, Y. AtPDR12 contributes to lead resistance in Arabidopsis. *Plant Physiol* 138, 827-836 (2005).
13. Kang, J. *et al.* PDR-type ABC transporter mediates cellular uptake of the phytohormone abscisic acid. *Proc Natl Acad Sci U S A* 107, 2355-2360 (2010c).

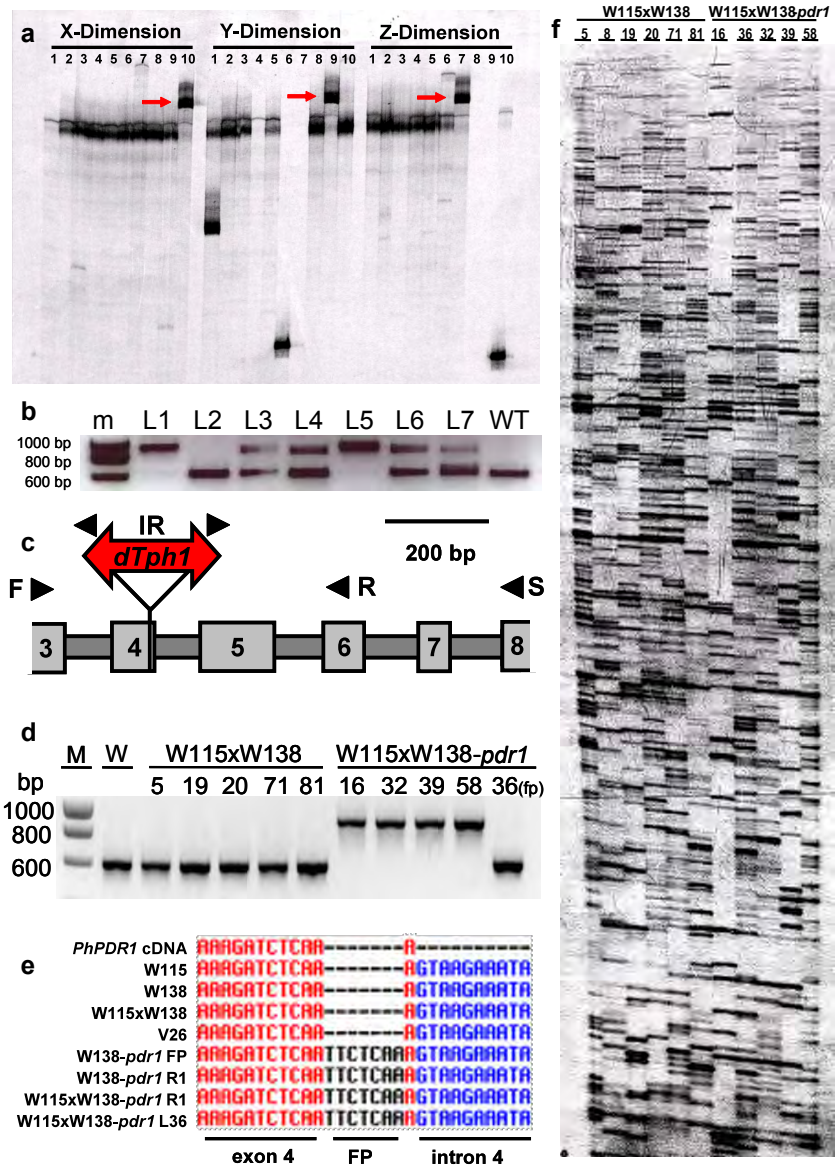

Supplementary Figure 2.4: Genetic analysis of a *dTph1* insertion in *PhPDR1* in the W138 and the W115xW138 background

a, PCR-based screen of a three dimensionally arranged gDNA library of 10x10x10 W138 individuals for *dTph1* insertion in *PhPDR1*. Amplification with a *dTph1*-specific primer **(IR in c)** and a *PhPDR1*-specific primer **(S in c)** resulted in one specific band per dimension (red arrows), giving coordinates for a single W138 individual (X-10, Y-9, Z-7). **b,** Homozygosity PCR with transposon flanking primers identifying homozygous *PhPDR1 dTph1* insertion mutants (L1 and L5), heterozygous individuals (L3, L4, L6, and L7) and a putative homozygous *PhPDR1* wild type (L2) in the selfed progeny of the retrieved candidate. W115 (WT) served as a wild type control (m, marker lane). Sequencing of L2 revealed homozygosity for a 7 bp target site duplication-derived footprint allele **(W138-*pdr1* FP in e). c,** Schematic of *dTph1* insertion in exon 4 of *PhPDR1*. Black triangles indicate positions of primers used in the screen (IR and S) and for homozygosity PCR (F and R). **d,** Homozygosity PCR for *dTph1* insertion on the selfed progeny of W115 crosses with W138-*pdr1* **(primers F and R in b).** M corresponds to marker lane and W115 (W) served as control. Five lanes correspond to homozygous *PhPDR1* wild type lines (W115xW138), four lanes correspond to homozygous *PhPDR1 dTph1* insertion lines (W115xW138-*pdr1*) and one lane corresponds to a homozygous *PhPDR1* footprint allele (36 (fp)). **e,** Alignment of the footprint flanking region of W115 cDNA with *PhPDR1* wild type and *PhPDR1* footprint alleles in various *P. hybrida* backgrounds. (FP = footprint, R = somatic revertant). **f,** Transposon display of *dTph1* insertions in the background of six W115xW138 and five W115xW138-*pdr1* lines. Line 8 was not used for phenotypic analysis in this study. Bands that co-segregate strictly with the presence or absence of the *PhPDR1 dTph1* insertion or the respective phenotypes indicate *dTph1* insertions that could also be responsible for the observed phenotypes. Note that the *dTph1* insertion in *PhPDR1* cannot be detected on this display due to an expected band size of 1.7 kb that is beyond the resolution of the display.

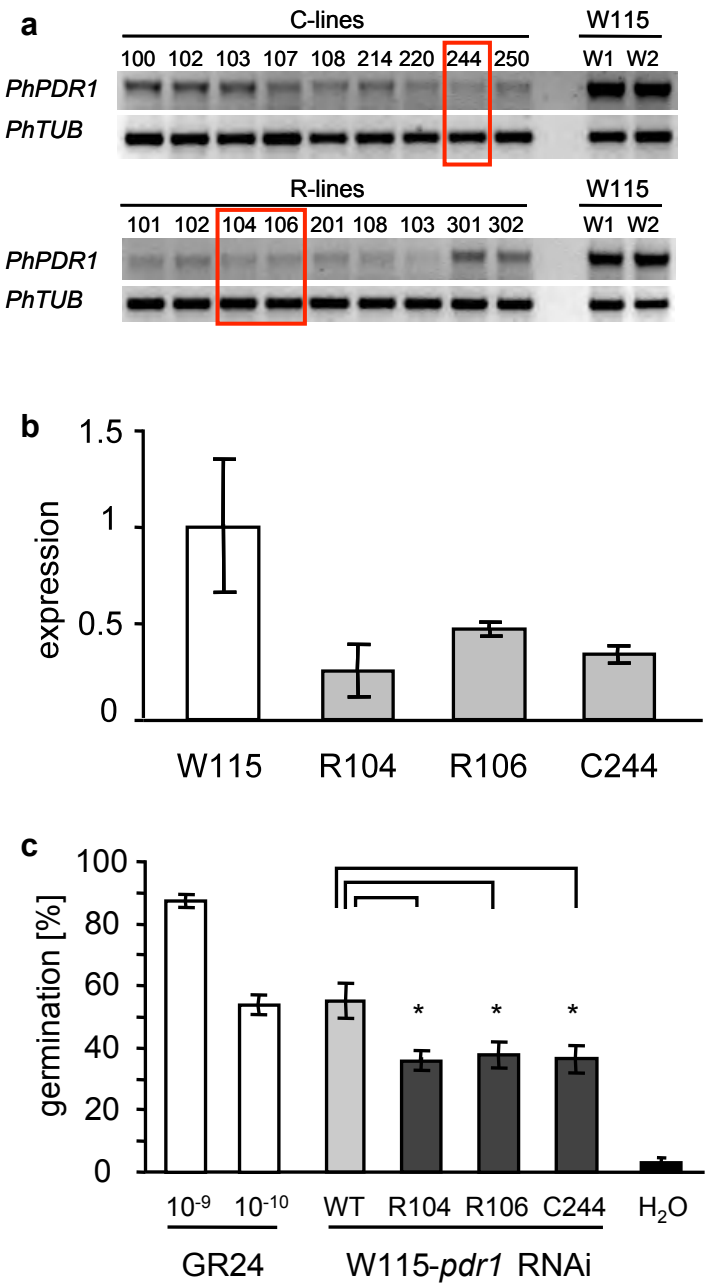

Supplementary Figure 2.5: *PhPDR1* transcript quantification and assessment of stimulation of germination of *Ph. ramosa* for *phpdr1*-RNAi lines

a, Semiquantitative RT-PCR for *PhPDR1* transcript in seedlings of W115 lines either transformed with a silencing construct targeting a non-conserved region in the center of *PhPDR1* (C-lines) or the 3` end and 3` untranslated region of *PhPDR1* (R-lines). Two untransformed W115 individuals (W1 and W2) served as wild-type controls and tubulin (*PhTub*) served as loading control. Red boxes indicate lines used in this study. **b,** qRT PCR targeting *PhPDR1* transcript in W115 seedlings and selected RNAi lines. Data was normalized against *Glyceraldehyde 3-phosphate dehydrogenase* and W115 *PhPDR1* expresssion. Data are means ± s.e.m. (N = 3). **c,** Germination of *P. ramosa* induced by root exudates from W115 and three independent *PhPDR1* silenced lines (N = 4). GR24 at 1 and 0.1 nM served as positive control and water (H_2O) served as negative control (N = 3). Data are means ± s.e.m. * = $p < 0.05$.

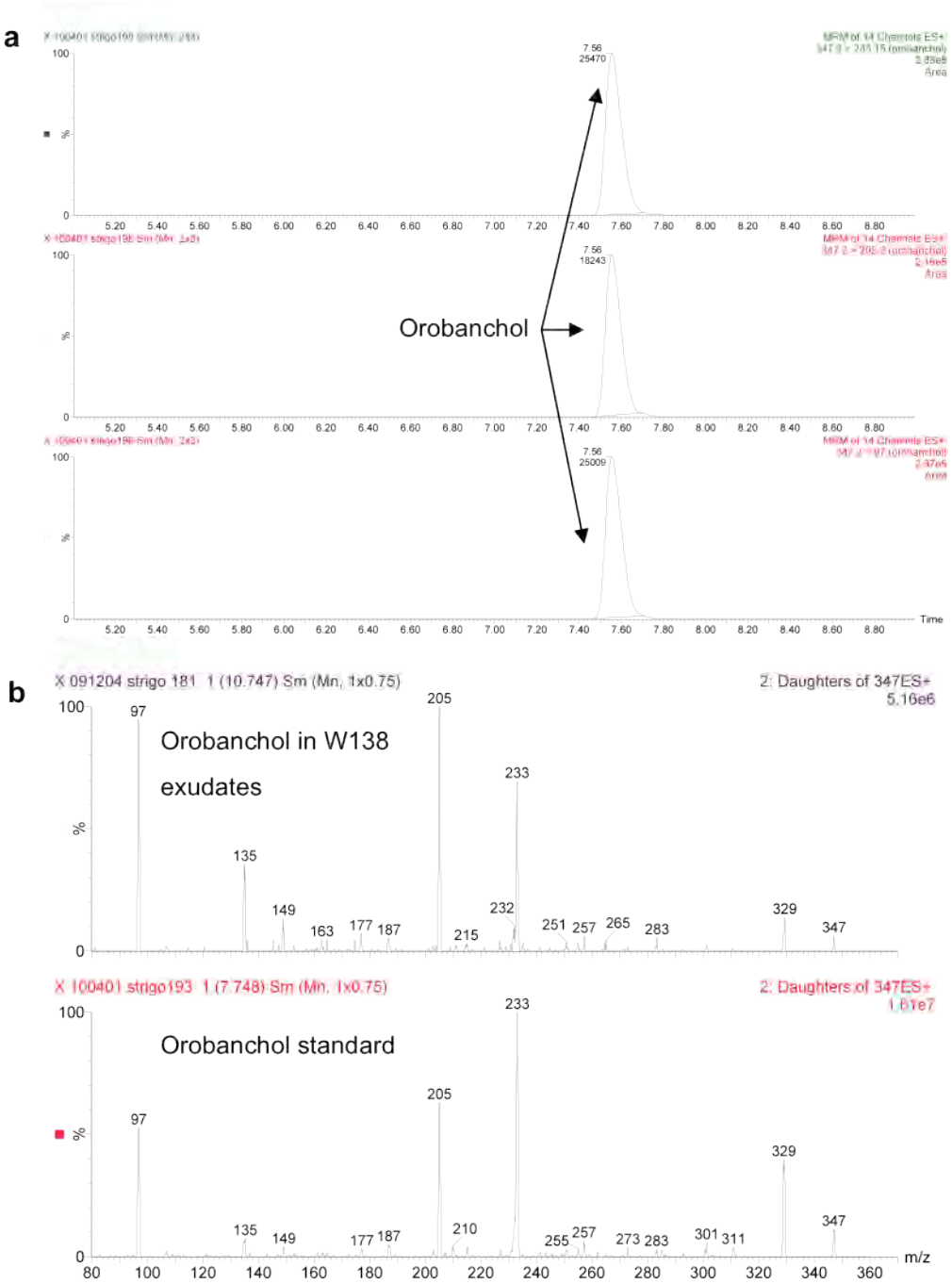

Supplementary Figure 2.6: Orobanchol identification in *Petunia hybrida*

a, MRM-LC-MS/MS chromatogram of W138 exudates showing transitions 347 > 233, 347 > 205 and 347 > 96.8, for orobanchol. **b,** full daughter ion scan MS/MS spectrum of orobanchol in W138 exudates and orobanchol standard.

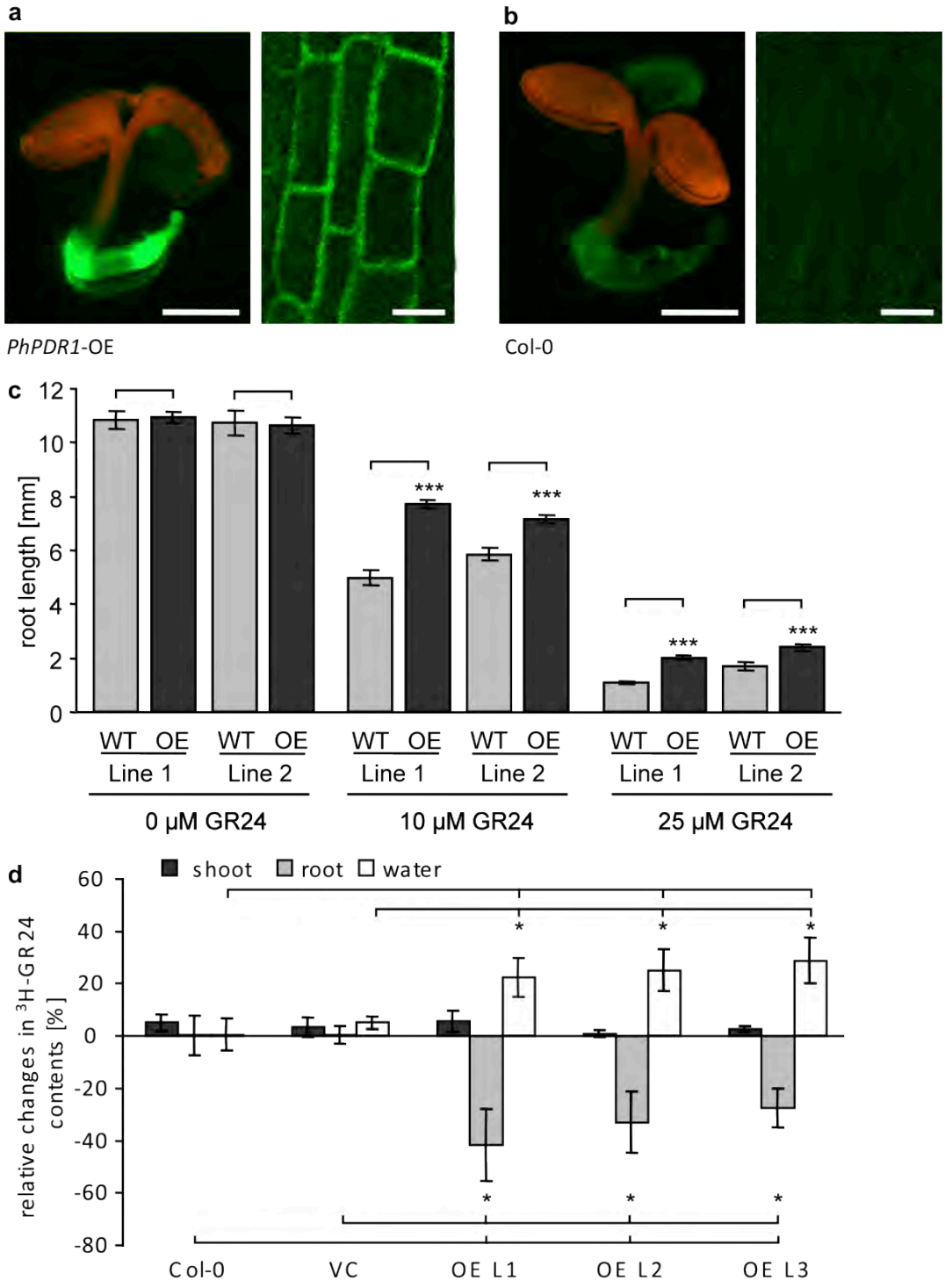

Supplementary Figure 2.7: Evaluation of *GFP::gPhPDR1* (*PhPDR1*-OE) lines

a-b, GFP signal in whole seedlings (left panels, Scale bar = 1 mm) and epidermal root cells (right panels, Scale bar = 10 µm) of a *GFP::gPhPDR1* over-expression line (*PhPDR1*-OE) **(a)** and autofluorescence in Col-0 **(b)**. **c,** Quantification of root length of two independent *PhPDR1*-OE lines (dark grey) (N > 36) and segregating wild types (grey) (N > 12) germinated and grown for 7 days on 0, 10 or 25 µM GR24. *** = $p < 0.001$. **d,** Transport-related changes in GR24 contents in shoots, roots and root exudates. GR24 contents of metabolically inactive tissues incubated for 1 h at 4 °C were subtracted from contents of metabolically active tissues incubated for 1 h at 23 °C. The differences are displayed in percent analogous to the graph in Fig. 3d. * = $p < 0.05$.

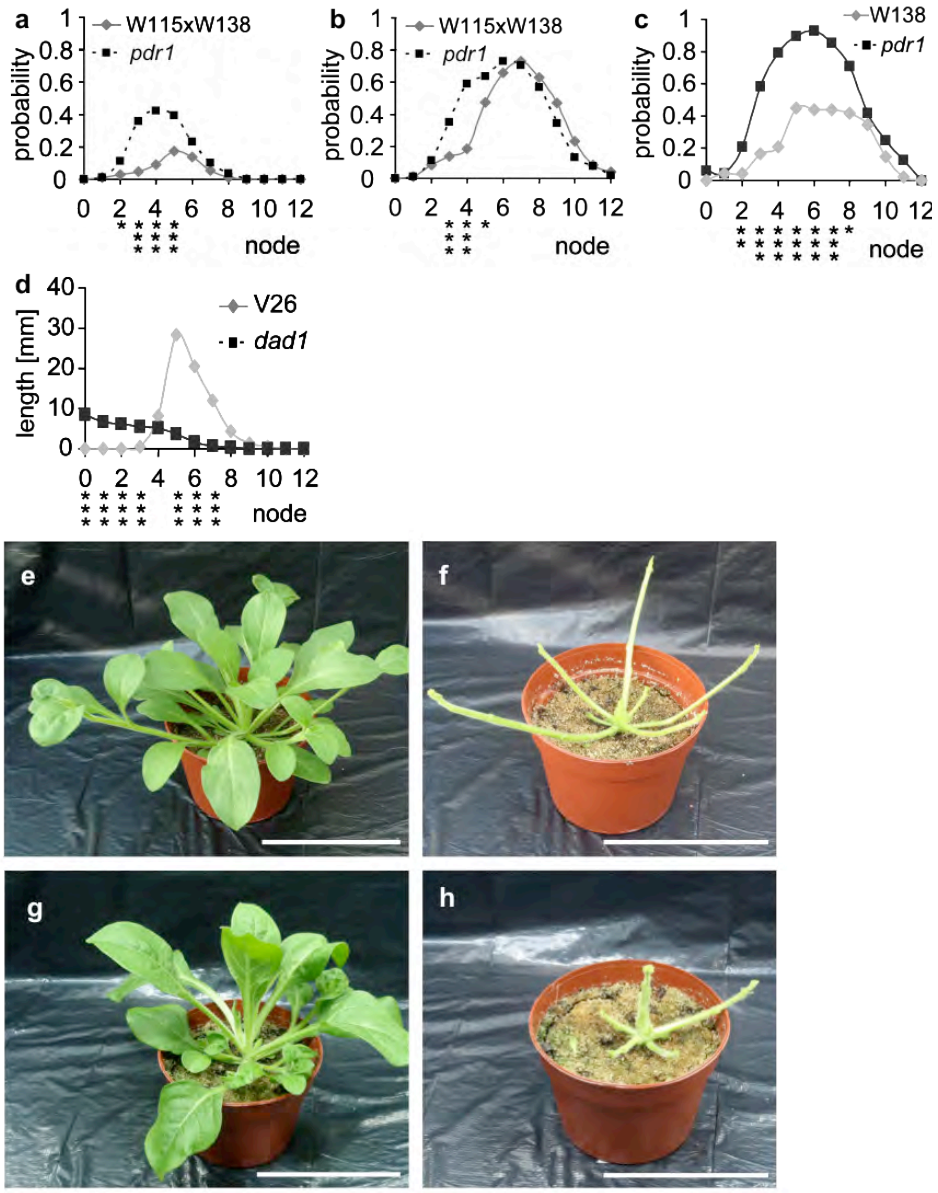

Supplementary Figure 2.8: Aboveground phenotype of *pdr1* and *dad1* lines

a-b, Analysis of branch development of W115xW138 (grey diamonds) and W115xW138-*pdr1* (black squares). Probability at a given node to produce a bud of more than 7 mm 29 dpg **(a)** and a fully developed branch at flowering time 55 dpg **(b)**. Data are means ± s.e.m. (N = 110 (5 x 22)). **c,** Probability at a given node to produce a fully developed branch for W138 and W138-*pdr1* at flowering time 64 dpg. Data are means ± s.e.m. (N = 49). Note: The comparably stronger branching phenotype of W138-*pdr1* over W115xW138-*pdr1* is attributed to the transposon backgrounds of W138 that are assumed to cause pleiotropic aboveground effects. These result in a relatively weaker branching performance of W138 and stronger response to lack of *PhPDR1*-dependent SL distribution in W138-*pdr1*. These effects are largely compensated in the W115xW138 backcrosses, which show a near identical branching phenotype as the *pdr1*-RNAi lines (Fig. 4e-f; Supplementary table 1). We believe that backcrosses and *phpdr1*-RNAi reflect the aboveground effects of *PhPDR1* impairments more adequately. As opposed to the complex trait of branching, SL exudation is dominantly PhPDR1-controlled, causing similar effects in all *phpdr1* backgrounds. **d,** Branch length at a given node for V26 and *dad1* 35 dpg. Data are means ± s.e.m. (N = 8) **e-h**, Visible branch length phenotype 41 dpg of a W115xW138-*pdr1* individual **(e)**, stripped of its leaves **(f)** as compared to a W115xW138 individual **(g)**, stripped of its leaves **(h)**. Scale bars = 10 cm.

	WT	*pdr1*	*pdr1*/WT	P-value	dpg
W138	2.7 +/- 0.28	5.9 +/- 0.24	2.19	>0.001 (n=49)	64
W115xW138	3.8 +/- 0.02	4.3 +/- 0.02	1.13	>0.001 (n=110)	58
W115 (RNAi)	3.6 +/- 0.37	4.2 +/- 0.38	1.17	n.s. (n=15)	58
	WT	*dad1*	*dad1*/WT		
V26	3.4 +/- 0.48*	9.9 +/- 0.99*	2.91	>0.001 (n=7)*	70

Supplementary Table 2-1: Number of branches at flowering time in *pdr1* and *dad1* lines

Total number of full branches of *pdr1* mutants and the respective wild types at flowering time were scored according to a *Petunia* branch definition[1]. For comparison full branch numbers of V26 and *dad1* as presented by Napoli[2] (*) are shown. dpg = days post germination; Note: The comparably stronger branching phenotype of W138-*pdr1* over W115xW138-*pdr1* is attributed to the transposon backgrounds of W138 that are assumed to cause pleiotropic aboveground effects. These result in a relatively weaker branching performance of W138 and stronger response to lack of *PhPDR1*-dependent SL distribution in W138-*pdr1*. These effects are largely compensated in the W115xW138 backcrosses, which show a near identical branching phenotype as the *pdr1*-RNAi lines (Fig. 4e-f). We believe that backcrosses and *phpdr1*-RNAi reflect the aboveground effects of *PhPDR1* impairments more adequately.

References:

1. Snowden, K. C. & Napoli, C. A. A quantitative study of lateral branching in petunia. *Functional Plant Biology* 30, 987-994 (2003).

2. Napoli, C. Highly Branched Phenotype of the Petunia dad1-1 Mutant Is Reversed by Grafting. *Plant Physiol* 111, 27-37 (1996).

3 The asymmetric and cell-specific localization of PhPDR1 regulates the polar transport of the phytohormone strigolactone in plant roots.

Joëlle Sasse[1], Sibu Simon[2], Christian Gübeli[1], Jiři Friml[2], Enrico Martinoia[1] and Lorenzo Borghi[1]

[1] Institute of Plant Biology, University of Zürich, Zürich, Switzerland

[2] Institute of Science and Technology Austria, Klosterneuburg, Austria

Short title: PhPDR1 asymmetric localization regulates strigolactone polar transport

submitted to Cell Reports

3.1 Summary

Strigolactones are phytohormones playing major roles in shaping plant architecture and in promoting plant-mycorrhiza symbiosis. Much was discovered on strigolactone function and biosynthesis, still little is known on strigolactone transport. Here we show that the recently discovered strigolactone transporter from *Petunia axillaris* (PaPDR1) exhibits a cell-type, specific polar localization. In root tips PaPDR1 is co-expressed with the strigolactone biosynthetic gene *DAD1 (CCD8)* and is localized at the apical ends of root cortex cells, where it catalyzes cell-to-cell transport. In hypodermal passage cells (HPC) PaPDR1 is present at the outer-lateral side allowing strigolactone excretion. Transport experiments using radioactive-labeled strigolactone identified directional, shoot-ward transport of strigolactone that is reduced in *pdr1* mutants. Accordingly, *pdr1* mutants have morphological and gene expression alterations in the root tip that reflect increased strigolactone contents. In conclusion, our results indicate that specific polar localization of PaPDR1 is a prerequisite for the correct allocation of strigolactones within a plant.

3.2 Introduction

Strigolactones are carotenoid-derived phytohormones with functions that have evolved along with the green lineage (Delaux *et al.*, 2012), from inducers of algal rhizoid elongation to inhibitors of lateral shoot branching (Gomez-Roldan *et al.*, 2008; Umehara *et al.*, 2008). In higher plants, strigolactones have first been discovered as germination stimulants for parasitic weeds (Cook *et al.*, 1966). Much later these compounds have been shown to be involved in establishing the first steps of mycorrhizal symbiosis between host plants and arbuscular mycorrhiza fungi (Akiyama *et al.*, 2005) and in synchronizing nutrient availability to plant development (Foo *et al.*, 2013; Ruyter-Spira *et al.*, 2011; Xie and Yoneyama, 2010). More in detail, recently discovered roles for strigolactones include regulation of lateral (Ruyter-Spira *et al.*, 2011) and adventitious (Rasmussen *et al.*, 2012) root development, root cell division (Ruyter-Spira *et al.*, 2011) , secondary growth (Agusti *et al.*, 2011) and leaf senescence (Snowden *et al.*, 2005). Strigolactones are negative regulators of lateral shoot branching, either by acting into axillary buds as direct promoters for dormancy (Brewer *et al.*, 2009; Gomez-Roldan *et al.*, 2008) or by dampening the levels of the auxin transporter PIN1 (Crawford *et al.*, 2010; Shinohara *et al.*, 2013). The enzymes required for strigolactone biosynthesis are conserved in several species (Alder *et al.*, 2012; Ruyter-Spira *et al.*, 2013). The carotenoid cleavage dioxygenase CCD8 (DAD1/MAX4/D10/RMS1) takes part into the synthesis of the first strigolactone active molecule, carlactone (Alder *et al.*, 2012), together with the iron-binding D27 and CCD7 (Umehara *et al.*, 2008; Wang and Li, 2011; Xie and Yoneyama, 2010). Localization of strigolactone biosynthesis was mainly studied via grafting experiments and is reported to take place in root tips and close to shoot axils (Bainbridge *et al.*, 2005; Sorefan *et al.*, 2003). Recently, first steps were carried on the strigolactone signaling mechanism, composed of a DAD2 (PhMAX2) F-box protein interacting with a D14 α/β hydrolase in presence of strigolactone or its synthetic analog GR24 (Hamiaux *et al.*, 2012; Smith and Waters, 2012b). Additional findings (Nakamura *et al.*, 2013; Zhao *et al.*, 2013) showed that the binding and hydrolysis of strigolactones to the D14 (DAD2) complex is required to activate proteasome-mediated degradation of the strigolactone signaling repressor DWARF53 (Jiang *et al.*, 2013; Zhou *et al.*, 2013) by the Skp1-Cullin-F-box $(SCF)^{MAX2}$ complex.

On the other side, the knowledge on strigolactone transport is still scant. We recently published (Kretzschmar *et al.*, 2012) the isolation and characterization of a strigolactone transporter, PaPDR1, a *Petunia axillaris* ABCG class transporter. PaPDR1 transports strigolactone also in the model plant *Arabidopsis thaliana*, despite its closest Arabidopsis sequence homologue *AtABCG40* is a known ABA transporter (Kang *et al.*, 2010c). In tomato and Arabidopsis strigolactone was detected in the xylem sap (Kohlen *et al.*, 2011). Root-derived strigolactone influences shoot lateral branching in several plant species (Beveridge *et al.*, 1994; Foo *et al.*, 2001; Napoli, 1996), despite the fact that strigolactone is also synthetized at the base of shoot axils (Bainbridge *et al.*, 2005; Booker *et al.*, 2005; Sorefan *et al.*, 2003). These findings suggest that strigolactone root-to-shoot transport regulates the shoot architecture and happens via the xylem.

PaPDR1 is expressed in root tips and HPC of Petunia (Kretzschmar *et al.*, 2012). On one hand, the activity of *pPDR1:GUS* in root tips is intriguing, as strigolactone is reported to be synthetized in columella root cells of Arabidopsis (Sorefan *et al.*, 2003). We hypothesized that PaPDR1 might have a role into xylem loading of strigolactone from the root tip, thus to avoid strigolactone accumulation in the root meristem, which was reported to be sensitive to small alterations in strigolactone concentration (Ruyter-Spira *et al.*, 2011). On the other hand, the presence of *pPDR1:GUS* in HPC fits the model which indicates strigolactone as the beacon guiding arbuscular mycorrhizal fungi (AMF). Through yet unknown paths, strigolactone might be transported / diffuse from the xylem to the exodermis and there exuded into the rhizosphere.

A directional transport from root tips up into the xylem and from the vasculature to the rhizosphere might be eased by a polar strigolactone transport and therefore a polar localization of PaPDR1. Polar localization of transporters is known for auxin influx and efflux carriers belonging to the AUX and PIN families (Bennett *et al.*, 1996; Kleine-Vehn and Friml, 2008) and also for ABCG36 and ABCG37, transporters of auxinic precursors (Ruzicka *et al.*, 2010; Strader and Bartel, 2009). The different localization domains for these transporters are regulated by endocytosis, vesicle recycling and cell wall components (Feraru *et al.*, 2011; Kleine-Vehn *et al.*, 2011).

Here we report that PaPDR1 is apically localized in root tip cells and that its absence alters root-to-shoot strigolactone transport, feedbacks *DAD1* expression levels and influence cell homeostasis in the root tip. We also show that PaPDR1 is distally localized in HPC, which fits PaPDR1 role in strigolactone exudation to soil. This is the first time to

our knowledge that a transmembrane protein is asymmetrically localized either in the apical-basal or in the lateral membrane domain depending on the cell-type where it is expressed. We finally suggest that PaPDR1 shares BFA-sensitive vesicle traffic (Geldner *et al.*, 2001) with PIN proteins.

3.3 Results

3.3.1 PaPDR1 is apically localized in Petunia root cortex cells

Strigolactones are either exuded into the soil via the hypodermis (Supplementary figure 3.1a-f for Petunia root morphology), or transported via the xylem to the shoot. In order to elucidate how strigolactones are allocated to the shoot and HPC, Petunia W115 wild-type cultivar and Arabidopsis *rdr6* plants - the latter used to reduce silencing effects on transgenes (Butaye *et al.*, 2004) - were transformed with the strigolactone transporter PaPDR1 fused to a GFP at its C-terminal end. The transgenic protein levels were quantified in 2 week-old seedlings using a GFP antibody, negative in WT plants (Figure 3.1a). In both Petunia and Arabidopsis, GFP-PDR1 levels were low when driven by the endogenous promoter (np-PDR1) compared to the respective ectopic lines (PDR1-OE) transformed with a CaMV p35S variant (compare Figure 3.1b to c and Figure 3.1d to e). This difference in GFP-PDR1 amounts fits the limited and rather low expression observed in *pPDR1:GUS* plants (Kretzschmar *et al.*, 2012). PaPDR1 was shown to be induced by auxin, strigolactone and low phosphate (Kretzschmar *et al.*, 2012).

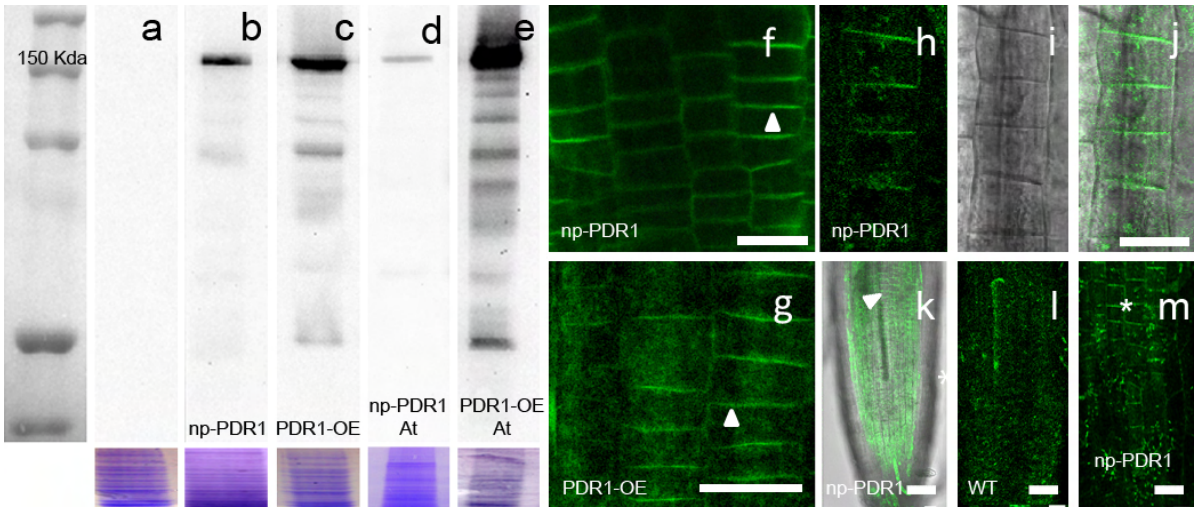

Figure 3.1: Quantification and cell localization of GFP-PDR1

(a-e) GFP-PDR1 in 10 day-old **(a)** WT, **(b)** *pPDR1:GFP-PDR1* (np-PDR1), **(c)** *p35S:GFP-PDR1* (PDR1-OE) Petunia seedlings and in **(d)** *pPDR1:GFP-PDR1;rdr6* and **(e)** *p35S:GFP-PDR1;rdr6* (PDR1-OE At) Arabidopsis seedlings. (f, arrowhead) GFP-PDR1 in root tip cortex cells of 2-month old np-PDR1 Petunia starved on clay. (g, arrowhead) GFP-PDR1 in root tips of PDR1-OE Petunia. **(h)** np-PDR1 in 4 week-old Petunia root tips after 2 week of phosphate starvation, **(i)** light channel and **(j)** overlap. **(k)** Overlay between white light and GFP channels; the arrowhead points to the GFP-PDR1 domain in the root tip. **(l)** Autofluorescent background in WT Petunia root tip compared to **(m)** np-PDR1 signal. In picture labels: plant genotypes. Scale bars = 15 μm.

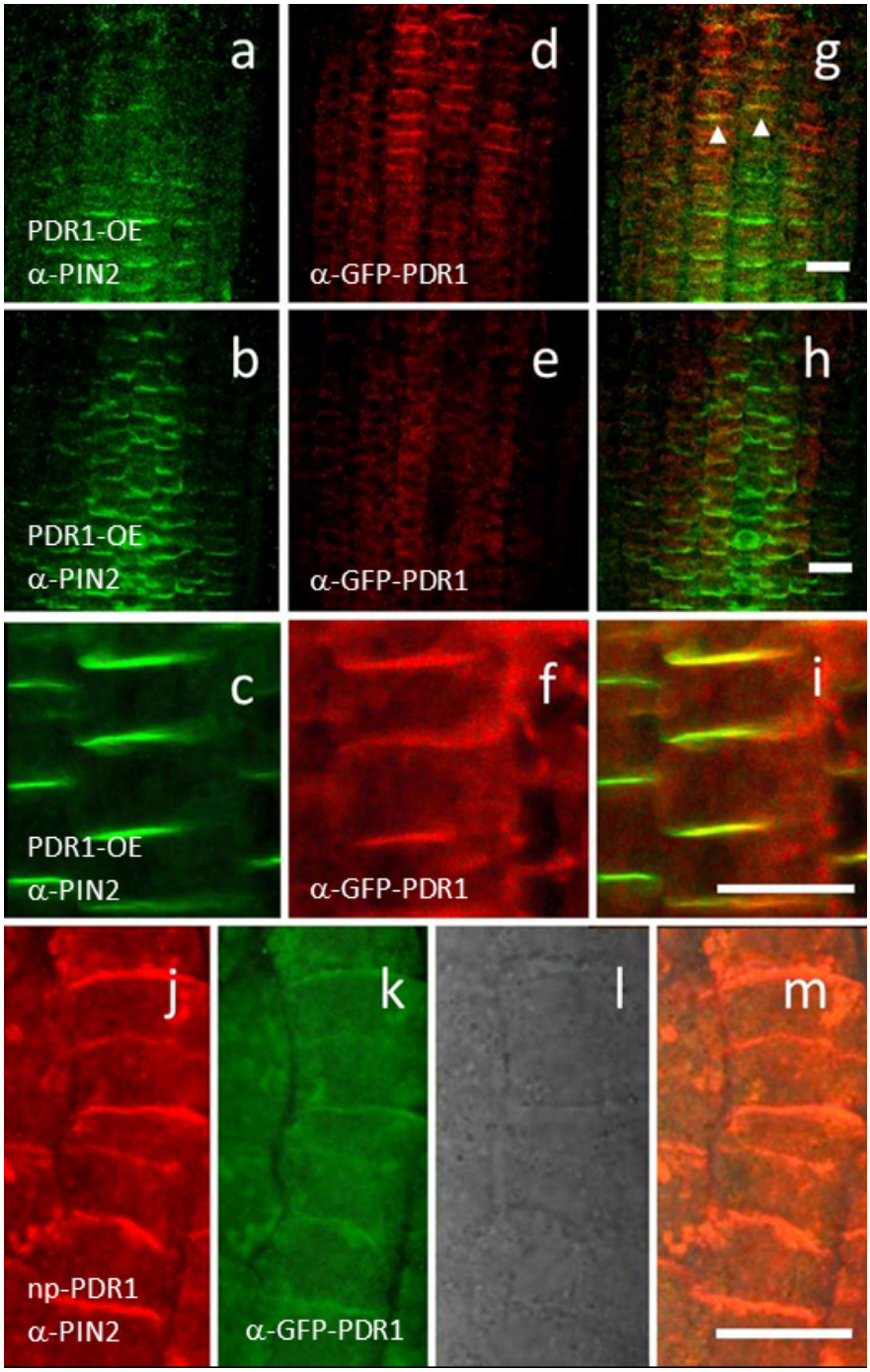

Figure 3.2: GFP-PDR1 sub-cellular localization.

(a-i) Immuno-localizations on PhPIN2 (Alexa488 secondary antibody, AtPIN2 primary anitbody, green channel) and GFP-PDR1 (Cy3 secondary antibody, GFP primary antibody, red channel) in PDR1-OE root tips: **(a, b, c)** PhPIN2, (d, e, f) GFP-PDR1 and **(g, h, i)** respective co-localizations from hypodermis **(a, d, g)** to inner cortex **(b, e, h)**. **(g, arrowheads)** Co-localization of GFP-PDR1 and PhPIN2. **(c, f, i)** Co-localization of PhPIN2 (green) and GFP-PDR1 (red) in root cortex of PDR1-OE roots. **(j, m)** One month-old np-PDR1 Petunia seedlings starved on MS agar plates with low phosphate for 2 weeks: **(j,** Cy3 secondary antibody, AtPIN2 primary antibody, **red** channel) apical localized PhPIN2 signal and (k, Alexa488 secondary antibody, GFP primary antibody, green) GFP-PDR1 **(l, grey)** transmitted light and **(m)** overlap. In picture labels: plant genotypes / antibodies. Scale bars = 20 μm.

Previous studies showed that the auxin transporters AtPIN1 and AtPIN2 are asymmetric in the root tip cells of Arabidopsis. AtPIN1 is basally localized in the root stele and AtPIN2 is apical localized in epidermis and cortex cells out of the meristem region (Krecek *et al.*, 2009). To identify the polarity of the asymmetric PaPDR1 signal as apical or basal, we compared GFP-PDR1 localization to the *Petunia hybrida* homologues PhPIN1 and PhPIN2. Petunia has a strong auto-fluorescent background in most root tissues, although lower in the root tip (Figure 3.1l), therefore immunolocalization was chosen to reduce the autofluorescence-to-signal ratio. Immunolocalizations with anti-PhPIN1, PhPIN2 or GFP in 8 week-old np-PDR1 plants starved on clay did not show any signal (data not shown), possibly due to a difficulty in infiltration into suberized root tissues. Similarly, GFP-PDR1 immunolocalizations in *np-PDR1* Arabidopsis were negative (data not shown), possibly because of the low GFP-PDR1 protein levels in Arabidopsis (see Figure 3.1d). Protein co-localizations were then carried on with GFP and AtPIN2 antibodies in 2 week-old PDR1-OE and 4 week-old np-PDR1 Petunia plantlets, the latter pre-starved on MS agar plates with low phosphate for two weeks. The GFP-PDR1 signal in PDR1-OE plants was absent in lateral root cap and epidermis (Supplementary Figure 3.1g) but strong and asymmetrically localized in hypodermis (Supplementary Figure 3.1h), partially overlapping with the PhPIN2 expression domain (Figure 3.2a, d, g arrowheads). PhPIN2 was present also in cortex layers deeper than the hypodermis (Figure 3.2b) in contrast to GFP-PDR1, confined to the hypodermis (Figure 3.2e and Supplementary Figure 3.2i). The cortex cells expressing both GFP-PDR1 and PhPIN2 showed a co-localization of GFP-PDR1 and PhPIN2 in PDR1-OE roots (Figure 3.2g, i) and in np-PDR1 plantlets (Figure 3.2j-m), indicating that PaPDR1 is targeted to the apical domain of the plasma membrane.

3.3.2 PaPDR1 is asymmetrically localized in Arabidopsis root tip cells

PaPDR1 is a functional strigolactone transporter also in *Arabidopsis thaliana* (Kretzschmar *et al.*, 2012). Therefore we were interested whether in Arabidopsis, which lacks a PaPDR1 functional homologue, PaPDR1 would also be asymmetrically localized. If so, thanks to the extensive molecular toolbox available in Arabidopsis several questions regarding the mechanism of PaPDR1 polar localization could be answered. Despite the aid of the *rdr6* mutant background (Butaye *et al.*, 2004),

we could not detect GFP-PDR1 in root tips of *np-PDR1* Arabidopsis either via live cell imaging or immunolocalization.

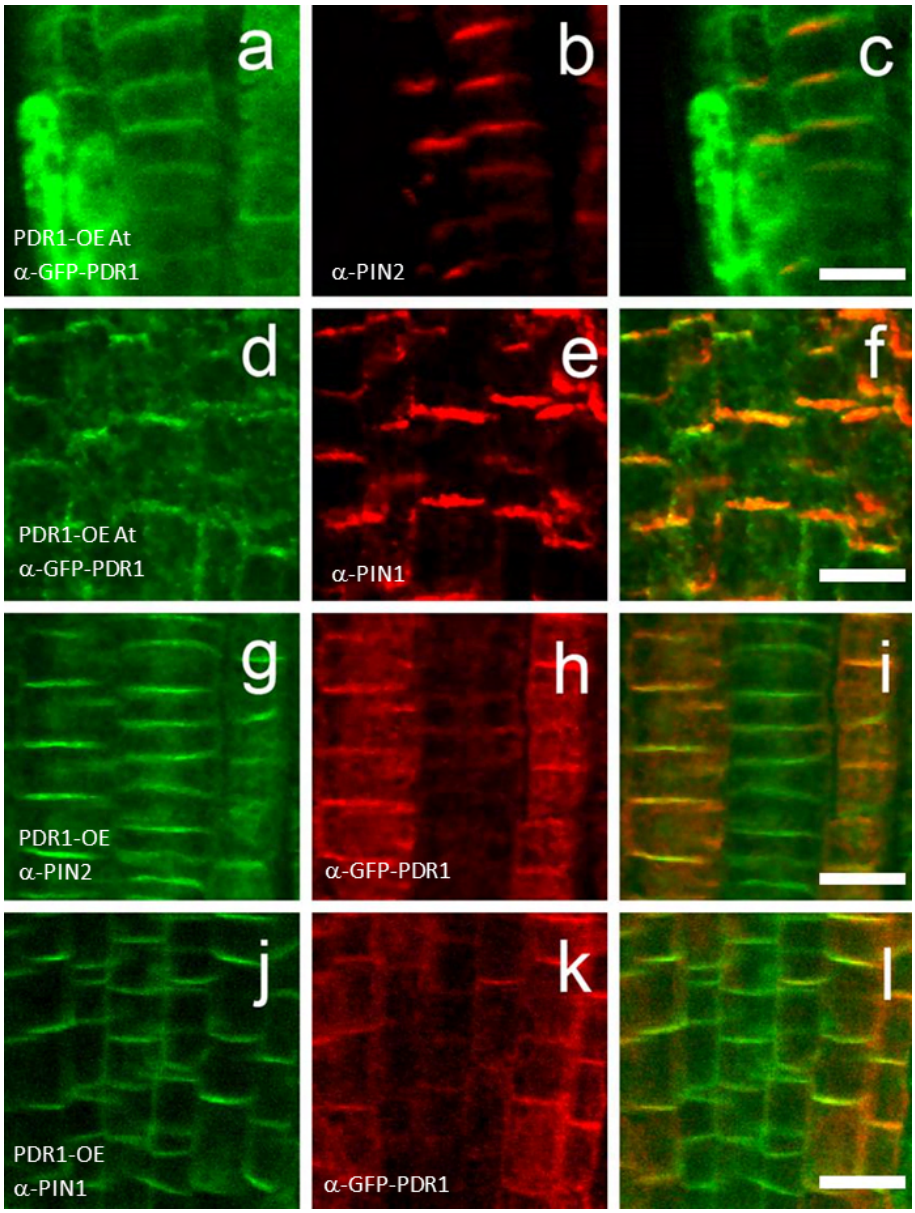

Figure 3.3: GFP-PDR1 co-localization with PIN proteins

(a-f) Immuno-localizations on GFP-PDR1 (Alexa488 secondary antibody, GFP primary antibody, green channel) and AtPIN1 and AtPIN2 (Cy3 secondary antibody, AtPIN1 + AtPIN2 primary antibodies, red channel) in 10 day-old PDR1-OE At seedlings. GFP-PDR1 in Arabidopsis is apically localized in cortex cells of root tips **(a-c)** where it co-localizes with AtPIN2. GFP-PDR1 in PDR1-OE At seedlings is present in the root stele (d-f), where it co-localizes with AtPIN1. **(g-l)** Immuno-localizations on PhPIN2 (**g**, Alexa488 secondary antibody, AtPIN2 primary antibody, root cortex cells), PhPIN1 (**j,** Alexa488 secondary antibody, AtPIN1 primary antibody, root stele) and GFP (**h, k,** Cy3 secondary antibody, GFP primary antibody, red channel) of 10 day-old Petunia roots incubated with 10 μM exogenous GR24 for 6 hours. After GR24 incubation GFP-PDR1 is detected not only in hypodermis **(h)** co-localized with PhPIN2 **(yellow overlap, i)** but also in the root stele **(k)** co-localizing with PhPIN1 **(yellow overlap, l)**. In picture labels: plant genotypes / antibodies. Scale bars = 20 μm.

This negative result might be either due to the low protein levels (see Figure 3.1d) or to the possibility that the Petunia promoter is not as functional in Arabidopsis root tips. On

the other hand, GFP-PDR1 was detectable in *PDR1-OE* Arabidopsis plants (PDR1-OE-At) in root epidermal and cortex cells (Figure 3.3a-c) and in the root stele (Figure 3.3d-f). GFP-PDR1 showed asymmetric distribution in cells co-localizing with AtPIN2 in epidermal and cortex cells (Figure 3.3c), and with AtPIN1 in root stele cells (Figure 3.3f). GFP-PDR1 asymmetric localization in cortex cells (Supplementary Figure 3.2) was confirmed to be predominantly apical by co-staining of cell walls with propidium iodide (Supplementary Figure 3.3).

The ectopic GFP-PDR1 expression pattern we detected in Arabidopsis root tips was also visible in Petunia PDR1-OE roots only if the latter were pre-incubated 6 hour-long with 10 μM GR24. Like in Arabidopsis, also in Petunia GFP-PDR1 became present not only co-localized with PhPIN2 in the cortex (Figure 3.3g-i) but also with PhPIN1 in the root stele (Figure 3.3j-l). Protein quantification confirmed that 6 hour-long incubation in 10 μM GR24 is sufficient to boost GFP-PDR1 protein levels (Supplementary Figure 3.4) and that such protein boost is long lasting, as we could still detect it 3 weeks after germination on GR24 concentrations as low as 2.5 μM (Supplementary Figure 3.4).

3.3.3 GFP-PDR1 is localized at the outer lateral side in HPC of Petunia roots

Hypodermal passage cells are the entry point for mycorrhizal fungi (Sharda and Koide, 2008). The endogenous promoter *pPDR1* is exclusively active in these cells (Kretzschmar *et al.*, 2012). We therefore analyzed the sub-cellular localization of GFP-PDR1 in Petunia HPC. Root cells above the root tip of Petunia are strongly auto-fluorescent (Figure 3.4a). However, a stronger-than-background GFP signal was visible in the outer lateral side of a few hypodermal cells of np-PDR1 roots, *bona fide* HPC (Figure 3.4b, c arrows). GFP immunolocalizations on root slices from WT (Figure 3.4 d-i) and np-PDR1 (Figure 3.4 j-o) plants (both starved on clay for 2 months) confirmed the presence and asymmetrical localization of GFP-PDR1 at the distal-lateral plasma membrane of HPC.

3.3.4 Regulation of GFP-PDR1 targeting to the plasma membrane of root tip and HPC

Our results describe that PaPDR1 is asymmetrically localized in root tips, where it is located at the apical membrane side and in HPC where it is polarly localized at the outer lateral side. Hence, the different asymmetrical localization of GFP-PDR1 seems to be cell type-specific. In order to learn more about the mechanisms involved in the polar distribution of PaPDR1, we performed experiments aimed to modify the respectively apical and outer lateral localization of PaPDR1 by treatments with auxin, GR24, or Brefeldin-A (BFA). The latter has been reported to alter the vesicle traffic responsible for targeting e.g. the auxin carriers PINs (Geldner *et al.*, 2001) and the auxinic precursor transporters ABCG36 and ABCG37 to the plasma membrane (Ruzicka *et al.*, 2010; Strader and Bartel, 2009).

We applied the same range of single treatments on fragments of Petunia roots, which still showed a strong GFP-PDR1 signal in mock liquid cultures up to 24 hours after incubation (Supplementary Figure 3.5a, b). A 6 hour-long 25 µM BFA treatment resulted in accumulation of small vesicles (Supplementary Figure 3.5c, d) in 20% of the analyzed HPC, but not in root tips. We supposed that 2 month-old Petunia roots have a low permeability to exogenous compounds, as previously experienced with negative immunolocalizations on same age material. Indeed, only by mild vacuum infiltrations with higher BFA concentrations (50 µM) and 90 minute-long incubation we could confirm the accumulation of GFP-PDR1 vesicles in the analyzed HPC (Figure 3.4p, q) and root cortex cells (Figure 3.4r, s). Auxin and GR24 treatments slightly boosted the GFP-PDR1 signal intensity 24 hours after induction, in accordance with the auxin-dependent increase of *PaPDR1* previously observed (Kretzschmar *et al.*, 2012) (Supplementary Figure 3.5e-h).

Arabidopsis PDR1-OE root tips responded to these exogenous treatments like Petunia. The asymmetric localization of GFP-PDR1 was not altered by a mock incubation in MS medium for 1.5 to 24 hours (compare Supplementary Figure 3.6a and 3.5b). Exposure to 25 µM BFA for 90 minutes caused the accumulation of intracellular signal in root cortex cells (Supplementary Figure 3.6c), similarly to what we obtained for PhPIN2 in 2 week-old Petunia after the same treatment (Supplementary Figure 3.6d). 16 hour-long incubation with 10 µM GR24 did not alter GFP-PDR1 polar

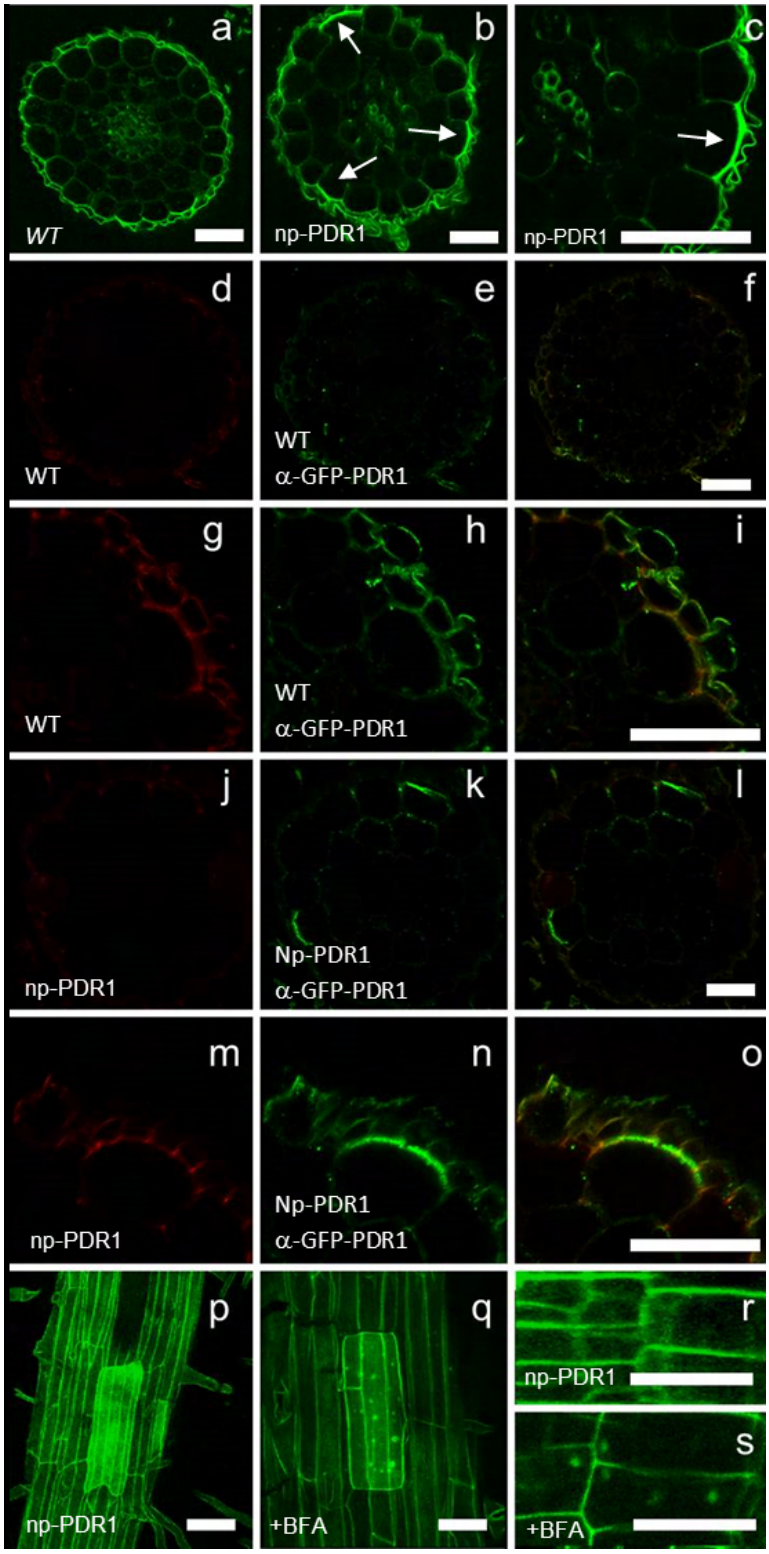

Figure 3.4: GFP-PDR1 localization in HPC and sensitivity to BFA

Polar localization of np-PDR1 in HPC of 2-month old Petunia starved on clay for 6 weeks. **(a-c)** Vibratome-operated transversal sections of Petunia roots. **(a)** Despite the strong auto-fluorescence of Petunia tissues, a GFP-PDR1 stronger-than-background signal can be detected in hypodermal cells **(b, arrows)** and in these cells it is asymmetrical localized **(c, arrowhead)**. GFP immunolocalizations on **(d-i)** WT and **(j-o)** np-PDR1 roots, transversal sections: autofluorescence (red channel and green channel), GFP signal (Alexa488 secondary antibody, GFP primary antibody, green channel in **k,n**) and overlap **(l,o)**. Only in np-PDR1 cells the GFP signal does not overlap with the red channel. **(p-s)** BFA treatments on np-PDR1 roots. **(p)** In mock treated roots, GFP-PDR1 is visible in HPC. **(q)** Vesicles accumulate in HPC after BFA incubation. **(r)** Hypodermal cells or Petunia root tip after mock treatment. **(s)** After BFA, vesicles are visible in the hypodermis. In picture labels: plant genotypes / treatments / antibodies. Scale bars = 20 μm.

localization (Supplementary Figure 3.6 e, f), while auxin treatments strongly increased the GFP-PDR1 signal (Supplementary Figure 3.6g). This loss of GFP-PDR1 asymmetrical localization could be due either directly to auxin or to a strong expression of GFP-PDR1 due to the activation of *pPDR1* (Kretzschmar *et al.*, 2012).

3.3.5 Petunia pdr1 roots have reduced strigolactone transport

We hypothesized that PaPDR1 polar localization in roots might direct a polar strigolactone transport from the root tip up to the xylem, where strigolactone was previously detected in both tomato and Arabidopsis (Kohlen *et al.*, 2011). Such polar transport might also help regulating the accumulation of strigolactone in the root biosynthetic tissue. We first investigated the expression pattern of *CCD8/DAD1*, thus to understand where strigolactones are synthetized in Petunia roots. A 1.7 Kb-long DAD1 promoter (*pDAD1*) was amplified from *Petunia hybrida* and cloned upstream of a nuclear localization signal in frame with a nuclear localized, YFP coding sequence (De Rybel *et al.*, 2011). Two week-old *pDAD1:nls-YFP* seedlings showed YFP-positive nuclei only in root tips (Supplementary Figure 3.7a) with no signal in other root tissues (Supplementary Figure 3.7b, c, d). Similar to *pPDR1:GFP-PDR1*, *pDAD1:nls-YFP* is present in cortex cells and absent in epidermal, endodermal and stele cells of the root tip (Supplementary Figure 3.7e-h). To test if the apical localized PaPDR1 contributes to strigolactone transport out of the strigolactone-synthesizing root tip up into xylem, we evaluated strigolactone transport (see Experimental procedures) in phosphate starved roots of Petunia *pdr1* mutants compared to their WT background (W115 x W138). The transport of a radiolabelled GR24 was quantified (Figure 3.5a). Root tips of *pdr1* mutants (n = 11) showed a significant, higher accumulation of radioactivity compared to WT. On the contrary, radioactivity in agar surrounding the plantlets, in upper root segments and in shoots was weaker in *pdr1* seedlings compared to WT. This result shows an accumulation of radiolabelled GR24 in *pdr1* root tips compatible with an impaired polar transport of strigolactone from the root tip up into the root vasculature. A similar, although less pronounced trend could be observed in plants not grown under P deficiency (Supplementary Figure 3.8). Such results are compatible with our hypothesis that without PaPDR1 less strigolactone is acropetally transported to the xylem. The directional transport of radiolabelled GR24

and the apical localization of GFP-PDR1 show that strigolactone polar transport plays a role in the shootward distribution of strigolactone out of the root tip.

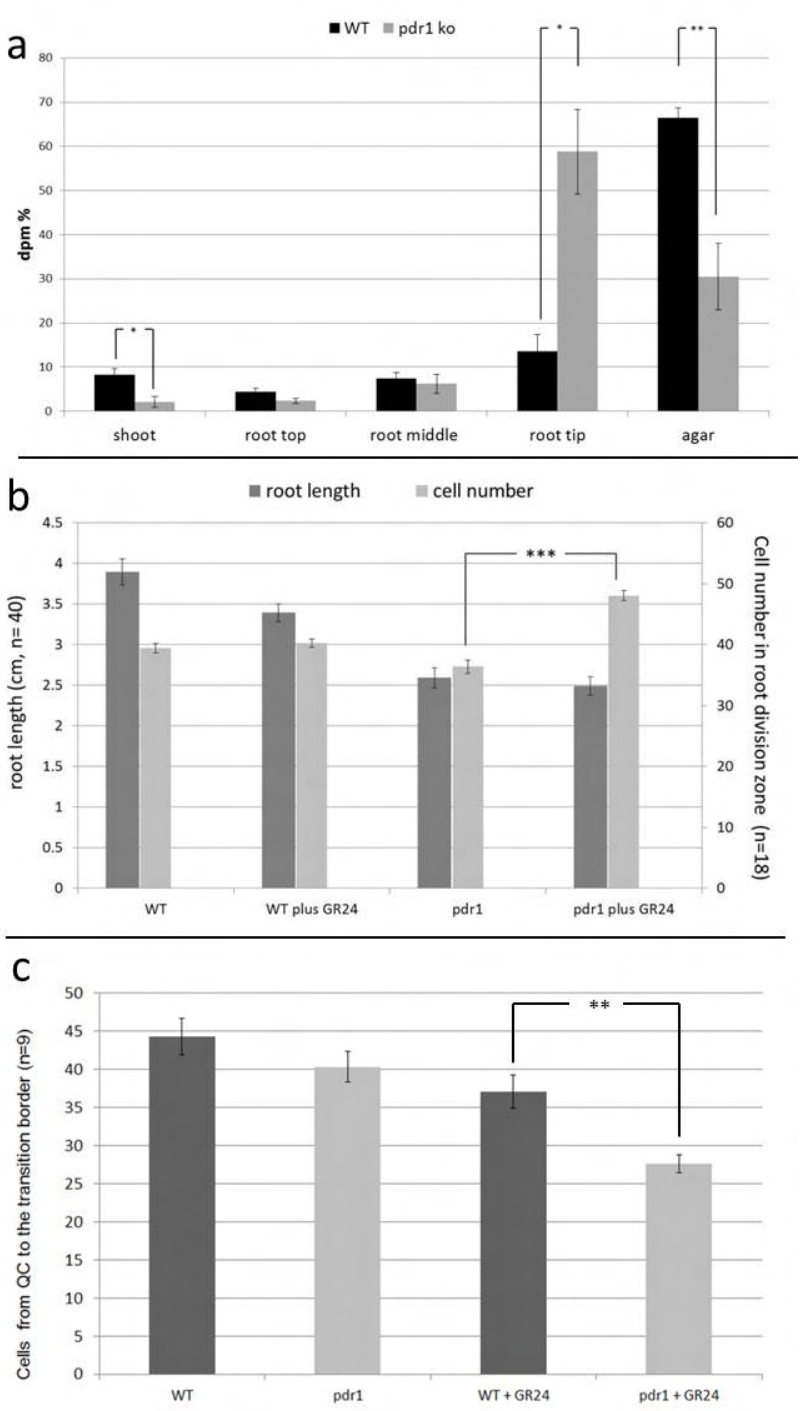

Figure 3.5: Effects of *pdr1* loss-of-function on strigolactone transport and root tip homeostasis.

(a) Transport quantification of radiolabelled GR24 in root tips, root segments (middle and top) and shoots in WT and *pdr1* Petunia (n = 11). Root-tip radioactivity counts are higher in *pdr1* than in WT and lower in shoots and roots, showing accumulation of GR24 in *pdr1* root tips and impaired root-to-shoot transport capacity. **(b)** Main root lengths (dark grey bars) (n = 40) and cell number (light grey bars) in root division zones (n = 18) of 2 week-old WT and *pdr1* mutants. Exogenous GR24 (2.5 μM) does not significantly affect root length of WT or *pdr1* roots but it alters the cell numbers in root division zones of *pdr1* mutants **(c)**. Two week-old WT and *pdr1* mutants did not show significant differences in numbers of cells between quiescent center and transition zone. When germinated on 10 μM GR24, *pdr1* mutants scored 37% less cells compared to their mock, in contrast to a not significant decrease of 17% detected in wildtype roots. (* = $P < 0.05$; ** = $P < 0.005$).

3.3.6 Effects of exogenous GR24 on the main root of WT and pdr1 Petunia mutants.

To obtain further evidence whether strigolactones are ectopically accumulated in the root tip in the absence of PaPDR1, we tested if WT and *pdr1* root tips were responding differently to exogenous GR24. GR24 concentrations as low as 2.5 µM were reported to increase the number of cells in the meristem zone in Arabidopsis root tips (Ruyter-Spira *et al.*, 2011). Two week-old *pdr1* seedlings germinated on 1% sucrose plus/minus 2.5 µM GR24 and relative WT background were scored for main root length and cells in the division zone of the root tip. Roots were stained with propidium iodide, and the cells between quiescent center (QC) and the border with the elongation zone quantified (Supplementary Figure 3.9a-b). The number of cells in the root division zone in *pdr1* mutants, but not in WT plants, was significantly increased by 2.5 µM GR24 (Figure 3.5b light grey bars). The total length of wild-type and *pdr1* main roots was not significantly affected by GR24 (Figure 3.5b dark grey bars). *Pdr1* main root length, independent of the treatment, was shorter than WT. Levels as high as 10 µM GR24 inhibit main root growth in Arabidopsis (Kretzschmar *et al.*, 2012). Therefore, we additionally scored main root lengths of WT and *pdr1* Petunia roots germinated on 10 µM GR24 MS plates. WT main roots had 17% fewer cells in the meristem zone compared to WT mock plants. The effect of 10 µM GR24 levels was stronger in *pdr1* mutants, which scored 37% fewer cells between QC and elongation border (Figure 3.5c and Supplementary Figure 3.9g-j). We propose that high GR24 levels have higher toxicity in *pdr1* mutants because of their defective strigolactone transport out of the root tip up into the xylem.

Main root lengths of WT and pdr1 mutants vertically grown in agar plates are different. However, without the abovementioned treatments with exogenous GR24 we could not score alterations in cell numbers of their respective root division zones (Figure 3.5c). We hypothesized that *DAD1/CCD8* expression levels might be negatively regulated by accumulation of strigolactone in *pdr1* root tips, thus to maintain homeostasis in the root meristem. By quantitative PCR we measured DAD1 expression levels in WT and *pdr1* mutants at 7 and 10 days after germination (dag): DAD1 levels are lower in root tips of *pdr1* mutants compared to WT (Supplementary Figure 3.10a). Additionally, short, mild treatments with exogenous GR24 decreased DAD1 expression in Petunia root

tip (Supplementary Figure 3.10b), compatibly to what was shown for *MAX4 (DgCCD8/CCD8)* (Hayward *et al.*, 2009; Liang *et al.*, 2010). Therefore, we interpret *DAD1* downregulation in *pdr1* root tips as a consequence of strigolactone accumulation due to an impaired strigolactone polar transport in *pdr1* loss-of-function plants. Strigolactone altered biosynthetic levels might be then responsible for the differential growth of the main root in WT and *pdr1* mutants, either via crosstalks with auxins (Hayward *et al.*, 2009; Shinohara *et al.*, 2013) or other yet unknown, more direct pathways.

3.4 Discussion

We describe here the distinct and asymmetrical localization of *Petunia axillaris* PDR1 in cortex cells of Petunia and Arabidopsis root tips and in HPC of Petunia. PaPDR1 is apically localized in hypodermal cells of the root tip, co-localized with PhPIN2 and overlapping with *DAD1 (CCD8)*. In the root tip, PaPDR1 contributes to loading strigolactone into the xylem. In *pdr1* root rips we detected accumulation of radiolabelled GR24 higher than in WT and lower in upper root segments and shoot. We could still measure radiolabelled GR24 in the shoot: since we applied exogenous GR24 it is likely that part of it could also move in the apoplast via the transpiration stream.

Despite the transpiration stream, root tips of *pdr1* mutants show a reduced *DAD1* expression levels compared to wild type, compatible with a negative feedback due to strigolactone accumulation. Therefore PaPDR1 function is not restricted to xylem loading but it is also important for removing strigolactone from the root tip, thus to maintain the root tip homeostasis.

We propose that the cell-to-cell transport of strigolactone out of the root tip is also related to its function as beacon to mycorrhization (Gutjahr and Parniske, 2013). The distribution, more than the number, of HPC has been reported to influence the amount of mycorrhization events per plant (Sharda and Koide, 2008). Strigolactones are weakly polar molecules and we showed that they can be taken up by root tips. Root tips in Petunia as well as in other Solanaceae do not build in root tips an impermeable hypodermis with Casparian strips (Enstone *et al.*, 2002), and without PaPDR1 endogenous strigolactones might diffuse from the root tip cortex out into the rhizosphere. Hence, not-optimal concentrations of strigolactone in the root tip could also build a misplaced signal to attract arbuscular mycorrhiza fungi instead of directing them to HPC.

Additional investigations are needed to analyze the localization of PaPDR1 in the shoot. Strigolactones play important roles in inhibiting lateral bud outgrowth either by directly downregulating transcription factors necessary for bud growth or by inhibiting auxin export from dormant buds via dampening PIN1 (Shinohara *et al.*, 2013). In both cases, a polar cell-to-cell transport of strigolactone from the xylem to the axillary buds might be necessary to avoid crosstalks with auxins in neighboring districts. Further analyses need

to be conducted in these tissues where strigolactones and auxins, or other hormones, have been shown to have overlapping domains, e.g. for secondary growth (Agusti *et al.*, 2011), lateral (Ruyter-Spira *et al.*, 2011) and adventitious roots (Rasmussen *et al.*, 2012) and internode elongation (de Saint Germain *et al.*, 2013). New approaches have to be developed to map PaPDR1 out of the root tip, where analyses are difficult because of Petunia autofluorescence.

PaPDR1 is outer-laterally localized in HPC. The 50% reduction of GR24 exudation from *pdr1* roots we report is consistent with previous observations (Kretzschmar *et al.*, 2012). The outer lateral localization of ABCG class proteins was also reported for auxinic exporters (Ruzicka *et al.*, 2010; Strader and Bartel, 2009). These transporters are localized in root tips but do not build any cell-to-cell transport: they export IBA from the root epidermis out into the rhizosphere. As well, ABCG11 and ABCG12 were reported to be required for lipid export towards to cuticle (McFarlane *et al.*, 2010). They are both expressed in the stem epidermis and their function is confined to this tissue.

PaPDR1, similar to PIN2 (Krecek *et al.*, 2009), can target different membrane domain in distinct cell population. However, to our knowledge this is the first time a transmembrane protein is detected either in the apical/basal or in the lateral domain. The peculiar role of the outer-lateral membrane domain of HPC as entry- or exit-points for mycorrhization or strigolactone might play a role in re-shaping PaPDR1 targeting from the apical-basal to the lateral domain. Nothing is known yet about the expressome of HPC, it is therefore difficult to speculate if and which novel mechanisms might be behind PaPDR1 targeting. In Petunia hypodermal cells, PaPDR1 co-localizes with PIN2 (Krecek *et al.*, 2009; Muller *et al.*, 1998). Interestingly, in PDR1-OE Arabidopsis and in GR24 treated PDR1-OE Petunia seedlings, PaPDR1 additionally co-localizes with PIN1 in the root stele. Such additional co-localization suggests that PaPDR1 might share the vesicle targeting system responsible for PIN localization (Korbei and Luschnig, 2013b; Offringa and Huang, 2013). We inhibited the intracellular vesicle recycling via Brefeldin A and detected the presence of vesicle aggregates in GFP-PDR1 positive cells. BFA is reported to alter the endocytic recycling of auxin transporters belonging to PIN and ABCG families (Geldner *et al.*, 2001; Ruzicka *et al.*, 2010; Strader and Bartel, 2009). We propose that PaPDR1 shares at least part of its membrane targeting system with auxin transporters. For PIN proteins, the amino acid motif TPRXS(N/S) situated on the large central hydrophilic loop is crucial for phosphorylation and polar localization but absent

in PaPDR1. Different, yet unknown phosphorylation sites or post translational modifications (Korbei and Luschnig, 2013a) could play a role in PaPDR1 targeting.

In HPC of Petunia roots, exogenous IAA or GR24 could not alter PaPDR1 polar localization but still enhanced the protein levels. Interestingly, IAA treatments altered the signal intensity of GFP-PDR1 in root tips of Arabidopsis roots up to a loss of asymmetric localization. PaPDR1 is auxin and GR24 inducible (Kretzschmar *et al.*, 2012). Hence it is not clear yet if higher auxin accumulation in root tips causes symmetric localization of PaPDR1 or if excessive levels of PaPDR1 are mis-targeted to the plasma membrane.

A polar phytohormone transport was reported exclusively for auxins (Petrasek and Friml, 2009). Cytokinins, jasmonate and its metabolite methyl-jasmonate are transported either via xylem or phloem for long-distance signaling (Sakakibara, 2006; Thorpe *et al.*, 2007). The characterization of a cytokinin transporter is limited to low-affinity systems for both cytokinins and adenine (Cedzich *et al.*, 2008). Transporters for abscisic acid (ABA) were recently identified in Arabidopsis as the ABCG class protein *AtPDR12* (Kang *et al.*, 2010c) and the low-affinity nitrate transporter NRT1.2 (Kanno *et al.*, 2012). They both regulate cellular uptake of ABA but no asymmetrical localization on the plasma membrane is known. Brassinosteroids are not reported for long-distance transport (Symons *et al.*, 2008) and gibberellins are suggested to be transported symplastically and follow a diffusive transport (Bruggeman *et al.*, 2001). Similar to auxins, strigolactones need polar transport out of their biosynthetic tissues, in this case the root tip, and towards their target domains, either the shoot or the rhizosphere. However, in contrast to the large family of auxin transporters (Zazimalova *et al.*, 2010), at present only PaPDR1 was characterized as transporter for strigolactone. Additionally, no importer for strigolactone, probably necessary for a directional cell-to-cell transport, has been isolated. The characterization of new strigolactone transporters from different plant species will show if the presence of a single strigolactone transporter is specific to Petunia. The ectopic GR24-induced PaPDR1 pattern, extending from the root cortex deep down in the root stele of Petunia, suggests that strigolactone might play a role not only in enhancing *PaPDR1* expression but also in increasing PaPDR1 stability. Strigolactone, similar to what is known for auxins (Paciorek *et al.*, 2005), might promote its own polar transport in cells where it is present by increasing the half-life of PaPDR1.

Strigolactone transport from its biosynthetic to target tissues is highly regulated by endogenous and exogenous signals and synchronized with strigolactone biosynthesis. Both strigolactone transport and biosynthesis are upregulated by scarcity of phosphate and nitrogen into soil (Kretzschmar *et al.*, 2012; Lopez-Raez and Bouwmeester, 2008), and hence are both involved into the synchronization of root and shoot development to nutrient availability. Also, PaPDR1 is asymmetrically localized in root tips and HPC, thus setting a directional strigolactone transport in and outside plants. Additionally, *PaPDR1* and *DAD1* are positively regulated at least by another phytohormone, auxin (Bainbridge *et al.*, 2005; Kretzschmar *et al.*, 2012). Such hormonal crosstalks and gene expression synchronizations in root cells are not only necessary to keep the root meristem homeostasis, but might also modulate the amount of strigolactone loaded into the xylem and transported shootward. PaPDR1 therefore plays an important role in integrating feedback signals generated by nutrient availability, strigolactone and auxin distributions thus to synchronize root and shoot development.

3.5 Experimental procedures

Plant growth: Petunia plants were grown under long day conditions (16 h light / 8 h darkness regime), at 60% relative humidity and 25 °C in soil (ED 73, Einheitserde) or in clay granules (Oil Dri US-Special, Damolin) or plated on 0.85% (w/v) Phyto Agar (Duchefa) medium containing 2.2 g L^{-1} MS medium (Duchefa) at 21 °C. Low phosphate MS medium for PaPDR1 induction equals to 0.25 mM instead of 1.25 mM KH_2PO_4.

Protein Quantification: Western blot analyses were carried out following (Banasiak *et al.*, 2013) with minor modifications. The membrane was incubated with the GFP antibody (Sigma G6539).

Whole-mount immunolocalizations with Arabidopsis AtPIN1, AtPIN2 and GFP (Sigma G6539) antibodies were carried on as described in (Sauer *et al.*, 2006) with minor modifications. Antibodies were dilutes as follows AtPIN1 (1:1000) (Robert *et al.*, 2010), AtPIN2 (1:1000) (Wisniewska *et al.*, 2006) and GFP (1:600) (Sigma G6539) antibodies.

For immunolocalizations on vibratome sectioned roots, 150-µm thick cross-sections were obtained via vibratome and fixed in 4% parafomaldehyde. A 1 h fixation under

vacuum followed at RT. The slices were washed with PBS plus 1 mM glycine 5 x 5 min at RT and shaken in 3% BSA for 2 h at 4 °C. Primary antibody (Sigma G6539, 1:1000) incubation was carried on overnight at 4 °C on shaker. The next day, the slices were rinsed 5 x 10 min in PBS. Secondary antibody incubation (Life Technologies, A-11001, 1:1000) was carried on for 2.5 h at 37° C.

Microscopy Analysis: A Leica SP5 and a Zeiss LSM 710 were used for confocal microscopy, both systems with settings recommended by the manufacturer. Propidium iodide was applied at a concentration of 10 µg ml^{-1} .

Transport assay of radiolabelled strigolactone: Petunia plants were grown for 10 days on plates. For each line, eight plants were arranged on a plate, with the root tip on a parafilm strip. A 1 mm^3 cube of 2.2 g L^{-1} MS, 0.8% (w/v) phyto agar, and 62.5 nM ^{3}H-GR24 (specific activity 40 Ci $mmol^{-1}$, American Radiolabeled Chemicals) was arranged touching the root tip. After incubation 3 h at RT, root tips were immersed for 10 s in a 4 °C 1 µM GR24 solution. The root was sectioned in 5 mm root tip and above root fragments. Shoots were immersed for 30 min in 24% (w/v) trichloroacetic acid. Shoot and root sections were immersed in 3 ml ULTIMA Gold LSC cocktail (Perkin Elmer). Tritium counts were determined for with a Liquid Scintillation Analyser Tri-Carb 2900 TR (Packard BioScience) and displayed in percentage of total counts.

Hormonal and chemical treatments: Petunia or Arabidopsis seedlings grown on plates were exposed for 6 to 24 h to final concentrations of 10 µM of the synthetic strigolactone analogue GR24 (Chiralix) or 10 µM IAA, 25 µM or 50 µM BFA for 90 minutes. A 30 minute-long vacuum was applied to 2 month-old Petunia roots to ease BFA infiltration.

Quantitative PCR: RNA was extracted with RNeasy Plant Mini Kit (Qiagen) and cDNA was synthesized with polyT oligonucleotide (Promega) and M-MLV Reverse Transcriptase (Promega) for 1 h at 40 °C. DAD1 expression was quantified with AGAACTGGTATGATGAGGGT and TTTCTTTGGAACCCAGCAAC oligonucleotides. The expression levels of Glyceraldehyde-3-phosphate dehydrogenase were determined with the oligonucleotides GACTGGAGAGGTGGAAGAGC and CCGTTAAGAGCTGGGAGAAC as housekeeping gene. Quantitative PCR was performed in SYBR Green PCR Master Mix (Applied Biosystems) with a 7500 Fast Real-Time PCR System (Applied Biosystems).

3.6 Acknowledgements

We thank Dr. José María Mateos (University of Zurich, Switzerland) for providing us with the vibratome. Prof. Dolf Weijers (Wageningen University, the Netherlands) for shipping us his set of Ligation-Independent-Cloning vectors. Prof. Bruno Humbel (University of Lausanne, Switzerland) for suggestions on GFP-PDR1 detection. Dr. Undine Krügel (University of Zurich, Switzerland) and Prof. Michal Jasinski (Polish Academy of Science, Poland) for hints on protein quantification. Olivia and Otto Sasse for designing the graphical abstract.

3.7 References

Agusti, J., Herold, S., Schwarz, M., Sanchez, P., Ljung, K., Dun, E.A., Brewer, P.B., Beveridge, C.A., Sieberer, T., Sehr, E.M., *et al.* (2011). Strigolactone signaling is required for auxin-dependent stimulation of secondary growth in plants. Proc Natl Acad Sci U S A *108*, 20242-20247.

Akiyama, K., Matsuzaki, K., and Hayashi, H. (2005). Plant sesquiterpenes induce hyphal branching in arbuscular mycorrhizal fungi. Nature *435*, 824-827.

Alder, A., Jamil, M., Marzorati, M., Bruno, M., Vermathen, M., Bigler, P., Ghisla, S., Bouwmeester, H., Beyer, P., and Al-Babili, S. (2012). The Path from beta-Carotene to Carlactone, a Strigolactone-Like Plant Hormone. Science *335*, 1348-1351.

Bainbridge, K., Sorefan, K., Ward, S., and Leyser, O. (2005). Hormonally controlled expression of the Arabidopsis MAX4 shoot branching regulatory gene. Plant J *44*, 569-580.

Banasiak, J., Biala, W., Staszkow, A., Swarcewicz, B., Kepczynska, E., Figlerowicz, M., and Jasinski, M. (2013). A Medicago truncatula ABC transporter belonging to subfamily G modulates the level of isoflavonoids. J Exp Bot *64*, 1005-1015.

Bennett, M.J., Marchant, A., Green, H.G., May, S.T., Ward, S.P., Millner, P.A., Walker, A.R., Schulz, B., and Feldmann, K.A. (1996). Arabidopsis AUX1 gene: a permease-like regulator of root gravitropism. Science *273*, 948-950.

Beveridge, C.A., Ross, J.J., and Murfet, I.C. (1994). Branching Mutant rms-2 in Pisum sativum (Grafting Studies and Endogenous Indole-3-Acetic Acid Levels). Plant Physiol *104*, 953-959.

Booker, J., Sieberer, T., Wright, W., Williamson, L., Willett, B., Stirnberg, P., Turnbull, C., Srinivasan, M., Goddard, P., and Leyser, O. (2005). MAX1 encodes a cytochrome P450 family member that acts downstream of MAX3/4 to produce a carotenoid-derived branch-inhibiting hormone. Dev Cell *8*, 443-449.

Brewer, P.B., Dun, E.A., Ferguson, B.J., Rameau, C., and Beveridge, C.A. (2009). Strigolactone acts downstream of auxin to regulate bud outgrowth in pea and Arabidopsis. Plant Physiol *150*, 482-493.

Bruggeman, F.J., Libbenga, K.R., and Van Duijn, B. (2001). The diffusive transport of gibberellins and abscisic acid through the aleurone layer of germinating barley grain: a mathematical model. Planta *214*, 89-96.

Butaye, K.M., Goderis, I.J., Wouters, P.F., Pues, J.M., Delaure, S.L., Broekaert, W.F., Depicker, A., Cammue, B.P., and De Bolle, M.F. (2004). Stable high-level transgene expression in Arabidopsis thaliana using gene silencing mutants and matrix attachment regions. Plant J *39*, 440-449.

Cedzich, A., Stransky, H., Schulz, B., and Frommer, W.B. (2008). Characterization of cytokinin and adenine transport in Arabidopsis cell cultures. Plant Physiol *148*, 1857-1867.

Cook, C.E., Whichard, L.P., Turner, B., Wall, M.E., and Egley, G.H. (1966). Germination of Witchweed (Striga lutea Lour.): Isolation and Properties of a Potent Stimulant. Science *154*, 1189-1190.

Crawford, S., Shinohara, N., Sieberer, T., Williamson, L., George, G., Hepworth, J., Muller, D., Domagalska, M.A., and Leyser, O. (2010). Strigolactones enhance competition between shoot branches by dampening auxin transport. Development *137*, 2905-2913.

De Rybel, B., van den Berg, W., Lokerse, A., Liao, C.Y., van Mourik, H., Moller, B., Peris, C.L., and Weijers, D. (2011). A versatile set of ligation-independent cloning vectors for functional studies in plants. Plant Physiol *156*, 1292-1299.

de Saint Germain, A., Ligerot, Y., Dun, E.A., Pillot, J.P., Ross, J.J., Beveridge, C.A., and Rameau, C. (2013). Strigolactones stimulate internode elongation independently of gibberellins. Plant Physiol *163*, 1012-1025.

Delaux, P.M., Xie, X., Timme, R.E., Puech-Pages, V., Dunand, C., Lecompte, E., Delwiche, C.F., Yoneyama, K., Becard, G., and Sejalon-Delmas, N. (2012). Origin of strigolactones in the green lineage. New Phytol *195*, 857-871.

Dhonukshe, P., Huang, F., Galvan-Ampudia, C.S., Mahonen, A.P., Kleine-Vehn, J., Xu, J.A., Quint, A., Prasad, K., Friml, J., Scheres, B., *et al.* (2010). Plasma membrane-bound AGC3 kinases phosphorylate PIN auxin carriers at TPRXS(N/S) motifs to direct apical PIN recycling. Development *137*, 3245-3255.

Enstone, D.E., Peterson, C.A., and Ma, F.S. (2002). Root endodermis and exodermis: Structure, function, and responses to the environment. J Plant Growth Regul *21*, 335-351.

Feraru, E., Feraru, M.I., Kleine-Vehn, J., Martiniere, A., Mouille, G., Vanneste, S., Vernhettes, S., Runions, J., and Friml, J. (2011). PIN Polarity Maintenance by the Cell Wall in Arabidopsis. Current Biology *21*, 338-343.

Foo, E., Turnbull, C.G., and Beveridge, C.A. (2001). Long-distance signaling and the control of branching in the rms1 mutant of pea. Plant Physiol *126*, 203-209.

Foo, E., Yoneyama, K., Hugill, C., Quittenden, L.J., and Reid, J.B. (2013). Strigolactones: Internal and external signals in

plant symbioses? Plant Signal Behav *8*.

Geldner, N., Friml, J., Stierhof, Y.D., Jurgens, G., and Palme, K. (2001). Auxin transport inhibitors block PIN1 cycling and vesicle trafficking. Nature *413*, 425-428.

Gomez-Roldan, V., Fermas, S., Brewer, P.B., Puech-Pages, V., Dun, E.A., Pillot, J.P., Letisse, F., Matusova, R., Danoun, S., Portais, J.C.*, et al.* (2008). Strigolactone inhibition of shoot branching. Nature *455*, 189-194.

Gutjahr, C., and Parniske, M. (2013). Cell and developmental biology of arbuscular mycorrhiza symbiosis. Annu Rev Cell Dev Biol *29*, 593-617.

Hamiaux, C., Drummond, R.S., Janssen, B.J., Ledger, S.E., Cooney, J.M., Newcomb, R.D., and Snowden, K.C. (2012). DAD2 is an alpha/beta hydrolase likely to be involved in the perception of the plant branching hormone, strigolactone. Curr Biol *22*, 2032-2036.

Hayward, A., Stirnberg, P., Beveridge, C., and Leyser, O. (2009). Interactions between auxin and strigolactone in shoot branching control. Plant Physiol *151*, 400-412.

Huang, F., Zago, M.K., Abas, L., van Marion, A., Galvan-Ampudia, C.S., and Offringa, R. (2010). Phosphorylation of conserved PIN motifs directs Arabidopsis PIN1 polarity and auxin transport. Plant Cell *22*, 1129-1142.

Jiang, L., Liu, X., Xiong, G., Liu, H., Chen, F., Wang, L., Meng, X., Liu, G., Yu, H., Yuan, Y.*, et al.* (2013). DWARF 53 acts as a repressor of strigolactone signalling in rice. Nature *504*, 401-405.

Kang, J., Hwang, J.U., Lee, M., Kim, Y.Y., Assmann, S.M., Martinoia, E., and Lee, Y. (2010c). PDR-type ABC transporter mediates cellular uptake of the phytohormone abscisic acid. Proc Natl Acad Sci U S A *107*, 2355-2360.

Kanno, Y., Hanada, A., Chiba, Y., Ichikawa, T., Nakazawa, M., Matsui, M., Koshiba, T., Kamiya, Y., and Seo, M. (2012). Identification of an abscisic acid transporter by functional screening using the receptor complex as a sensor. Proc Natl Acad Sci U S A *109*, 9653-9658.

Kleine-Vehn, J., and Friml, J. (2008). Polar targeting and endocytic recycling in auxin-dependent plant development. Annu Rev Cell Dev Biol *24*, 447-473.

Kleine-Vehn, J., Wabnik, K., Martiniere, A., Langowski, L., Willig, K., Naramoto, S., Leitner, J., Tanaka, H., Jakobs, S., Robert, S.*, et al.* (2011). Recycling, clustering, and endocytosis jointly maintain PIN auxin carrier polarity at the plasma membrane. Mol Syst Biol *7*.

Kohlen, W., Charnikhova, T., Liu, Q., Bours, R., Domagalska, M.A., Beguerie, S., Verstappen, F., Leyser, O., Bouwmeester, H., and Ruyter-Spira, C. (2011). Strigolactones are transported through the xylem and play a key role in shoot architectural response to phosphate deficiency in nonarbuscular mycorrhizal host Arabidopsis. Plant Physiol *155*, 974-987.

Korbei, B., and Luschnig, C. (2013a). Plasma membrane protein ubiquitylation and degradation as determinants of positional growth in plants. J Integr Plant Biol *55*, 809-823.

Korbei, B., and Luschnig, C. (2013b). Plasma membrane protein ubiquitylation and degradation as determinants of positional growth in plants. J Integr Plant Biol *55*, 809-823.

Krecek, P., Skupa, P., Libus, J., Naramoto, S., Tejos, R., Friml, J., and Zazimalova, E. (2009). The PIN-FORMED (PIN) protein family of auxin transporters. Genome Biol *10*.

Kretzschmar, T., Kohlen, W., Sasse, J., Borghi, L., Schlegel, M., Bachelier, J.B., Reinhardt, D., Bours, R., Bouwmeester, H.J., and Martinoia, E. (2012). A petunia ABC protein controls strigolactone-dependent symbiotic signalling and branching. Nature *483*, 341-U135.

Liang, J., Zhao, L., Challis, R., and Leyser, O. (2010). Strigolactone regulation of shoot branching in chrysanthemum (Dendranthema grandiflorum). J Exp Bot *61*, 3069-3078.

Lopez-Raez, J.A., and Bouwmeester, H. (2008). Fine-tuning regulation of strigolactone biosynthesis under phosphate starvation. Plant Signal Behav *3*, 963-965.

McFarlane, H.E., Shin, J.J., Bird, D.A., and Samuels, A.L. (2010). Arabidopsis ABCG transporters, which are required for export of diverse cuticular lipids, dimerize in different combinations. Plant Cell *22*, 3066-3075.

Muller, A., Guan, C., Galweiler, L., Tanzler, P., Huijser, P., Marchant, A., Parry, G., Bennett, M., Wisman, E., and Palme, K. (1998). AtPIN2 defines a locus of Arabidopsis for root gravitropism control. EMBO J *17*, 6903-6911.

Nakamura, H., Xue, Y.L., Miyakawa, T., Hou, F., Qin, H.M., Fukui, K., Shi, X., Ito, E., Ito, S., Park, S.H.*, et al.* (2013). Molecular mechanism of strigolactone perception by DWARF14. Nat Commun *4*, 2613.

Napoli, C. (1996). Highly Branched Phenotype of the Petunia dad1-1 Mutant Is Reversed by Grafting. Plant Physiol *111*, 27-37.

Offringa, R., and Huang, F. (2013). Phosphorylation-dependent Trafficking of Plasma Membrane Proteins in Animal and Plant Cells. J Integr Plant Biol *55*, 789-808.

Paciorek, T., Zazimalova, E., Ruthardt, N., Petrasek, J., Stierhof, Y.D., Kleine-Vehn, J., Morris, D.A., Emans, N., Jurgens, G., Geldner, N., *et al.* (2005). Auxin inhibits endocytosis and promotes its own efflux from cells. Nature *435*, 1251-1256.

Petrasek, J., and Friml, J. (2009). Auxin transport routes in plant development. Development *136*, 2675-2688.

Rasmussen, A., Mason, M.G., De Cuyper, C., Brewer, P.B., Herold, S., Agusti, J., Geelen, D., Greb, T., Goormachtig, S., Beeckman, T., *et al.* (2012). Strigolactones Suppress Adventitious Rooting in Arabidopsis and Pea. Plant Physiology *158*, 1976-1987.

Robert, S., Kleine-Vehn, J., Barbez, E., Sauer, M., Paciorek, T., Baster, P., Vanneste, S., Zhang, J., Simon, S., Covanova, M., *et al.* (2010). ABP1 Mediates Auxin Inhibition of Clathrin-Dependent Endocytosis in Arabidopsis. Cell *143*, 111-121.

Ruyter-Spira, C., Al-Babili, S., van der Krol, S., and Bouwmeester, H. (2013). The biology of strigolactones. Trends Plant Sci *18*, 72-83.

Ruyter-Spira, C., Kohlen, W., Charnikhova, T., van Zeijl, A., van Bezouwen, L., de Ruijter, N., Cardoso, C., Lopez-Raez, J.A., Matusova, R., Bours, R., *et al.* (2011). Physiological effects of the synthetic strigolactone analog GR24 on root system architecture in Arabidopsis: another belowground role for strigolactones? Plant Physiol *155*, 721-734.

Ruzicka, K., Strader, L.C., Bailly, A., Yang, H.B., Blakeslee, J., Langowski, L., Nejedla, E., Fujita, H., Itoh, H., Syono, K., *et al.* (2010). Arabidopsis PIS1 encodes the ABCG37 transporter of auxinic compounds including the auxin precursor indole-3-butyric acid. P Natl Acad Sci USA *107*, 10749-10753.

Sakakibara, H. (2006). Cytokinins: activity, biosynthesis, and translocation. Annu Rev Plant Biol *57*, 431-449.

Sauer, M., Paciorek, T., Benkova, E., and Friml, J. (2006). Immunocytochemical techniques for whole-mount in situ protein localization in plants. Nat Protoc *1*, 98-103.

Sharda, J.N., and Koide, R.T. (2008). Can hypodermal passage cell distribution limit root penetration by mycorrhizal fungi? New Phytol *180*, 696-701.

Shinohara, N., Taylor, C., and Leyser, O. (2013). Strigolactone can promote or inhibit shoot branching by triggering rapid depletion of the auxin efflux protein PIN1 from the plasma membrane. PLoS Biol *11*, e1001474.

Smith, S.M., and Waters, M.T. (2012). Strigolactones: destruction-dependent perception? Curr Biol *22*, R924-927.

Snowden, K.C., Simkin, A.J., Janssen, B.J., Templeton, K.R., Loucas, H.M., Simons, J.L., Karunairetnam, S., Gleave, A.P., Clark, D.G., and Klee, H.J. (2005). The Decreased apical dominance 1/petunia hybrida carotenoid cleavage dioxygenase8 gene affects branch production and plays a role in leaf senescence, root growth, and flower development. Plant Cell *17*, 746-759.

Sorefan, K., Booker, J., Haurogne, K., Goussot, M., Bainbridge, K., Foo, E., Chatfield, S., Ward, S., Beveridge, C., Rameau, C., *et al.* (2003). MAX4 and RMS1 are orthologous dioxygenase-like genes that regulate shoot branching in Arabidopsis and pea. Gene Dev *17*, 1469-1474.

Strader, L.C., and Bartel, B. (2009). The Arabidopsis PLEIOTROPIC DRUG RESISTANCE8/ABCG36 ATP Binding Cassette Transporter Modulates Sensitivity to the Auxin Precursor Indole-3-Butyric Acid. Plant Cell *21*, 1992-2007.

Symons, G.M., Ross, J.J., Jager, C.E., and Reid, J.B. (2008). Brassinosteroid transport. J Exp Bot *59*, 17-24.

Thorpe, M.R., Ferrieri, A.P., Herth, M.M., and Ferrieri, R.A. (2007). 11C-imaging: methyl jasmonate moves in both phloem and xylem, promotes transport of jasmonate, and of photoassimilate even after proton transport is decoupled. Planta *226*, 541-551.

Umehara, M., Hanada, A., Yoshida, S., Akiyama, K., Arite, T., Takeda-Kamiya, N., Magome, H., Kamiya, Y., Shirasu, K., Yoneyama, K., *et al.* (2008). Inhibition of shoot branching by new terpenoid plant hormones. Nature *455*, 195-200.

Wang, Y., and Li, J. (2011). Branching in rice. Curr Opin Plant Biol *14*, 94-99.

Wisniewska, J., Xu, J., Seifertova, D., Brewer, P.B., Ruzicka, K., Blilou, I., Rouquie, D., Benkova, E., Scheres, B., and Friml, J. (2006). Polar PIN localization directs auxin flow in plants. Science *312*, 883.

Xie, X., and Yoneyama, K. (2010). The strigolactone story. Annu Rev Phytopathol *48*, 93-117.

Yang, S.Y., and Paszkowski, U. (2011). Phosphate import at the arbuscule: just a nutrient? Mol Plant Microbe Interact *24*, 1296-1299.

Zazimalova, E., Murphy, A.S., Yang, H.B., Hoyerova, K., and Hosek, P. (2010). Auxin Transporters - Why So Many? Csh Perspect Biol *2*.

Zhao, L.H., Zhou, X.E., Wu, Z.S., Yi, W., Xu, Y., Li, S., Xu, T.H., Liu, Y., Chen, R.Z., Kovach, A., *et al.* (2013). Crystal structures of two phytohormone signal-transducing alpha/beta hydrolases: karrikin-signaling KAI2 and strigolactone-signaling DWARF14. Cell Res *23*, 436-439.

Zhou, F., Lin, Q., Zhu, L., Ren, Y., Zhou, K., Shabek, N., Wu, F., Mao, H., Dong, W., Gan, L., *et al.* (2013). D14-SCFD3-dependent degradation of D53 regulates strigolactone signalling. Nature *504*, 406-410.

3.1 Supplementary: Figures

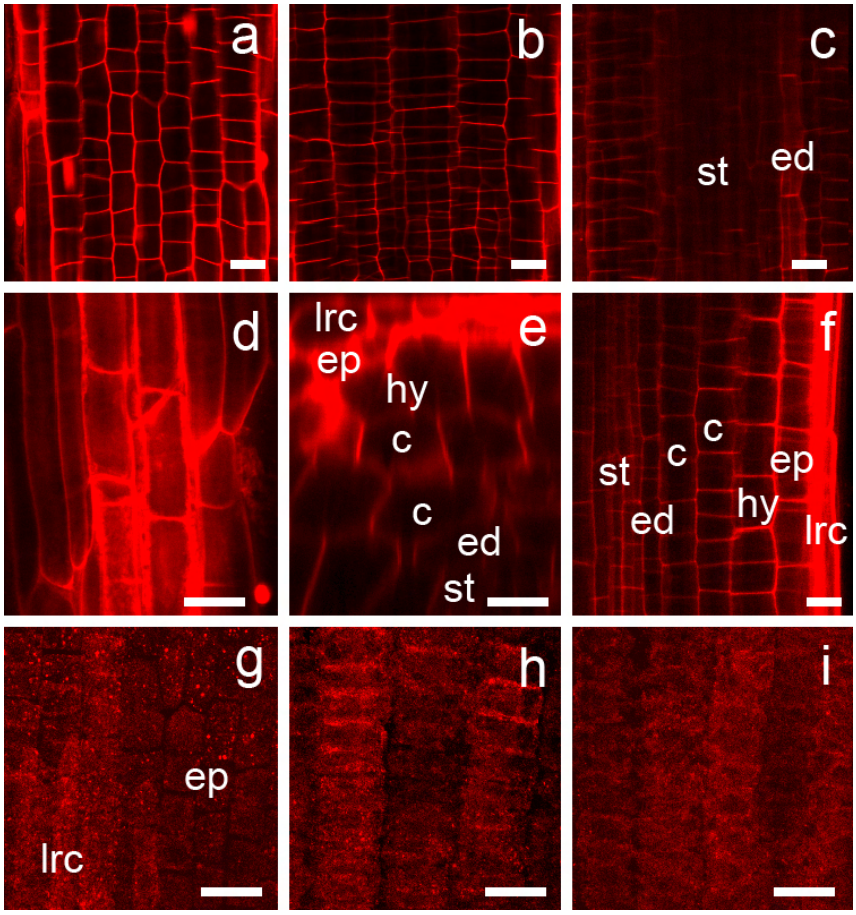

Supplementary Figure 3.1

(a-f) Morphology of cell layers in Petunia root tip, cells walls stained with propidium iodide. **(a)** epidermis. **(b)** hypodermis. **(c)** stele (st) and endodermis (ed). **(d)** lateral root cap cells. **(e)** transversal scanning via confocal microscope of the main root tip, top to bottom from the outer to inner layer: lateral root cap (lrc), epidermis (ep), hypodermis (hy), cortex **(c)**, endodermis and stele. **(f)** longitudinal section of main root tip **(g-i)** Immunolocalization on PDR1-OE seedlings with anti-GFP: **(g)** epidermis (ep) and lateral root cap (lrc), **(h)** hypodermis and **(i)** cortex.

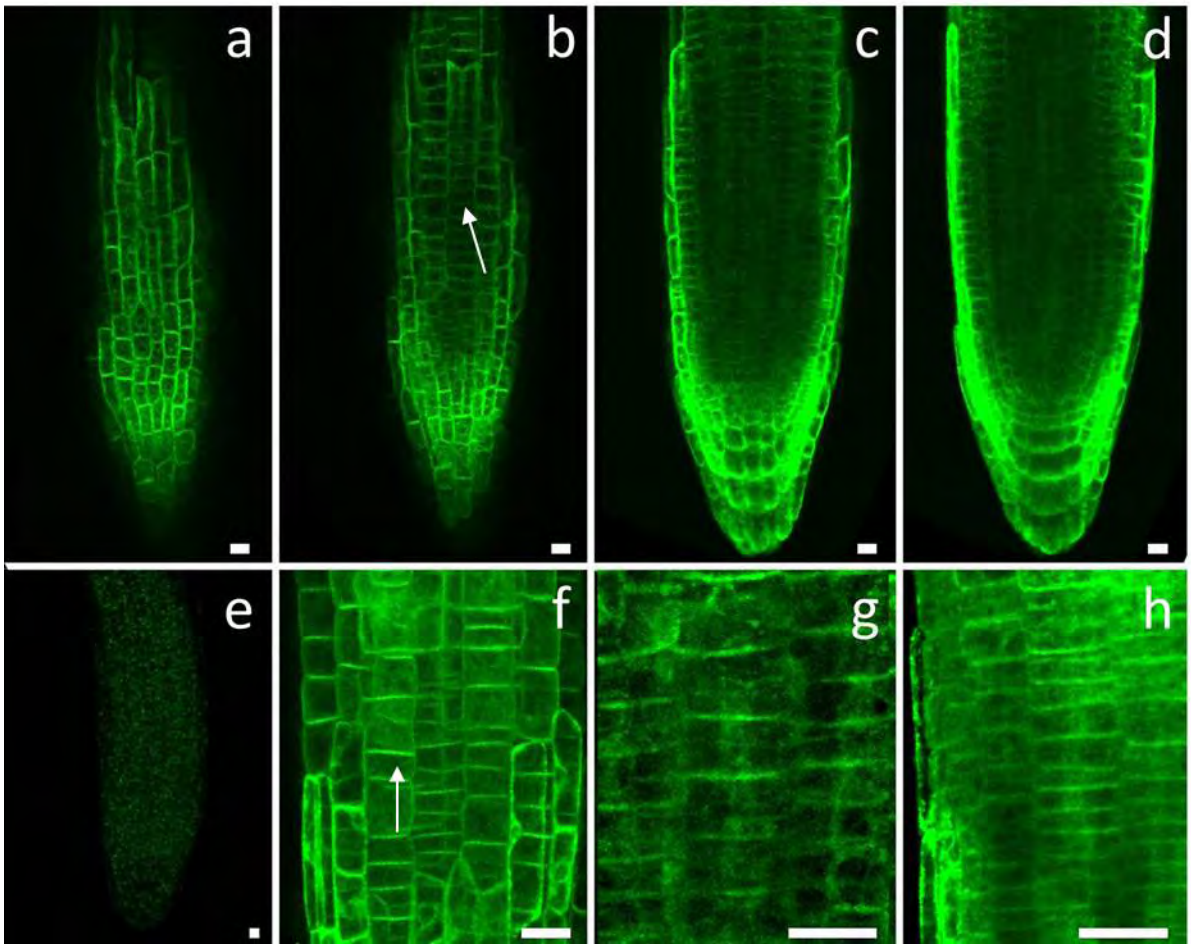

Supplementary Figure 3.2

GFP-PDR1 is asymmetrically localized in root tips of 2 week-old PDR1-OE Arabidopsis, not in the root cap **(a)** but in epidermal **(b, f arrows)** and cortex cells **(c, d)** and magnifications **(g, h). (e)** WT autofluorescence. Scale bars = 20 μm.

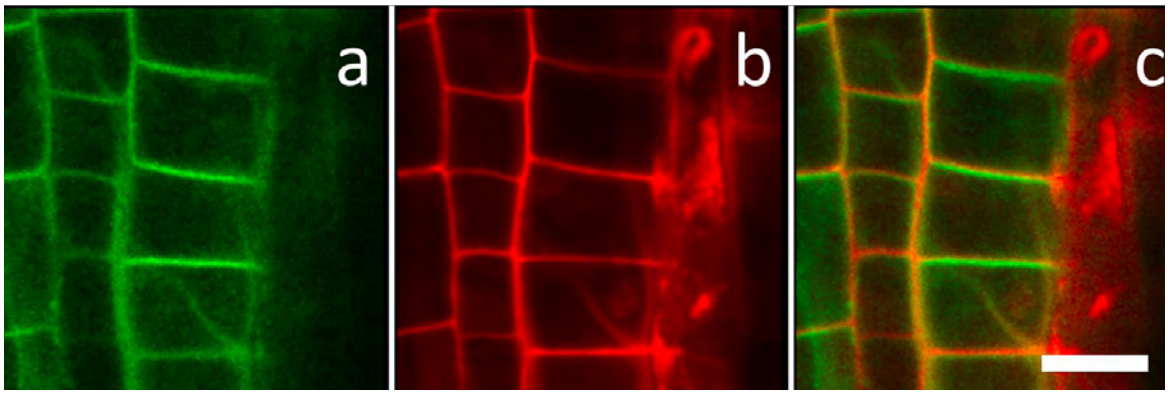

Supplementary Figure 3.3

GFP-PDR1 (green) propidium iodide (red) and co-localization of fully differentiated, root-tip cortex cells **(a-c)** of 10 day-old PDR1-OE Arabidopsis seedlings. GFP-PDR1 is apically localized in cortex cells of root tips. Scale bars = 20 μm.

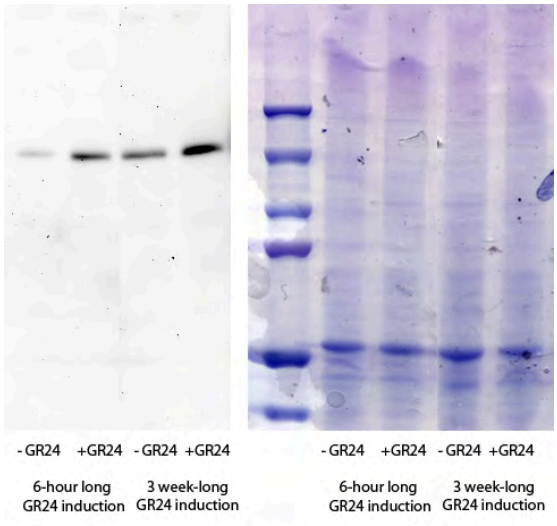

Supplementary Figure 3.4

(a) Protein quantification of GFP-PDR1 via GFP-antibody in 10 day-old PDR1 OE Petunia seedlings induced with 10 μM GR24 for 6 hours and in 3 week-old seedlings germinated on 2.5 μM GR24 MS plates. **(b)** Comassie blue staining: 200 μg of protein (microsomal fraction) were loaded per lane. Both short and long GR24 inductions caused a boost in GFP-PDR1 protein levels, respectively 5 fold and 2 fold, as digitally quantified via ImageJ (http://rsbweb.nih.gov/ij/).

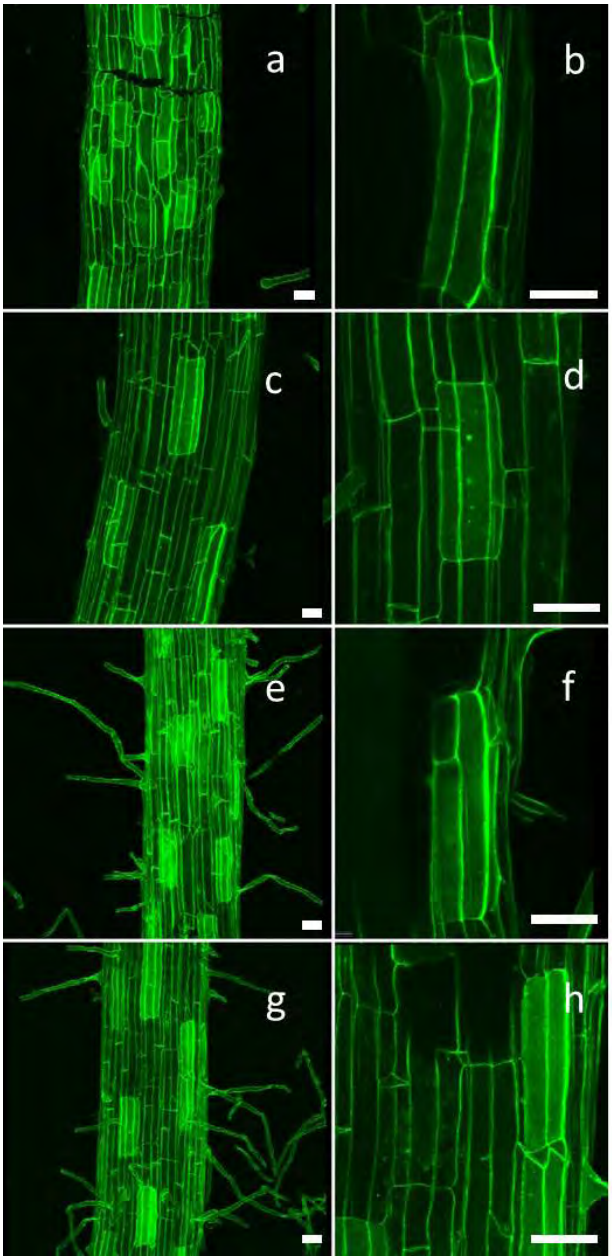

Supplementary Figure 3.5

GFP-PDR1 distal localization in hypodermal passage cells of np-PDR1 Petunia starved on clay and 6 hour-long treated in ½ MS liquid medium **(a, b, mock)** plus either 25 μM BFA **(c, d)** or 10 μM IAA **(e, f)** or 10 μM GR24 **(g, h)**. Incubation with 25 μM BFA triggers the accumulation of small GFP positive vesicles **(d)** in 20% of the analyzed HPC (n = 20). IAA and GR24 treatments boost GFP-PDR1 signaling respectively by 1.6 x and 1.5 x (GFP intensity digital quantified via ImageJ) but none of these treatments alter GFP-PDR1 polarity **(compare f and g to b)**. Scale bars = 20 μm.

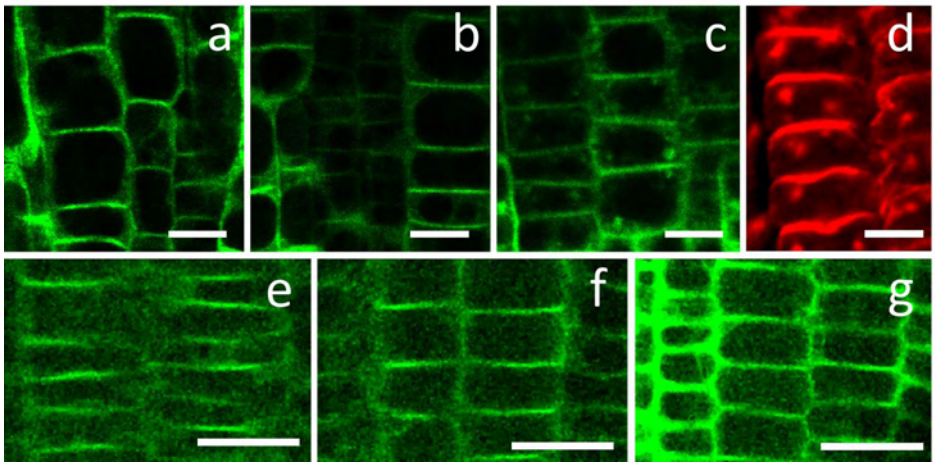

Supplementary Figure 3.6

(a-c) BFA treatments of PDR1-OE Arabidopsis visualized via CLSM. Not treated **(a)** and mock treated plants **(b)** did not show accumulation of GFP positive vesicles, which are present in BFA incubated seedlings in root cortex cells **(c)**. The vesicle accumulation in root tip cells is reminiscent of PIN2 vesicles **(d)** after BFA incubation (AtPIN2 immunolocalization). Mock **(e)** and 24 hour-long treatment with 10 μM GR24 **(f)** and 10 μM IAA **(g)** incubations on 10 day-old PDR1-OE Arabidopsis seedlings in ½ MS medium. Scale bars = 20 μm.

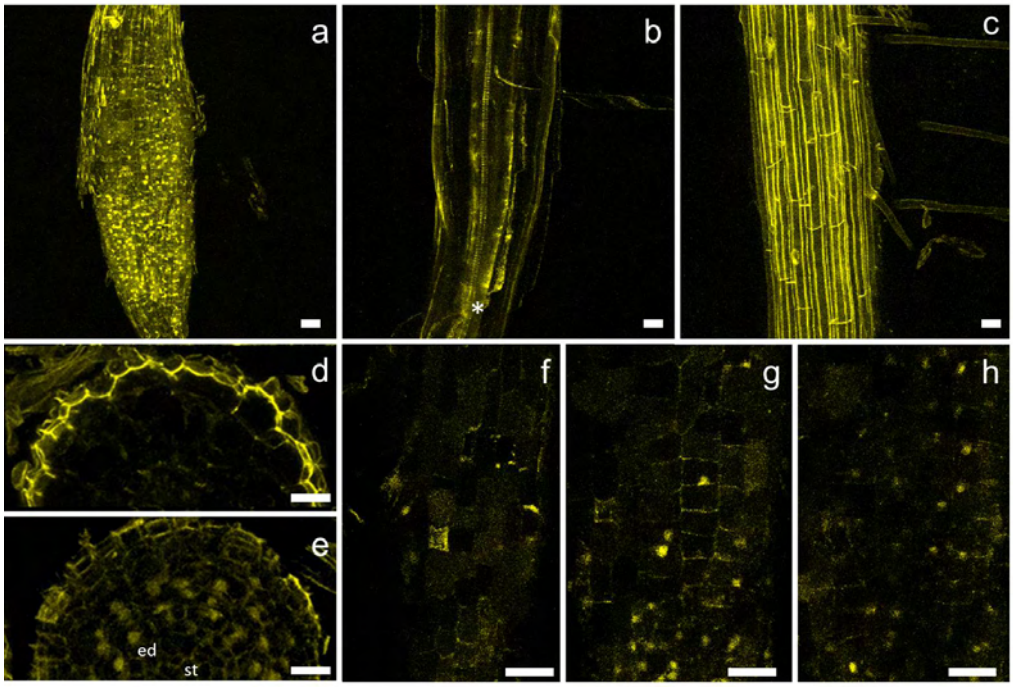

Supplementary Figure 3.7

pDAD1:nls-YFP expression analysis in Petunia root via CLSM. **(a)** DAD1 is expressed in root tips but not in above-root-tip regions where the vasculature **(b, star)** differentiates or in upper root regions (**c** longitudinal, **d** transversal section). **(e, h)** DAD1 is expressed in cortex layers **(e, g, h)** between epidermis (**f**) and endodermis **(e, red)** and absent in the stele (**st**). Scale bars = 20 μm.

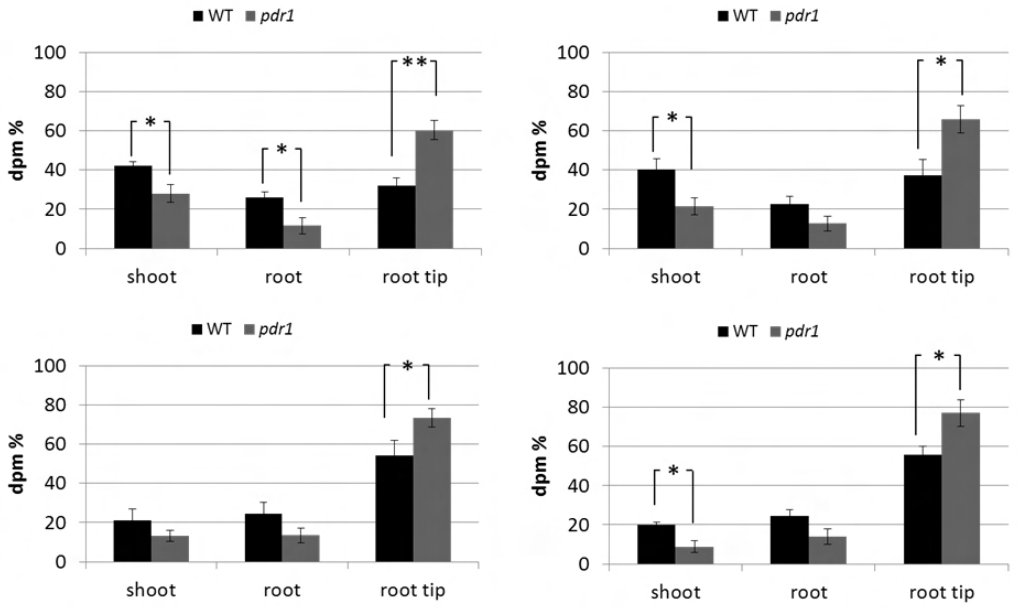

Supplementary Figure 3.8

Transport quantification of radiolabelled GR24 in 0.5 cm root tips, root and shoots in WT and *pdr1* Petunia (4 biological replicates shown, n = 5 to 8 each genotype/experiment). We identified a compatible trend in 7 out of 10 experiments. In 4 out of the 7 abovementioned tests we scored statistically significant differences between wild type and *pdr1* mutants. Root tips covered with a 0.8% agar cube containing 62.5 nM of [H^3]GR24 were incubated 3 hour-long under a neon lamp. Root-tip radioactivity counts were higher in *pdr1* than in WT and lower in shoots and roots, showing accumulation of GR24 in *pdr1* root tips and low root-to-shoot transport capacity. (* = $P < 0.05$; ** = $P < 0.005$; when not indicated, $0.05 < P < 0.1$).

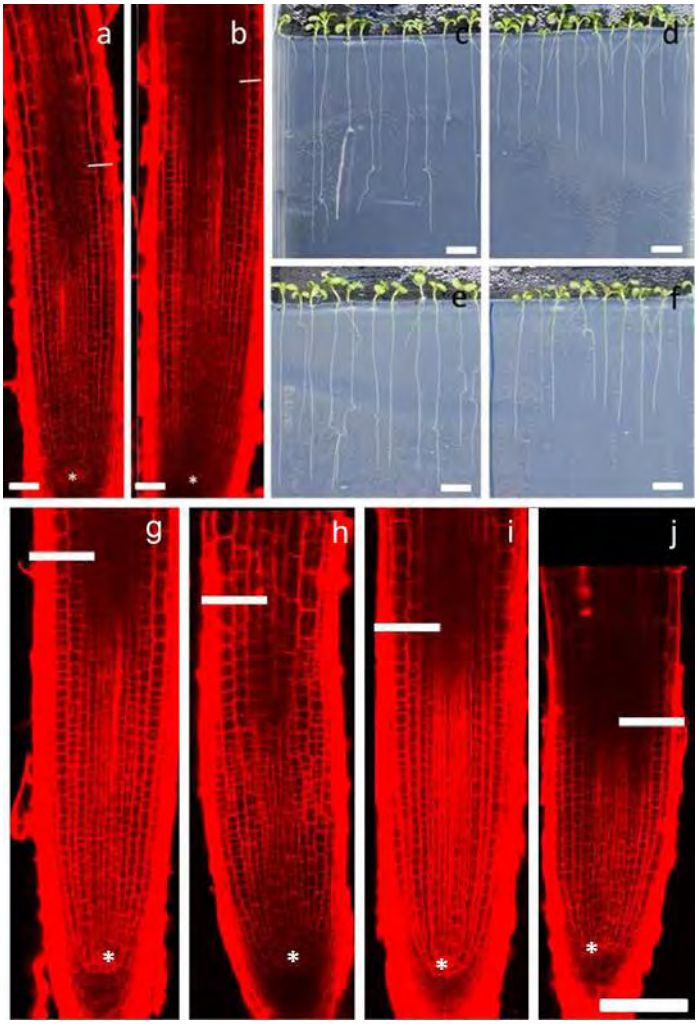

Supplementary Figure 3.9

(a, b) Propidium iodide stained, 2 week-old root tips of WT **(a)** and *pdr1* **(b)** mutant **(star = quiescent center; white line = elongation border)** germinated on 1% sucrose MS plates plus 2.5 μM GR24 and **(c, d)** respective root lengths of the two lines on MS vertical plates. **(e, f)** 2 week-old WT and *pdr1* seedlings grown in 1% sucrose MS plates without additional 2.5 μM GR24. **(g-j)** Propidium iodide staining of Petunia root tips from WT mock **(g)**, *pdr1* mock **(h)**, WT plus 10 μM GR24 **(i)**, *pdr1* plus 10 μM GR24 **(j)** Petunia. Pictures representative of 9 plants each genotype/treatment. Quiescent center (white star) and elongation border (white bar). Scale bars a, b = 100 μm; c - f = 1.5 cm; g - j = 150 μm-

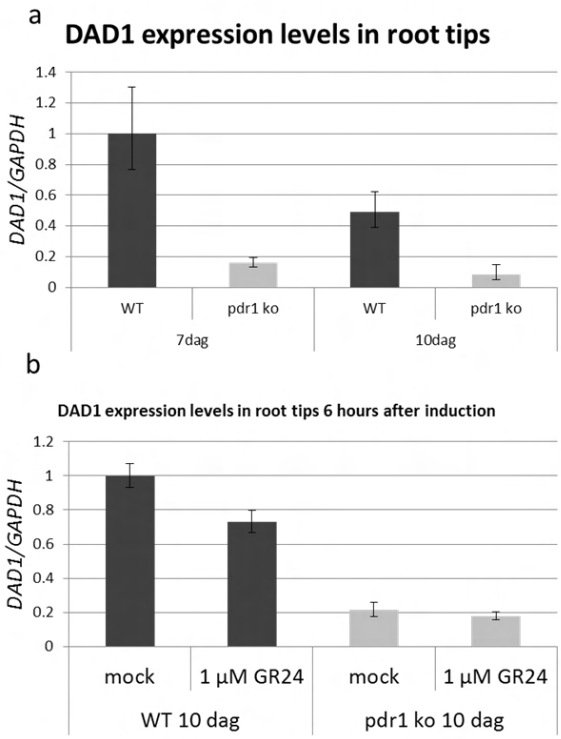

Supplementary Figure 3.10

DAD1 expression relative to *GAPDH* in Petunia root tips. **(a)** *DAD1* is 6x dowregulated in *pdr1* root tips compared to wild type at 7 and 10 days after germination. **(b)** After 6 hours incubation in 1 µM GR24, *DAD1* expression level is 30% decreased in WT seedlings.

4 *Petunia hybrida* PDR2 is Involved in Herbivore Defense by Controlling Sterol Contents

Joëlle Sasse[1], Markus Schlegel[1], Miyoung Lee[1], Lorenzo Borghi[1], José-L. Giner[3], Laurent Bigler[2*], Enrico Martinoia[1*], and Tobias Kretzschmar[1,4]

[1]Institute of Plant Biology, University of Zürich, Zürich, Switzerland

[2]Department of Chemistry, University of Zürich, Zürich, Switzerland

[3]Department of Chemistry, State University of New York, Syracuse, USA

[4]International Rice Research Institute, Manila, Philippines

[*]Corresponding authors

in preparation for submission

4.1 Abstract

Secondary metabolites are of utmost importance for plant defense against herbivores. Many of these substances are stored at high concentrations in glandular trichomes as a first line of defense against pathogens and herbivores. Several Pleiotropic Drug Resistance (PDR) type ABC transporters were described to play a role in pathogen or herbivore defense (Sasabe *et al.*, 2002; Jasinski *et al.*, 2001; Stukkens *et al.*, 2005; Bienert *et al.*, 2012). Here, we report on *Petunia hybrida PDR2*, the first ABC protein involved in herbivore defense for which a biologically active substrate is proposed. PhPDR2 localizes to the plasma membrane and is predominantly expressed in leaf and stem multicellular glandular trichomes. Downregulation of *PhPDR2* activity via RNA interference (*phpdr2*) resulted in a markedly higher susceptibility of the transgenic plants to the generalist foliage feeder *Spodoptera littoralis*. Untargeted screening of *phpdr2* trichome metabolite contents by HPLC showed a significant decrease in petuniasterone and petuniolide content. Those compounds were shown to act as potent toxins against various insects, and they are sterol derived. Therefore, *Ph*PDR2 sheds a new light on sterol transport in plants. Our findings suggest that *Ph*PDR2 plays a leading role in herbivore defense by translocation of sterol-derived compounds in trichomes of Petunia.

4.2 Results and Discussion

Trichomes are epidermal protrusions that have distinct roles in abiotic and biotic stress. On one side, they lower irradiation and hinder movement of organisms on the leaf surface. On the other side, glandular trichomes store high levels of secondary metabolites in their heads that are poisonous, or that attract predators of the herbivores (Wagner, 1991; Allmann and Baldwin, 2010). Most of these metabolites are toxic not only for the pathogens and herbivores but similarly for the plant. It is therefore crucial for the plant to actively maintain a steep metabolite concentration gradient between the trichome and leaf cells, as well as between trichome stalk and head. Such transporters involved in establishment and maintenance of high concentrations of secondary metabolites in trichomes are largely unknown.

ATP-binding cassette (ABC) transporters constitute a large protein family present in all phyla. They can create steep concentration gradients since they are directly energized by ATP (Theodoulou, 2000; Verrier *et al.*, 2008). All members of the full-size ABCG (former PDR) subfamily characterized to date in plants localize to the plasma membrane, and many of them have been described to be involved in terpenoid transport (Kang, 2010c; Kretzschmar *et al.*, 2012; van den Brule *et al.*, 2002; Jasinski *et al.*, 2001). These characteristics make ABCGs good candidates to enrich secondary metabolites in trichomes (Yazaki, 2006). We were therefore interested in ABCG sequences that show elevated expression in trichome tissue compared to leaf tissue. We extracted *Petunia hybrida* cultivar W115 cDNA of mechanically collected trichomes and of leaves devoid of trichomes. We then amplified 0.5 kilobase (kb) fragments from both tissues with primers annealing to conserved regions of the second nucleotide binding domain (NBD).

The 44 cloned and sequenced fragments could be assigned to four of the five clusters of PDR proteins (Figure 4.1 A, Crouzet *et al.*, 2006), and the sequence fragments were named in ascending order starting with *PhPDR2*. We first investigated phylogenetic relationships of the newly identified *Petunia* PDR sequences to already described members of this subclass (Figure 4.1 B).

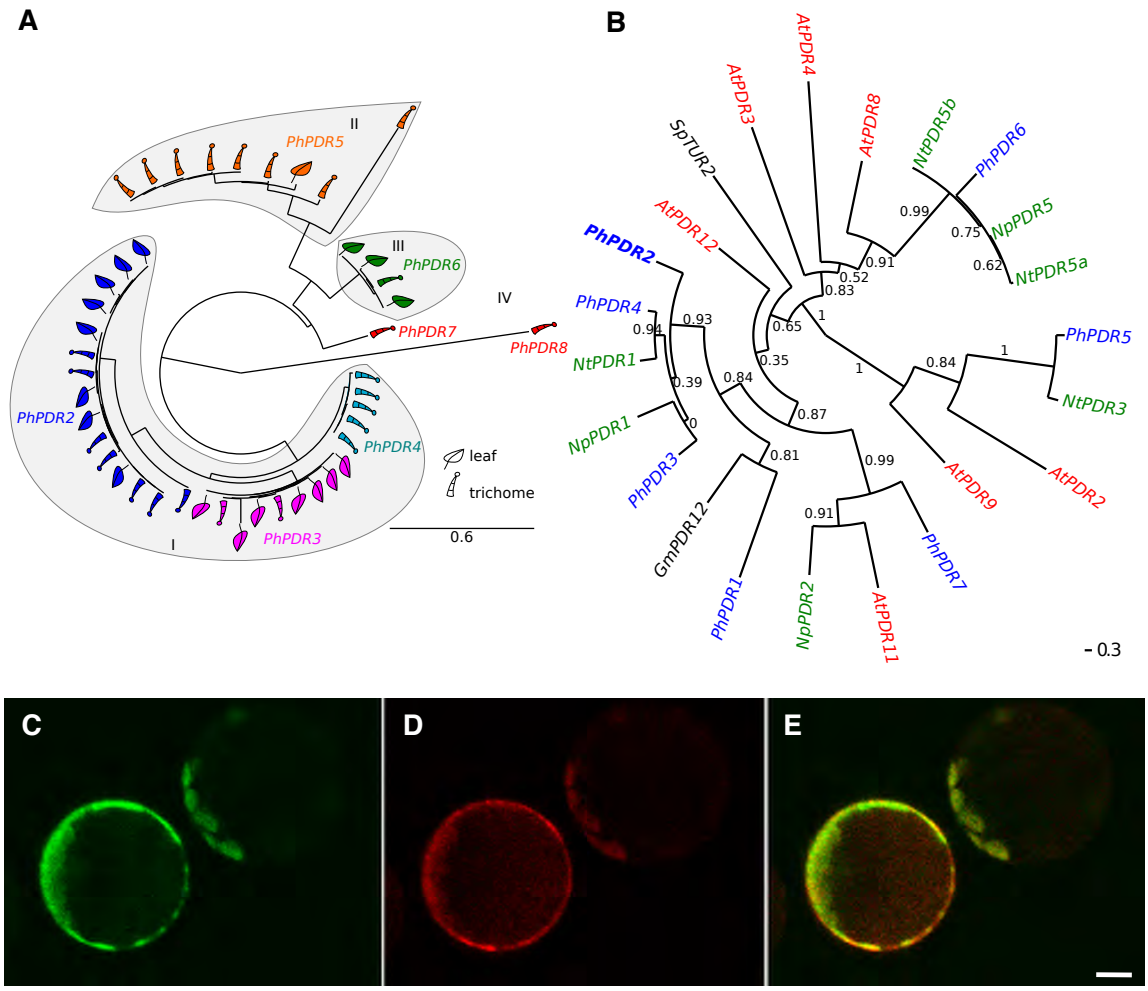

Figure 4.1: PhPDR2 is expressed in leaves and trichomes and localizes to the plasma membrane

A, Maximum likelihood tree for *PhPDR* fragments amplified with primers binding to Walker A and PDR signature 4 of second NBD, expressed in leaves and trichomes. Sequences are named with ascending numbers. PDR clusters are visualized with grey shading, and the cluster number is indicated with roman numerals. **B**, Phylogeny of *PhPDR2 - PhPDR7* fragments (blue) and the respective fragments, identified by sequence similarity, of reported PDR sequences of *A. thaliana* (red), *N. tabacum* and *N. plumbaginifolia* (green), *Spirodela polyrrhiza* (black), and *Glycine max* (black). PhPDR8 was excluded from the analysis due to low sequence similarity. **C-E,** *A. thaliana* protoplasts were transiently transformed with *35S::GFP-PDR2* **(C)** and a plasma membrane marker **(D).** E, overlay. Scale bar: 5 µm.

A well-characterized gene of cluster III is *Nicotiana tabacum PDR5* (*NtPDR5*) that is induced in leaves upon several treatments, but is absent from trichomes (Bienert *et al.*, 2012). The *PhPDR6* fragment showed high similarity to *NtPDR5*, and was mainly expressed in leaves. As trichomes were mechanically collected, it could be that the one clone identified in trichome tissue resulted from a contamination of the trichome tissue sample with some epidermal leaf cells. For *NtPDR3,* a member of cluster II (Ducos *et al.*, 2005), tissue specific expression was not reported. Highly similar *PhPDR5* fragments originated from trichome tissue only. Likewise, the expression pattern of cluster IV *N. plumbaginifolia PDR2* (*NpPDR2*, Trombik *et al.*, 2008) was not reported yet, whereas

the *Petunia* fragments *PhPDR7* and *PhPDR8* that were most similar to *NpPDR2* originated from trichome tissue. However, the *Petunia* sample size was in this case not big enough to be able to speculate about gene expression patterns. Among the best characterized PDR proteins is the trichome-localized *NtPDR1* belonging to cluster I of PDR proteins (Crouzet *et al.*, 2013; Stukkens *et al.*, 2005). The *PhPDR4* fragments showed high similarity to *NtPDR1*, and were similarly only identified in trichome, but not in leaf tissue. *PhPDR3* sequences originated mainly from leaf tissue and clustered with *NpPDR1* that was reported to be expressed in leaf tissue upon pathogen infection and constitutively in glandular trichomes (Bultreys *et al.*, 2009; Stukkens *et al.*, 2005). The largest set of eight leaf and seven trichome *Petunia PhPDR2* fragments did not cluster with a published PDR sequence. We thus decided to investigate its role in *Petunia*. A complete phylogenetic tree with all reported PDR sequences of Petunia, tomato, rice, Arabiopsis, and *Nicotiana sp*. can be found in Supplementary Figure 4.1.

The full length *PhPDR2* cDNA sequence was cloned from W115 trichome cDNA, revealing an ORF of 4293 base pairs (bp), an 5' UTR of 136 bp, 3' UTR of 253 bp followed by a poly-A tail, resulting in a cDNA size of 4705 bp (Supplementary Figure 4.2 A, see 9.1). The predicted polypeptide residues features a reverse organization of the two NBDs and the transmembrane domains (TMDs), which is exclusively found in full size ABCG type transporters (Supplementary Figure 4.2 B). The *PhPDR2* NBDs embody the ATP-binding Walker A and B motifs, the ABC signatures (Martinoia *et al.*, 2002), and all four PDR signatures (Supplementary Figure 4.2 C). Phylogenetic analysis placed *Ph*PDR2 within Cluster I of PDR subclusters, with *Np*PDR1, *Nt*PDR1, *Gm*PDR12, and *At*PDR12 as closest relatives (Supplementary Figure 4.1). The 7544 bp DNA sequence of *PhPDR2* was cloned from W115 leaf DNA, revealing presence of 20 exons (Supplementary Figure 4.2 A, see 9.1). The sequence was fused to an N-terminal GFP reporter under the control of the *35S* promoter. *Arabidopsis thaliana* mesophyll protoplasts were transiently co-transformed with the *35S:GFP-gPDR2* construct and a plasma membrane marker. The two signals co-localized, indicating presence of *Ph*PDR2 at the plasma membrane (Figure 4.1 C-E).

Analysis of *PhPDR2* transcript abundance in various plant tissues revealed ubiquitous expression in full, intact leaves and more prominently in trichomes. Additionally, transcripts were detected in stems, seedlings, roots, and at low amounts in flowers (Figure 4.2 A). In order to obtain a more detailed picture of *PhPDR2* expression

on a sub tissue level, a 1.2 kb genomic fragment upstream of the *PhPDR2* CDS was fused with the GUS reporter gene and stably transformed into W115 (see 9.2). In foliar tissue, *PhPDR2* promoter activity was found exclusively around the leaf margins (Figure 4.2 B) and in the multicellular glandular trichomes (Figure 4.2 C, D), as well as in epidermal cells basal to the trichomes (Figure 4.2 E, F). In stem tissue, expression was likewise confined to trichomes (Figure 4.2 G). Belowground, promoter activity was pronounced in and around developing and emerging lateral root primordial (Figure 4.2 H), whereas emerging lateral root tips were devoid of signal (Figure 4.2 I). The presence of *PhPDR2* transcript in flower tissue was confirmed similarly (Figure 4.2 J).

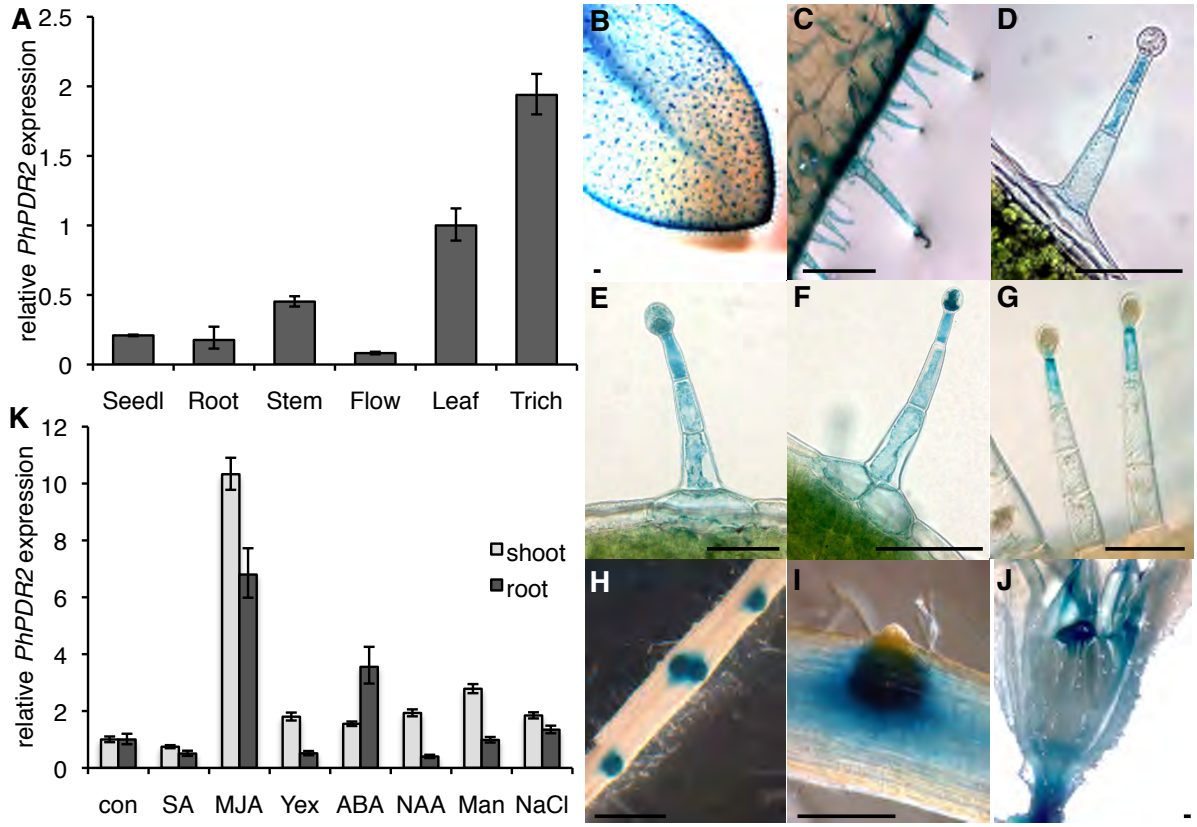

Figure 4.2: *PhPDR2* is expressed in leaf and stem trichomes and it is induced by jasmonic acid

A, Quantitative PCR for *PhPDR2* in aboveground parts of 14-day-old seedlings and in different organs of a 2-month-old plant. Abbreviations: seedling (Seedl), flower (Flow), trichome (Trich). Data are depicted as means ± S.E.M (n = 3). **B-J**, p*PhPDR2*::GUS signal of a two-month-old W115 plant in leaf **(B),** in leaf trichomes with one or two basal epidermal cells **(C - F)**, and in stem trichomes **(G)**, in the main root **(H)**, at site of lateral root emergence **(I)**, in a flower **(J)**. Scale bars are 1 mm. **K,** Quantitative *PhPDR2* PCR in 24-day-old seedling root (light grey) and shoot (dark grew) treated with water, salicylic acid (SA), methyl jasmonate (MJA), abscisic acid (Aba), auxin (Naa), yeast extract (Yex), mannitol (Man), and sodium chloride (NaCl). Data are depicted as means ± S.E.M. (n = 3).

PhPDR2 expression at leaf borders (Figure 4.2 B) suggested a deposition of *Ph*PDR2 substrates in this tissue. The deposition of deterrents and toxins in leaf borders can serve as a first line of defense. The same is true for trichome-localized substances since

some herbivore preferentially initiate their feeding at this location. In addition, *PhPDR2* expression was detected in all trichome cells (Figure 4.2 C-F), and although intensities of GUS signals have to be interpreted with caution, the increasing GUS stain intensity from the base towards the top of the trichome could suggest increasing transporter amounts towards the top that could enrich secondary metabolites in the trichome head. An apical plasma membrane localization of *Ph*PDR2 would result in transport of substances from basal to apical trichome cells, and in a considerable increase of substrates in trichome heads. This mechanism would avoid interference of the substrates with plant leaf metabolism and ensure a most powerful effect on herbivores that burst the head of trichomes, either by movement or by feeding. Further studies with GFP-*Ph*PDR2 fusion proteins under control of constitutive and native promoters are necessary to resolve the outstanding localization questions.

PhPDR2 expression in trichomes pointed towards an involvement in plant defense. Generally, plant responses to microorganisms depend on salicylic acid (SA), whereas responses to herbivory attack induce jasmonic acid (JA) dependent signaling pathways (Bodenhausen and Reymond, 2007). Multiple *ABCGs* are responsive to JA or methyl jasmonate (MJA) treatment (Moons, 2008; Sasabe *et al.*, 2002; Stukkens *et al.*, 2005; Ducos *et al.*, 2005; Bienert *et al.*, 2012), indicating that many ABCGs may be involved in herbivore response. Thus, *PhPDR2* response in seedlings to SA and JA treatment was investigated. Simultaneously, the response to the general fungal elicitor yeast extract was tested. To examine *PhPDR2* involvement in abiotic stress, we analyzed its transcriptional response to abscisic acid (ABA), a phytohormone involved in water stress, and in response to mannitol and sodium chloride, representing osmotic and salt stress factors, respectively (Figure 4.2 K). *PhPDR2* transcripts accumulated markedly in seedling roots and shoots treated with MJA, pointing towards an involvement of *PhPDR2* in herbivore defense. However in mature plants, *PhPDR2* was not responsive to MJA treatment any more (Supplementary Figure 4.3 D-G). The inducibility of *PhPDR2* in seedlings but not in adult plants might reflect a specific defense strategy*:* In young plants, energy could be invested mainly in growth and to a lower extent in synthesis of defense compounds that are only produced upon attack, whereas in older plants, energy could be directed more to reproduction and stress protection, resulting in higher average levels of defense compounds and in a lower responsiveness to herbivory. Consistent with this hypothesis is the fact that *PhPDR2* expression level in leaves of

adult plants are about four fold higher than in seedlings, and that treatment of seedlings with MJA results in *PhPDR2* expression levels comparable to the one of adult plants (Figure 4.2 A).

To further investigate our hypothesis of *Ph*PDR2 involvement in herbivore defense, the gene was silenced with a RNAi construct targeting the 3' end and the 3' UTR of the gene. As Petunia is not sequenced yet, it is not possible to exclude that the RNAi targeted against *PhPDR2* affected close *PhPDR2* homologues. We show that the construct targets *PhPDR2* (Figure 4.3 A), and the following results are discussed in this respect. The three W115 *PhPDR2*-RNAi lines *phpdr2*^{1}, *phpdr2*^{2}, and *phpdr2*^{3}, displayed high to moderate *PhPDR2* transcript silencing, and thus, they were chosen for further analysis (Figure 4.3 A).

Caterpillars of the generalist herbivore *Spodoptera littoralis* were fed on *phpdr2* and on the respective wild-type leaves. Absolute increase in larval weight and larval mortality were monitored for second instar larvae displaying the same initial average weight. From day 5 until day 16 of feeding, significantly higher increase in average weight and lower mortality could be detected in larvae feeding on *phpdr2* leaves compared to such feeding on W115 leaves. For example on day 13, changes of survival were nine times higher on *phpdr2* leaves than on wild-type leaves, and weight gain of larvae was 3.8 fold higher (Figure 4.3 B, C). Silencing of *PhPDR2* most probably leads to a decrease of *Ph*PDR2 protein and transport capacity levels. From the abovementioned experiments we concluded that *phpdr2* leaves are less toxic to the caterpillars that the corresponding wild-type leaves. The lower toxicity level of *phpdr2* lines can either be explained by a decreased transport of the toxin itself, possibly coupled to a negative feedback on the toxin biosynthesis, or by a decreased transport of a precursor for a toxin.

The reduced toxicity of *phpdr2* leaves compared to the respective wild type (Figure 4.3 B), together with the induction of *PhPDR2* by MJA in seedlings (Figure 4.2 A), indicate a role of *Ph*PDR2 in herbivore defense. To date, *Nt*PDR5 is the only PDR protein reported to be involved in herbivore defense. Similar to *PhPDR2*, *NtPDR5* silenced plants are more susceptible to herbivore feeding, and protein levels are increased upon MJA treatment (see Figure 4.2 K, Figure 4.3, Bienert *et al.*, 2012). Unlike *PhPDR2*, *NtPDR5* is induced in leaf tissue upon mechanical wounding, application of *Manduca sexta* oral secret or feeding (see Supplementary Figure 4.3, Bienert *et al.*, 2012). *Nt*PDR5 is not detected in trichomes (Bienert *et al.*, 2012). The differential expression of *PhPDR2* in

trichomes and leaf borders and *Nt*PDR5 in leaf, respectively, suggest deviating roles of the two proteins in defense responses. The expression of *PhPDR2* at the borders of the leaves and in trichomes indicate that this transporter is involved in the first line of defense, whereas *Nt*PDR5 appear to be more part of a general defense strategy.

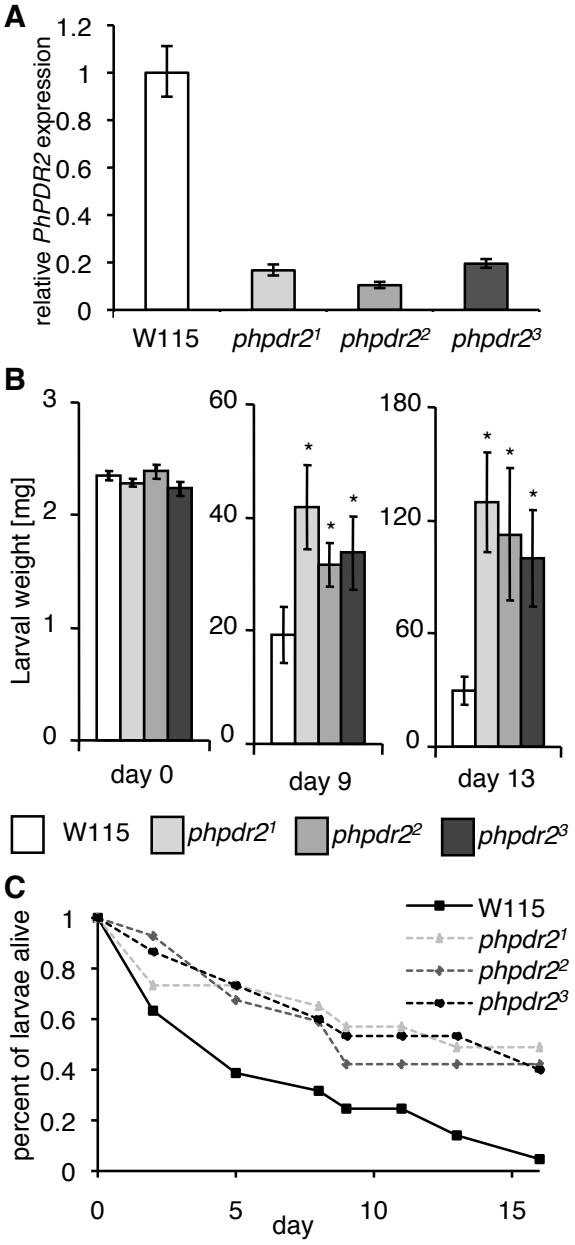

Figure 4.3: *Spodoptera littoralis* feeding on *phpdr2* and wild-type plants

A, Quantitative PCR shows downregulation of *PhPDR2* in *phpdr2* lines compared to wild type. **B-C**, *S. littoralis* second instar larvae feeding experiments over 16 days on 3-month-old *phpdr2* lines 1 – 3 (grey bars and symbols) or on wild type (white bars and symbols). Depicted are weight gain over time **(B)**, data are means ± S.E.M. (n = 30), $P = 0.05$, or as survival rate over time **(C)**. The experiments shown are representatives for three experiments performed.

A second indication for deviating roles of *Ph*PDR2 and *Nt*PDR5 in herbivore defense is their distant phylogenetic relationship (Supplementary Figure 4.1). The *Ph*PDR2 sequence is more closely related to *Nt*PDR1 and *Np*PDR1, which were only described to play a role in pathogen response to date. Similar to *PhPDR2*, the Nicotiana proteins are induced by JA treatment, and they localize to trichomes (Sasabe *et al.*, 2002; Stukkens *et al.*, 2005; Crouzet *et al.*, 2013; Bultreys *et al.*, 2009).

Glandular trichomes store a wide variety of metabolites belonging to different secondary metabolite classes. Among them are terpenoids, phenylpropenes, polyketides, fatty acid derivatives, and acyl sugars (Schilmiller *et al.*, 2008; Slocombe *et al.*, 2008; Wang *et al.*, 2001). PDR proteins of cluster I were shown to be involved either in terpenoid transport or more specifically, many were shown to be involved in sclareol transport (van den Brule *et al.*, 2002; Campbell *et al.*, 2003; Jasinski *et al.*, 2001; Crouzet *et al.*, 2013). Sclareol is an antifungal diterpene that is secreted on the plant surface in *Nicotiana sp.*, also affecting plant growth (Cutler *et al.*, 1977). In consequence, we performed assays to investigate whether *PhPDR2* may be involved in this process, but our observations did not point towards an involvement of *Ph*PDR2 in sclareol transport (Supplementary Figure 4.4). As our targeted approach did not result in identification of a substrate, we chose a broader approach to learn about *Ph*PDR2 substrates by performing an untargeted metabolomic approach.

Trichome metabolite contents have been investigated in tomato (Kang *et al.*, 2010a; Kang *et al.*, 2010b). The authors showed that mechanical removal of trichomes and a leaf dip approach resulted in similar metabolite detections. Hence, we applied both sampling methods to trichomes of *phpdr2* and W115 wild-type lines, following the extraction and analysis protocols of the abovementioned publications. Experiment 1 included mechanical removal of trichomes, whereas experiments 2 and 3 included leaf washes of greenhouse-grown, and sterile-grown plants, respectively. The extracts were analyzed with ultra-high performance (UHPLC) high-resolution mass spectrometry (HR-MS). The resulting LC-MS data was statistically evaluated with the Bruker ProfileAnalysis™ application, a statistic tool enabling unsupervised principal component analysis (PCA). Sixteen conspicuous candidate masses with MS signal intensities lower than 50% were identified in two or more *phpdr2* lines compared to the wild type (Supplementary Table 4-1). Chemical database searches on SciFinder® revealed that nine chemical formulae could be attributed to Petunia sterol compounds (Table 4-1). The structure of the

further seven metabolites could not be identified so far. The intensities of two Flavonoids reported for Petunia were analyzed to investigate whether the reduction of Petunia sterol compounds in *phpdr2* lines was specific for this compound class or if in general, secondary metabolite amounts were lower compared to wild type. The two Flavonoids were detected in similar amounts in *phpdr2* and wild type, suggesting that the lower amounts of Petunia sterols in *phpdr2* lines is a specific effect (Table 4-1, Zerback *et al.*, 1989).

Table 4-1: Petunia sterol content reduction in *phpdr2* line pools of experiment 2

Compound	Mass	Time	EIC integration			XCMS analysis		
	m/z	(min)	Intensity	Fold	*P*-value	Intensity	Fold	*P*-value
Petuniasterone A acetate	601.3197	6.6	5	2.0	0.017	5	2.1	0.012
Petuniolide E	487.3055	5.82	3	3.3	1.73E-04	4	3.5	2.90E-04
Petuniolide F	503.3010	4.99	2	2.5	6.31E-03	3	2.6	8.20E-03
	503.3004	4.70	3	1.9	1.17E-03	3	2.2	1.40E-03
		3.90	1	1.9	0.010	1	1.7	0.028
		5.60	2	3.7	1.13E-04	2	3.6	1.80E-04
Petuniasterone G	461.3262	4.22	2	4.9	5.09E-03	4	5.6	0.010
		5.13	2	7.04	7.12E-03	3	7.8	0.013
Petuniolide C	501.2850	4.85	2	6.9	3.44E-03	3	6.0	9.70E-03
Petuniasterone J	601.3368	5.13	1	2.3	0.019	1	2.3	0.017
Petuniasterone H	521.3465	4.79	1	4.9	7.44E-04	1	5.1	3.30E-04
Q-3-GluGal	625.1410	2.20	2	1.0	0.954	2	1.2	0.505
K-3-GluGal	609.1462	2.35	2	1.0	0.709	2	1.1	0.603

List of metabolites with a sterol structure found to be reduced in *phpdr2* leaves and of two flavonoids (depicted are fold differences of means of *phpdr2,*[1] *phpdr2*[2]*, and phpdr2*[3] compared to wild-type leaves). The accurate masses and retention times of the respective compounds are given. Signals corresponding to the mass of petuniolide F and petuniasterone G, respectively, were detected at several retention times and could not be assigned. The relative peak area of the respective masses is given (mean integrated peak areas, 5 = high, 1 = low), as well as the fold reduction of the *phpdr2* lines compared to wild type, and the *P*-value of the reduction, for both, extracted ion chromatograms (EIC) manually integrated, and for unpaired parametric t-test (Welch t-test) data processing with the XCMS software (Tautenhahn *et al.*, 2012), respectively. All Petunia sterol candidates were identified in (+) ESI, whereas the Flavonoids were identified in the (-) ESI, respectively. Q-3-GluGal: Quercetin 3-*O*-(2''-*O*-*β*-D-glucopyranosyl)-*β*-D-galactopyranoside. K-3-GluGal: Kaempferol 3-*O*-(2''-*O*-*β*-D-glucopyranosyl)-*β*-D-galactopyranoside (Zerback *et al.*, 1989). The chemical formula of the candidates is depicted in Supplementary Table 4-2.

Petunia sterols were first identified in Petunia leaves 1988 (Elliger *et al.*, 1988b; Elliger *et al.*, 1989b) within a screen for substances exhibiting toxicity to insect larvae. The compounds identified contained a ketone mojety on the A-ring, and thus, the substances were termed petuniasterones. Follow up studies described several more petuniasterones, petuniolides, and their derivatives of high, low, or no toxicity to a whole variety of caterpillars, among them the *Solanaceae* specialist *M. sexta*, or the

Spodoptera sp. generalists (Elliger and Waiss, 1991). Because we applied a similar extraction protocol as described for the characterization of petuniasterones, because of the reduced amounts of Petunia sterols masses in *phpdr2* samples, and because of the decreased toxicity effect observed in *phpdr2* leaves, we concluded that *Ph*PDR2 could be involved in transport of Petunia sterols.

According to literature, approximately 50 different Petunia sterols were characterized in several Petunia species, such as *P. hybrida, P. integrifolia*, *P. inflata*, *P. axillaris*, and *P. parodii*. Because some of the them share the same chemical formula, 37 extracted ion chromatograms (EICs) were calculated out of the UHPLC-HR-ESI-MS-data. We identified 62.2% of these chemical formulae in our dataset, whereof 65.2% were of lower intensities in *phpdr2* leaves compared to wild-type leaves (*P*-value ≤ 0.05). Among the formulae detected in lower amounts in *phpdr2* lines were several petuniasterones and petuniolides. Intensities of formulae corresponding to several petuniasterones remained unchanged, and other sterol structures such as glycosylated molecules or sterols coupled to a pyridine ring that have been described were not detected (see Supplementary Table 4-2, Elliger *et al.*, 1992b; Shingu *et al.*, 1994). This may be due to an absence of these substances from our samples, or due to the extraction method applied. Still, we cannot exclude the possibility that they are substrates of *Ph*PDR2.

It was suggested that petuniolide C is the most relevant toxin in *P. parodii* because of its high toxicity (amount causing reduction to 50% growth of untreated, ED_{50}: *Heliothis zea* 3 ppm, *S. littoralis* 69 ppm) and abundance (average 300 mg kg^{-1} DW, Elliger and Waiss, 1991). Indeed, we identified petuniolide C in our samples; however, it was present in lower amounts than petuniolide E or F. The divergence to published data could be due to different metabolite abundance in *P. hybrida*, or due to the slightly different extraction methods. It was further suggested that the total petuniolide content of *P parodii* leaves is approximately 20 times ED_{50}. We were not able to determine absolute amounts of petuniasterones or petuniolides in our samples. Despite this, we observed a 50% or more reduction of prominent candidate masses in *phpdr2* lines compared to wild type, and also in *S. littoralis* feeding experiments, we observed a 50% reduction in mortality (Figure 4.3). Thus, we conclude that in *phpdr2* lines, major defense compounds are less abundant. We observed considerable variation in candidate masses within single lines of one experiment, and within lines between different

experiments. Similarly, published results showed up to four-fold variation of petuniolide C in field-grown *P. parodii* (240 - 920 mg kg^{-1} DW). The authors could not explain the trend by seasonal variation (Elliger and Waiss, 1991), and we could not correlate the variation to a specific line or collection method. Despite this, the mean of single Petunia sterols, as well as the sum of all Petunia sterols of *phpdr2* lines versus the wild type, was significantly reduced in all experiments.

Besides the masses corresponding to known Petunia sterols, further masses were present in lower amount in *phphdr2* lines (Supplementary Table 4-1). The corresponding chemical formulae have not been described for Petunia so far. We could not further characterize these candidates , *e.g.* with MS/MS experiments, and therefore, we cannot exclude that some of them may also be involved in herbivore responses of Petunia. However, Petunia sterols were shown to be very potent toxins, and considering the vast amount of structures stored in databases even for *Petunia sp*., we are convinced that the identification of more than 50% of the compounds as petuniasterones and petuniolides is not casual. We therefore conclude that *Ph*PDR2 is involved in transport of Petunia sterols, or of their biosynthetic precursor.

With our analysis, we cannot determine if the Petunia sterols are themselves substrates of *Ph*PDR2 or if a precursor in the biosynthesis of Petunia sterols is transported. Both hypothesis are equitable, as some ABCGs have a narrow (van den Brule *et al.*, 2002), others a broad substrate specificity (Kang *et al.*, 2010c; Lee *et al.*, 2005). Synthesis and labeling of various Petunia sterols followed by transport assays would reveal which of the two hypothesis is more reasonable, and which structural features are crucial for substrate recognition. However it should be mentioned that the petuniasterone biosynthesis pathway is still enigmatic.

*Ph*PDR2 is the first transporter described to be involved in herbivore defense for which a substrate is proposed. For *phpdr2* plants, a marked decrease in toxicity against caterpillars was observed, making *Ph*PDR2 a crucial component in Petunia defense. The presence of petuniasterones in trichomes make them a target for industrial applications. Glandular trichomes of Solanaceae species have been focus of plant metabolic engineering strategies because of their accessibility and the ability to produce large amounts of secondary metabolites (Schilmiller *et al.*, 2008). Therefore, elucidation of the Petunia sterol synthetic pathway could result in the development of novel insecticides or in elevated resistance of plants against herbivores.

The results presented here lead to the conclusion that *Ph*PDR2 is involved in herbivore response in *Petunia hybrida*. Several lines of evidence, such as its expression in glandular trichomes of leaf and stem, its induction by MJA treatment, as well as the increased susceptibility of *phpdr2* lines to herbivory support this conclusion. With an untargeted metabolite analysis approach, Petunia sterols were identified to be present in lower amounts in *phpdr2*, suggesting an involvement of *Ph*PDR2 in allocation of these sterol-derived compounds.

4.2.1 Work in progress

During the time this thesis was written, work on this manuscript was still in progress. For some of the Figures and Tables, data sets were not complete and thus, this data was not included. In next steps, an additional Figure depicting chromatograms of some Petunia sterols found in wild type and *phpdr2* lines will be included. Further, a Table listing the most significant metabolites reduced in *phpdr2* lines identified by XCMS analysis will be shown, and MS/MS data of these Petunia sterols will be added, confirming their identity.

4.3 Materials and methods

Plant growth conditions: All Petunia plants were grown under long day conditions with 16 h of continuous light at 40% relative humidity. Plants were either grown on soil (ED 73 Einheitserde) or on clay granules (Oil Dry US Special from Damolin) supplemented once a week with 1x Hoagland solution. On plate, plants were grown on medium containing 2.2 g L^{-1} MS (Duchefa) and with or without 15 g L^{-1} sucrose (0.5 MS - Suc, 0.5 MS + Suc plates, respectively), supplemented with 9 g L^{-1} phyto agar (Duchefa) at 16 h of light and 25 °C.

PDR2 transcriptional induction and quantitative PCR: For hormone and elicitor treatment 14 d old W115 seedlings grown on plate were exposed for 24 h with final concentrations of 100 µM salicylic acid (SA), 0.1 ml L^{-1} methyl-jasmonate (MJa), 10 g L^{-1} yeast extract, 10 µM abscisic acid (ABA), 25 µM 1-naphthaleneacetic acid (NAA), or 500 µM sclareol.

RNA was isolated with the RNeasy Plant Mini Kit (Qiagen USA) and reverse transcribed to cDNA with M-MLV Reverse Transcriptase (Promega, USA). Quantitative PCR was performed with 5'-TCAAGGCATTCAACTTCCAG and 5'-TACTGACCGAGTCTCCACCA for PDR2 5'-GACTGGAGAGGTGGAAGAGC and 5'-CCGTTAAGAGCTGGGAGAAC for the housekeeping gene glyceraldehyde-3-phosphate dehydrogenase in SYBR Green PCR Master Mix (Applied Biosystems) on a 7500 Fast Real-Time PCR system (Applied Biosystems).

For mechanical wounding and *M. sexta* oral secret treatment, *pPhPDR2-GUS* W115 plants (see below) were pre-selected by Basta spraying and grown on soil for 4 - 6 weeks. Plants were wounded at the youngest fully unfolded leaf by forceps pressure or by a fabric pattern wheel (Kallenbach *et al.*, 2012). For oral secret treatment, 20 µl of secret (kindly provided by I. Baldwin, Max Planck Institute for Chemical Ecology, Jena, Germany), 33 mM MJA, or water was applied to the wounded parts of the leaf. After 24 h, plants were collected for GUS staining.

***PhPDR2* cloning strategy:** Partial sequences of putative ABCG/*PDR* transcripts were amplified from total cDNA obtained from the roots of W115 individuals. NBD1-specific amplicons of around 0.5 kb were obtained with 5`-mgwatgactctdytkytkggacctcc

targeting PDR signature1 and 5`-gyttcytytgncchcchgaaatwcc targeting the ABC signature. NBD2-specific amplicons of around 0.5 kb were obtained with 5`-gggwaaracggwgtyagtggwgcw targeting the Walker A box and 5`-ctcatnacaatdgcwgcwgctctwgc targeting PDR signature 3. Fragments for the respective NBDs were aligned and the *ABCG/PDR* subfamily specific consensus primers (F 5'-tattgggacttgaaatttgtgccgatac, R 5'-gctccactaacacccatcagagctgtc) were designed to amplify putative *ABCG/PDR* coding regions spanning NBD1 and NBD2 from W115 trichome cDNA.

Amplification of upstream and downstream sequences of *PhPDR2* full length transcript was achieved via 5`RACE and 3`RACE PCRs using the SMART-RACE cDNA Amplification Kit (Clontech, Takara Bio Company, USA) according to the manufacturers specifications. 5' RACE primer and 5' nested RACE primer had the following sequence: 5'-atggattcgaagaaggccagaacgtcttc and 5'-cccttaccatgtcatctcccaccaaag. 3' RACE primer and nested 3' RACE primer sequences were: 5'-gatcagggtgcctctgaagatagattgg and 5'-caggaggatatattgagggtagaatccaca.

The *PhPDR2* genomic DNA sequence was cloned in two sequential steps from W115 DNA. First, a 2.6 kb 5' part was amplified (F 5'-atcccgggataatggaaccagtaaac, R 5'-ttaaggatccggatcccgtcatgtgaccaa, F contains a *Xma*I site and R a endogenous *Bam*HI site (underlined)). The PCR product was T/A cloned into pGEM®-T easy (Promega). Second, the 3' 5.3 kb part of *PhPDR2* was amplified in to single PCRs. PCR1: F1 5'-ttaaggatccttggtcacatgacgggatcc with the endogenous *Bam*HI site (underlined), R1 5'-catcatcggtgaagtccagt. PCR2: F2 5'-gaagaaatggtggat, R2 5'-taagcggccgcctatcttgtctggaagtt with a *Not*I site (underlined). A second PCR (F1 and R2) resulted in amplification of the full 5.3 kb. The PCR product was cloned into pGEM®-T easy (Promega). Both genomic fragments were transferred into the binary pGreenII0229 vector system (Hellens *et al.*, 2000). A *CaMV 35S* promoter was added with 5'-gggcccgtcaaagattcaaatagaggac and 5'-ctcgagtgtcctctccaaatgaaatg containing an *Apa*I and *Xho*I restriction site, respectively (underlined), a N-terminal *GFP5* was added with 5'-gtcgacatgagtaaaggagaagaac and 5'-ctgcagatctttcgaaagggcagatt containing a *Sal*I and *Pst*I restriction site, respectively (underlined), and an *OCE3* terminator was added with 5'-agcggccgcaatttccccgatcgttca and 5'-gcggccgccgatctagtaacatagatga containing *Not*I restriction sites (underlined).

Conserved PDR domain amplification: For the investigation of Petunia *PDR* sequences expressed in leaf and trichome tissue, primers were designed on a CDS alignment of *PDRs* from different Solanaceae species because for Petunia, only two *PDRs* are described so far. *Solanum lycopersicum* sequences were obtained from a Blast of *PhPDR2* and *PhPDR1* against the tomato database (http://mips.helmholtz-muenchen.de/plant/tomato/database). The search resulted in the following sequences: Solyc02g081870.2.1, Solyc06g076930.1.1, Solyc05g018510.2.1, Solyc11g007300.1.1, Solyc06g036240.1.1, Solyc12g098210.1.1, Solyc09g091660.2.1, Solyc12g100190.1.1, Solyc12g100180.1.1, Solyc12g019640.1.1, Solyc11g067000.1.1, Solyc11g007290.1.1, Solyc11g007280.1.1, Solyc09g091670.2.1, Solyc08g067620.2.1, Solyc08g067610.2.1, Solyc06g065670.2.1, Solyc05g055330.2.1, Solyc05g053610.2.1, Solyc05g053600.2.1, Solyc05g053590.2.1, Solyc05g053570.2.1, and Solyc03g120980.2.1. *Solanum tuberosum* CDS were obtained from GenBank for *StPDR1* (JF720054.1), *StPDR2* (JF440348.1), *StPDR3* (JF720055.1), *StPDR4* (JF720056.1), and by a Blast search with *PhPDR1* and *PhPDR2* against the *Solanum tuberosum* database (http://solgenomics.net), which resulted in the CDS of PGSC0003DMC400041247 PGSC0003DMT400061280, PGSC0003DMC400051611 PGSC0003DMT400076208, PGSC0003DMC400023214 PGSC0003DMT400034124, PGSC0003DMC400051609 PGSC0003DMT400076206, PGSC0003DMC400023219 PGSC0003DMT400034130, PGSC0003DMC400051612 PGSC0003DMT400076209, PGSC0003DMC400033296 PGSC0003DMT400049313, PGSC0003DMC400033294 PGSC0003DMT400049311, PGSC0003DMC400029466 PGSC0003DMT400043433, PGSC0003DMC400033295 PGSC0003DMT400049312, PGSC0003DMC400004038 PGSC0003DMT400005783, PGSC0003DMC400004040 PGSC0003DMT400005785, PGSC0003DMC400032813: 1-1200 PGSC0003DMT400048449, PGSC0003DMC400050377 PGSC0003DMT400074382, PGSC0003DMC400050376. Furthermore, the *Nicotiana plumbaginifolia* CDS *NpPDR1* (AJ404328.1), *NpPDR2* (AJ831424.1), *NpPDR3* (AJ831379.1), *NpPDR5* (JQ808000.1), the *Nicotiana tabacum* CDS *NtPDR1* (AB075550.1), *NtPDR3* (AJ831379.1), *NtPDR4* (AJ831380.1), *NtPDR5a* (JQ808002.1), and *NtPDR5b* (JQ808003.1) were included. The Walker A box of NBD 2 and the PDR signature 4 were part of the most conserved part of the alignment. Thus, PCR was performed on this region (F 5'-agcwytrrtgggwgtyagtggdgctgg, R 5'-ctcatcaaadgcttcaaawatgtc) and the fragments were cloned into pGEM®-T easy

vector (Promega, USA), sequenced and aligned with the MultAlin software (http://multalin.toulouse.inra.fr/multalin/).

***PhPDR2* phylogenetic analysis:** To set PhPDR2 in relation to described PDR proteins, a maximum-likelihood tree was created on Phylogeny.fr (http://www.phylogeny.fr/). The well-established *Oryza sativa* and the *A. thaliana* PDR proteins, as well as *Spirodela polyrrhiza SpTUR2*, *Glycine max GmPDR12*, the *N. plumbaginifola NpPDR1, NpPDR2, NpPDR3, NpPDR5*, the *N. tabacum NtPDR1, NtPDR3, NtPDR4, NtPDR5a, NtPDR5b,* the *Petunia hybrida* PhPDR1 were included in the tree. *OsPDR15*, which is a pseudogene, and *OsPDR19*, with no detectable cDNA (Moons, 2008), were excluded from the analysis. PDR Clusters were annotated after Crouzet et. al, 2005. Accessions: *AtPDR1* (BK001001), *AtPDR2* (BK001000), *AtPDR3* (BK001002), *AtPDR4* (BK001003), *AtPDR5* (BK001004), *AtPDR6* (BK001005), *AtPDR7* (BK001006), *AtPDR8* (BK001007), *AtPDR9* (BK001008), *AtPDR10* (BK001009), *AtPDR11* (BK001010), *AtPDR12* (BK001011), *AtPDR13* (BK001012), *AtPDR14* (BK001013), *AtPDR15* (BK001014), *GmPDR12* (Q1M2R7), *NpPDR1* (AJ404328.1), *NpPDR2* (AJ831424.1), *NpPDR3* (AJ831379.1), *NpPDR5* (JQ808000.1), *NtPDR1* (AB075550.1), *NtPDR3* (AJ831379.1), *NtPDR4* (AJ831380.1), *NtPDR5a* (JQ808002.1), *NtPDR5b* (JQ808003.1), *OsPDR1* (BK001015), *OsPDR2* (BK001016), *OsPDR3* (BK001017), *OsPDR4* (BK001018), *OsPDR5* (AJ535050), *OsPDR6* (AJ535049), *OsPDR7* (AJ535048), *OsPDR8* (AJ535047), *OsPDR9* (AJ535046), *OsPDR10* (AJ535045), *OsPDR11* (AJ535044), *OsPDR12* (AJ535043), *OsPDR13* (AJ535042), *OsPDR15* (AJ535041), *OsPDR16* (AAQ01165.1), *OsPDR17* (AK100858), *OsPDR18* (AK072827), *OsPDR20* (EAZ44307.1), *OsPDR21* (AK070409), *OsPDR22* (AK107869), *OsPDR23*_1 (AK102367), *OsPDR23*_2 (AK103110), *PhPDR1* (JQ292813), *SpTUR2* (CAA94437).

The conserved region (see Conserved domain analysis) of the respective genes was identified and phylogeny of the 0.5 kb fragments was analyzed with a maximum likelihood tree, using standard settings (http://www.phylogeny.fr/, Dereeper *et al.*, 2008).

***PhPDR2* promoter GUS constructs and GUS staining assay:** Amplification of a 1.2 kb promoter fragment upstream of the *PhPDR2* gene was accomplished via use of the Genome Walker Universal Kit (Clontech, Takara Bio Company, USA) with the primer 5'-caagagctgcccatttaagtgcttcttc and the nested primer 5'-cgcttaaacttccccttgcacttcctc. The

fragment was T/A cloned into pGEM-T Easy vector system (Promega, USA) and subsequently reamplified with the primer 5'-ggaaccaagctttgtgtaggaaaattttgc containing a *Hind*III restriction site (underlined) and the primer 5'-tacatctagagacccccctctagctcag containing an *Xba*I restriction site (underlined). The respective restriction sites were used to clone the *PhPDR2* promoter fragment into the *GUS* gene-containing pGPTV-Bar (Becker *et al.*, 1992) vector system.

For GUS staining trials tissues to be investigated were submerged in an appropriate amount of GUS-staining buffer (100 mM sodium phosphate buffer pH 7.0, 10 mM NaEDTA, 1.5 mM potassium hexacyanoferrate(II) trihydrate, 0.25 mM potassium hexacyanoferrate(III), 0.1% (v/v) Triton X-100 and 1 mM 5-bromo-4-chloro-3-indolyl β-D-glucuronide cyclohexylammonium salt) vacuum infiltrated three times for 30 s and incubated in the dark at 37 °C for 12 – 24 h. After staining samples were cleared and stored in 70% ethanol.

***PhPDR2* RNA interference constructs:** Silencing of *PhPDR2* specific transcripts was attempted via the generation of double stranded hairpin RNA fragments utilizing the pKANIBAL vector system (Wesley *et al.*, 2001). A 407 bp fragment containing parts of the 3' end and the 3' UTR of *PhPDR2* was amplified from *PhPDR2* cDNA with 5'-cgatggatcctcgagctgatgatgaaacagtggaa, containing *BamH*I and *Xho*I restriction sites (underlined) and 5'-cgatatcgatggtaccgaataaatatgccgctttca containing *Cla*I and *Kpn*I sites (underlined). The resulting amplicon was cloned in sense and antisense direction in the two MCS of pKANIBAL flanking the hairpin intron sequence. The pKANIBAL RNAi cassette containing *CaMV 35S* promoter RNAi construct and *OCE3* terminator was excised from the vector backbone using the *Not*I restriction sites and transferred into the binary pGreenII0229 vector system (Hellens *et al.*, 2000), conferring Glufosinate Ammonium resistance as a selection marker in plants.

After stable transformation of W115 plants the degree of down-regulation in several independent *phpdr2* lines was estimated via semi-quantitative RT-PCR using the *PhPDR2* specific primers 5'-ggaatgtattctgccttacc and 5'-gtaatctccaaattgtgatgc. Petunia tubulin 1 transcript, partially amplified with 5'-cattggtcaagccggttattc and 5`'acccttgaagaccagtacagt served as a housekeeping and loading control.

Transient *Arabidopsis thaliana* transformation: *Arabidopsis thaliana* Col-0 plants were grown in a 8 h light, 16 h dark cycle at 21 °C at 60% relative humidity. Leaves of 2-month-old plants were collected, the abaxial cuticule removed with sand paper, and

digested at 23 °C, gentle shaking, for 1.5 h in 0.4 M mannitol, 20 mM KCl, 20 mM MES, 0.4% [w/v] macerozyme R10 (Yakult Honsha, Japan), 1% [w/v] cellulase R10 (Yakult Honsha, Japan), pH 5.7. After the digestion, 10 mM $CaCl_2$ was added, and protoplasts were collected at 400 g for 5 min at 4 °C with low break. Supernatant was removed and the pellet was solubilized in W5 solution (154 mM NaCl, 125 mM $CaCl^2$, 5 mM KCl, 2 mM MES, pH 5.7) was moved to a tube containing 21% [w/v] sucrose. The protoplasts were collected at 400 g for 6 min at 4 °C with low break, the supernatant removed, and cells were transferred to a new tube. W5 solution was added, the protoplasts were incubated 30 min on ice, and collected at 400 g for 3 min at 4 °C with low break. Protoplasts were collected and density was adjusted to $2 * 10^5$ cells ml^{-1} in MMg solution (0.4 M mannitol, 15 mM $MgCl_2$, 4 mM MES pH 5.7).

The pGreen179 plasmid containing the 35S:GFP-PDR2 construct was purified with the Plasmid Plus Midi Kit (Qiagen); 10 µg of the construct and 10 µg of the plasma membrane marker *AtAHA2-RFP* (Lee *et al.*, 2003) was added to the protoplasts, as well as 220 µl of PEG solution (40% [w/v] PEG 4000, 0.2 M mannitol, 0.1 M $CaCl_2$). Protoplasts were incubated for 5 min at 23 °C. Further, 800 µl of W5 solution was added, and cells were collected 400 g for 3 min at 4 °C with low break. The supernatant was removed fully, and 100 µl of W5 solution was added. Protoplasts were incubated in the dark for 2 d at 23 °C.

Stable Petunia transformation: *PhPDR2* promoter GUS constructs and *phpdr2* RNAi constructs were transferred into the W115 background via *Agrobacterium tumefaciens* mediated transformation of leaf explants, callus induction and plant regeneration (Lutke, 2006). 0.45% phytagel were used instead of 0.9% agar in all media and the concentrations of BAP and NAA in the Selection Medium was adjusted between 1 - 2 mg L^{-1} for the former and 0.05 - 0.15 mg L^{-1} for the latter to maximize shoot induction for each individual transformation.

Regenerated plantlets were tested for successful construct insertion via PCR on genomic DNA. The primers 5'-acggtccacatgccggtatatacgatg and 5'-gatggcatttgtaggagccaccttcc, targeting the *CaMV 35S* promoter, were used to confirm RNAi construct insertion. The primers 5'-gaattgatcagcgttggtgggaaagc and 5'-ggtaatgcgaggtacggtaggagttg, targeting the GUS gene, were used to confirm GUS construct insertion.

***Spodoptera littoralis* feeding trials:** All larvae for the leaf feeding experiments were kindly provided by Syngenta, Switzerland. Second instar *S. littoralis* larvae were placed in transparent plastic containers (10 * 10.5 * 4.5 cm). Eight holes (0.5 - 1 mm diameter) were punched in two opposite walls to ensure ventilation. The bottom was covered with a moist paper towel, which was exchanged regularly and every 1 - 2 days larvae were supplied with fresh leaves. It was taken care, that their position and developmental stage were the same. Frequently, the uppermost fully expanded leaves were taken, since they were constantly renewed during plant growth. It was also tried to chose plants from the same size, when available, although this was not always possible. To ensure that excised leaves kept their turgor, cut petioles ends were inserted into small water containers and sealed with parafilm. Starting from a certain size, it was possible to identify each larva with a high probability due to apparent differences in size. Thus weight gain could be calculated for each larvae between two timepoints.

Survival probabilities were calculated as Kaplan-Meier curves which also tolerate data censoring. A tutorial found at www.cancerguide.org/scurve_km.html was used for curve construction. In contrast to graphs produced by statistical software, graphs presented in this thesis were not plotted as step graphs, and without indications for censored data.

Trichome collection and leaf washes: In experiment 1, stem trichomes of four greenhouse-grown, 3-month-old W115 plants, and of three *phpdr2*^{1}, *phphdr2*^{2}, and *phpdr2*^{3} plants each were collected by freezing the stem for 5 s in liquid nitrogen, and mechanical removal with a spatula. The fresh weight of the collected trichomes was quantified and later used for normalization of the samples. For each 10 mg of trichomes, 100 µl of isopropanol:acetonitrile:water 3:3:2 solution (Kang *et al.*, 2010b) containing two internal standards, (+) 0.05% camphor-10-sulfonic acid (purum, Fluka, Germany) and 0.05% lidocaine hydrochloride monohydrate (Sigma, Germany). Samples were suspended in an ultrasonic bath for 1 min, centrifuged at 13'000 g at 4 °C for 5 min. Of the supernatant, 5 µl were used for UHPLC-MS analysis.

For experiment 2, the seventh leaf of seven 3-month-old, greenhouse-grown W115, *phpdr2*^{1}, *phphdr2*^{2}, and *phpdr2*^{3} plants was incubated with the adaxial surface in a glass petri dish with 8 ml of isopropanol:acetonitrile:water 3:3:2 solution for 5 min at 23 °C with gentle shaking. The solution was collected and stored at -20 °C for further use. Samples were concentrated using Oasis HLB 6cc extraction cartridges (Waters). The cartridges were conditioned with methanol, equilibrated with water, and loaded with

the samples. After washing with 5 mL water, the cartridges were eluted with 6 mL methanol. Samples were dried under N_2, and resuspended in 200 µl of the isopropanol:acetonitrile:water solution containing internal standards that has been described above.

For experiment 3, all leaves of 2.5-month-old, sterile-grown W115, *phpdr2*[1], *phphdr2*[2], and *phpdr2*[3] plants were washed and concentrated as described before for experiment 2.

UHPLC-HR-ESI-MS analyses: Samples were analyzed with an ultra-high performance (UHPLC) high-resolution mass spectrometry (HR-MS), which was composed of a Waters Acquity UPLC system (Waters, USA) connected to a maXis quadrupole time-of-flight MS (Bruker Daltonics, Germany). Plant metabolites were separated at 40 °C on a Waters Acquity UPLC BEH column (1 x 50 mm, 1.7 µm) with a flow rate of 0.2 ml min^{-1}, and a mobile phase composed of water (solution A) and acetonitrile (solution B), both of which containing 0.1% HCOOH. The gradient program conditions were (the values indicate the proportion of percentage of solvent B used): 3% at 0.0 min, isocratic of 0.5 min followed by a linear gradient up to 99.5% within 8 min. The gradient was followed by a washing step with 99.5% solvent B for 2.5 min and a re-equilibration step to the initial composition for 2 min. The UHPLC was connected to the MS equipped with an electrospray ion source (ESI) operated either in positive (+) or in negative (-) ionization mode. Nitrogen was used as nebulizer (2.0 bar) and as dry gas (9 L min^{-1}, 205 °C). MS acquisitions were performed in the mass range from m/z 50 to 1500 at 20'000 resolution (full width at half maximum) and 1.5 scan s^{-1}. Masses were calibrated below 2 ppm accuracy with a 2 mM solution of sodium formate over m/z 158 up to 1450 mass range prior analysis.

The Bruker ProfileAnalysis™ application (Version 2.1, Bruker Daltonics, Germany) was used for unsupervised principal component analysis (PCA) processing of the HR-ESI-MS data. Conspicuous masses having more than 50% reduction of signal intensity in *phpdr2* lines compared to W115 were selected. The corresponding molecular formulas of these masses were calculated with DataAnalysis™ (Bruker Daltonics, Germany) at 2 ppm mass accuracy and used for identifying the metabolites of interest for *Petunia sp.* with SciFinder® database (www.cas.org, American Chemical Society) and literature data (Elliger and Waiss, 1991; Elliger *et al.*, 1993; Elliger *et al.*, 1990a; Elliger *et al.*, 1988a; Elliger *et al.*, 1989a; Elliger *et al.*, 1992a; Elliger *et al.*, 1990b; Elliger *et al.*, 1992b).

The peak areas of the metabolite of interest were obtained after manual integration of the theoretical extracted ion chromatograms (EIC) with ± 0.05 Da width.

The UHPLC-HR-ESI-MS data was in addition processed with XCMS Online (http://metlin.scripps.edu/xcms/, Metlin, Tautenhahn *et al.*, 2012) for experiment 2, analyzing all *phpdr2* lines versus W115. Following parameters were selected: centwave detection method, 10 ppm mass accuracy, 5 < UHPLC peak width < 20, obiwarp retention time correction, unpaired parametric t-test (Welch t-test, unequal variances), 0.001 statistical threshold. Masses of the aforementioned phytosterols were identified in the XCMS results file.

Sclareol phenotype assays: Three-week-old *pPDR2-GUS* plants grown on 0.5 MS + Suc plates were grown for further 24 h on 0.5 MS + Suc supplemented with 0, 100, or 500 µM sclareol to monitor if *PhPDR2* was sclareol responsive. Subsequently, plants were stained (see GUS staining).

Wild type and *phpdr2* seeds were germinated on plates containing 0, 50, 250, or 500 µM sclareol and germination was scored after 11 days of growth (Campbell *et al.*, 2003).

Wild type and *phpdr2* plants were grown for two weeks on 0.5 MS – Suc, or on plates additionally supplemented with 30 mg L^{-1} Hygromycin, respectively. Subsequently, plants were transferred to 0.5 MS + Suc supplemented with 0, 100, 250, or 500 µM sclareol. Root length difference between day 0 and 6 on sclareol-containing plates was quantified and expressed as mean change of root length (Campbell *et al.*, 2003).

Statistical analyses: Data were analyzed using the R software (R Development Core Team 2009), version 2.9.2. For comparing weight (resp. weight gain) of larvae on wildtype versus phpdr2 plants, a linear model using generalized least squares (gls) was applied from the package *nlme.* W115 data were set to represent the intercept of the model, against which each line is compared. In contrast to a simple t-test, this method is more powerful since it can correct for of unequal variances – a problem which was commonly faced – by using the *varIdent* function. The distribution of the data was reasonably normal, thus no transformation had to be applied.

From survival data, Kaplan-Meier estimates were calculated using the *survival* package in R, and *phpdr2* survival curves were then tested for significant differences compared to the W115 curve.

For all statistical analyzes, significance was reported at the level $\alpha = 0.05$.

4.4 References

Allmann, S. and Baldwin, I. T. (2010) Insects betray themselves in nature to predators by rapid isomerization of green leaf volatiles. *Science*, 329, 1075–1078.

Becker, D., Kemper, E., Schell, J. and Masterson, R. (1992) New plant binary vectors with selectable markers located proximal to the left T-DNA border. *Plant Mol. Biol.*, 20, 1195–1197.

Bienert, M. D., Siegmund, S. E., Drozak, A. *et al.* (2012) A pleiotropic drug resistance transporter in *Nicotiana tabacum* is involved in defense against the herbivore *Manduca sexta*. *Plant Journal*, 72, 745–757.

Bodenhausen, N. and Reymond, P. (2007) Signaling pathways controlling induced resistance to insect herbivores in Arabidopsis. *Mol. Plant Microbe Interact.*, 20, 1406–1420.

Brewer, P. B., Dun, E. A., Ferguson, B. J. *et al.* (2009) Strigolactone acts downstream of auxin to regulate bud outgrowth in pea and Arabidopsis. *Plant Physiol.*, 150, 482–493.

Bultreys, A., Trombik, T., Drozak, A. and Boutry, M. (2009) *Nicotiana plumbaginifolia* plants silenced for the ATP-binding cassette transporter gene *NpPDR1* show increased susceptibility to a group of fungal and oomycete pathogens. *Mol. Plant Pathol.*, 10, 651–663.

Campbell, E. J., Schenk, P. M., Kazan, K. *et al.* (2003) Pathogen-responsive expression of a putative ATP-binding cassette transporter gene conferring resistance to the diterpenoid sclareol is regulated by multiple defense signaling pathways in Arabidopsis. *Plant Physiol.*, 133, 1272–1284.

Crouzet, J., Roland, J., Peeters, E. *et al.* (2013) NtPDR1, a plasma membrane ABC transporter from *Nicotiana tabacum*, is involved in diterpene transport. *Plant Mol. Biol*. 82, 181-192.

Crouzet, J., Trombik, T., Fraysse, A. S. and Boutry, M. (2006) Organization and function of the plant pleiotropic drug resistance ABC transporter family. *FEBS Letters*, 580, 1123–1130.

Cutler, H. G., Reid, W. W. and Delétang, J. (1977) Plant-Growth Inhibiting Properties of Diterpenes From Tobacco. *Plant Cell Physiol.*, 18, 711–714.

Dereeper, A., Guignon, V., Blanc, G. *et al.* (2008) Phylogeny.fr: robust phylogenetic analysis for the non-specialist. *Nucleic Acids Research*, 36, W465–W469.

Ducos, E., Fraysse, S. and Boutry, M. (2005) *NtPDR3*, an iron-deficiency inducible ABC transporter in *Nicotiana tabacum*. *FEBS Letters*, 579, 6791–6795.

Dun, E. A., Brewer, P. B. and Beveridge, C. A. (2009) Strigolactones: discovery of the elusive shoot branching hormone. *Trends in Plant Science*, 14, 364–372.

Elliger, C. A., Waiss, A. C., Benson, M. and Wong, R. Y. (1993) Ergostanoids From *Petunia inflata*. *Phytochemistry*, 33, 471–477.

Elliger, C. A., Waiss, A. C. Jr. and Benson, M. (1992a) Petuniasterone R, A New Ergostanoid From *Petunia parodii. Journal of Natural Products*, 55, 129–133.

Elliger, C. A., Wong, R. Y., Benson, M. and Waiss, A. C. Jr. (1992b) Petunianines, unusual steroidal nitrogenous bases from *Petunia inflata*. *J. Chem. Soc., Perkin Trans. 1*, 5-6.

Elliger, C. A. and Waiss, A. C. Jr. (1991) Insect Resistance Factors in Petunia. In *ACS Symposium Series*. ACS Symposium Series. Washington, DC: American Chemical Society, pp. 210–223.

Elliger, C. A., Waiss, A. C., Benson, M. and Wong, R. Y. (1990a) Ergostanoids From *Petunia parodii*. *Phytochemistry*, 29, 1–11.

Elliger, C. A., Wong, R. Y., Waiss, A. C. Jr. and Benson, M. (1990b) Petuniolides. Unusual ergostanoid lactones from Petunia species that inhibit insect development. *J. Chem. Soc., Perkin Trans. 1*, 525.

Elliger, C. A., Haddon, W. F., Waiss, A. C. Jr. and Benson, M. (1989a) Petuniasterone N, An Unusual Ergostanoid From Petunia Species. *Journal of natural Products*, 52, 576–580.

Elliger, C. A., Waiss, A. C. Jr., Wong, R. Y. and Benson, M. (1989b) Petuniasterones From *Petunia parodii* And *P. integrifolia*; Unusual Ergostane-Type Steroids. *Phytochemistry*, 28, 3443–3452.

Elliger, C. A., Benson, M., Lundin, R. E. and Waiss, A. C. Jr. (1988a) Minor Petuniasterones from *Petunia hybrida*. *Phytochemistry*, 27, 3597–3603.

Elliger, C.A., Benson, M.E., Haddon, W.F. *et al.* (1988b) Petuniasterones, Novel Ergostane-Type Steroids of *Petunia*

hybridia Vilm. (Solanaceae) Having Insect-Inhibitory Activity. X-Ray Molecular Structure of the 22,24,25-[(Methoxycarbonyl)Orthoacetate] of 7a,22,24,25-Tetrahydroxy Ergosta-1,4-Dien-3-One and of 1a-Acetoxy-24,25-Epoxy-7a-Hydroxy-22-(Methylthiocarbonyl)Acetoxyergost-4-en-3-One. *J. Chem. Soc., Perkin Trans. 1*, 711–717.

Granado, J., Felix G. and Boller T. (1995) Perception of Fungal Sterols in Plants (Subnanomolar Concentrations of Ergosterol Elicit Extracellular Alkalinization in Tomato Cells). *Plant Physiol.*, 107, 485–490.

Hellens, R. P., Edwards, E. A., Leyland, N. R. *et al.* (2000) pGreen: a versatile and flexible binary Ti vector for Agrobacterium-mediated plant transformation. *Plant Mol. Biol.*, 42, 819–832.

Jasinski, M., Stukkens, Y., Degand, H. *et al.* (2001) A plant plasma membrane ATP binding cassette-type transporter is involved in antifungal terpenoid secretion. *Plant Cell*, 13, 1095–1107.

Kallenbach, M., Bonaventure, G., Gilardoni, P.A. *et al*. (2012) *Empoasca* leafhoppers attack wild tobacco plants in a jasmonate-dependent manner and identify jasmonate mutants in natural populations. *Proc. Natl. Acad. Sci. U.S.A.*, 109, E1548–57.

Kang, J. H., Shi, F., Jones, A. D. *et al.* (2010a) Distortion of trichome morphology by the *hairless* mutation of tomato affects leaf surface chemistry. *J. Exp. Bot.*, 61, 1053–1064.

Kang, J. H., Liu, G., Shi, F. *et al.* (2010b) The tomato *odorless-2* mutant is defective in trichome-based production of diverse specialized metabolites and broad-spectrum resistance to insect herbivores. *Plant Physiol.*, 154, 262–272.

Kang, J., Hwang, J. U., Lee, M., *et al.* (2010c) PDR-type ABC transporter mediates cellular uptake of the phytohormone abscisic acid. *Proc. Natl. Acad. Sci. U.S.A.*, 107, 2355–2360.

Kretzschmar, T., Kohlen, W., Sasse, J. *et al.* (2012) A petunia ABC protein controls strigolactone-dependent symbiotic signalling and branching. *Nature*, 483, 341–344.

Lee J., Bae H., Jeong J. *et al.* (2003) Functional expression of a bacterial heavy metal transporter in Arabidopsis enhances resistance to and decreases uptake of heavy metals. *Plant Physiol.* 133, 589-596.

Lee, M., Lee, K., Lee, J. *et al.* (2005) AtPDR12 contributes to lead resistance in Arabidopsis. *Plant Physiol.*, 138, 827–836.

Lutke, W. K. (2006) Petunia (*Petunia hybrida*). *Methods Mol. Biol.*, 344, 339–349.

Martinoia, E., Klein, M., Geisler, M. *et al.* (2002) Multifunctionality of plant ABC transporters--more than just detoxifiers. *Planta*, 214, 345–355.

Moons, A. (2008) Transcriptional profiling of the PDR gene family in rice roots in response to plant growth regulators, redox perturbations and weak organic acid stresses. *Planta*, 229, 53–71.

Rossard, S., Roblin, G. and Atanassova, R. (2010) Ergosterol triggers characteristic elicitation steps in *Beta vulgaris* leaf tissues. *Journal of Experimental Botany*, 61, 1807–1816.

Sasabe, M., Toyoda, K., Shiraishi, T. *et al.* (2002) cDNA cloning and characterization of tobacco ABC transporter: *NtPDR1* is a novel elicitor-responsive gene. *FEBS Letters*, 518, 164–168.

Schilmiller, A. L., Last, R. L. and Pichersky, E. (2008) Harnessing plant trichome biochemistry for the production of useful compounds. *Plant Journal*, 54, 702–711.

Shingu, K., Fujii, H., Mizuki, K. *et al.* (1994) Ergostane Glycosides From *Petunia hybrida*. *Phytochemistry*, 36, 1307–1314.

Slocombe, S. P., Schauvinhold, I., McQuinn, R. P. *et al.* (2008) Transcriptomic and Reverse Genetic Analyses of Branched-Chain Fatty Acid and Acyl Sugar Production in *Solanum pennellii* and *Nicotiana benthamiana*. *Plant Physiol.*, 148, 1830–1846.

Stukkens, Y., Bultreys, A., Grec, S. *et al.* (2005) NpPDR1, a pleiotropic drug resistance-type ATP-binding cassette transporter from *Nicotiana plumbaginifolia*, plays a major role in plant pathogen defense. *Plant Physiol.*, 139, 341–352.

Tautenhahn, R., Patti, G. J., Rinehart, D. and Siuzdak, G. (2012) XCMS Online: A Web-Based Platform to Process Untargeted Metabolomic Data. *Anal. Chem.*, 84, 5035–5039.

Theodoulou, F.L. (2000) Plant ABC transporters. *Biochim. Biophys. Acta*, 1465, 79–7103.

Trombik, T., Jasinski, M., Crouzet, J. and Boutry, M. (2008) Identification of a cluster IV pleiotropic drug resistance transporter gene expressed in the style of *Nicotiana plumbaginifolia. Plant Mol. Biol.*, 66, 165–175.

Tugizimana, F., Steenkamp, P. A., Piater, L. A. and Dubery, I. A. (2012) Ergosterol-Induced Sesquiterpenoid Synthesis in Tobacco Cells. *Molecules*, 17, 1698–1715.

van den Brule, S., Muller, A., Fleming, A. J. and Smart, C. C. (2002) The ABC transporter SpTUR2 confers resistance to the antifungal diterpene sclareol. *Plant Journal*, 30, 649–662.

Verhoef, N., Yokota, T., Shibata, K. *et al.* (2013) Brassinosteroid biosynthesis and signalling in *Petunia hybrida. J. Exp.*

Bot., 64, 2435–2448.

Verrier, P. J., Bird, D., Burla, B. *et al.* (2008) Plant ABC proteins - a unified nomenclature and updated inventory. *Trends in Plant Science*, 13, 151–159.

Wagner, G. J. (1991) Secreting Glandular Trichomes: More than Just Hairs. *Plant Physiol.*, 96, 675–679.

Wang, E. M., Wang, R., DeParasis, J. *et al.* (2001) Suppression of a P450 hydroxylase gene in plant trichome glands enhances natural-product-based aphid resistance. *Nature Biotechnology*, 19, 371–374.

Wesley, S. V., Helliwell, C. A., Smith, N. A. *et al.* (2001) Construct design for efficient, effective and high-throughput gene silencing in plants. *Plant Journal*, 27, 581–590.

Yazaki, K. (2006) ABC transporters involved in the transport of plant secondary metabolites. *FEBS Letters*, 580, 1183–1191.

Zerback R., Bokel M., Geiger H. and Hess D. (1989) A Kaempferol 3-Glucosylgalactoside and further Flavonoids from Pollen of *Petunia hybrida. Phytochemistry,* 28: 897–899.

4.5 Supplemental Material

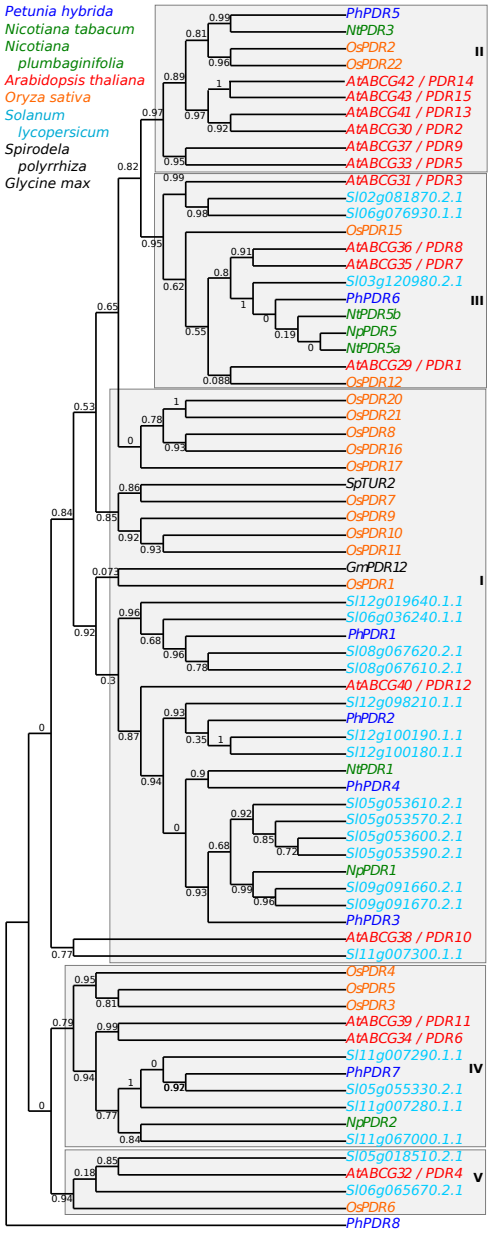

Supplementary Figure 4.1: *PhPDR2* phylogeny in comparison to other species

Maximum likelihood tree for 500 bp cDNA of PDR domains of *Petunia hybrida* (Ph, dark blue), *Oryza sativa* (Os, orange), *Arabidopsis thaliana* (At, red), *N. tabacum* (Nt, green), *N. plumbaginifolia* (Np, green), *Solanum lycopersicum* (Sl, light blue), *Spirodela polyrrhiza* (Sp, black), and *Glycine max* (Gm, black). Petunia sequences originate from amplification with primers aligning to Walker A domain and to PDR signature 4 on the second NBD. The same domain was identified in the sequences of non-Petunia species depicted by similarity search. Probabilities are depicted as numbers at branching points. PDR clusters are annotated after Crouzet *et al.* 2005. Note that the fragment of *OsPDR1* is present in cluster IV rather than in cluster I described for the protein sequence. The *OsPDR14* pseudogene was excluded from the analysis, as well as *OsODR23* and *OsPDR22* that did not contain the fragment of interest.

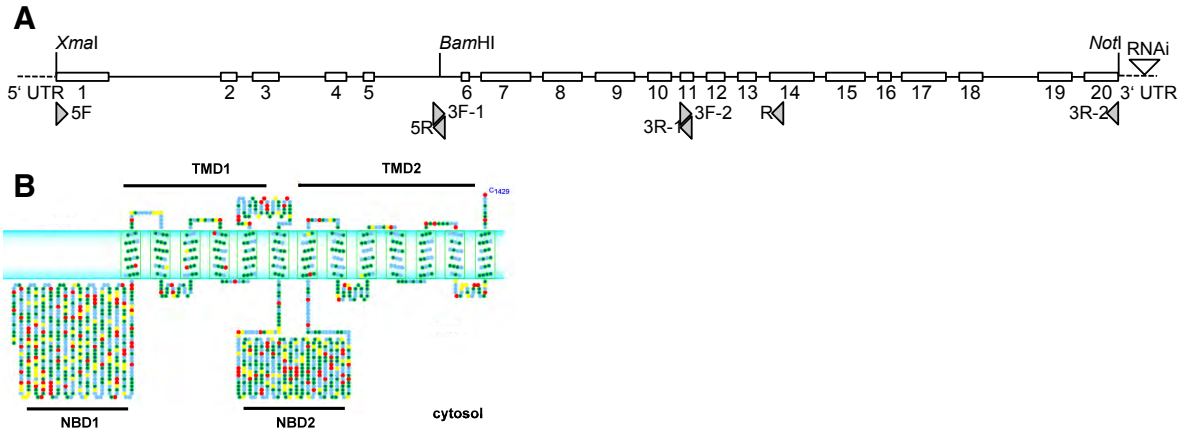

C

MEPVNLGNLRAASLRGSARGSLSGSLRANSNSIWRNDNVFTRSSRDENDEEALKWAALEKLPTFDRLTKGLL

FGSEGTAPSQIDIHDISFQERQGLLDRLVKDPDEDNEKFLLKLRDRIDRVGLDLPTIEVRYEHLHVVADAYIGGR

ALPTFTNFVTNFLESLLTSLHILPSKKRKLTILNDVSGIIKPCRLTLLLGPPGSGKTTFLLALAGKLDPELKVTGKV

Signature 1 Walker A

TYNGHDMTEFVPQRTAAYISQHDLHIGEMTVRETLEFSARCQGIGTRYEMLAELSRREKAANIKPDPDIDIYMK

ASATEGQEANVVTDYVLKILGLDICADTLVGDDMVRGISGGQKKRVTTGEMLVGPSKALFMDEISTGLDSSTT

ABC Walker B Signature 2

YSIVNSLRQTVQILKETAVISLLQPAPETYNLFDDIILLTDGLVVYGPREDVLAFFESMGFKCPDRKGVADFLQE

VTSKKDQQQYWARRDEPYRFITSKEFAEAYQSFHVGRKQLDELGAPFDKSKSHPAALSNQKYGIGKKQLLKV

CTEREYLLMKRNSFLFIFKFFQLLIMAILTMTMFLRTEMHHNTEEDGGTYVGALFFVIVMIMFNGMTELGMVLF

KLPVFYRQRDLFFYPSWAYAIPSWILKIPITFVEVALWVFLTYYVIGFDPNPERLFKQFFLLIIVNQMAGLFRFIGA

AGRTLGIAATFGAFALLLQFALGGFVLSRDMMKKWWIWGYWTSPMMYSVNAILVNEFHGKRWRRIAPNGTPL

GDAVVRGRGFFPDASWYWIGVGALIGFTVLFNILYSLALAYLNPIGKPQAMMPEDSEDAKTTSTEKEGYNSEG

QNKKRGMVLPFEPHSITFDDVIYSVDMPQEMKDQGASEDRLVLLNGVSGAFRPGVLTALMGVSGAGKTTLM

Walker A

DVLAGRKTGGYIEGRIHISGYPKKQETFARISGYCEQNDIHSPYVTVYESLVYSAWMRLPHDVDERTRKMFVG

EVKDLVELRPIRSALVGLPGVDGLSTEQRKRLTIAVELVANPSIIFMDEPTSGLDARAAAIVMRAVRNTVDTGRT

ABC Walker B Signature 3

VVCTIHQPSIDIFEAFDELFLMKRGGQEIYVGPLGRNSCHLIKYFESMPGVSKIKDGYNPATWMLEVTTPGQET

Signature 4

MFGVDFTDLYKKSDLYGRNEALITELSVPRPGTKDLHFDTQYSQPFWTQCMACLWKQHWSYWRNPAYTAVR

FLFTVMISLVFGTMFWDLGSKASRAQDLSNAMGCLYAAVLFIGTQSASSVQPVVAVERTVFYRERAAGMYSAL

PYAFAQAFIEIPYIFVQATFCGIIIYAMIGFEWTVEKYFWYLFFMFFTLMYYTYYGMVTVAITPNVNVAQVVSAFF

YGLWNLFSGFIVPRPRMAIWWRWYYWICPTAWTLYGLIASQFGDYQNKLTDDETVEQYLRRFFGFKHEFLPV

VGVVTAGFTVLFAFTFAFGIKAFNFQTR

Supplementary Figure 4.2: *PhPDR2* predicted structure

A, Genomic structure of *PhPDR2*, exons are depicted as squares. **B,** *Ph*PDR2 protein topology structure was predicted with ClustalW. Transmembrane domains (TMD) contain mainly hydrophobic (green circles) amino acids, whereas the nucleotide binding domains (NBD) contain additionally hydrophilic (blue), positive charged (red), and negatively charged (yellow) residues. **C,** The predicted *Ph*PDR2 amino acid sequence with PDR-specific domains 1-4 (underlined), ABC signature (orange), Walker A (blue) and Walker B (red) domains indicated.

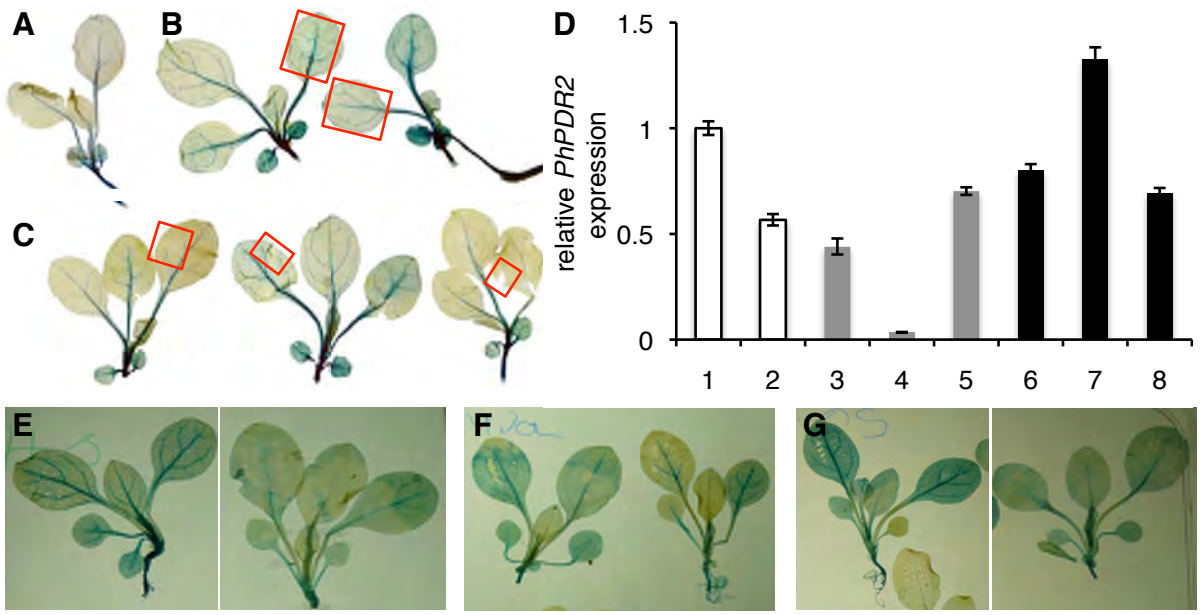

Supplementary Figure 4.3: Transcriptional responses of *PhPDR2*

A-C, Six-weeks-old, sterile-grown *pPDR2-GUS* plants were wounded (red squares) mechanically with a forceps **(B)** or a scissor **(C)**. A, Negative control. **D,** Relative *PhPDR2* expression quantified with real-time PCR in two-month-old, greenhouse-grown W115 plants. Control leaves were sampled at the day of treatment (1) and collection (2). One leaf of three plants each were wounded with a fabric pattern wheel with subsequent application of water (3-5), or 33 mM MJa (6-8), and collected after 24 h of treatment. **E-G**, one-month-old, sterile-grown *pPDR2-GUS* plants were wounded with a fabric pattern wheel with subsequent application of water **(E)**, 33 mM methyl jasmonate **(F)**, or *M. sexta* oral secret **(G)**. **A-C**, **E-G** plants were GUS-stained after 24 h of treatment.

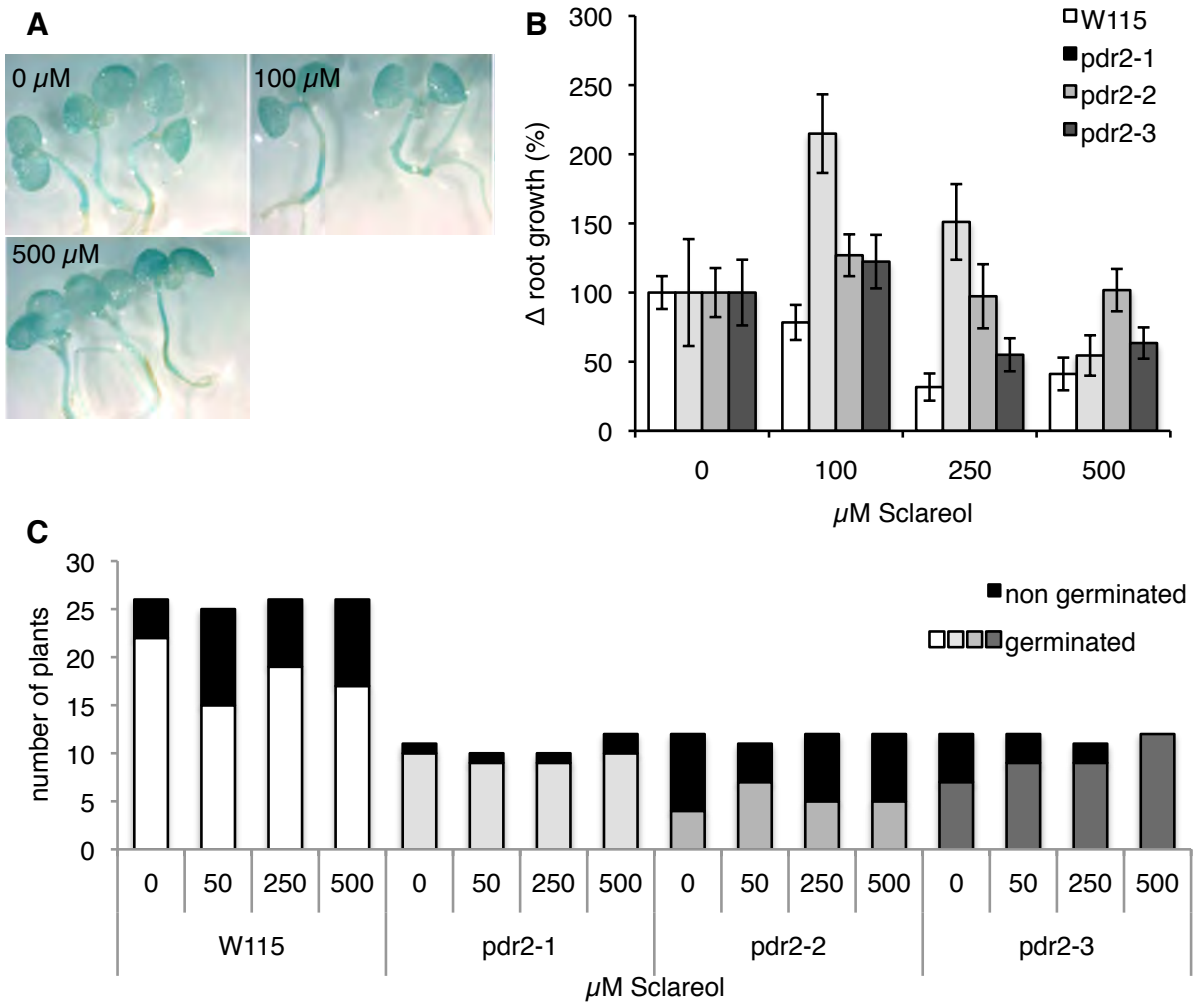

Supplementary Figure 4.4: Sclareol assays

A, Three-week-old *pPDR2-GUS* seedlings were grown on different sclareol concentrations for 24 h and stained for GUS activity. **B,** W115 and *phpdr2* plants were grown on plates with and without sclareol. Difference in root length are depicted as means ± S.E.M. (n = 15). **C,** Seeds of W115 and *phpdr2* plants were grown for 11 d on different sclareol concentrations. Number of germinated (white, grey) and non-germinated (black) seeds are depicted.

Supplementary Table 4-1: Candidate masses in Bruker analysis

					1: trichomes			2: leafwash			3: leafwash			avg		
m/z	**time**	**PS, PL**	**ESI mode**	**Inten-sity**	***pdr¹***	***pdr²***	***pdr³***	***pdr¹***	***pdr²***	***pdr³***	***pdr¹***	***pdr²***	***pdr³***	**1**	**2**	**3**
601.32	6.6	PS A	pos	5	143	24	26	n.d.	n.d.	n.d.	n.d.	n.d.	n.d.	64	n.d.	n.d.
487.31	5.8	PL E	pos	4	68	18	59	52	28	75	n.d.	n.d.	n.d.	48	52	n.d.
503.3	4.7	PL F	pos	4	71	20	58	53	28	78	37	59	39	50	53	45
427.28	5.8		pos	3	86	64	73	185	154	268	n.d.	n.d.	n.d.	75	203	n.d.
545.31	5.6		pos	3	119	14	34	26	9	26	70	152	95	56	20	106
601.34	5.1	PS J	pos	3	122	14	33	45	28	55	31	86	38	57	43	51
461.33	4.2	PS G	pos	2	53	7	55	43	25	89	54	41	28	39	52	41
501.29	4.9	PL C	pos	2	72	19	46	41	36	42	38	74	47	46	40	53
503.3	5	PL F	pos	2	81	19	80	286	74	187	n.d.	n.d.	n.d.	60	182	n.d.
521.35	4.8	PS H	pos	2	69	23	59	99	56	371	n.d.	n.d.	n.d.	50	175	n.d.
575.32	4.9		pos	2	51	15	65	56	43	98	n.d.	n.d.	n.d.	44	66	n.d.
611.33	4.2		pos	2	17	65	72	33	54	71	50	71	107	51	53	76
503.3	3.9	PL F	pos	1	58	7	35	31	19	48	31	44	30	33	33	35
549.28	4.99		neg	1	58	8	40	27	16	48	32	44	30	35	30	35
549.28	5.09		neg	1	86	18	30	22	7	14	38	64	42	45	14	48
565.28			neg	1	106	9	14	27	14	20	21	96	38	43	20	51

Candidate masses with retention time, putative petuniasterone (PS), or petuniolide (PL) identity, identification in positive (pos) or negative (neg) ESI mode, as well as the relative intensity of the compound (5: high, 1: low). Data is given for experiment 1 in which trichomes were sampled mechanically, experiment 2, in which greenhouse-grown leaves were washed in buffer, and experiment 3, in which sterile-grown leaves were washed in buffer. For each phpdr line in each experiment, the amount in percent of wild-type levels is given. To the right, the average (avg) of all *phpdr2* lines for each experiment is given. Color code: dark blue: *phpdr2* levels lower than 30% of wild type, blue: levels 31-50% of wild type, light blue: levels 51-70% of wild type. n.d., not detected.

Supplementary Table 4-2: Analysis of petunia sterol masses of experiment 2 by XCMS

Compound	Molecular formula	Time (min)	Mass m/z	Fold change	*P*-value	Intensity	toxicity (ED50, ppm) *Heliothis zea*	toxicity (ED50, ppm) *Spodoptera frigiperda*	Detected in species	CAS number
Petuniasterone A	$C_{32}H_{46}O_6S$	6.33	559.3088	4.5	0.023	1	130	150	*P. hybrida*	114175-99-4
Petuniasterone A	$C_{32}H_{46}O_6S$	5.12	559.3088	1.7	0.033	1				114175-99-4
30-hydoxypetuniasterone A	$C_{32}H_{46}O_7S$	4.2	575.3037	4.9	0.0054	1	>400		*P. hybrida*	
17β-hydoxypetuniasterone A	$C_{32}H_{46}O_7S$	4.2	575.3037	4.9	0.0054	1	>400		*P. hybrida*	
30-hydoxypetuniasterone A 7-acetate	$C_{34}H_{48}O_8S$	5.6	617.3143	1.2	0.43	3	144		*P. hybrid*, *P. parodii*	
Petuniasterone P4	$C_{34}H_{48}O_8S$	5.6	617.3143							131549-59-2
Petuniasterone Q	$C_{34}H_{48}O_8S$	5.6	617.3143				185			131569-68-1
16-ketopetuniasterone A 7-acetate	$C_{32}H_{46}O_8S$	n.d.	591.2986	n.d.	n.d.	n.d.	700		*P. parodii*	
Petuniasterone A acetate	**$C_{34}H_{48}O_7S$**	**6.6**	**601.3194**	**2.1**	**0.012**	**5**				
Petuniasterone A acetate	**$C_{34}H_{48}O_7S$**	**5.1**	**601.3194**	**2.3**	**0.017**	**1**				
12ξ-acetoxy-11β-hydroxy petuniasterone D 7-acetate	$C_{34}H_{48}O_9$	5.1	601.3371	2.3	0.017	1			*P. integrifolia*	
Petuniasterone J	**$C_{34}H_{48}O_9$**	**5.1**	**601.3371**				**>1000**		***P. parodii*, *P. integrifolia***	**126240-10-6**
Petuniasterone B	$C_{30}H_{46}O_6$	5.4	503.3367	1.5	0.059	1	no		*P. hybrida*	114176-00-0
Petuniasterone C	$C_{28}H_{42}O_4$	4.2	443.3156	5.4	0.0072		no		*P. hybrida*	114176-01-1
Petuniasterone D	$C_{30}H_{44}O_5$	n.d.	485.3262	n.d.	n.d.	n.d.	130	325	*P. hybrida*	119259-63-1
12α-acetoxypetuniasterone D 7-acetate	$C_{34}H_{48}O_8$	5.3	585.3422	1.5	0.15	1	115		*P. hybrida*	
16-ketopetuniasterone D 7-acetate	$C_{32}H_{44}O_7$	5.1	541.3160	2.2	0.0089	1			*P. parodii*	
Petuniasterone K	$C_{32}H_{44}O_7$	5.1	541.3160				>800		*P. parodii*	126240-11-7
Petuniasterone E	$C_{34}H_{50}O_8S$	5.7	619.3299	1.2	0.4	1			*P. hybrida*	119513-59-6
Petuniasterone G1, G2	**$C_{28}H_{44}O_5$**	**4.2**	**461.3262**	**5.6**	**0.01**	**4**	**no**			**119513-57-4**
Petuniasterone G1, G2	**$C_{28}H_{44}O_5$**	**5.2**	**461.3262**	**7.8**	**0.013**	**3**				**119513-57-4**
Petuniasterone H1, H2	**$C_{30}H_{48}O_7$**	**4.8**	**461.3262**	**5.1**	**0.00033**	**1**			***P. hybrida***	
Petuniasterone I	$C_{34}H_{48}O_9S$	5.5	633.3092	1.7	0.0032	2	125		*P. parodii*	126240-09-3
Petuniasterone P3	$C_{34}H_{48}O_9S$	5.5	633.3092						*P. parodii*	131549-58-1
Petuniasterone L	$C_{34}H_{46}O_8S$	5.6	615.2986	2.5	0.0002	2			*P. parodii*	126240-12-8
Petuniasterone L	$C_{34}H_{46}O_8S$	5.25	615.2986	2.4	0.00183	1			*P. parodii*	126240-12-8
Petuniasterone R	$C_{34}H_{46}O_8S$	5.6	615.2986	2.5	0.0002	2	400		*P. parodii*	127592-89-6
Petuniasterone R	$C_{34}H_{46}O_8S$	5.25	615.2986	2.4	0.00183	1			*P. parodii*	127592-89-6
7-deacetylpetuniasterone L	$C_{32}H_{44}O_7S$	n.d.	573.2986	n.d.	n.d.	n.d.			*P. parodii*	
Petuniasterone M	$C_{31}H_{46}O_5$	n.d.	499.3418	n.d.	n.d.	n.d.			*P. parodii*	126240-13-9
12α-acetoxypetuniasterone M	$C_{33}H_{48}O_7$	n.d.	557.3473	n.d.	n.d.	n.d.			*P. integrifolia*	
12ξ-acetoxy-11β hydroxypetuniasterone M 7-acetate	$C_{35}H_{50}O_9$	n.d.	615.3528	n.d.	n.d.	n.d.			*P. integrifolia*	

Compound	Molecular formula	Time (min)	Mass m/z	Fold change	*P*-value	Intensity	toxicity (ED50, ppm) *Heliothis zea*	toxicity (ED50, ppm) *Spodoptera frigiperda*	Detected in species	CAS number
Petuniasterone N	$C_{34}H_{46}O_{10}S$	n.d.	647.2884	n.d.	n.d.	n.d.	75		*P. hybrid, P. parodii, P. integrifolia*	123458-54-8
Petuniasterone O	$C_{32}H_{48}O_8$	n.d.	561.3422	n.d.	n.d.	n.d.	165		*P. parodii*	126589-94-4
Petuniasterone P1	$C_{32}H_{46}O_8$	n.d.	559.3265	n.d.	n.d.	n.d.			*P. parodii*	131549-56-9
Petuniasterone P2	$C_{32}H_{46}O_8$	n.d.	559.3265						*P. parodii*	131549-57-0
Petuniolide B	$C_{32}H_{46}O_8$	n.d.	559.3265				10		*P. parodii*	128255-51-6
Petuniasterone S	$C_{32}H_{48}O_7$	6	545.3473	1.1	0.65	2			*P. inflata*	149725-27-9
Petuniolide A	$C_{31}H_{44}O_8$	5.6	545.3109	1.7	0.012	2				128255-50-5
Petuniolide A	$C_{31}H_{44}O_8$	4.9	545.3109	1.3	0.3	1	13		*P. parodii*	128255-50-5
Petuniolide C	**$C_{29}H_{40}O_7$**	**4.9**	**501.2847**	**6**	**0.0097**	**3**	**3-4**	**69**	***P. axillaris, P. parodii, P.inflata***	**128255-52-7**
Petuniolide D	$C_{30}H_{42}O_7$	5.4	515.3003	1.6	0.046	1	2		*P. parodii*	128255-53-8
Petuniolide E	**$C_{29}H_{42}O_6$**	**5.8**	**487.3054**	**3.5**	**0.00029**	**4**	**21**		***P. parodii***	**131549-54-7**
Petuniolide F (5.0)	**$C_{29}H_{42}O_7$**	**5**	**503.3003**	**2.6**	**0.0082**	**3**	**170**		***P. parodii***	**131569-66-9**
Petuniolide F (3.9)	**$C_{29}H_{42}O_7$**	**3.9**	**503.3003**	**1.7**	**0.028**	**1**				**131569-66-9**
Petuniolide F (4.7)	**$C_{29}H_{42}O_7$**	**4.7**	**503.3003**	**2.2**	**0.0014**	**3**				**131569-66-9**
Petuniolide F (5.6)	**$C_{29}H_{42}O_7$**	**5.6**	**503.3003**	**3.6**	**0.00018**	**2**				**131569-66-9**
Petuniolide G	$C_{29}H_{40}O_8$	3.9	517.2796	1.6	0.21	1	12		*P. parodii*	131569-67-0
Petuniolide G	$C_{29}H_{40}O_8$	4.4	517.2796	1.7	0.14	1				131569-67-0
Petunianine A	$C_{34}H_{45}NO_6$	n.d.	564.332	n.d.	n.d.	n.d.			*P. inflata, P. hybrida*	
Petunianine C	$C_{36}H_{49}NO_7$	n.d.	608.3582	n.d.	n.d.	n.d.				149725-28-0
Petunianine D	$C_{34}H_{45}NO_5$	n.d.	548.3371	n.d.	n.d.	n.d.				149725-26-8
Petunianine D 7-acetate	$C_{36}H_{47}NO_6$	n.d.	590.3476	n.d.	n.d.	n.d.				157773-35-8
Petunioside A	$C_{44}H_{70}O_{19}S$	8.2	935.4305	1.1	0.28	1			*P. hybrida*	157810-77-0
Petunioside B	$C_{40}H_{68}O_{17}$	n.d.	821.4529	n.d.	n.d.	n.d.			*P. hybrida*	

Analysis of reported petunia sterol masses with XCMS for experiment 2. Compound name, chemical formula and mass are given, as well as the retention time, the reduction (fold change) in the pooled PDR2-RNAi lines compared to wild type with the respective p-value, and the respective intensity of the peak (fold of the mean maximum intensities, 5 = high, 1 = low). Further, reported growth arrest amounts in ppm for two herbivores are given, the detection in Petunia sp, and the CAS number of the respective compound. Compounds identified by manual analysis with Bruker are depicted in bold. n.d., not detected.

5 Data so far not integrated in publications

5.1 Results

5.1.1 Characterization of *PDR1* over-expression plants

5.1.1.1 Over-expression of PDR1 *alters plant morphology in Petunia*

To learn more about the PDR1 function, PDR1 over-expression (PDR1-OE) W115 lines expressing the *P. axillaris PDR1* genomic DNA (Genbank Accession JQ292812) with an N-terminal GFP fusion under the control of the 35S promoter were created. Transgenic lines with high *PDR1* expression levels were selected and plant morphology was investigated (Figure 5.1, Figure 5.2). Transgenic lines with wild-type *PDR1* expression levels (PDR1-OE silenced) showed wild-type morphology. Plants with high *PDR1* expression levels showed a tilted stem, first growing laterally in the pot until reaching the pot edge, followed by vertical growth (Figure 5.1 A, B). PDR1-OE lines formed less and shorter branches, a characteristic which was observed at different developmental stages (Figure 5.1 B - E). Leaf morphology was altered for PDR1-OE leaves in the middle stem section (leaves 5 - 13), whereas the oldest and youngest leaves displayed wild-type morphology (youngest leaves not shown, Figure 5.1 F - K).

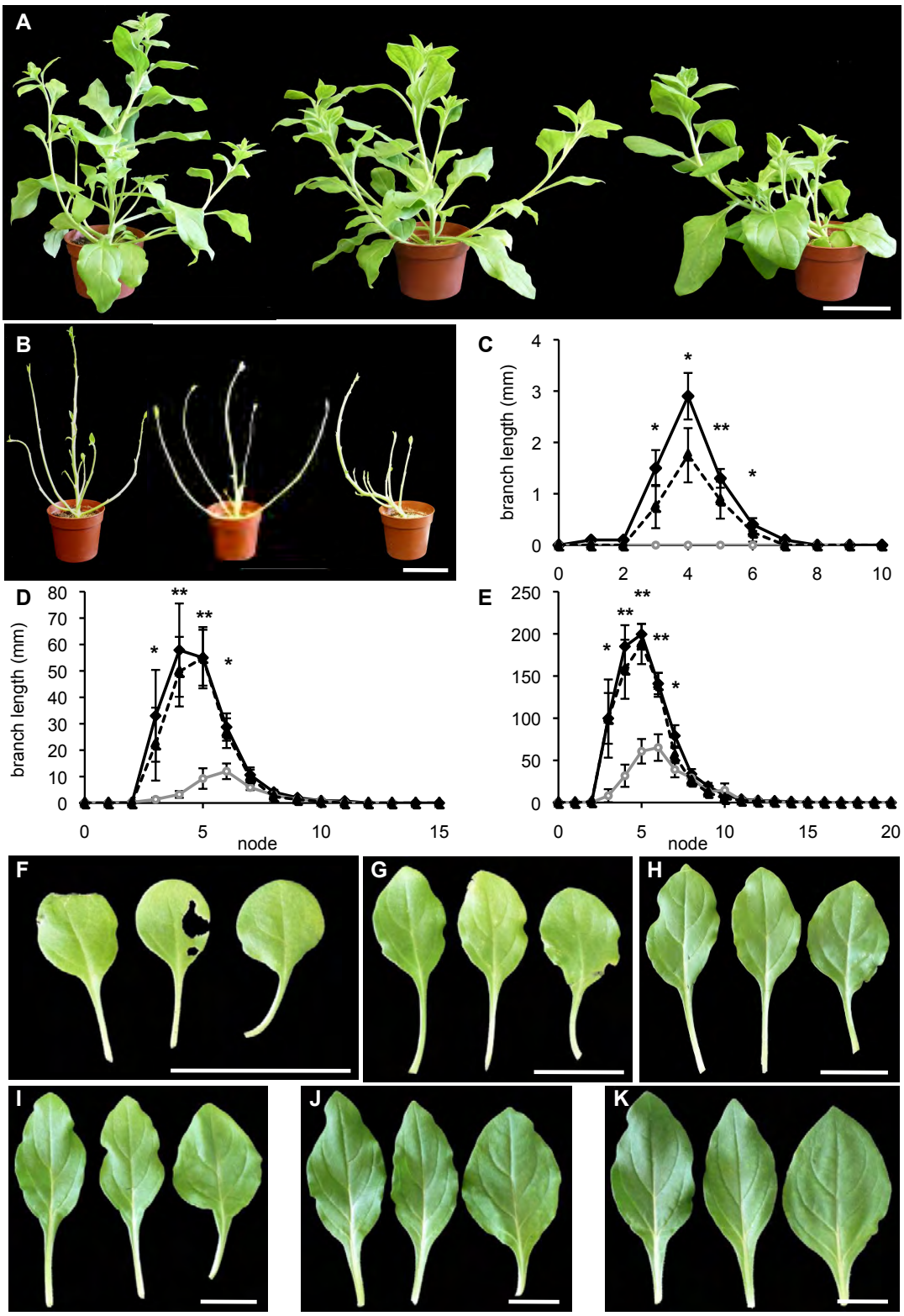

Figure 5.1: Aboveground morphological changes in Pdr1-OE lines

W115 plants transformed with 35S::GFP-*gPaPDR1*. **A,** Appearance of untransformed W115, PDR1-OE silenced, and PDR1-OE plants. Photograph taken 53 days after germination (dag). **B,** The same plants as in A with leaves striped off. **C-E,** Quantification of branch length 35 dag **(C)**, 46 dag **(D)**, 53 dag **(E)**, of W115 (black solid line), PDR1-OE silenced (black dashed line), and PDR1-OE (grey solid line with open circles) plants. Displayed are means ± S.E.M. (n = 8). **F-K,** Morphology of leaf 3 **(F)**, leaf 5 **(G)**, leaf 6 **(H)**, leaf 8 **(I)**, leaf 11 **(J)**, leaf 13 **(K)** of one representative W115, PDR1-OE silenced, and PDR1-OE plant 53 dag. Scale bars are 10 cm in A, B, and 5 cm in F-K. * = $P \leq 0.05$, ** = $P \leq 0.005$; values are given for differences between PDR1-OE and W115 / PDR1-OE silenced.

To learn more about aboveground morphological differences between PDR1-OE and the corresponding wild type, RNA was extracted from pooled nodes 4 - 6 that showed the largest differences in branching, for node 8 and 13, where differences were smaller or absent, for an internode section between nodes 7 and 8, and for the petiole of leaf 6 that showed a difference in morphology compared to wild type. Expression levels of *PDR1*, the auxin transporter *PIN1*, and the strigolactone (SL) synthesis gene *DAD1* were analyzed with semiquantitative PCR (Figure 5.2 A - C). Untransformed wild-type lines generally displayed higher gene expression levels than PDR1-OE silenced lines. Assuming that the *PDR1* construct present in the PDR1-OE silenced lines does not cause off-target effects, this leads to the conclusion that expression of *PDR1, PIN1*, and *DAD1* is quite variable in different lines, even with the same genetic background. Thus, by comparing PDR1-OE data with data of its *PDR1* silenced sister line revealed that *PIN1* expression was enhanced in the nodal parts, and *DAD1* expression levels were reduced in node 13 and internode 7, 8. This data is in contrast with the phenotypic observation of reduced branching, which implies higher SL levels, and thus higher SL synthesis and lower PIN1 levels (see 1.2.2.1, Crawford *et al.*, 2010). However, transcription levels do not necessarily depict protein amounts, so PIN1 levels could still be decreased in PDR1-OE lines, and SL synthesis could be enhanced. To better understand the interaction of SL and auxin in bud outgrowth and leaf morphology, antibodies should be used to monitor protein levels.

In addition to the aboveground characterization of PDR1-OE, belowground gene expression and root morphology were investigated. To test whether there is a feedback of SL transport on SL synthesis, *DAD1* expression was investigated in the lowermost part of the root, where the SL synthesis gene *MAX4* was reported to be highly expressed (Mashiguchi *et al.*, 2009; Bainbridge *et al.*, 2005). Roots of big and small plants were analyzed for different developmental stages. *DAD1* levels were not altered in PDR1-OE lines compared to wild type (Figure 5.2 D). This finding could indicate first that over-expression of *PDR1* does not influence SL synthesis in the root tip, second that PDR1-OE influences SL synthesis not in root tips but maybe in other plant tissues, or third that SL synthesis is only regulated post-transcriptionally by SLs.

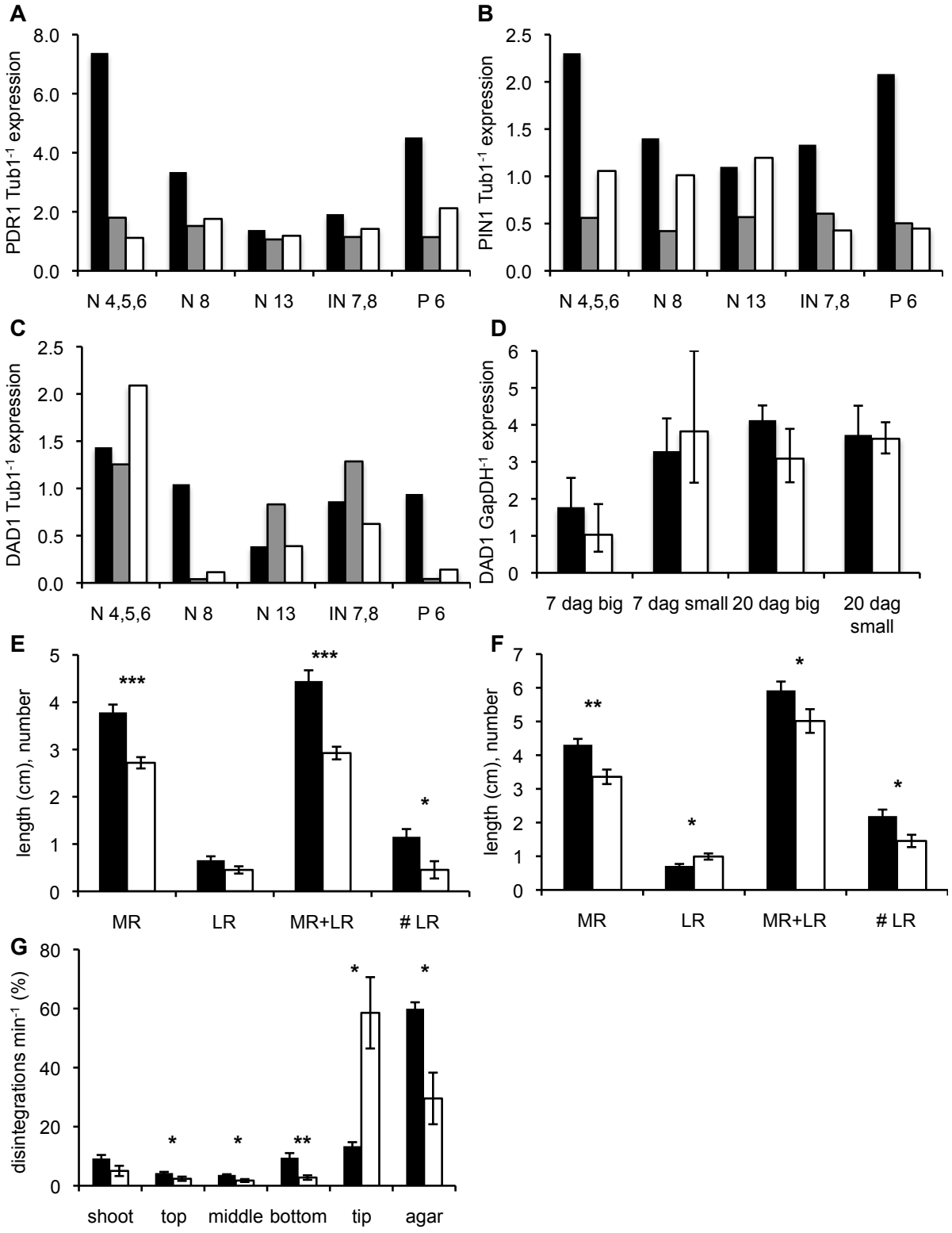

Figure 5.2: Additional phenotypes of PDR1-OE plants

Expression data, morphology and GR24 transport for wild type (black columns), PDR1-OE silenced (gray columns), and PDR1-OE (white columns) plant tissues. **A-C,** Expression levels of *PDR1* **(A)**, *PIN1* **(B)**, and *DAD1* **(C)** determined by semiquantitative PCR and normalized by *Tubulin 1* expression in various nodes (N), in internode between nodes 7 and 8 (IN 7,8), and in petiole of node 6 (P6) of 56 dag plants. **D,** Quantitative PCR for *DAD1* in the lowermost 1 cm of roots of big and small plants, 7 dag and 20 dag. **E, F,** Quantification of the length of primary root (MR), the sum of lateral roots (LR), the sum of MR and LR, and the number of lateral roots per plant (# LR) at 13 **(E)** and 20 **(F)** dag. **G,** Uptake of radiolabeled GR24 to the root tip (tip), transport to upper root parts (bottom, middle, and top), to shoot, and exudation of GR24 from root to agar. Values are mean ± S.E.M. (n = 8). * = $P \leq 0.05$, ** = $P \leq 0.005$, *** = $P \leq 0.0005$.

SL levels were shown to influence root morphology (see 1.2.2.2). Therefore, the length of primary roots, as well as the length and number of lateral roots was analyzed in PDR1-OE and in wild type. PDR1-OE plants showed shorter primary root length, and shorter overall root length, which was defined as the sum of the length of primary and lateral roots. In addition, PDR1-OE lines displayed a reduction in lateral root length and number (Figure 5.2 E, F); however, it was noticed that results regarding root morphology were not consistent between experiments, which might be due to the light installation of the growth chamber. Experiments should therefore be repeated.

Transport experiments with the radiolabelled synthetic SL GR24 were performed to evaluate further if SL transport and distribution are altered in PDR1-OE plants compared to the respective wild type (Figure 5.2 G). A passive or active uptake of GR24 was assumed into the root from an agar block that was brought into contact with the root tip, and a subsequent PDR1-dependent transport of GR24 to the more apical plant parts, as well as a PDR1-dependent exudation of GR24 to the agar-containing medium on which the plants were placed. In PDR1-OE plants, GR24 accumulated in the root tip, and less GR24 compared to the wild type was transported to the upper plant parts or exuded to the medium. If in PDR1-OE plants, PDR1 allocation was wild-type like, one would expect elevated transport to the upper parts of the plant, as well as higher exudation to the medium (see 3.3). As this is not the case in transport experiments, it has to be concluded that PDR1 location in PDR1-OE lines is altered.

5.1.1.2 Over-expression of PDR1 *in Arabidopsis*

Arabidopsis thaliana Col-0 and silencing-deficient *rdr6* plants in a Col-0 background were transformed with *GFP-PaPDR1* under the control of the 35S promoter to analyze the protein function in a non-native system. It has been shown that the SL transporter is functional in this system (Kretzschmar *et al.*, 2012), and thus, an aim of this work was to investigate if the presence of *PDR1* altered the morphology of Arabidopsis plants.

Arabidopsis PDR1-OE plants grown for one month on soil in the greenhouse showed a slight but significant decrease in aboveground lateral branching compared to wild-type Col-0 lines (Figure 5.3 A). Cotylimide VI (CTL-VI) was reported to increase SL synthesis in plants (Tsuchiya *et al.*, 2010), and as SLs inhibit branching, it was hypothesized that CTL-VI application would result in a decrease in branching. Interestingly, plants treated with the chemical showed the opposite behaviour, namely an increased branching

phenotype. The difference observed between PDR1-OE and the wild type was undone by CTL-VI treatment (Figure 5.3 A). CTL-VI significantly induced the formation of lateral buds in PDR1-OE lines relative to the wild type, whereas the inducing effect was not significant in Col-0. This indicates an increased sensitivity of PDR1-OE lines to CTL-VI, and possibly to SL amounts.

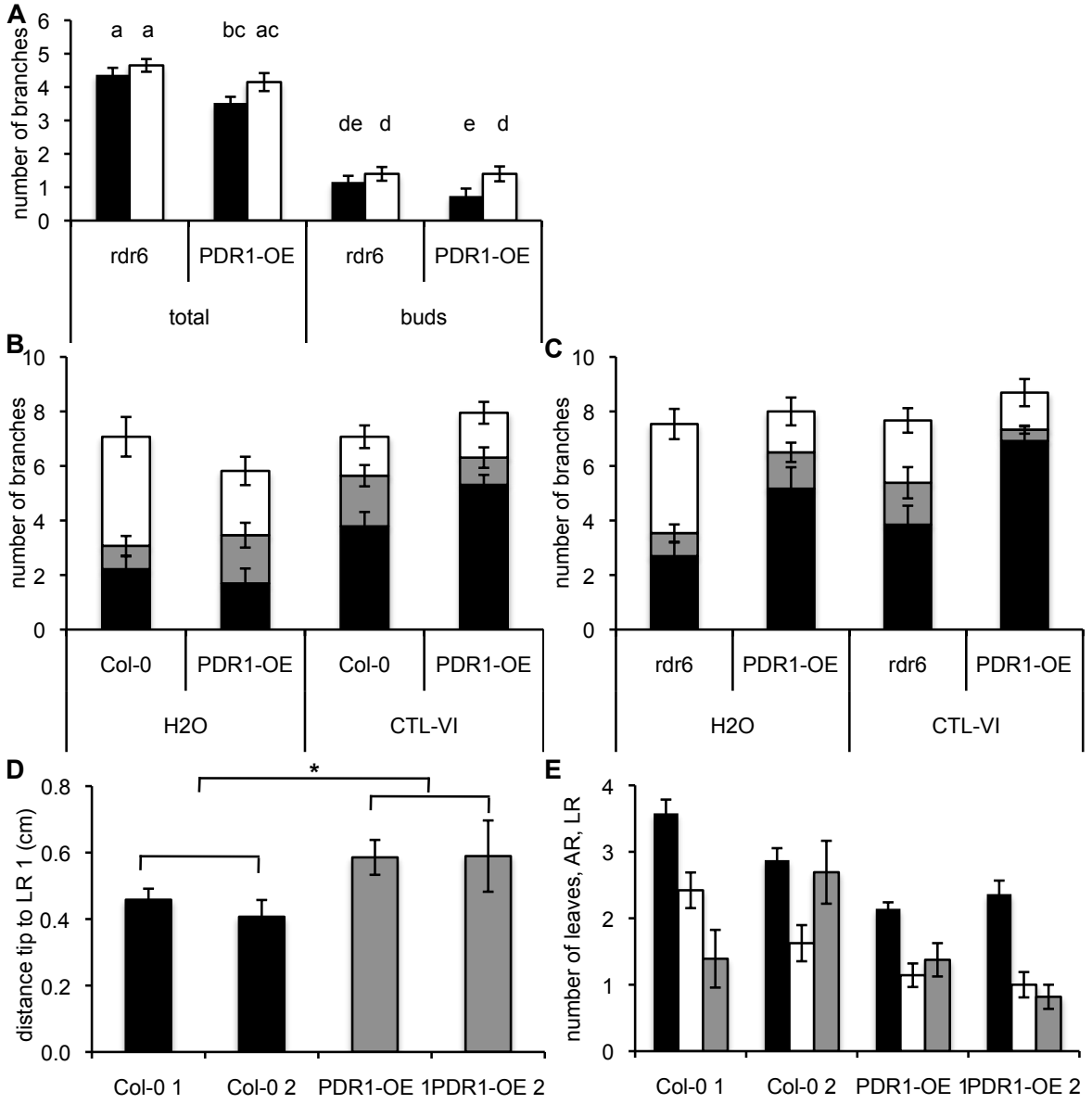

Figure 5.3: PDR1-OE in Arabidopsis

A, Aboveground total number of branches (outgrown and buds) in Col-0 or rdr6 wild type and PDR1-OE in rdr6 background 42 dag with CTL-VI treatment (white bars) or without (black bars). Data are means ± S.E.M. (n = 20). **B-C,** Aboveground number of branches 0 – 1 cm (white), 1 - 3.2 cm (grey), and longer than 3.2 cm (black) for Col-0 **(B)** and rdr6 **(C)** backgrounds with their respective PDR1-OE line, treated with water or with CTL-VI. Plants were grown as described by Waters et al 2012a. Data are means ± S.E.M (n ≥ 12). **D,** Distance from the root tip to the first lateral root primordium in two wild-type (black) and two PDR1-OE lines (grey) 3 dag. Data are means ± S.E.M. (n = 4, 6). **E,** Number of leaves (black), adventitious roots (white), and lateral roots (grey) in two wild type and two PDR1-OE lines. Plants were grown for 3 d in dark and 6 d in light. Data are means ± S.E.M. (n ≥ 11). * = $P \leq 0.05$

The experiment was repeated with plants first grown under short day conditions with subsequent shift to continuous light, which induced bolting and branching. Arabidopsis SL mutant plants were shown to have a more pronounced root branching phenotype under these conditions (Waters *et al.*, 2012a). PDR1-OE lines did not show a significant difference in overall branch number, and neither in the length distribution of the branches (Figure 5.3 B, C). CTL-VI addition increased the ratio of long branches in PDR1-OE, and did not significantly affect the respective wild-type roots. The stimulatory effect of CTL-VI on branching in Arabidopsis observed in the earlier experiment was thus confirmed. There is no straightforward explanation for the stimulatory effect on branching upon CTL-VI addition; however, it is clear that CTL-VI does not simply upregulate SL production in Arabidopsis. From the aforementioned experiments, it was concluded that the PDR1-OE construct does not alter aboveground branching in Arabidopsis considerably.

For the investigation of belowground morphology, PDR1-OE and the respective wild type were transformed with GUS reporter constructs under the control of a *DR5* promoter to visualize auxin accumulation of root primordia and thus, lateral root formation. The distance of the root tip to the first lateral root primordium, a measure for lateral root induction, was increased in PDR1-OE lines (Figure 5.3 D), indicating that lateral roots are formed with a lower frequency.

Adventitious root formation is induced by etiolated growth, therefore, Col-0 and PDR1-OE plants were grown 3 d in dark, followed by 6 d growth in light. Wild-type plants showed etiolated growth, whereas PDR1-OE lines only started to grow in the subsequent light period. Therefore, it was not surprising that PDR1-OE lines showed a delay in growth (lower number of leaves) and lower numbers of lateral and adventitious roots (Figure 5.3 E). If the lower developmental stage is taken into account, PDR1-OE lines still show a lower number of lateral roots compared to wild type, which is in agreement with the observations described above.

5.1.2 Petunia rootstock and scion are both involved in branching

Grafting experiments have been used for a long time to investigate mobility of signal compounds (Müller and Leyser, 2011). It was shown by such means that the branch-inhibiting, root-derived signal is mobile, and moves from the root towards the shoot. Experiments with SL synthesis and signalling mutants have been

performed (see 1.2.2.1). It was thus examined if SL transport mutant plants exhibited a similar of different behavior compared to synthesis mutants, and if PDR1-OE plants showed a distinct phenotype.

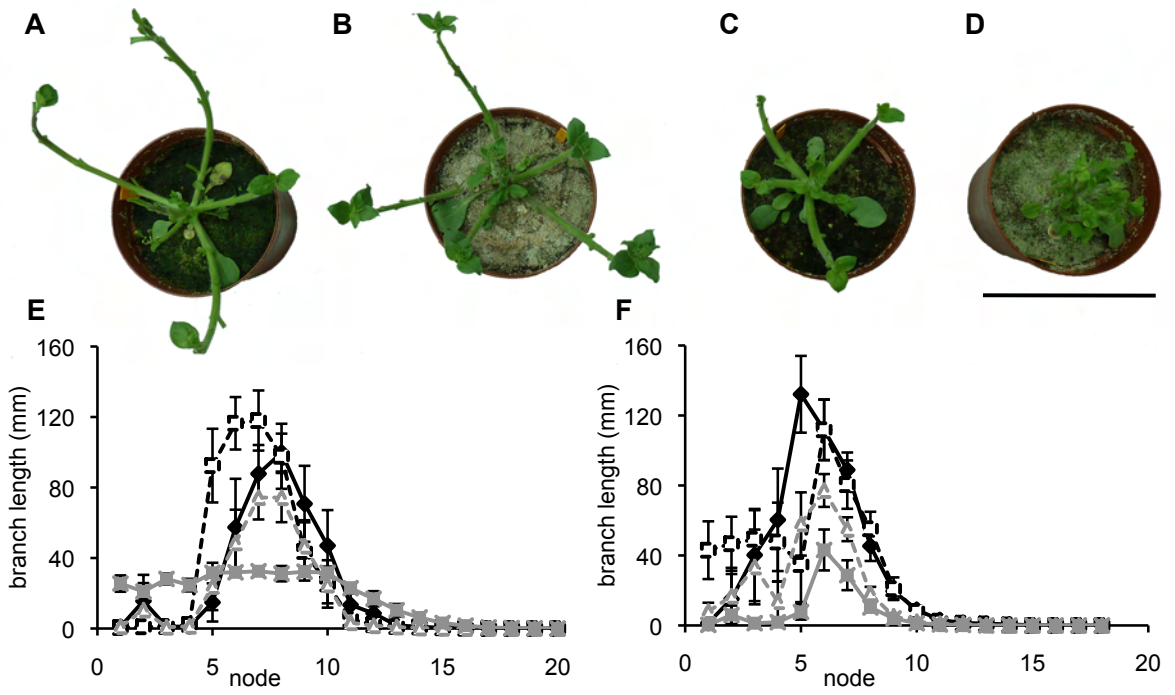

Figure 5.4: Grafting experiments

Grafting of V26 wild type on the SL mutant *dad1* (**B, E**: black dashed) and vice versa (**C, E**: grey dashed), and the control graftings of V26 (**A, E**: black solid), and of DAD1 (**D, E:** grey solid) **F,** Grafting of W115 wild type on PDR1-OE (black dashed) and vice versa (grey dashed), and the control graftings of W115 (black solid), and of PDR1-OE (grey solid) of 61 dag plants. **E, F:** Data are means ± S.E.M. (n = 7). of 59 dag plants. Scale bar = xx cm.

Grafting experiments described for the SL synthesis mutant *dad1* with its wild type cultivar V26 (Napoli, 1996) were repeated in this work. The high branching phenotype of *dad1* scions was reported to be partially rescued when grafted onto a wild-type stock. Note that the morphology of dad1 is different from V26, and the graftings show an intermediate phenotype (Figure 5.4 A-D). In the experiments presented here, the branching phenotypes of *dad1* scions could be partially rescued by a wild-type stock likewise, and branch length of such graftings was shorter than for the reverse grafting of a wild-type scion on a *dad1* stock (Figure 5.4 E). PDR1-OE plants displayed reduced overall branching and branch length compared to wild-type plants (see 5.1.1, Figure 5.1). Grafting experiments showed an elevated branching of PDR1-OE scions on wild-type stocks compared to the PDR1-OE control (Figure 5.4 F). The reverse grafting of wild-type scion on PDR1-OE stock showed even longer branches, but not as long as the wild type control grafting. These results indicate that the SL synthesis, as well as the SL

transport capacity of the scion and the stock, are important to modulate branching, whereas the impact of the scion genotype is bigger than the one of the stock.

Grafting experiments were performed with PDR1-KO lines likewise but the PDR1 deficient lines showed aberrant phenotypes, and thus, the experiments need to be repeated. In contrast to previous observations (Kretzschmar *et al.*, 2012), PDR1-KO plants showed slower growth, reduced branching and more aberrant phenotypes than the corresponding wild-type lines even if the plants were not manipulated by grafting. One possible reason for this behaviour could be the nutrient levels of the soil, because they are of major importance for branch outgrowth. Therefore, various substrates and substrate combinations were tested to understand if the observed phenotype could be rescued. On nutrient depleted substrates, still the same growth delay and reduced branching was observed for PDR1-KO plants. It was therefore concluded that the observed phenotype was likely not due to nutrient levels in the substrate, but due to a faster decline in seed quality in PDR1-KO plants compared to the respective wild-type lines (all the seeds were harvested in September 2011). Indeed, a role for SLs in seed germination was reported (see 1.2.2.3). Currently, new seed batches are produced for the repetition of the experiment.

5.1.2.1 Involvement of SLs in wilting

Earlier observations by T. Kretzschmar suggested an involvement of SL transport in wilting. Therefore, wilting experiments were performed with *dad1*, PDR1-KO, and PDR1-OE lines. For *dad1* plants, a fast-wilting phenotype was observed (Figure 5.5 A - C). PDR1-KO and PDR1-OE lines showed an inconsistent pattern in the three experiments performed (Figure 5.5 D - F, and G, H), indicating that SL synthesis, but not SL transporter levels are important for water balance of Petunia.

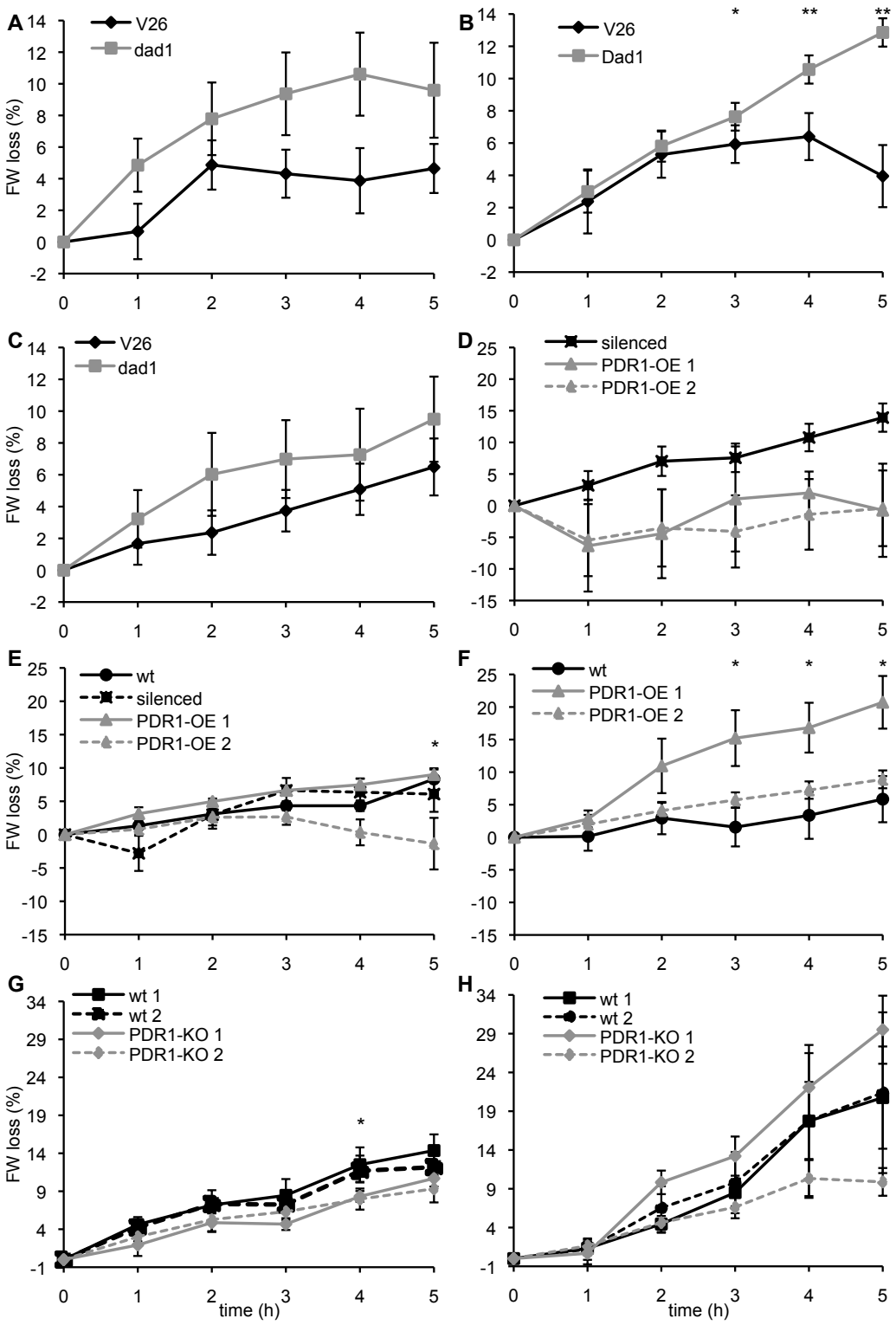

Figure 5.5: Wilting experiments

A-H, Fresh weight (FW) loss in percent for 28 dag SL synthesis mutant (*dad1*, grey squares), SL transport mutant (PDR1-KO, grey diamonds), SL transport *PDR1* over-expression plants (PDR1-OE, grey triangles), SL transport *PDR1* silenced lines (silenced, black squares), and their respective wild types (black diamonds, circles, and squares). Note that y-axis scales are identical for A-C, D-F, and G-H. Experiment 1 included data of A, D, and G; experiment 2 included data of B, E, and H; and experiment 3 included data of C and F. Data are given as means ± S.E.M. (n = 5). P-values are given for differences between V26 and *dad1* **(A - C)**, wild type and PDR1-OE 1 **(D - F)**, and wild type 1 / 2 and PDR1-KO 1 / 2 **(G-H)**, * = P ≤ 0.05, ** = P ≤ 0.005.

5.2 Discussion

5.2.1 Are SL levels altered in PDR1-OE Petunia lines?

Analysis of PDR1-OE plants resulted in some interesting observations: the plants exhibited reduced axillary branching (Figure 5.1), an increased resistance to high GR24 concentrations, and higher arbuscular mycorrhizal fungi (AMF) colonization rates (L. Borghi, University of Zürich, Switzerland, personal communication), implying the presence of high SLs levels at nodes and in roots (see 5.1.1). However, a transcriptional increase of *DAD1* could not be detected in nodes that show a strong reduction in branching (Figure 5.1), or in root tips (Figure 5.2), which were reported to be a main site of SL synthetic gene expression (Sorefan, 2003; Mashiguchi *et al.*, 2009). As many proteins are regulated post-transcriptionally, it is still possible that SL levels are increased in PDR1-OE lines. An alternative hypothesis is that SL turnover is reduced, resulting in higher overall SL levels. Our collaborators (group of Prof. H. Bouwmeester, Wageningen University, The Netherlands) will investigate the hypothesis of elevated SL levels in PDR1-OE tissues by quantification of SLs in the different lines. In case SL amounts are not elevated, the observed phenotypes likely result from an altered SL distribution in the tissue.

The increased resistance of PDR1-OE plants to high GR24 levels, the increased AMF colonization, the lower number of lateral roots (see 5.1.1.1, 5.1.1.2), and the increased number of meristematic cells in the root tip (see 3.3) point towards increased SL levels in roots, and an increased SL exudation. However, SL transport rates by the root tip were not enhanced in PDR1-OE lines (Figure 5.2), indicating that SL transport capacity is not elevated. A root exudation assay with radiolabeled GR24 will show if the exudation capacity of the root is enhanced for PDR1-OE plants, which could explain the observed phenotypes.

Over-expression of PDR1 resulted in elevated AMF colonization rates. This trait may be applicable to agriculture biotechnology. To date, high yields depend heavily on inorganic fertilizers, resources that are limiting and energetically expensive to produce. Furthermore, growth of crops with AMF was shown to be beneficial in regions where nutrient levels are suboptimal, with plants showing increased stress resistance (Estrada

et al., 2013; Nadeem *et al.*, 2014; Sawers *et al.*, 2008). Therefore, investigations of altered SL transport to enhance AMF colonization might be of interest for crop improvement.

5.2.2 Does *PDR1* over-expression influence *Ph*MAX2?

The inhibitory function of SLs in axillary branching is well described (see 1.2.2.1). However, in PDR1-OE lines, not only branching behaviour is altered. Plants exhibit altered main axis growth pattern (Figure 5.1), and they have an altered vasculature patterning (L. Borghi, personal communication). Those phenotypes could be due to a reduction of lignin content in the stem, a hypothesis that is currently being tested in our laboratory. In addition, PDR1-OE plants have altered leaf shapes (Figure 5.2), and *dad1* mutant plants wilt faster (Figure 5.5). Arabidopsis *max2* deficient plants were reported to display altered leaf shapes, a delay in leaf senescence, and a reduced resistance to drought stress (Woo *et al.*, 2001; Stirnberg *et al.*, 2002). Thus, it was hypothesized that in PDR1-KO, PDR1-OE, and *dad1* plants, *PhMAX2* levels could be altered, causing the observed phenotypes (see 1.2.2.3). Analysis of *MAX2* transcription and protein levels in PDR1-KO, PDR1-OE, and *dad1* plants will show if the observed phenotypes are due to an altered SL signalling.

5.2.3 Differences among Arabidopsis and Petunia PDR1-OE lines

Petunia PDR1-OE lines exhibit a strong reduction in axillary branching and other distinct morphological changes (see 5.1.1.1). Arabidopsis PDR1-OE plants in turn do not show these distinct features, only a rather minor branching difference under some conditions (Figure 5.3). However, experiments with PDR1-OE Arabidopsis lines showed that *PaPDR1* is a functional SL exporter in roots (Kretzschmar *et al.*, 2012), and also, Arabidopsis root morphology is altered in PDR1-OE lines (Figure 5.3). Thus, the lack of a distinct aboveground phenotype in PDR1-OE Arabidopsis plants was not due to an incompatibility of the Petunia gene with Arabidopsis. A reason for the different phenotypes observed could potentially involve different regulatory mechanisms for *PDR1* expression or activity in shoot tissue between the two species. An observation in line with this hypothesis is that Arabidopsis *PaPDR1* promoter GUS reporter lines showed GUS staining in roots, but the signal was absent in aboveground tissue (L. Borghi, personal communication). As the GUS signal is present in Petunia lines in above- and

belowground tissues (Kretzschmar *et al.*, 2012), this finding indicates that promoter activity is differentially regulated in the shoots of Arabidopsis and Petunia.

In both, Arabidopsis and Petunia plants respectively, SLs are synthesized not only in the root, but also locally in the shoot (Napoli, 1996; Bainbridge *et al.*, 2005). In Arabidopsis grafting experiments, a wild-type scion grafted on a SL mutant stock fully restores wild-type branching behaviour, indicating that shoot-derived SL is sufficient to restore branching (Sorefan, 2003). The opposite grafting of a mutant scion on a wild-type stock similarly results in wild-type branching (Sorefan, 2003). However, in Petunia, only a partial rescue was observed in graftings with *dad1* or *pdr1* plants with their respective wild types, irrespective of the direction of grafting (Figure 5.4, Napoli, 1996). These results indicate that in Petunia, the SL status of the scion is more important than the one of the root, as wild-type scions cause a branching behaviour more similar to wild-type control graftings than wild-type stocks grafted with mutant scions. The distinct reactions of the two species on grafting experiments may indicate that SL production and transport is of different importance. Arabidopsis plants are able to restore wild-type branching when SLs are present either in the root or in the shoot, whereas Petunia plants require an integration of SL signals from both plant parts. One possible explanation for this fact arises from the different growth strategies and architectures of the two species.

Vegetative growing Arabidopsis plants do not branch, whereas Petunia plants display elongated internodes and lateral branches. This is perhaps an adaptation to the respective growth environment: Arabidopsis is a pioneer plant, and grows preferentially in areas where competition with other plants for resources is low. Petunia however, originates from South America grassland regions, where competition with grasses and shrubs for space and light is much higher. The short generation time of Arabidopsis allows fast growth and reproduction when conditions are good, whereas the longer generation time of Petunia requires plastic growth, and adaptation to various conditions. Arabidopsis only bolts upon flowering induction, to allow seed dispersal by wind, and thus might require a less fine-tuned branching control system than Petunia. In the case of Petunia, SL synthesis in the root followed by transport to the shoot probably transfers the belowground status of nutrients into a decision whether more branches are formed or not, a crucial signal that avoids nutrient depletion upon unfavourable conditions. For Arabidopsis, this signal might not be of major importance, as the plant senesces soon

after bolting and seed production. It would be interesting to test these hypothesis in future with other species exhibiting growth strategies similar to Arabidopsis or Petunia.

In summary, plants altered in SL transport displayed phenotypes similar to such described for SL synthesis mutant plants. Despite this, the severity of the phenotype was often lower in transport mutant plants. These findings highlight the importance of transporter studies in addition to the research performed on biosynthesis of SLs.

5.3 Materials and Methods

Growth conditions: Petunia plants were grown in the greenhouse in a 16 h light, 8 h dark regime at 60% relative humidity, and 25 °C on ED 73 Einheitserde. Arabidopsis plants were grown on the same substrate in a 16 h light, 8 h dark regime at 60% relative humidity, and 22 °C. Petunia seeds were sterilized for 3 min in 70% [v/v] ethanol, and washed 3 times with ddH_2O. Plants were grown on 0.5 MS – Suc (2.2 g L^{-1} MS medium, 9 g L^{-1} phyto agar, pH 5.7) or on 0.5 MS + Suc (2.2 g L^{-1} MS medium, 15 g L^{-1} sucrose, 9 g L^{-1} phyto agar, pH 5.7) in a 16 h light, 8 h dark regime at 60% relative humidity, and 21 °C. Arabidopsis seeds were sterilized for 15 min in 70% [v/v] ethanol, followed by 15 min 100% ethanol, dried, and plated on the medium mentioned above. Before incubation in the growth chamber, plates were stratified in the dark for 3 days at 4 °C. For the Arabidopsis lateral branching experiment, conditions are mentioned in the respective section.

Petunia transformation: *Petunia hybrida* W115 plants were grown on MS + Suc (30 g L^{-1} sucrose, 4.4 g L^{-1} MS basal salts, 0.112 g L^{-1} Gambourg vitamins, 9 g L^{-1} phyto agar, pH 5.7) for 2 months. Leaves were cut in squares, stems in 1 cm long pieces, both were placed on filter paper that was wet with liquid MS and incubated in the growth chamber for two days. *Agrobacterium tumefaciens* cultures transformed with the respective constructs were grown for 16 h at 28 °C, centrifuged for 5 min at 4000 g, 23 °C, and subsequently resuspended in liquid Petunia medium (30 g L^{-1} sucrose, 4.4 g L^{-1} MS basal salts, pH 5.7, 0.112 g L^{-1} Gambourg vitamins, 100 µg L^{-1} 1-naphthalene acetic acid, 2 mg L^{-1} 6-benzylaminopurine, 1 mg L^{-1} folic acid, 1 µM $CuSO_4$, 20 µM acetosyringone), and adjusted to optical density (OD) 0.5. The Petunia tissues were transferred to Co-Cultivation medium plates and placed on filter paper (30 g L^{-1} sucrose, 4.4 g L^{-1} MS basal salts, 0.112 g L^{-1} Gambourg vitamins, pH 5.7, 100 µg L^{-1} 1-naphthalene acetic acid, 2 mg L^{-1} 6-benzylaminopurine, 1 mg L^{-1} folic acid, 1 µM $CuSO_4$, 9 g L^{-1} phyto agar). The *A. tumefaciens* suspension was added onto the filter paper, and incubated for 30 min with occasional shaking. Residual liquid was removed and the plates were incubated for 3 days in a growth chamber. Next, Petunia tissues were transferred to selective plates (Co-cultivation plate composition with additionally 100 mg L^{-1} Timenten, 500 mg L^{-1} Carbencillin, and the respective selective agent for the

construct). Petunia tissues were transferred to new selective plates every three weeks, until callus tissue was formed. Callus with a diameter of 0.5 cm was removed from the residual tissue, and grown further on selective media. Leaflets with a size of 1 cm were removed from the callus and transferred to selective media without auxin and cytokinin supplements. If roots were formed, plants were transferred to soil and grown for seeds in the greenhouse.

RNA isolation, cDNA synthesis, semiquantitative and quantitative PCR: RNA was isolated with the RNeasy Plant Mini Kit (Qiagen), cDNA was synthesized from 1 µg RNA with M-MLV Reverse Transcriptase (Promega) and oligodT(18) primers for 1 h at 40 °C. For semiquantitative expression analysis, PCR was performed with GoTaq polymerase (Promega) with its respective buffer, 53 °C annealing temperature, 38 cycles, 1 min elongation, and 0.2 µl cDNA template per reaction. Quantitative PCR was performed with a 7500 Fast Real-Time PCR machine (Applied Biosystems) with SYBR Green master mix, 100 nM primers, 1.2 µl cDNA per reaction, and a PCR program as described (Kretzschmar *et al.*, 2012). An overview on the primers used can be found in Table 9-1.

Hygromycin leaf test: Petunia lines transformed with a construct carrying Hygromycin resistance were tested for construct presence by cutting four 1 cm^2 squares of a leaf. Two squares each were placed on 0.5 MS - Suc, the other 0.5 MS - Suc + 20 mg L^{-1} Hygromycin. Survival of the leaflets was monitored after 2 weeks incubation of plates in a growth chamber. The protocol was modified from (Wang and Waterhouse, 1997).

Grafting experiments with Petunia: Petunia plants were grown for 14 d on 0.5 MS - Suc. Cotyledons and possible emerging leaves were removed with a microscissor, the hypocotyl was cut in half, and scions were moved to another plate to join with stocks of another or the same genotype. With the help of a binocular, scion and stock were joined as well as possible, and plates were incubated for two more weeks in continuous light, 60% relative humidity, 25 °C. Roots that formed at the junction of scion and stock were removed, and plants were transferred to soil in the greenhouse.

Lateral branching in Petunia: Plants were grown in 0.55 L pots in the greenhouse as described above. Branches were quantified at different time points for wild type W115, the PDR1-OE silenced line 447, and various PDR1-OE lines. Depicted are results for line

455, similar results were obtained for the T1 line 459 and its T2 lines 459-16, 459-17, and 459-19.

Lateral branching in Arabidopsis: Col-0 *rdr6* and PDR1-OE (line 42) were stratified for 3 days, transferred to a 16 h light, 8 h dark regime (for conditions, see above), GFP-positive plants were marked 3 days after germination (dag), transferred to soil after 11 dag, and grown for 31 days in the greenhouse. For the branching experiment with the shift from short to long day conditions (Waters *et al.*, 2012a), Col-0, PDR1-OE (line 113), Col-0 *rdr6*, and PDR1-OE (line 42) were stratified for 4 d and grown for 44 d in 8 h light, 16 h dark regime, 60% relative humidiy, 20 °C, then shifted to continuous light, 60% relative humidity, 21°C, 3 klux light, for 20 d. In all experiments, plants were watered with 3 ml 5 µM CTL-VI (CTL-VI stock solution: 10 mM in DMSO) or water with 0.05% [v/v] DMSO three times a week. Lateral branches were quantified.

Leaf quantification in Petunia: Leaves were removed from 52 dag plants, and arranged in ascending order. Leaf area, leaf blade length and with, and petiole length were quantified from pictures with ImageJ 1.44 software (http://rsbweb.- nih.gov/ij).

Wilting assay: Petunia plants were grown for 28 days on clay granules (Oil Dri US-Special, Damolin) in the greenhouse. Roots were cut to a total length of 3 cm, and kept in a petri dish in buffer (2 mM $CaCl_2$, 2 mM KSO_4, 2 mM Na_2EDTA) under a neon lamp at 27 °C. After an equilibration time of 30 min, the start fresh weight was determined and further measurements were performed after 1 h incubation steps.

Lateral roots and adventitious root formation in wild type and PDR1-OE Arabidopsis: To visualize formation of lateral root primordial a DR5-GUS reporter construct was transformed into Col-0 *Arabidopsis thaliana* (wild type) or into 35S::*GFP-gPaPDR1* Col-0 lines (PDR1-OE). Homozygous lines were grown on 0.5 MS + Suc. Initially, plates were incubated for 3 h at 23 °C in sterile bench, and for 3 d at 4 °C in the dark for stratification. Further, plants were incubated 3 d in dark in a growth chamber to enable etiolated growth and subsequently, 6 d in light in a growth chamber. Plants were stained (Kretzschmar *et al.*, 2012), and numbers of lateral and adventitious roots as well as number of leaves were determined.

Lateral roots and main root quantification in Petunia: Plants were grown vertically on 0.5 MS - Suc plates for various time spans in a growth chamber as described above.

Plates were scanned and length of lateral and main roots were quantified for wild type and PDR1-OE (459-17) using the ImageJ 1.44 software (http://rsbweb.- nih.gov/ij).

Transport assay: W115 and PDR1-OE (line 459-17) plants were grown vertically for 10 d on 0.5 MS - Suc plates in a growth chamber. Eight plants for each line were placed on one 0.5 MS - Suc plate such that the root tips were located on strip of parafilm. Eighty microliters of 0.5 MS - Suc medium containing 0.8% agarose was melted, 0.2 µl of [3H]GR24 (specific activity 40 Ci mmol^{-1}, American Radiolabeled Chemicals) was added, the drop of agar was allowed to solidify, cut in cubes, and the pieces were localized such that they touched the root tips basipetally. Arrangement of the agar cubes was verified using a binocular. The plate was incubated for three hours at 23 °C, light. Plants were subsequently washed in 4 °C ddH_2O, the lowest most 0.5 cm of the roots (tip), the upper parts of the root (1 cm bottom, 1 cm middle, remaining ~ 1 cm tip), the shoot, and the agar on which the plants were localized was sampled. Shoot tissue was immersed in 24% [w/v] trichloroacetic acid as described (Kretzschmar *et al.*, 2012). Tritium counts were determined and expressed as percentages of total counts (see also 3.5).

6 Conclusions and Outlook

The aim of this study was to characterize two PDR transporters identified in *Petunia hybrida* by T. Kretzschmar during his PhD thesis work (*Pleiotropic Drug Resistance Type ABC Transporters in* Petunia hybrida*: Novel Roles in Symbiotic Interactions, Branch Development and Herbivory Defense,* T. Kretzschmar, Universität Zürich, Zürich, 2009). Here it is shown that PDR1 is involved in strigolactone (SL) transport and that it is crucial for some developmental processes in Petunia. Furthermore, polar localization of the protein in root tip cells and in hypodermal passage cells is reported. Conversely, PDR2 is involved in transport of sterol-derived compounds in Petunia leaf and stem glandular trichomes as well as in defense against herbivores.

6.1 PDR1 is a strigolactone transporter

6.1.1 PDR1 transports strigolactones away from the root tip, and it interacts with auxin to regulate root morphology

Strigolactones (SLs) were only recently identified as plant hormones. Their biosynthesis and signaling capabilities were elucidated to a great extent, but information about the mode of transport of the hormone was still missing. In this thesis, the first publication about a SL transporter, PDR1 of *Petunia hybrida,* is described (Kretzschmar *et al.*, 2012). The identity of PDR1 as a SL exporter was confirmed by the use of *Arabidopsis thaliana* as a heterologous system.

Transcription of SL synthesis genes was reported to be present in the root tip (Sorefan, 2003; Bainbridge *et al.*, 2005). Consistent with these data, *DAD1* transcripts were detected in this tissue. Compared to *DAD1*, *PDR1* is expressed in a slight more shootward layer of the root tip (see 3.3.2). Further, polar transport of SLs seems to be established in

a similar manner as for auxin, namely by polar localization of hormone exporters in the plasma membrane. The apical plasma membrane localization of PDR1 in root tip cells indicates a polar transport of SLs from the root tip to the more apical regions of the plant. Indeed, feeding radiolabeled synthetic SL GR24 to PDR1-KO root tips resulted in lower count detection in the tissues above the root tip, compared to wild-type plants (see 3.3.5). Unfortunately, due to the high autofluorescence above the root tip, it was not possible to elucidate so far to which tissues SLs are transported from the root tip. SLs were detected in xylem sap of Arabidopsis and tomato (Kohlen *et al.*, 2010). Given this, PDR1 could be involved in SL loading to the xylem. Alternative to the transport via the xylem, a cell-to-cell transport mechanism, as is reported for auxin, can be postulated for SLs. Auxin enters the cells mainly by AUX/LAX importers that are polar or apolar localized, and to a small part by diffusion (Bandyopadhyay *et al.*, 2007). Auxin export from a cell is catalyzed by the polar localization of PINs, resulting in an overall directed auxin flux in a tissue. The same mechanism can be imagined for SL transport in plants, where PDRs would take the role of the PINs in auxin transport. However, no information is available to date for the putative SL import proteins.

Auxins and SLs were found to interact tightly in regulating developmental processes, whereas the exact mode of signal integration of the two plant hormones is still not fully resolved. In-depth analysis of roots expressing tagged PDR1 and PIN proteins could reveal the interplay of auxin and SLs. The subcellular localization of PDR1 in respect to the various PIN proteins reported could add to the characterization of PDR1 function (Krecek *et al.*, 2009). The easiest approach would be to study PDR1 in Arabidopsis, because in this species, the different PIN family members are well described. However, heterologous expression of a Petunia protein in Arabidopsis may lead to the observation of artifacts. To avoid this, such studies should be performed with endogenous proteins only. This requires either the identification of PDR1 homologues in for example Arabidopsis, or the identification of the PINs in Petunia. The closest homologue of PDR1 in Arabidopsis is PDR12, which is involved in abscisic acid (ABA) and lead transport (Hwang, *et al.*, 2010; Lee *et al.*, 2005). It was investigated whether *pdr12* mutant plants showed any phenotype related to SL mutant plants (see 1.2.2); however, no role for PDR12 in SL metabolism was identified (E. Martinoia, University of Zürich, Switzerland, personal communication). Moreover, Arabidopsis ABCG full-size and half-size members were screened for impaired growth on plates containing high

levels of cotylimide VI, a chemical reported to enhance endogenous SL production, but no SL related phenotype could be observed for another ABCG candidate (E. Martinoia, personal communication). Thus, the easier approach to understand SL and auxin interactions may be to identify the PIN proteins in Petunia. Besides the challenge of PIN family member characterization, microscopy studies with Petunia are a challenge in general. Petunia roots are thick compared to Arabidopsis roots, and they exhibit strong autofluorescence. Thus, elaborated experimental techniques are required performing this kind of experiments.

6.1.2 Reported and putative functions of PDR1 in mycorrhization

In addition to the root tip, *PDR1* is expressed in single, subepidermal cells in roots that were identified as hypodermal passage cells (HPCs) by histochemical staining (Kretzschmar *et al.*, 2012). Arbuscular mycorrhizal fungi (AMF) hyphae enter the root through HPCs to form a symbiosis with their host plant. Further, the results included in this thesis revealed that PDR1 is laterally localized in HPC, facing towards the outside of the root (see 3.3.3). This finding is in line with the directed export of SLs observed from roots into the rhizosphere to attract AMF. The importance of PDR1 in early stages of mycorrhization is illustrated by the finding that PDR1-KO plants exude less SLs and consequently, show lower levels of AMF symbiosis (Kretzschmar *et al.*, 2012), whereas PDR1-OE lines are mycorrhized at higher rates than wild-type lines (L. Borghi, personal communication).

Upon successful mycorrhization, SL exudation from roots is reduced (Lopez-Raez *et al.*, 2010). However, upon mycorrhization, *PDR1* expression remains high, and it co-localizes with fungal structures in the root (Kretzschmar *et al.*, 2012). Currently, the function of SLs and SL transport after establishment of mycorrhization is unknown. One can hypothesize that SLs are necessary for fungal growth within the plant, in which SL presence would guide hyphal growth, and the continued survival of the arbuscules. However, although AMF colonization levels are lower in SL deficient mutants such as *dad1*, arbuscule morphology is not altered (Kretzschmar *et al.*, 2012), indicating that SLs are not needed for AMF symbiosis maintenance.

AMF symbiosis not only induces symbiosis-related genes in the host, but as well genes that are induced in response to pathogens (Güimil *et al.*, 2005; Liu *et al.*, 2003). The common agreement is that this response is due to the fungal identity of the symbiotic

partner. Although *PDR1* transcription is not induced by yeast extract, which is a fungal elicitor (Kretzschmar *et al.*, 2012), it cannot be excluded that *PDR1* induction during mycorrhization is due to an non-specific, ancient response.

A third explanation for *PDR1* expression during mycorrhization could be that *PDR1* is involved in transport of substrates other than SLs. Indeed, some ABCG proteins were reported to have a broad substrate specificity (see 1.1.2). PDR1 could thus be involved in transport of another carotenoid-derived compound, such as mycorrhadicin or cyclohexenone, which are produced upon mycorrhization in a number of plants. In fact, CCD7 was reported to be not only involved in SL synthesis, but as well in the production of apocarotenoids (Walter *et al.*, 2010). To date, the function of mycorrhadicin is unknown, but it was associated only with later stages of mycorrhization, and maybe with already senescing arbuscules (Fester *et al.*, 2002). To date, it is unclear if these apocarotenoids are transported. To investigate if PDR1 is involved in this process, *PDR1* transcript levels could be analyzed in respect to *CCD1* transcription, which is a carotenoid cleavage dioxigenase that is predicted to be involved in later steps of the apocarotenoid synthesis pathway (Walter *et al.*, 2007; Sun *et al.*, 2008). Co-regulation of *CCD1* and *PDR1* could point towards an involvement in the same pathway. In general, PDR1 function in later stages of mycorrhization could be analyzed by growing plants carrying PDR1 reporter constructs on plates with AMF. *PDR* expression could be monitored with a high time resolution to understand if SL transport happens before, during, and/or after mycorrhization.

6.1.3 Hints to the post-transcriptional regulation of PDR1 and its polar localization to the plasma membrane

Clues for post-transcriptional regulation of PDR1 come from the observation that in Petunia, promoter signals differed from protein signals: signals of the *PDR1* promoter GPF construct were present in many more cells than the GFP-PDR1 fusion protein, irrespective if the expression of the protein was under the control of the native promoter or the 35S promoter (L. Borghi, personal communication). In addition, PDR1-OE plants do not show ubiquitous *PDR1* expression as expected, but a specific protein signal restricted to the root tip and to hypodermal passage cells in roots. It was therefore concluded that PDR1 is regulated post-transcriptionally.

Polar auxin transport is established by polar localization of the AUX/LAX and PIN proteins. The plasma membrane localization of PIN proteins was shown to be dynamic, PIN1 for example cycles between endosomal compartments and the plasma membrane (Geldner *et al.*, 2001), a mechanism that can be inhibited by several drugs. Among them is Brefeldin A (BFA), which blocks endocytotic recycling to the plasma membrane, and thus leads to the accumulation of cytoplasmic bodies (Grunewald and Friml, 2010). It was shown that initial PIN1 synthesis and transport to the plasma membrane is apolar. Phosphorylation at the plasma membrane and subsequent invagination by vesicles with different affinity for the phosphorylation status of PIN1 result in polar localization of the protein (Offringa and Huang, 2013). In Arabidopsis, the three at least partially redundant kinases WAG1, WAG2 and PID likely phosphorylate PINs at different sites, among which is a conserved motif in the central hydrophilic loop. In addition, phosphatases have been described (Offringa and Huang, 2013). Similar to PIN1, PDR1 localization is BFA sensitive (see 3.3.4), but the conserved phosphorylation motif described for PINs is absent in PDR1. Triple knockouts of *wag1 wag2 pid* Arabidopsis plants are arrested early in development, and PIN1 polar localization is lost (Offringa and Huang, 2013). Therefore, a plan was developed to cross PDR1-OE Arabidopsis plants with the aforementioned triple mutant, to analyze if PDR1 polar localization is lost similarly. However, other kinases and phosphorylases have been described to affect PIN localization in addition to other regulatory mechanisms such as ubiquitination that influences its localization (Offringa and Huang, 2013). Therefore, it is possible that PDR1 polar localization could be regulated by mechanisms other than those currently described for PIN proteins.

6.1.4 The role of PDR1 in aboveground branching regulation

Aboveground, *PDR1* is expressed in nodal tissue. PDR1-KO plants exhibit higher branching than the corresponding wild-type plants, and PDR1-OE lines display reduced branching (see 5.1.1, Kretzschmar *et al.*, 2012). Compared to SL synthesis mutants, PDR1-KO lines have a less severe phenotype: *dad1* plants form a branch at every node and have a dwarf phenotype (Napoli, 1996), whereas PDR1-KO plants initiate branching earlier and form longer branches, but some of the buds remain dormant and a dwarf phenotype was not observed (Kretzschmar *et al.*, 2012). Both, *dad1* and PDR1-KO plants

can be rescued by the addition of GR24 (Kretzschmar *et al.*, 2012), indicating that both mutants are SL sensitive.

In the field of axillary branching, a major open question is the detailed regulation of branching inhibition and bud outgrowth, and the regulation of this development by the interplay of auxin, SLs and cytokinins. Recently, even brassinosteroids have been shown to influence branching (Janssen *et al.*, 2014). The cloning of the first SL transporter *PDR1* now enables studies investigating auxin and SL transport in nodal tissue to analyze the interplay of the hormones. In Petunia, a mutant in auxin synthesis was described that showed increased branching (Tobena-Santamaria, 2002; Gallavotti, 2013). Crossing of auxin mutant plants with *dad1* and PDR1-KO plants would reveal if the signals of the two hormones are integrated into the same pathway or if the hormones act independently. In addition, a cytokinin synthesis gene was described in Petunia (Zubko *et al.*, 2002) that could be integrated into the analysis of auxin and SL metabolism in nodal tissue. Ideally, a future study would incorporate a cytokinin transporter, analogous to PIN1 for auxin and PDR1 for SLs; however, to date, no *in vivo* studies exist that characterize cytokinin transporters. In Arabidopsis, two proteins were shown to transport cytokinins in yeast assays, but evidence for a role in plant metabolism is still missing (Kudo *et al.*, 2010).

6.1.5 How crucial is strigolactone transport within a plant?

A hormone is a substance that is in most cases produced in some spots, and perceived in others. Thus by definition, for many phytohormones, there are some transport processes involved. For SLs, the sites of synthesis and perception are not well described. Given this, it remains unclear between which sites SL transport has to occur. Hormones can be produced and sensed locally, or they can be transported over long distances before detection. For SLs, long-distance transport via the xylem was reported (Kohlen *et al.*, 2010), but in addition, local SL production seems to be important (Sorefan, 2003; Napoli, 1996). Analogous to SLs, cytokinins are well-described plant hormones, for which both, long-distance transport and local synthesis has been reported (Kudo *et al.*, 2010). Specific cytokinins are produced in the root and transported to the upper parts of the plant via the xylem, whereas other cytokinins are synthesized locally in tissues such as leaves and stem. Xylem-transported cytokinin levels are regulated by environmental factors, and are thought to signal for nutrient stress (*e.g.* nitrate status of the root to the

shoot). Local cytokinins likely serve as local messengers, and some evidence exists for phloem transport of these cytokinins (Kudo *et al.*, 2010). Likewise for SLs, it is not resolved to which amount local and distal cytokinin pools influence developmental processes such as branching. In analogy to cytokinins, different SL molecules could be produced in roots and shoots, and local and distal production could serve different functions. Likewise, transport could take place via the xylem, the phloem, cell-to-cell transport, and/or a combination of the processes. The latter two hypotheses remain to be tested.

To investigate the importance of SL transport within a plant, studies should be performed to elucidate SL synthesis and perception sites. Gene expression data is available for some of the SL synthesis and perception genes (Stirnberg *et al.*, 2007; Zou *et al.*, 2006; Bennett *et al.*, 2006; Sorefan, 2003; Bainbridge *et al.*, 2005; Vogel *et al.*, 2009; Kohlen *et al.*, 2012; Arite *et al.*, 2007), but so far, no protein localization studies have been performed. The results presented in this thesis show at least for PDR1 that gene expression and protein localization data are incongruent (in collaboration with L. Borghi, see 3.3). Future studies should therefore address the cell-specific localization of SL synthesis, perception, and transport proteins.

With the current knowledge, it can still be postulated that SL transport is important in several tissues. First, SL transport out of biosynthetic tissues is important to avoid negative feedback of accumulating SLs on the biosynthetic genes (Snowden *et al.*, 2005; Hayward *et al.*, 2009; Ruyter-Spira *et al.*, 2011). A major site of SL synthesis is the root tip (Bainbridge *et al.*, 2005; Sorefan, 2003), and apical localization of PDR1 in this tissue is reported (see 3.3.1), which is consistent with the proposed hypothesis. Another site of SL synthesis is stem tissue (Kohlen *et al.*, 2012; Napoli, 1996; Foo, 2005), or more specific, nodal tissue (Bainbridge *et al.*, 2005), which is also consistent with PDR1 expression in nodes (Kretzschmar *et al.*, 2012). The altered aboveground branching phenotype of PDR1-KO and PDR1-OE lines highlight the importance of PDR1 in this developmental process (see 5.1.1.1).

Second, SL transport from root to shoot tissue was postulated in grafting experiments performed in several species (Sorefan, 2003; Napoli, 1996; Beveridge *et al.*, 2009). The presence of SLs in the xylem (Kohlen *et al.*, 2010) supports this idea. SL transport via the xylem would require SL loading to and unloading from the xylem; for the former, an SL exporter, and for the latter, an SL importer. PDR1 could be involved in xylem loading in

the root tip; however, this remains to be demonstrated. Future studies should aim to identify candidates for an SL importer. Assays similar to the ones described for the identification of PDR1 (Kretzschmar *et al.*, 2012) could be performed.

Third, SLs are perceived in the nodal tissue and exuded from HPCs, which again implies a directed SL transport mechanism to avoid off-target effects in other tissues. It is unresolved to date if SLs are locally produced in these tissues, or if long-distance transport of SLs is involved. The availability of an SL synthesis inhibitor that could be applied locally would help to dissect the differential functions of long and short distance SL transport. For example, local, aboveground SL synthesis could be inhibited, and effects of root-derived SL on shoot morphology could be investigated.

For some of the developmental processes such as the aforementioned branching regulation and SL exudation, an involvement of PDR1 is evident. For other processes such as regulation of root morphology, secondary growth and germination, the role of SL transport has not yet been investigated; however, preliminary results presented here suggest that SL transport is also involved in some of these processes. The results suggest an involvement of PDR1 in regulation of root morphology (see Figure 5.2, Figure 5.3) and in controlling the number of meristematic cells in the root tip (see 3.3.6). Further, evidence for a role in vasculature formation (L. Borghi, and 5.2.2), secondary growth (Figure 5.1) and abiotic stress resistance (see 5.2.2, Figure 5.5) can also be seen.

Several findings suggest that PDR1 might not be the only SL exporter in Petunia. First, the branching phenotype of PDR1-KO plants is not as strong as in SL deficient plants. Second, AMF colonization levels in PDR1-KO are higher than in *dad1* plants, and some residual SL exudation is detected (Kretzschmar *et al.*, 2012). Third, although passive diffusion into cells was reported for auxin (for a review, see Leyser, 2006), and absence of transport was formerly postulated for ABA (for a review, see Boursiac *et al.*, 2013), transporters have been identified in both systems. For auxin, members of several protein families were reported to take part in cellular import and export, among them members of the PIN, AUX/LAX, and PGP families (Bandyopadhyay *et al.*, 2007). This may suggest that for SLs, importers and exporters belonging to various protein families could exist. Screening of mutant plants displaying similar phenotypes as PDR1-KO or *dad1*, or for proteins with increased transcription upon auxin/GR24/mycorrhization treatment might help in the identification of such candidates.

6.1.6 It will be difficult to dissect strigolactone specific effects from the effects of other phytohormones

In the past few years it was recognized that SLs play a role in a plethora of processes (see 1.2.2, 1.2.3). For only a few of the processes, a direct effect of SLs on transcription factors or target genes was described (see 1.2.2). In most of the cases, it was realized that SL effects depend on, or are due to, an interplay with other plant hormones; in particular auxins, cytokinins, GA, ABA, brassinosteroids, and ethylene. SLs were shown to regulate auxin transport (Ruyter-Spira *et al.*, 2011; Koltai and Kapulnik, 2013; Shinohara *et al.*, 2013), and auxin was shown to increase SL biosynthesis (Bainbridge *et al.*, 2005; Foo, 2005; Zou *et al.*, 2006; Arite *et al.*, 2007; Brewer *et al.*, 2013). Thus, if the level of one hormone is altered, either by mutation of pathways or by exogenous application, levels of the second hormone will be altered in parallel. Mutations of genes involved in synthesis or transport of hormones or external application of hormones inevitably lead to an alteration of the system, and thus maybe to observation of artifacts. To further complicate the picture, it was shown that that environmental factors such as light, sugars, and nutrient levels modulate SL responses of the plant (see 1.2.2.3). Further, the F-box protein *MAX2* is not only involved in SL signaling, but additionally binds other α/β-hydrolases that are involved in other signaling pathways (see 1.2.2.3). Careful experimentation is required to dissect the effect of the different hormones on various developmental processes. Ideally, sensors for the different hormones would be created, enabling real-time observations of the hormonal interplay. Alternatively, tagging of hormone transporters such as PIN1 and PDR1 would illustrate presence and possible interplay of the hormones (see 6.1.1). Studies about the target genes such as the transcription factor FC1 involved in branching (see 1.2.2.1) will reveal also more about the integration of the different hormonal responses.

6.2 PDR2 is the first plant transporter described to be involved in sterol transport

Characterization of *Petunia hybrida* PDR2 points towards an involvement of the protein in herbivore response (see 2). The gene is expressed in multicellular, glandular trichomes of leaves and stem, at the borders of leaves, and in lower amounts at the sites of lateral root emergence and flower tissues (Figure 4.2 A). In seedlings, PDR2 transcription is induced by jasmonic acid (Figure 4.2 K), implying a role in herbivore defense. Indeed, larvae of the generalist herbivore *Spodoptera littoralis* gain weight faster on *phpdr2* leaves than on the respective wild type, and lower mortality rates are observed (Figure 4.3). An untargeted HPLC-MS approach identified several candidate masses present in lower abundance in *phpdr2* trichomes and leaf washes. More than half of the candidate masses were identified as petuniasterones or petuniolides (Table 4-1, Supplementary Table 4-1), which are sterol-dervied compounds that have been reported to be very toxic even in small amounts against a range of insects (see 1.4.5, Elliger and Waiss, 1991). So far, no sterol transporters have been characterized in plants, although members of the ABCG family were shown to transport sterols in humans and yeast (see 1.4.2, 1.4.3). Thus, PDR2 is the first plant transporter reported to be involved in sterol compound accumulation.

Future studies should be undertaken to examine the biosynthetic pathway of Petunia sterols. Sterols are synthesized mostly via the mevalonate (MVA) pathway, from which also some terpenoids are derived (see 1.4.4). The pathway has been described to be active in tomato and *Nicotiana* trichomes (Besser *et al.*, 2009; Bleeker *et al.*, 2012; Tissier *et al.*, 2013), and given the solanaceous identity of these species, the pathway is likely active in Petunia too. Petunia trichomes are pale green, suggesting that they are photosynthetically active, and likely energetically at least partially independent from leaf tissue. In case the MVA pathway is found to be active, precursors for sterol synthesis would be present in trichome tissue, and Petunia sterols may be synthesized in the trichome directly. An alternative hypothesis is the synthesis of Petunia sterol precursors or of the mature compounds in the leaf, succeeded by the import into trichomes. PDR2 could be involved in this process, as analysis of its transcriptional activity by PDR2 promoter GUS fusion constructs revealed expression of PDR2 in trichomes and

epidermal cells basal to the trichome (Figure 4.2 E, F). Future studies should investigate whether PDR2 is polarly localized, which would reveal if PDR2 could be involved in the import of sterols into the trichome. Moreover, substrate specificity of PDR2 should be examined in subsequent studies. Some PDR proteins have been shown to have a broad substrate specificity, whereas others display a narrow substrate range (see 1.1.2). For PDR2, both can be imagined; if PDR2 transports a precursor of Petunia sterols, its substrate range may be narrow, whereas if it transports a variety of petuniasterones and petuniolides, its substrate range may be broad.

Besides Petunia sterols, other masses were found to be decreased in *phpdr2* leaves compared to wild type (Supplementary Table 4-1). These masses have not been described in *Petunia sp*. yet, and it would be interesting to learn about their molecular identity and function in future experiments. Therefore, it cannot be excluded that some of these candidate masses are as well involved in herbivore responses of Petunia.

6.2.1 Trichomes as factories for secondary metabolites

Humans have been utilizing plants throughout their existence to exploit their medicinal value, taste, and effect against pathogens and herbivores (Schilmiller *et al.*, 2008). Still, major drugs, such as artemisinin that exerts an antimalarial function, or the analgesic morphine, are extracted from plants (Gershenzon and Dudareva, 2007). In addition, plant secondary metabolites, often produced in trichomes, are basis of perfumes, are used as food additives, or as natural pesticides (Schilmiller *et al.*, 2008). Given the importance of secondary metabolites, it is surprising how little research is performed in this field nowadays. One of the reasons may be that each species, even each cultivar, may show a discrete composition of secondary metabolites, which can further be influenced by environmental factors and pests (Gershenzon and Dudareva, 2007; van Schie *et al.*, 2007; Besser *et al.*, 2009). Future studies should aim to examine biosynthetic pathways of secondary metabolites such as Petunia sterols more closely, as the identification of biosynthetic enzymes and transport processes would open many new possibilities. On the one hand, rate-limiting steps could be identified, production enhanced, or extraction from the plant could be made easier: for example, exudation of the compounds onto the leaf surface, or accumulation of compounds in the trichomes could be engineered (Wagner, 1991). Alternatively, biosynthetic pathways could be transferred from plants that are difficult to handle, such as trees, to plants that are easily grown in a

greenhouse. The biosynthetic pathway of some terpenoids and flavonoids has been revealed (Slocombe *et al.*, 2008; Schilmiller *et al.*, 2010; Schmidt *et al.*, 2011), and it was shown that bioengineering lead to plants less susceptible against pathogen and herbivore attack (Schilmiller *et al.*, 2008; Bleeker *et al.*, 2012; Tissier *et al.*, 2013). Studies analyzing plant defense mechanisms against pests and herbivores could lead to the production of new insecticides, fungicides, and defenses against other pests (Miresmailli and Isman, 2013).

Plants are still poorly characterized for their potential for human use, and even bigger is the lack of research performed to understand the function of secondary metabolites in plants (Gershenzon and Dudareva, 2007). Generally, it is assumed that secondary metabolites evolved as means of defense, but only for a few examples this was adressed in an experimental setting that allows this conclusion (for reviews, see Schilmiller *et al.*, 2008; Gershenzon and Dudareva, 2007). Future studies should be undertaken to examine secondary metabolite functions in plants, and if a function in plant defense is identified, the potential for use as pesticide should be evaluated. Glandular trichomes are an excellent organ to perform such studies, as many secondary compounds are stored in those organs at very high concentrations (Tissier, 2012). Trichomes are readily accessible, and for several species, protocols are published how to collect trichomes, or even trichomes of a single type (Kang *et al.*, 2010a; McDowell *et al.*, 2010; Schilmiller *et al.*, 2010). The identification of petuniasterones in a screen for toxic metabolites of Petunia trichomes illustrates the potential of untargeted metabolite analysis of trichomes. Petunia sterols would be good candidates to develop a new insecticide, given their high toxicity against insects, and their ineffectiveness against other arthropods as for example crustaceans (Elliger and Waiss, 1991).

6.3 Advantages and difficulties of the model system Petunia

Petunias are considered the first bedding plants cultivated, and they are still one of the major ornamentals found today (Gerats and Vandenbussche, 2005). A considerable amount of research has been dedicated to the development of new flower colors, scent, and altered plant morphology (Gerats and Vandenbussche, 2005). Recently, Petunia has gained more attention also in other research areas, because similar to *Nicotiana* species, it is a member of the Solanaceae. Thus, it can serve as a model plant for crop species such as tomato, potato, and eggplant. Because of its close relation to crop plants, research of Petunia might be easier to apply than for example research on Arabidopsis. Moreover, there are certain research fields that are easier to investigate in Petunia. For example, in contrast to Arabidopsis, Petunia is a host for mycorrhizal fungi (Bouwmeester *et al.*, 2007), Petunia shows a branching development distinct from Arabidopsis (see 5.2.3), and Petunia trichomes contain significant amounts of secondary metabolites, whereas this is not the case for Arabidopsis (Clauss *et al.*, 2006).

The *Petunia hybrida* W115 cultivar is a model plant that is quite easy to handle, its generation time of approximately three months is reasonable for greenhouse experiments, such as seed production, generation of transgenic plants, or generation-spanning experiments. The W115 cultivar produces considerable amounts of seeds, although manual fertilization is required. Molecular biology protocols can be adapted easily from Arabidopsis, *Nicotiana*, or rice. The presence of a endogenous transposon insertion library allows screening for non-transgenic gene knockouts in the W138 cultivar (Koes *et al.*, 1995; De Keukeleire *et al.*, 2001), which subsequently can be introgressed into the W115 cultivar. With this transposon insertion system, field experiments are possible, in contrast to T-DNA generated mutant plants.

A downside of Petunia as a model system is the time consuming transformation of plants, which requires plantlet regeneration from callus tissue (see 5.3). In addition, many transgenes are silenced, requiring the screening of a considerable number of plants for non-silenced individuals. Silencing can also only occur in the second generation of plants, making careful monitoring of gene expression levels over several generations mandatory. Although the morphology of Petunia resemble more the one of certain crop species, its size poses certain problems. Root thickness in combination with massive cell

walls for example prevent microscopy of inner cell layers of intact roots (see 3), and embedding and sectioning of tissue is required for investigation of root and shoot tissues. In addition, more space is needed for growth and propagation of the plants.

Various Petunia species, and various *Petunia hybrida* cultivars have been in the focus of research. On one hand, this reflects the variations found in this species, but on the other hand, the use of different genetic backgrounds hinders direct comparison of results. This is true for example for branching studies, as W115, W138, and V26 cultivars all exhibit specific branching patterns (see Figure 5.4, Kretzschmar *et al.*, 2012). Further, Petunia originates from South America (Chen *et al.*, 2007), and thus, seeds cannot be stratified, making plant growth less uniform than for example for Arabidopsis, and morphological studies more difficult. The variation in plant size and in developmental timing is even more obvious when Petunia plants are grown in the greenhouse, for example for branching quantification. The three months required for a plant to reach the size for evaluation gives space for all sorts of environmental impact on plants, resulting in variable growth pattern and speed. Generally, careful monitoring of growth conditions and plant status is required to ensure good experimental conditions.

7 Literature

Aguilar-Martinez, J. A., Poza-Carrion, C. and Cubas, P. (2007) Arabidopsis *BRANCHED1* acts as an integrator of branching signals within axillary buds. *Plant Cell*, 19, 458–472.

Agusti, J., Herold, S., Schwarz, M., *et al.* (2011) Strigolactone signaling is required for auxin-dependent stimulation of secondary growth in plants. *Proc. Natl. Acad. Sci. U.S.A.,* 108, 20242–20247.

Akiyama, K., Ogasawara, S., Ito, S. and Hayashi, H. (2010) Structural requirements of strigolactones for hyphal branching in AM fungi. *Plant Cell Physiol.*, 51, 1104–1117.

Akiyama, K., Matsuzaki, K.-I. and Hayashi, H. (2005) Plant sesquiterpenes induce hyphal branching in arbuscular mycorrhizal fungi. *Nature*, 435, 824–827.

Alder, A., Jamil, M., Marzorati, M., *et al.* (2012) The path from beta-carotene to carlactone, a strigolactone-like plant hormone. *Science*, 335, 1348–1351.

Ambrosio, S. R., Oki, Y., Heleno, V. C. *et al.* (2008) Constituents of glandular trichomes of *Tithonia diversifolia*: relationships to herbivory and antifeedant activity. *Phytochemistry*, 69, 2052–2060.

Arite, T., Iwata, H., Ohshima, K. *et al.* (2007) *DWARF10*, an *RMS1/MAX4/DAD1* ortholog, controls lateral bud outgrowth in rice. *The Plant Journal*, 51, 1019–1029.

Auldridge, M. E., Block, A., Vogel, J. T., *et al.* (2006) Characterization of three members of the Arabidopsis carotenoid cleavage dioxygenase family demonstrates the divergent roles of this multifunctional enzyme family. *The Plant Journal*, 45, 982–993.

Bainbridge, K., Sorefan, K., Ward, S. and Leyser, O. (2005) Hormonally controlled expression of the Arabidopsis *MAX4* shoot branching regulatory gene. *The Plant Journal*, 44, 569–580.

Balla, J., Kalousek, P., Reinohl, V. *et al.* (2011) Competitive canalization of PIN-dependent auxin flow from axillary buds controls pea bud outgrowth. *The Plant Journal*, 65, 571–577.

Bandyopadhyay, A., Blakeslee, J. J., Lee, O. R., *et al.* (2007) Interactions of PIN and PGP auxin transport mechanisms. *Biochem. Soc. Trans.*, 35, 137–141.

Bari, R. and Jones, J. D. G. (2008) Role of plant hormones in plant defence responses. *Plant Mol. Biol.*, 69, 473–488.

Bennett, T., Sieberer, T., Willett B. *et al.* (2006) The *Arabidopsis MAX* pathway controls shoot branching by regulating auxin transport. *Current Biology*, 16, 553–563.

Besser, K., Harper, A., Welsby, N. *et al.* (2009) Divergent regulation of terpenoid metabolism in the trichomes of wild and cultivated tomato species. *Plant Physiol.*, 149, 499–514.

Besserer, A., Puech-Pages, V., Kiefer, P., *et al.* (2006) Strigolactones stimulate arbuscular mycorrhizal fungi by activating mitochondria. *PLoS Biol.*, 4, 1239-1247.

Beveridge, C. A., Dun, E. A. and Rameau, C. (2009) Pea has its tendrils in branching discoveries spanning a century from auxin to strigolactones. *Plant Physiol.*, 151, 985–990.

Bishop, G. J. and Yokota, T. (2001) Plants steroid hormones, brassinosteroids: Current highlights of molecular aspects on their synthesis/metabolism, transport, perception and response. *Plant Cell Physiol.*, 42, 114–120.

Bleeker, P. M., Mirabella, R., Diergaarde, P. J., *et al.* (2012) Improved herbivore resistance in cultivated tomato with the sesquiterpene biosynthetic pathway from a wild relative. *Proc. Natl. Acad. Sci. U.S.A.*, 109, 20124–20129.

Bodenhausen, N. and Reymond, P. (2007) Signaling pathways controlling induced resistance to insect herbivores in *Arabidopsis. Mol. Plant Microbe Interact.*, 20, 1406–1420.

Booker, J., Sieberer, T., Wright, W. *et al.* (2005) *MAX1* Encodes a Cytochrome P450 Family Member that Acts Downstream of *MAX3/4* to Produce a Carotenoid-Derived Branch-Inhibiting Hormone. *Developmental Cell*, 8, 443–449.

Booker, J., Auldridge, M., Wills, S. *et al.* (2004) MAX3/CCD7 Is a Carotenoid Cleavage Dioxygenase Required for the Synthesis of a Novel Plant Signaling Molecule. *Current Biology*, 14, 1232–1238.

Booker, J. (2003) Auxin Acts in Xylem-Associated or Medullary Cells to Mediate Apical Dominance. *The Plant Cell,* 15, 495–507.

Boughton, A. J., Hoover, K. and Felton, G. W. (2005) Methyl jasmonate application induces increased densities of glandular trichomes on tomato, *Lycopersicon esculentum*. *J. Chem. Ecol.*, 31, 2211–2216.

Boursiac, Y., Léran, S., Corratgé-Faillie, C., G *et al.* (2013) ABA transport and transporters. *Trends in Plant Science*, 18, 325–333.

Bouwmeester, H. J., Roux, C., Lopez-Raez, J. A. and Becard, G. (2007) Rhizosphere communication of plants, parasitic plants and AM fungi. *Trends in Plant Science*, 12, 224–230.

Bouwmeester, H. J., Matusova, R., Zhongkui, S. and Beale, M. H. (2003) Secondary metabolite signalling in host-parasitic plant interactions. *Curr. Opin. Plant Biol.*, 6, 358–364.

Boyer, F.-D., de Saint Germain, A., Pouvreau, J.-B., *et al.* (2013) New Strigolactone Analogs as Plant Hormones with Low Activities in the Rhizosphere. *Molecular Plant*., 7, 675-690.

Braun, N., de Saint Germain, A., Pillot, J. P., *et al.* (2012) The pea TCP transcription factor PsBRC1 acts downstream of strigolactones to control shoot branching. *Plant Physiol.* 158, 225-238.

Brewer, P. B., Koltai, H. and Beveridge, C. A. (2013) Diverse roles of strigolactones in plant development. *Molecular Plant*, 6, 18–28.

Brewer, P. B., Dun, E. A., Ferguson, B. J. *et al.* (2009) Strigolactone acts downstream of auxin to regulate bud outgrowth in pea and Arabidopsis. *Plant Physiol.*, 150, 482–493.

Brundrett, M. C. (2009) Mycorrhizal associations and other means of nutrition of vascular plants: understanding the global diversity of host plants by resolving conflicting information and developing reliable means of diagnosis. *Plant Soil*, 320, 37–77.

Bu, Q., Lv, T., Shen, H., *et al.* (2013) Regulation of drought tolerance by the F-box protein MAX2 in Arabidopsis. *Plant Physiol.* 164, 424-439.

Bultreys, A., Trombik, T., Drozak, A. and Boutry, M. (2009) *Nicotiana plumbaginifolia* plants silenced for the ATP-binding cassette transporter gene *NpPDR1* show increased susceptibility to a group of fungal and oomycete pathogens. *Mol. Plant Pathol.*, 10, 651–663.

Cabrito, T. R., Teixeira, M. C., Singh, A. *et al.* (2011) The yeast ABC transporter Pdr18 (ORF *YNR070w*) controls plasma membrane sterol composition, playing a role in multidrug resistance. *Biochem. J.*, 440, 195–202.

Campbell, E. J., Schenk, P. M., Kazan, K. *et al.* (2003) Pathogen-responsive expression of a putative ATP-binding cassette transporter gene conferring resistance to the diterpenoid sclareol is regulated by multiple defense signaling pathways in Arabidopsis. *Plant Physiol.*, 133, 1272–1284.

Cardoso, C., Zhang, Y., Jamil, M., *et al.* (2014) Natural variation of rice strigolactone biosynthesis is associated with the deletion of two *MAX1* orthologs. *Proc. Natl. Acad. Sci. U.S.A.*, 111, 2379–2384.

Cardoso, C., Ruyter-Spira, C. and Bouwmeester, H.J. (2011) Strigolactones and root infestation by plant-parasitic *Striga*, *Orobanche* and *Phelipanche* spp. *Plant Sci.*, 180, 414–420.

Challis, R., Hepworth, J., Mouchel, C. *et al.* (2013) A role for *MORE AXILLARY GROWTH (MAX1)* in evolutionary diversity in strigolactone signalling upstream of *MAX2*. *Plant Physiol.* 161, 1885-1902.

Chen, C., Gao, M., Liu, J. and Zhu, H. (2007) Fungal symbiosis in rice requires an ortholog of a legume common symbiosis gene encoding a Ca^{2+}/calmodulin-dependent protein kinase. *Plant Physiol.*, 145, 1619–1628.

Cheng, X., Ruyter-Spira, C. and Bouwmeester, H. (2013) The interaction between strigolactones and other plant hormones in the regulation of plant development. *Front. Plant Sci.*, 4, 1-16.

Choudhary, S. P., Yu, J.-Q., Yamaguchi-Shinozaki, K. *et al.* (2012) Benefits of brassinosteroid crosstalk. *Trends in Plant Science*, 17, 594–605.

Cissoko, M., Boisnard, A., Rodenburg, J. *et al.* (2011) New Rice for Africa (NERICA) cultivars exhibit different levels of post-attachment resistance against the parasitic weeds *Striga hermonthica* and *Striga asiatica*. *New Phytol.*, 192, 952–963.

Clauss, M. J., Dietel, S., Schubert, G. and Mitchell-Olds, T. (2006) Glucosinolate and trichome defenses in a natural *Arabidopsis lyrata* population. *J. Chem. Ecol.*, 32, 2351–2373.

Cohen, M., Prandi, C., Occhiato, E. G. *et al.* (2013) Structure-function relations of strigolactone analogs: activity as plant hormones and plant interactions. *Molecular Plant*, 6, 141–152.

Crawford, S., Shinohara, N., Sieberer, T. *et al.* (2010) Strigolactones enhance competition between shoot branches by dampening auxin transport. *Development*, 137, 2905–2913.

Crouzet, J., Roland, J., Peeters, E. *et al.* (2013) NtPDR1, a plasma membrane ABC transporter from *Nicotiana tabacum*, is involved in diterpene transport. *Plant Mol. Biol*. 82, 181-192.

Crouzet, J., Trombik, T., Fraysse, A. S. and Boutry, M. (2006) Organization and function of the plant pleiotropic drug resistance ABC transporter family. *FEBS Letters*, 580, 1123–1130.

De Keukeleire, P., Maes, T., Sauer, M. *et al.* (2001) Analysis by Transposon Display of the behavior of the *dTph1* element family during ontogeny and inbreeding of *Petunia hybrida*. *Mol. Genet. Genomics*, 265, 72–81.

de Saint Germain, A., Ligerot, Y., Dun, E. A. *et al.* (2013) Strigolactones stimulate internode elongation independently of gibberellins. *Plant Physiol.*, 163, 1012–1025.

Dean, M., Hamon, Y. and Chimini, G. (2001) The human ATP-binding cassette (ABC) transporter superfamily. *Journal of Lipid Research*, 42, 1–11.

Delaux, P. M., Xie, X., Timme, R. E., *et al.* (2012) Origin of strigolactones in the green lineage. *New Phytol.*, 195, 857–871.

Domagalska, M. A. and Leyser, O. (2011) Signal integration in the control of shoot branching. *Nat. Rev. Mol. Cell Biol.*, 12, 211–221.

Drummond, R. S. M., Sheehan, H., Simons, J. L., *et al.* (2012) The expression of petunia strigolactone pathway genes is altered as part of the endogenous developmental program. *Front. Plant Sci.* 2, 1–14.

Drummond, R. S. M., Martinez-Sanchez, N. M., Janssen, B. J. *et al.* (2009) *Petunia hybrida CAROTENOID CLEAVAGE DIOXYGENASE7* Is Involved in the Production of Negative and Positive Branching Signals in Petunia. *Plant Physiol.*, 151, 1867–1877.

Ducos, E., Fraysse, S. and Boutry, M. (2005) *NtPDR3*, an iron-deficiency inducible ABC transporter in *Nicotiana tabacum*. *FEBS Letters*, 579, 6791–6795.

Dun, E. A., de Saint Germain, A., Rameau, C. and Beveridge, C. A. (2012) Dynamics of strigolactone function and shoot branching responses in *Pisum sativum*. *Plant Physiol.,* 6, 128-140.

Dun, E. A., Brewer, P. B. and Beveridge, C. A. (2009) Strigolactones: discovery of the elusive shoot branching hormone. *Trends in Plant Science*, 14, 364–372.

Ehrhardt, D. W., Wais, R. and Long, S. R. (1996) Calcium spiking in plant root hairs responding to Rhizobium nodulation signals. *Cell*, 85, 673–681.

El-Showk, S., Ruonala, R. and Helariutta, Y. (2013) Crossing paths: cytokinin signalling and crosstalk. *Development*, 140, 1373–1383.

Elliger, C. A., Wong, R. Y., Benson, M. and Waiss, A. C. Jr. (1992) Petunianines, unusual steroidal nitrogenous bases from *Petunia inflata*. *J. Chem. Soc., Perkin Trans.* 1, 5-6.

Elliger, C. A. and Waiss, A. C. Jr. (1991) Insect Resistance Factors in Petunia. In *ACS Symposium Series*. ACS Symposium Series. Washington, DC: American Chemical Society, pp. 210–223.

Elliger, C. A., Wong, R. Y., Benson, M. and Waiss, A. C. Jr. (1989a) X-Ray Crystal Structure Of Petuniasterone O, A Novel Ergostanoid From *Petunia parodii*. *Journal of Natural Products*, 52, 1345–1349.

Elliger, C.A., Waiss, A. C. Jr., Wong, R. Y. and Benson, M. (1989b) Petuniasterones From *Petunia parodii* And *P. integrifolia*; Unusual Ergostane-Type Steroids. *Phytochemistry*, 28, 3443–3452.

Elliger, C. A., Benson, M., Lundin, R. E. and Waiss, A. C. Jr. (1988) Minor Petuniasterones from *Petunia hybrida*. *Phytochemistry*, 27, 3597–3603.

Emechebe, A. M., Ellis-Jones, J., Schulz, S. *et al.* (2004) Farmers' perception of the Striga problem and its control in Northern Nigeria. *Experimental Agriculture*, 40, 215–232.

Estrada, B., Aroca, R., Maathuis, F. J. M. *et al.* (2013) Arbuscular mycorrhizal fungi native from a Mediterranean saline area enhance maize tolerance to salinity through improved ion homeostasis. *Plant Cell Environ*, 36, 1771–1782.

Fellbaum, C. R., Gachomo, E. W., Beesetty, Y., *et al.* (2012) Carbon availability triggers fungal nitrogen uptake and transport in arbuscular mycorrhizal symbiosis. *Proc. Natl. Acad. Sci. U.S.A.*, 109, 2666–2671.

Ferguson, B. J. and Beveridge, C. A. (2009) Roles for auxin, cytokinin, and strigolactone in regulating shoot branching. *Plant Physiol.*, 149, 1929–1944.

Fester, T., Hause, B., Schmidt, D., *et al.* (2002) Occurrence and Localization of Apocarotenoids in Arbuscular Mycorrhizal Plant Roots. *Plant Cell Physiol.*, 43, 256–265.

Flematti, G.R., Waters, M.T., Scaffidi, A. *et al.* (2013) Karrikin and Cyanohydrin Smoke Signals Provide Clues to New Endogenous Plant Signaling Compounds. *Molecular Plant*, 6, 29–37.

Foo, E., Ferguson, B. J. and Reid, J. B. (2014) The potential roles of strigolactones and brassinosteroids in the autoregulation of nodulation pathway. *Ann. Bot.*

Foo, E., Ross, J. J., Jones, W. T. and Reid, J. B. (2013) Plant hormones in arbuscular mycorrhizal symbioses: an emerging role for gibberellins. *Ann. Bot.*, 111, 769–779.

Foo, E. and Davies, N. W. (2011) Strigolactones promote nodulation in pea. *Planta*, 234, 1073–1081.

Foo, E., Morris, S. E., Parmenter, K. *et al.* (2007) Feedback regulation of xylem cytokinin content is conserved in pea and Arabidopsis. *Plant Physiol.*, 143, 1418–1428.

Foo, E. (2005) The Branching Gene *RAMOSUS1* Mediates Interactions among Two Novel Signals and Auxin in Pea. *Plant Cell*, 17, 464–474.

Fourcroy, P., Sisó-Terraza, P., Sudre, D. *et al.* (2013) Involvement of the ABCG37 transporter in secretion of scopoletin and derivatives by *Arabidopsis* roots in response to iron deficiency. *New Phytol.*, 201, 155–167.

Fukui, K., Ito, S. and Asami, T. (2013) Selective mimics of strigolactone actions and their potential use for controlling damage caused by root parasitic weeds. *Molecular Plant*, 6, 88–99.

Gallavotti, A. (2013) The role of auxin in shaping shoot architecture. *J. Exp. Bot.*, 64, 2593–2608.

Geldner, N., Friml, J., Stierhof, Y. D. *et al.* (2001) Auxin transport inhibitors block PIN1 cycling and vesicle trafficking. *Nature*, 413, 425–428.

Genre, A., Ivanov, S., Fendrych, M. *et al.* (2011) Multiple exocytotic markers accumulate at the sites of perifungal membrane biogenesis in arbuscular mycorrhizas. *Plant Cell Physiol.*, 53, 244–255.

Genre, A., Chabaud, M., Timmers, T. *et al.* (2005) Arbuscular mycorrhizal fungi elicit a novel intracellular apparatus in *Medicago truncatula* root epidermal cells before infection. *Plant Cell*, 17, 3489–3499.

Gerats, T. and Vandenbussche, M. (2005) A model system for comparative research: *Petunia*. *Trends in Plant Science*, 10, 251–256.

Gershenzon, J. and Dudareva, N. (2007) The function of terpene natural products in the natural world. *Nat. Chem. Biol.*, 3, 408–414.

Gomez-Roldan, V., Fermas, S., Brewer, P. B. *et al.* (2008) Strigolactone inhibition of shoot branching. *Nature*, 455, 189–194.

Gonzalez-Chavez, M. D. C., Ortega-Larrocea, M. D. P., Carrillo-Gonzalez, R. *et al.* (2011) Arsenate induces the expression of fungal genes involved in As transport in arbuscular mycorrhiza. *Fungal Biol.*, 115, 1197–1209.

Granado, J., Felix G. and Boller T. (1995) Perception of Fungal Sterols in Plants (Subnanomolar Concentrations of Ergosterol Elicit Extracellular Alkalinization in Tomato Cells). *Plant Physiol.*, 107, 485–490.

Grebe, M., Xu, J., Möbius, W. *et al.* (2003) *Arabidopsis* Sterol Endocytosis Involves Actin-Mediated Trafficking via ARA6-Positive Early Endosomes. *Current Biology*, 13, 1378–1387.

Griebel, T. and Zeier, J. (2010) A role for β-sitosterol to stigmasterol conversion in plant-pathogen interactions. *The Plant Journal*, 63, 254–268.

Grunewald, W. and Friml, J. (2010) The march of the PINs: developmental plasticity by dynamic polar targeting in plant cells. *EMBO J.*, 29, 2700–2714.

Guan, J. C., Koch, K. E., Suzuki, M. *et al.* (2012) Diverse Roles of Strigolactone Signaling in Maize Architecture and the Uncoupling of a Branching-Specific Subnetwork. *Plant Physiol.*, 160, 1303–1317.

Gutjahr, C. and Parniske, M. (2013) Cell and Developmental Biology of Arbuscular Mycorrhiza Symbiosis. *Annu. Rev. Cell Dev. Biol.*, 29, 593–617.

Gutjahr, C., Banba, M., Croset, V. *et al.* (2008) Arbuscular mycorrhiza-specific signaling in rice transcends the common symbiosis signaling pathway. *Plant Cell*, 20, 2989–3005.

Güimil, S., Chang, H. S., Zhu, T., *et al.* (2005) Comparative transcriptomics of rice reveals an ancient pattern of response to microbial colonization. *Proc. Natl. Acad. Sci. U.S.A.*, 102, 8066–8070.

Ha, C. V., Leyva-González, M. A., Osakabe, Y. *et al.* (2013) Positive regulatory role of strigolactone in plant responses to drought and salt stress. *Proc. Natl. Acad. Sci. U.S.A.*, 111, 851-856.

Hamiaux, C., Drummond, R. S., Janssen, B. J. *et al.* (2012) DAD2 Is an α/β Hydrolase Likely to Be Involved in the Perception of the Plant Branching Hormone, Strigolactone. *Current Biology*, 22, 2032–2036.

Hare, J. D. (2005) Biological activity of acyl glucose esters from *Datura wrightii* glandular trichomes against three native insect herbivores. *J. Chem. Ecol.*, 31, 1475–1491.

Harrison, M. J. (2012) Cellular programs for arbuscular mycorrhizal symbiosis. *Curr. Opin. Plant Biol.*, 15, 691–698.

Hayward, A., Stirnberg, P., Beveridge, C. and Leyser, O. (2009) Interactions between auxin and strigolactone in shoot branching control. *Plant Physiol.*, 151, 400–412.

Hemmerlin, A. (2003) Cross-talk between the Cytosolic Mevalonate and the Plastidial Methylerythritol Phosphate Pathways in Tobacco Bright Yellow-2 Cells. *Journal of Biological Chemistry*, 278, 26666–26676.

Howe, G.A. and Jander, G. (2008) Plant immunity to insect herbivores. *Annu. Rev. Plant Biol.*, 59, 41–66.

Hu, Z., Yamauchi, T., Yang, J. *et al.* (2013) Strigolactone and Cytokinin Act Antagonistically in Regulating Rice Mesocotyl Elongation in Darkness. *Plant Cell Physiol.*, 55, 30-41.

Hu, Z., Yan, H., Yang, J. *et al.* (2010) Strigolactones Negatively Regulate Mesocotyl Elongation in Rice during Germination and Growth in Darkness. *Plant Cell Physiol.*, 51, 1136–1142.

Humphrey, A. J. and Beale, M. H. (2006) Strigol: biogenesis and physiological activity. *Phytochemistry*, 67, 636–640.

Imaizumi-Anraku, H., Takeda, N., Charpentier, M. *et al.* (2005) Plastid proteins crucial for symbiotic fungal and bacterial entry into plant roots. *Nature*, 433, 527–531.

Isman, M.B., Jeffs, L. B., Elliger, C. A. *et al.* (1998) Petuniolides, Natural Insecticides from *Petunia parodii,* Are Antagonists of $GABA_a$ Receptors. *Pesticide Biochemistry and Physiology*, 58, 103–107.

Ito, H. and Gray, W. M. (2006) A gain-of-function mutation in the Arabidopsis pleiotropic drug resistance transporter PDR9 confers resistance to auxinic herbicides. *Plant Physiol.*, 142, 63–74.

Ito, S., Umehara, M., Hanada, A. *et al.* (2011) Effects of triazole derivatives on strigolactone levels and growth retardation in rice. *PLoS ONE*, 6, e21723.

Jacquier, N. and Schneiter, R. (2012) Mechanisms of sterol uptake and transport in yeast. *Journal of Steroid Biochemistry and Molecular Biology*, 129, 70–78.

Jamil, M., Rodenburg, J., Charnikhova, T. and Bouwmeester, H. J. (2011) Pre-attachment *Striga hermonthica* resistance of New Rice for Africa (NERICA) cultivars based on low strigolactone production. *New Phytol.*, 192, 964–975.

Janssen, B. J., Drummond, R. S. and Snowden, K. C. (2014) Regulation of axillary shoot development. *Curr. Opin- Plant Biol.*, 17, 28–35.

Jasinski, M., Stukkens, Y., Degand, H. *et al.* (2001) A plant plasma membrane ATP binding cassette-type transporter is involved in antifungal terpenoid secretion. *Plant Cell*, 13, 1095–1107.

Javot, H., Penmetsa, R. V., Terzaghi, N. *et al.* (2007) A *Medicago truncatula* phosphate transporter indispensable for the arbuscular mycorrhizal symbiosis. *Proc. Natl. Acad. Sci. U.S.A.*, 104, 1720–1725.

Jiang, L., Liu, X., Xiong, G., *et al.* (2013) DWARF 53 acts as a repressor of strigolactone signalling in rice. *Nature*, 504, 401–405.

Jones, B., Andersson Gunneras, S., Petersson, S. V. *et al.* (2010) Cytokinin Regulation of Auxin Synthesis in Arabidopsis Involves a Homeostatic Feedback Loop Regulated via Auxin and Cytokinin Signal Transduction. *Plant Cell*, 22, 2956–2969.

Jungwirth, H. and Kuchler, K. (2006) Yeast ABC transporters – A tale of sex, stress, drugs and aging. *FEBS Letters*, 580, 1131–1138.

Kalousek, P., Buchtova, D., Balla, J. and Reinohl, V. (2010) Cytokinins and polar transport of auxin in axillary pea buds. *Acta Universitatis Agriculturae et Silviculturae Mendelianae Brunensis*, 1–10.

Kanamori, N., Madsen, L. H., Radutoiu, S. *et al.* (2006) A nucleoporin is required for induction of Ca^{2+} spiking in legume nodule development and essential for rhizobial and fungal symbiosis. *Proc. Natl. Acad. Sci. U.S.A.*, 103, 359–364.

Kang, J., Park, J., Choi, H., *et al.* (2011) Plant ABC Transporters. *Arabidopsis Book*, 9, e0153.

Kang, J., Hwang, J. U., Lee, M., *et al.* (2010a) PDR-type ABC transporter mediates cellular uptake of the phytohormone abscisic acid. *Proc. Natl. Acad. Sci. U.S.A.*, 107, 2355–2360.

Kang, J. H., Shi, F., Jones, A. D. *et al.* (2010b) Distortion of trichome morphology by the *hairless* mutation of tomato affects leaf surface chemistry. *J. Exp. Bot.*, 61, 1053–1064.

Kang, J. H., Liu, G., Shi, F. *et al.* (2010c) The tomato *odorless-2* mutant is defective in trichome-based production of diverse specialized metabolites and broad-spectrum resistance to insect herbivores. *Plant Physiol.*, 154, 262–272.

Kapulnik, Y., Resnick, N., Mayzlish-Gati, E. *et al.* (2011) Strigolactones interact with ethylene and auxin in regulating root-hair elongation in Arabidopsis. *J. Exp. Bot.*, 62, 2915–2924.

Kapulnik, Y., Delaux, P.M., Resnick, N. *et al.* (2010) Strigolactones affect lateral root formation and root-hair elongation in Arabidopsis. *Planta*, 233, 209–216.

Kennedy, G. G. (2003) Tomato, pests, parasitoids, and predators: tritrophic interactions involving the genus Lycopersicon. *Annu. Rev. Entomol.*, 48, 51–72.

Kiers, E. T., Duhamel, M., Beesetty, Y. *et al.* (2011) Reciprocal rewards stabilize cooperation in the mycorrhizal symbiosis. *Science*, 333, 880–882.

Kim, D.-Y., Bovet, L., Maeshima, M. *et al.* (2007) The ABC transporter AtPDR8 is a cadmium extrusion pump conferring heavy metal resistance. *The Plant Journal*, 50, 207–218.

Kivlin, S. N., Emery, S. M. and Rudgers, J. A. (2013) Fungal symbionts alter plant responses to global change. *Am. J. Bot.*, 100, 1445–1457.

Klett, E. L. and Patel, S. (2003) Genetic defenses against noncholesterol sterols. *Curr. Opin. Lipidol.*, 14, 341–345.

Koes, R., Souer, E., van Houwelingen, A. *et al.* (1995) Targeted gene inactivation in petunia by PCR-based selection of transposon insertion mutants. *Proc. Natl. Acad. Sci. U.S.A.*, 92, 8149–8153.

Kohlen, W., Charnikhova, T., Lammers, M. *et al.* (2012) The tomato *CAROTENOID CLEAVAGE DIOXYGENASE8 (SlCCD8)* regulates rhizosphere signaling, plant architecture and affects reproductive development through strigolactone biosynthesis. *New Phytol*., 196, 535-347.

Kohlen, W., Charnikhova, T., Liu, Q. *et al.* (2010) Strigolactones are transported through the xylem and play a key role in shoot architectural response to phosphate deficiency in non-AM host *Arabidopsis thaliana*. *Plant Physiol.*, 155, 974-987.

Koltai, H. and Kapulnik, Y. (2013) Unveiling Signaling Events in Root Responses to Strigolactone. *Molecular Plant*, 6, 589–591.

Koltai, H., Cohen, M., Chesin, O. *et al.* (2011) Light is a positive regulator of strigolactone levels in tomato roots. *J. Plant Physiol*. 168, 1993-1996.

Kos, M., Houshyani, B., Overeem, A.J. *et al.* (2012) Genetic engineering of plant volatile terpenoids: effects on a herbivore, a predator and a parasitoid. *Pest. Manag. Sci.,* 69, 302-311.

Krecek, P., Skupa, P., Libus, J. *et al.* (2009) The PIN-FORMED (PIN) protein family of auxin transporters. *Genome Biol*, 10, 249.

Kretzschmar, T., Kohlen, W., Sasse, J. *et al.* (2012) A petunia ABC protein controls strigolactone-dependent symbiotic signalling and branching. *Nature*, 483, 341–344.

Kudo, T., Kiba, T. and Sakakibara, H. (2010) Metabolism and long-distance translocation of cytokinins. *J. Integr. Plant Biol.*, 52, 53–60.

Lee, M., Lee, K., Lee, J. *et al.* (2005) AtPDR12 contributes to lead resistance in Arabidopsis. *Plant Physiol.*, 138, 827–836.

Leyser, O. (2006) Dynamic integration of auxin transport and signalling. *Current Biology*, 16, R424–33.

Li, Y. (2004) ATP-binding Cassette (ABC) Transporters Mediate Nonvesicular, Raft-modulated Sterol Movement from the Plasma Membrane to the Endoplasmic Reticulum. *Journal of Biological Chemistry*, 279, 45226–45234.

Liang, J., Zhao, L., Challis, R. and Leyser, O. (2010) Strigolactone regulation of shoot branching in chrysanthemum (*Dendranthema grandiflorum*). *J. Exp. Bot.*, 61, 3069–3078.

Liu, J., Novero, M., Charnikhova, T. *et al.* (2013) *CAROTENOID CLEAVAGE DIOXYGENASE 7* modulates plant growth, reproduction, senescence, and determinate nodulation in the model legume *Lotus japonicus. J. Exp. Bot.*, 64, 1967-1981.

Liu, J., Blaylock, L. A., Endre, G. *et al.* (2003) Transcript Profiling Coupled with Spatial Expression Analyses Reveals Genes Involved in Distinct Developmental Stages of an Arbuscular Mycorrhizal Symbiosis. *Plant Cell*, 15, 2106–2123.

Liu, W., Kohlen, W., Lillo, A. *et al.* (2011) Strigolactone biosynthesis in *Medicago truncatula* and rice requires the symbiotic GRAS-type transcription factors NSP1 and NSP2. *Plant Cell*, 23, 3853–3865.

Lopez-Raez, J. A., Charnikhova, T., Fernandez, I. *et al.* (2010) Arbuscular mycorrhizal symbiosis decreases strigolactone production in tomato. *J Plant Physiol*., 168, 294-297.

Lopez-Raez, J. A., Charnikhova, T., Gomez-Roldan, V. *et al.* (2008a) Tomato strigolactones are derived from carotenoids and their biosynthesis is promoted by phosphate starvation. *New Phytol*, 178, 863–874.

Lopez-Raez, J. A., Matusova, R., Cardoso, C. *et al.* (2008b) Strigolactones: ecological significance and use as a target for parasitic plant control. *Pest. Manag. Sci.*, 64, 471-477.

Maillet, F., Poinsot, V., Andre, O. *et al.* (2011) Fungal lipochitooligosaccharide symbiotic signals in arbuscular mycorrhiza. *Nature*, 469, 58–63.

Martinoia, E., Klein, M., Geisler, M. *et al.* (2002) Multifunctionality of plant ABC transporters--more than just detoxifiers. *Planta*, 214, 345–355.

Mashiguchi, K., Sasaki, E., Shimada, Y. *et al.* (2009) Feedback-regulation of strigolactone biosynthetic genes and strigolactone-regulated genes in Arabidopsis. *Biosci. Biotechnol. Biochem.*, 73, 2460–2465.

Maxfield, F. R. and Menon, A. K. (2006) Intracellular sterol transport and distribution. *Current Opinion in Cell Biology*, 18, 379–385.

Maxfield, F. R. and Tabas, I. (2005) Role of cholesterol and lipid organization in disease. *Nature*, 438, 612–621.

McDowell, E. T., Kapteyn, J., Schmidt, A, *et al.* (2010) Comparative functional genomic analysis of *Solanum* glandular trichome types. *Plant Physiol.*, 155, 524–539.

Medeiros, A. H. and Tingey, W. M. (2006) Glandular Trichomes of *Solanum berthaultii* and Its Hybrids with S*olanum tuberosum* Affect Nymphal Emergence, Development, and Survival of *Empoasca fabae* (Homoptera: Cicadellidae). *Journal Economic Entomology*, 99, 1483–1489.

Mesmin, B., Antonny, B. and Drin, G. (2013) Insights into the mechanisms of sterol transport between organelles. *Cell. Mol. Life Sci.*, 70, 3405–3421.

Miresmailli, S. and Isman, M. B. (2013) Botanical insecticides inspired by plant-herbivore chemical interactions. *Trends in Plant Science*., 19, 29-35.

Moitra, K., Silverton, L., Limpert, K. *et al.* (2011) Moving out: from sterol transport to drug resistance – the ABCG subfamily of efflux pumps. *Drug Metabolism and Drug Interactions*, 26, 105-111.

Moons, A. (2008) Transcriptional profiling of the PDR gene family in rice roots in response to plant growth regulators, redox perturbations and weak organic acid stresses. *Planta*, 229, 53–71.

Moons, A. (2003) *Ospdr9*, which encodes a PDR-type ABC transporter, is induced by heavy metals, hypoxic stress and redox perturbations in rice roots. *FEBS Letters*, 553, 370–376.

Moreau, P., Hartmann, M., Perret, A. *et al.* (1998) Transport of sterols to the plasma membrane of leek seedlings. *Plant Physiol.*, 117, 931–937.

Moser, D., Klaiber, I., Vogler, B. and Kraus, W. (1999) Molluscicidal and antibacterial compounds from *Petunia hybrida*. *Pesticide Science*, 55, 336–339.

Murray, J. D., Cousins, D. R., Jackson, K. J. and Liu, C. (2013) Signaling at the Root Surface: The Role of Cutin Monomers in Mycorrhization. *Molecular Plant*, 6, 1381–1383.

Müller, D. and Leyser, O. (2011) Auxin, cytokinin and the control of shoot branching. *Ann. Bot.*, 107, 1203–1212.

Mwakaboko, A. S. and Zwanenburg, B. (2011) Strigolactone Analogs Derived from Ketones Using a Working Model for Germination Stimulants as a Blueprint. *Plant Cell Physiol.*, 52, 699–715.

Nadeem, S. M., Ahmad, M., Zahir, Z. A. *et al.* (2014) The role of mycorrhizae and plant growth promoting rhizobacteria (PGPR) in improving crop productivity under stressful environments. *Biotechnology Advances*, 32, 429–448.

Nakamura, H., Xue, Y.-L., Miyakawa, T. *et al.* (2013) Molecular mechanism of strigolactone perception by DWARF14. *Nature Communications*, 4, 1–10.

Nakashita, H., Yasuda, M., Nitta, T. *et al.* (2003) Brassinosteroid functions in a broad range of disease resistance in tobacco and rice. *Plant Journal*, 33, 887–898.

Napoli, C. (1996) Highly Branched Phenotype of the Petunia *dad1-1* Mutant Is Reversed by Grafting. *Plant Physiol.*, 111, 27–37.

Navazio, L., Moscatiello, R., Genre, A. *et al.* (2007) A diffusible signal from arbuscular mycorrhizal fungi elicits a transient cytosolic calcium elevation in host plant cells. *Plant Physiol.*, 144, 673–681.

Nazeri, N. K., Lambers, H., Tibbett, M. and Ryan, M. H. (2013) Moderating mycorrhizas: arbuscular mycorrhizas modify rhizosphere chemistry and maintain plant phosphorus status within narrow boundaries. *Plant Cell Environ*., 37, 911-927.

Nelson, D. C., Scaffidi, A., Dun, E. A. *et al.* (2011) F-box protein MAX2 has dual roles in karrikin and strigolactone signaling in *Arabidopsis thaliana*. *Proc. Natl. Acad. Sci. U.S.A.*, 108, 8897–8902.

Offringa, R. and Huang, F. (2013) Phosphorylation-dependent Trafficking of Plasma Membrane Proteins in Animal and Plant Cells. *J. Integr. Plant Biol.*, 55, 789–808.

Ongaro, V. and Leyser, O. (2008) Hormonal control of shoot branching. *J. Exp. Bot.*, 59, 67–74.

Parniske, M. (2008) Arbuscular mycorrhiza: the mother of plant root endosymbioses. *Nat. Rev. Microbiol.*, 6, 763–775.

Parniske, M. (2004) Molecular genetics of the arbuscular mycorrhizal symbiosis. *Curr. Opin. Plant Biol.*, 7, 414–421.

Parniske, M. M. (2000) Intracellular accommodation of microbes by plants: a common developmental program for symbiosis and disease? *Curr. Opin. Plant Biol.*, 3, 320–328.

Pasare, S. A., Ducreux, L. J. M., Morris, W. L. *et al.* (2013) The role of the potato (*Solanum tuberosum*) *CCD8* gene in stolon and tuber development. *New Phytol.*, 198, 1108–1120.

Peiter, E., Sun, J., Heckmann, A. B,.*et al.* (2007) The *Medicago truncatula* DMI1 protein modulates cytosolic calcium signaling. *Plant Physiol.*, 145, 192–203.

Prasad, R. and Goffeau, A. (2012) Yeast ATP-Binding Cassette Transporters Conferring Multidrug Resistance. *Annu. Rev. Microbiol.*, 66, 39–63.

Proust, H., Hoffmann, B., Xie, X. *et al.* (2011) Strigolactones regulate protonema branching and act as a quorum sensing-like signal in the moss *Physcomitrella patens*. *Development*, 138, 1531–1539.

Rasmussen, A., Depuydt, S., Goormachtig, S. and Geelen, D. (2013) Strigolactones fine-tune the root system. *Planta*., 238, 615-626.

Rasmussen, A., Mason, M., De Cuyper, C. *et al.* (2012) Strigolactones suppress adventitious rooting in Arabidopsis and pea. *Plant Physiol.*, 158, 1976-1987.

Rea, P. A. (2007) Plant ATP-binding cassette transporters. *Annu. Rev. Plant Biol.*, 58, 347–375.

Redecker, D., Kodner, R. and Graham, L.E. (2000) Glomalean fungi from the Ordovician. *Science*, 289, 1920–1921.

Rossard, S., Roblin, G. and Atanassova, R. (2010) Ergosterol triggers characteristic elicitation steps in *Beta vulgaris* leaf tissues. *Journal of Experimental Botany*, 61, 1807–1816.

Ruiz-Lozano, J. M., Porcel, R., Azcon, C. and Aroca, R. (2012) Regulation by arbuscular mycorrhizae of the integrated physiological response to salinity in plants: new challenges in physiological and molecular studies. *J. Exp. Bot.*, 63, 4033–4044.

Ruocco, M., Ambrosino, P., Lanzuise, S. *et al.* (2011) Four potato (*Solanum tuberosum*) ABCG transporters and their expression in response to abiotic factors and *Phytophthora infestans* infection. *J. Plant Physiology*, 168, 2225–2233.

Ruyter-Spira, C. and Bouwmeester, H. (2012) Strigolactones affect development in primitive plants. The missing link between plants and arbuscular mycorrhizal fungi? *New Phytol*, 195, 730–733.

Ruyter-Spira, C., Kohlen, W., Charnikhova, T. *et al.* (2011) Physiological effects of the synthetic strigolactone analog GR24 on root system architecture in Arabidopsis: Another below-ground role for strigolactones? *Plant Physiol.*, 155, 721-734.

Ruzicka, K., Strader, L. C., Bailly, A. *et al.* (2010) *Arabidopsis PIS1* encodes the ABCG37 transporter of auxinic compounds including the auxin precursor indole-3-butyric acid. *Proc. Natl. Acad. Sci. U.S.A.*, 107, 10749–10753.

Sasabe, M., Toyoda, K., Shiraishi, T. *et al.* (2002) cDNA cloning and characterization of tobacco ABC transporter: *NtPDR1* is a novel elicitor-responsive gene. *FEBS Letters*, 518, 164–168.

Sawers, R. J., Gutjahr, C. and Paszkowski, U. (2008) Cereal mycorrhiza: an ancient symbiosis in modern agriculture. *Trends in Plant Science*, 13, 93–97.

Schaeffer, A., Bronner, R., Benveniste, P. and Schaller, H. (2001) The ratio of campesterol to sitosterol that modulates growth in Arabidopsis is controlled by STEROL METHYLTRANSFERASE 2;1. *Plant Journal*, 25, 605–615.

Schaller, H. (2004) New aspects of sterol biosynthesis in growth and development of higher plants. *Plant Physiology and Biochemistry*, 42, 465–476.

Schaller, H. (2003) The role of sterols in plant growth and development. *Progress in Lipid Research*, 42, 163–175.

Schilmiller, A. L., Shi, F., Kim, J. *et al.* (2010) Mass spectrometry screening reveals widespread diversity in trichome specialized metabolites of tomato chromosomal substitution lines. *Plant Journal*, 62, 391–403.

Schilmiller, A. L., Last, R. L. and Pichersky, E. (2008) Harnessing plant trichome biochemistry for the production of useful compounds. *Plant Journal*, 54, 702–711.

Schmidt, A., Li, C., Shi, F. *et al.* (2011) Polymethylated myricetin in trichomes of the wild tomato species *Solanum habrochaites* and characterization of trichome-specific 3'/5‘- and 7/4’-myricetin O-methyltransferases. *Plant Physiol.*, 155, 1999–2009.

Schulz, T. A. and Prinz, W. A. (2007) Sterol transport in yeast and the oxysterol binding protein homologue (OSH) family. *Biochimica et Biophysica Acta (BBA) - Molecular and Cell Biology of Lipids*, 1771, 769–780.

Seto, Y., Sado, A., Asami, K. *et al.* (2014) Carlactone is an endogenous biosynthetic precursor for strigolactones. *Proc. Natl. Acad. Sci. U.S.A.*, 111, 1640–1645.

Sharda, J. N. and Koide, R. T. (2008) Can hypodermal passage cell distribution limit root penetration by mycorrhizal fungi? *New Phytol.*, 180, 696–701.

Shen, H., Zhu, L., Bu, Q. Y. and Huq, E. (2012) MAX2 Affects Multiple Hormones to Promote Photomorphogenesis. *Molecular Plant*, 5, 224–236.

Shen, H., Luong, P. and Huq, E. (2007) The F-Box Protein MAX2 Functions as a Positive Regulator of Photomorphogenesis in Arabidopsis. *Plant Physiol.*, 145, 1471–1483.

Shimoda, Y., Han, L., Yamazaki, T. *et al.* (2012) Rhizobial and Fungal Symbioses Show Different Requirements for Calmodulin Binding to Calcium Calmodulin-Dependent Protein Kinase in *Lotus japonicus. Plant Cell*, 24, 304–321.

Shingu, K., Fujii, H., Mizuki, K. *et al.* (1994) Ergostane Glycosides From *Petunia hybrida*. *Phytochemistry*, 36, 1307–1314.

Shinohara, N., Taylor, C. and Leyser, O. (2013) Strigolactone Can Promote or Inhibit Shoot Branching by Triggering Rapid Depletion of the Auxin Efflux Protein PIN1 from the Plasma Membrane. *PLoS Biol.*, 11, e1001474.

Singh, S. and Parniske, M. (2012) Activation of calcium- and calmodulin-dependent protein kinase (CCaMK), the central regulator of plant root endosymbiosis. *Curr. Opin. Plant Biol.*, 1–10.

Singh, L. P., Gill, S. S. and Tuteja, N. (2011) Unraveling the role of fungal symbionts in plant abiotic stress tolerance. *Plant Signa.l Behav.*, 6, 175–191.

Slocombe, S. P., Schauvinhold, I., McQuinn, R. P. *et al.* (2008) Transcriptomic and Reverse Genetic Analyses of Branched-Chain Fatty Acid and Acyl Sugar Production in *Solanum pennellii* and *Nicotiana benthamiana*. *Plant Physiol.*, 148, 1830–1846.

Smith, J. L., De Moraes, C. M. and Mescher, M. C. (2009) Jasmonate- and salicylate-mediated plant defense responses to insect herbivores, pathogens and parasitic plants. *Pest. Manag. Sci.*, 65, 497–503.

Snowden, K. C., Simkin, A. J., Janssen, B. J. *et al.* (2005) The *Decreased apical dominance1/Petunia hybrida CAROTENOID CLEAVAGE DIOXYGENASE8* gene affects branch production and plays a role in leaf senescence, root growth, and flower development. *Plant Cell*, 17, 746–759.

Snowden, K. C. and Napoli, C. A. (2003) A quantitative study of lateral branching in petunia. *Functional Plant Biology*, 30, 987–994.

Sorefan, K. (2003) *MAX4* and *RMS1* are orthologous dioxygenase-like genes that regulate shoot branching in *Arabidopsis* and pea. *Genes & Development*, 17, 1469–1474.

Stanga, J. P., Smith, S. M., Briggs, W. R. and Nelson, D. C. (2013) *SUPPRESSOR OF MAX2 1 (SMAX1)* controls seed germination and seedling development in *Arabidopsis thaliana. Plant Physiol.*, 163, 318–330.

Stein, M., Dittgen, J., Sanchez-Rodriguez, C. *et al.* (2006) *Arabidopsis* PEN3/PDR8, an ATP binding cassette transporter, contributes to nonhost resistance to inappropriate pathogens that enter by direct penetration. *Plant Cell*, 18, 731–746.

Stirnberg, P., Furner, I. J. and Leyser, O. (2007) MAX2 participates in an SCF complex which acts locally at the node to suppress shoot branching. *The Plant Journal*, 50, 80–94.

Stirnberg, P., van De Sande, K.K. and Leyser, O. (2002) *MAX1* and *MAX2* control shoot lateral branching in Arabidopsis. *Development*, 129, 1131–1141.

Stukkens, Y., Bultreys, A., Grec, S. *et al.* (2005) NpPDR1, a pleiotropic drug resistance-type ATP-binding cassette transporter from *Nicotiana plumbaginifolia*, plays a major role in plant pathogen defense. *Plant Physiol.*, 139, 341–352.

Sugiyama, A., Shitan, N., Sato, S. *et al.* (2006) Genome-wide analysis of ATP-binding cassette (ABC) proteins in a model legume plant, *Lotus japonicus:* comparison with Arabidopsis ABC protein family. *DNA Res*, 13, 205–228.

Sun, Z., Hans, J., Walter, M. H. *et al.* (2008) Cloning and characterisation of a maize carotenoid cleavage dioxygenase (*ZmCCD1*) and its involvement in the biosynthesis of apocarotenoids with various roles in mutualistic and parasitic interactions. *Planta*, 228, 789–801.

Swarbrick, P. J., Huang, K., Liu, G. *et al.* (2008) Global patterns of gene expression in rice cultivars undergoing a susceptible or resistant interaction with the parasitic plant *Striga hermonthica. New Phytol.*, 179, 515–529.

Takeda, N., Tsuzuki, S., Suzaki, T. *et al.* (2013) *CERBERUS* and *NSP1* of *Lotus japonicus* are common symbiosis genes that modulate arbuscular mycorrhiza development. *Plant Cell Physiol.*, 54, 1711–1723.

Tamasloukht, M., Sejalon-Delmas, N., Kluever, A. *et al.* (2003) Root factors induce mitochondrial-related gene expression and fungal respiration during the developmental switch from asymbiosis to presymbiosis in the arbuscular mycorrhizal fungus *Gigaspora rosea. Plant Physiol.*, 131, 1468–1478.

Tanaka, M., Takei, K., Kojima, M. *et al.* (2006) Auxin controls local cytokinin biosynthesis in the nodal stem in apical dominance. *Plant Journal*, 45, 1028–1036.

Tarling, E. J., de Aguiar Vallim, T. Q. and Edwards, P. A. (2013) Role of ABC transporters in lipid transport and human disease. *Trends in Endocrinology & Metabolism*, 24, 342–350.

Theodoulou, F.L. (2000) Plant ABC transporters. *Biochim. Biophys. Acta*, 1465, 79–7103.

Tissier, A., Sallaud, C. and Rontein, D. (2013) Tobacco Trichomes as a Platform for Terpenoid Biosynthesis Engineering. In T. J. Bach and M. Rohmer, eds. Isoprenoid Synthesis in Plants and Microorganisms. *Springer New York,* pp. 271–283.

Tissier, A. (2012) Glandular trichomes: what comes after expressed sequence tags? *Plant Journal*, 70, 51–68.

Tobena-Santamaria, R. (2002) FLOOZY of petunia is a flavin mono-oxygenase-like protein required for the specification of leaf and flower architecture. *Genes & Development*, 16, 753–763.

Toh, S., Kamiya, Y., Kawakami, N. *et al.* (2011) Thermoinhibition uncovers a role for strigolactones in Arabidopsis seed germination. *Plant Cell Physiol.*, 53, 107–117.

Traw, M. B. (2003) Interactive Effects of Jasmonic Acid, Salicylic Acid, and Gibberellin on Induction of Trichomes in Arabidopsis. *Plant Physiol.*, 133, 1367–1375.

Tromas, A., Parizot, B., Diagne, N. *et al.* (2012) Heart of Endosymbioses: Transcriptomics Reveals a Conserved Genetic Program among Arbuscular Mycorrhizal, Actinorhizal and Legume-Rhizobial Symbioses. *PLoS ONE*, 7, e44742.

Tsuchiya, Y., Vidaurre, D., Toh, S. *et al.* (2010) A small-molecule screen identifies new functions for the plant hormone strigolactone. *Nat. Chem. Biol.*, 6, 741–749.

Tugizimana, F., Steenkamp, P. A., Piater, L. A. and Dubery, I. A. (2012) Ergosterol-Induced Sesquiterpenoid Synthesis in Tobacco Cells. *Molecules*, 17, 1698–1715.

Umehara, M., Hanada, A., Magome, H. *et al.* (2010) Contribution of strigolactones to the inhibition of tiller bud outgrowth under phosphate deficiency in rice. *Plant Cell Physiol.*, 51, 1118–1126.

Umehara, M., Hanada, A., Yoshida, S. *et al.* (2008) Inhibition of shoot branching by new terpenoid plant hormones. *Nature*, 455, 195–200.

van Dam, N. M. and Hare, J. D. (1998) Biological activity of *Datura wrightii* glandular trichome exudate against *Manduca sexta* larvae. *J. Chem. Ecol.*, 24, 1529–1549.

van den Brule, S. and Smart, C. C. (2002) The plant PDR family of ABC transporters. *Planta*, 216, 95–9106.

van den Brule, S., Muller, A., Fleming, A. J. and Smart, C. C. (2002) The ABC transporter SpTUR2 confers resistance to the antifungal diterpene sclareol. *Plant Journal*, 30, 649–662.

Van Norman, J. M., Xuan, W., Beeckman, T. and Benfey, P. N. (2013) To branch or not to branch: the role of pre-patterning in lateral root formation. *Development*, 140, 4301–4310.

van Schie, C. C. N., Haring, M. A. and Schuurink, R. C. (2007) Tomato linalool synthase is induced in trichomes by jasmonic acid. *Plant Mol. Biol.*, 64, 251–263.

Verhoef, N., Yokota, T., Shibata, K. *et al.* (2013) Brassinosteroid biosynthesis and signalling in *Petunia hybrida. J. Exp. Bot.*, 64, 2435–2448.

Verrier, P. J., Bird, D., Burla, B. *et al.* (2008) Plant ABC proteins - a unified nomenclature and updated inventory. *Trends in Plant Science*, 13, 151–159.

Vogel, J. T., Walter, M. H., Giavalisco, P. *et al.* (2009) SlCCD7 controls strigolactone biosynthesis, shoot branching and mycorrhiza-induced apocarotenoid formation in tomato. *The Plant Journal*, 61, 300–311.

Wagner, G. J. (1991) Secreting Glandular Trichomes: More than Just Hairs. *Plant Physiol.*, 96, 675–679.

Waldie, T., Hayward, A. and Beveridge, C. A. (2010) Axillary bud outgrowth in herbaceous shoots: how do strigolactones fit into the picture? *Plant Mol. Biol.*, 73, 27–36.

Walker, J. E., Saraste, M., Runswick, M. J. and Gay, N. J. (1982) Distantly related sequences in the α- and β-subunits of ATP synthase, myosin, kinases and other ATP-requiring enzymes and a common nucleotide binding fold. *EMBO J.*, 1, 945–951.

Walter, M. H., Floss, D. S. and Strack, D. (2010) Apocarotenoids: hormones, mycorrhizal metabolites and aroma volatiles. *Planta*, 232, 1–17.

Walter, M. H., Floss, D. S., Hans, J., Fester, T. and Strack, D. (2007) Apocarotenoid biosynthesis in arbuscular mycorrhizal roots: contributions from methylerythritol phosphate pathway isogenes and tools for its manipulation. *Phytochemistry*, 68, 130–138.

Wang, E. M., Wang, R., DeParasis, J. *et al.* (2001) Suppression of a P450 hydroxylase gene in plant trichome glands enhances natural-product-based aphid resistance. *Nature Biotechnology*, 19, 371–374.

Wang, J., Grishin, N., Kinch, L. *et al.* (2011) Sequences in the Nonconsensus Nucleotide-binding Domain of ABCG5/ABCG8 Required for Sterol Transport. *Journal of Biological Chemistry*, 286, 7308–7314.

Wang, K., Senthil-Kumar, M., Ryu, C. M. *et al.* (2012) Phytosterols Play a Key Role in Plant Innate Immunity against Bacterial Pathogens by Regulating Nutrient Efflux into the Apoplast. *Plant Physiol.*, 158, 1789–1802.

Wang, M. B. and Waterhouse, P. M. (1997) A rapid and simple method of assaying plants transformed with hygromycin or PPT resistance genes. *Plant Molecular Biology Reporter*, 15, 209–215.

Wang, Y. and Li, J. (2011) Branching in rice. *Curr. Opin. Plant Bio.l*, 14, 94–99.

Waters, M. T. and Smith, S. M. (2013) KAI2- and MAX2-Mediated Responses to Karrikins and Strigolactones Are Largely Independent of HY5 in *Arabidopsis* Seedlings. *Molecular Plant*, 6, 63–75.

Waters, M. T., Brewer, P. B., Bussell, J. D. *et al.* (2012a) The Arabidopsis ortholog of rice DWARF27 acts upstream of MAX1 in control of plant development by strigolactones. *Plant Physiol.,* 159, 1073-1085.

Waters, M. T., Nelson, D. C., Scaffidi, A. *et al.* (2012b) Specialisation within the DWARF14 protein family confers distinct responses to karrikins and strigolactones in Arabidopsis. *Development*, 139, 1285–1295.

Wigchert, S. C., Kuiper, E., Boelhouwer, G. J. *et al.* (1999) Dose-response of seeds of the parasitic weeds Striga and Orobanche toward the synthetic germination stimulants GR 24 and Nijmegen 1. *J. Agric. Food Chem.*, 47, 1705–1710.

Wittenburg, H. and Carey, M.C. (2002) Biliary cholesterol secretion by the twinned sterol half-transporters ABCG5 and ABCG8. *J. Clin. Invest.*, 110, 605–609.

Woo, H. R., Chung, K. M., Park, J. H. *et al.* (2001) ORE9, an F-box protein that regulates leaf senescence in *Arabidopsis*. *Plant Cell*, 13, 1779–1790.

Xie, X., Yoneyama, K., Kisugi, T.,*et al.* (2013) Confirming Stereochemical Structures of Strigolactones Produced by Rice and Tobacco. *Molecular Plant*, 6, 153–163.

Xie, X. and Yoneyama, K. (2010) The strigolactone story. *Annu. Rev. Phytopathol.*, 48, 93–117.

Yang, C. J., Zhang, C., Lu, Y .N. *et al*. (2011) The Mechanisms of Brassinosteroids' Action: From Signal Transduction to Plant Development. *Molecular Plant*, 4, 588–600.

Yang, S.-Y. and Paszkowski, U. (2011) Phosphate import at the arbuscule: just a nutrient? *Mol Plant Microbe Interact*, 24, 1296–1299.

Yoneyama, K., Xie, X., Kim, H. I. *et al.* (2011) How do nitrogen and phosphorus deficiencies affect strigolactone production and exudation? *Planta*, 235, 1197–1207.

Yoneyama, K., Xie, X., Sekimoto, H. *et al.* (2008) Strigolactones, host recognition signals for root parasitic plants and arbuscular mycorrhizal fungi, from Fabaceae plants. *New Phytol*, 179, 484–494.

Yoneyama, K., Xie, X., Kusumoto, D. *et al.* (2007a) Nitrogen deficiency as well as phosphorus deficiency in sorghum promotes the production and exudation of 5-deoxystrigol, the host recognition signal for arbuscular mycorrhizal fungi and root parasites. *Planta*, 227, 125–132.

Yoneyama, K., Yoneyama, K., Takeuchi, Y. and Sekimoto, H. (2007b) Phosphorus deficiency in red clover promotes exudation of orobanchol, the signal for mycorrhizal symbionts and germination stimulant for root parasites. *Planta*, 225, 1031–1038.

Zhang, S., Li, G., Fang, J. *et al.* (2010) The interactions among *DWARF10*, auxin and cytokinin underlie lateral bud outgrowth in rice. *J. Integr. Plant Biol.*, 52, 626–638.

Zhou, F., Lin, Q., Zhu, L. *et al.* (2013) D14-SCF^{D3}-dependent degradation of D53 regulates strigolactone signalling. *Nature*, 504, 406–410.

Zou, J., Zhang, S., Zhang, W. *et al.* (2006) The rice *HIGH-TILLERING DWARF1* encoding an ortholog of Arabidopsis MAX3 is required for negative regulation of the outgrowth of axillary buds. *Plant Journal*, 48, 687–698.

Zubko, E., Adams, C. J., Machaekova, I. *et al.* (2002) Activation tagging identifies a gene from *Petunia hybrida* responsible for the production of active cytokinins in plants. *Plant Journal*, 29, 797–808.

8 Acknowledgements

Foremost, my thanks go to Prof. Enrico Martinoia, who gave me the opportunity to work on this many-sided, demanding and fascinating project. Thank you for the support and input when I needed it, and for the freedom to develop my own ideas. I always enjoyed the conversations about science and various other topics.

Many thanks to my thesis committee Prof. Beat Keller, Dr. Uta Paszkowski, and Dr. Didier Reinhardt, you were very supportive with not only discussions, but also with hands-on solutions to challenges I had to meet. Many thanks also go to Dr. Laurent Bigler, you always took your time to analyze my data further, to do some more experiments, and to explain your work to me, despite you are always so busy.

Next, my thanks go to Dr. Tobias Kretzschmar who started off the projects that I was able to take one step further in my work. Without your careful supervision and guidance in the first half year the challenges would have even bigger. The PETS group: thanks to Dr. Lorenzo Borghi, Christian Gübeli, Dr. Guo-wei Liu, and all the baby technicians, you were a great team to work with. The discussion with you were fruitful, and without your technical help, many projects would not have been possible. Many thanks not only go to the PETS, but also to Dr. Miyoung Lee and Dr. Undine Krügel for the nice lab atmosphere, the discussions about highlights, frustrating moments and the shared laughs. To the aforementioned people and to the other P1 members: thank you for the great working atmosphere, the fast support in critical situations, the great coffee and lunch breaks in the garden. Moreover, I would like to thank the staff of the Institute for their support, special thanks go to Kari who was always worried about the Petunia's wellbeing.

Further, I would like to thank Enrico, Dr. Glen R. Uhrig, Undine, and Laurent, for critical reading of the manuscript, and I would like to thank Dr. Pascal Schläpfer for providing nice figures and tables, critical comments, new ideas and for the careful reading of my thesis.

I would like to thank my family, my dad, my mum, Noémie, Nina, and Olivia for the continuous support in various areas, for the trust you put in me, and for the distraction from my work when I needed it. Many thanks as well to my second family Daniela, Bruno, and Marc, to let me be part of your life. Thank you for many great discussions, for the critical questions, and the continuous support.

Last, my thanks go to my husband Pascal. What can I say- your support, your love and ideas have been helping me through all challenges of science and life. I am looking forward to spend my life with you; and no matter where we will end up, I will feel at home with you by my side.

9 Appendix

Table 9-1:Overview on *Petunia hybrida* primers for semiquantitative and quantitative PCR

Gene	sq / q	annealing temp (°C)	Stock #	fw / rv	Sequence
DAD1	sq	61.2	15	fw	tagataagcctcgcaggcaactctc
		61.4	16	rv	catgcagtccataggggagac
DAD1	q	53.4	352	fw	agaactggtatgatgagggt
		53.4	9	rv	tttctttggaacccagcaac
GAPDH	q	59.2	214	fw	gactggagaggtggaagagc
		57.2	215	rv	ccgttaagagctgggagaac
PDR1	sq	53.0	54	fw	aaatgctactacagtgcag
		55.4	56	rv	catataatgtccaggaaatgg
	q	55.1	217	fw	gatggtattggattggagca
		53.1	216	rv	cctgaggtttaccaaatggg
PDR2	sq	56.4	191	fw	tcaaggcattcaacttccag
		60.5	192	rv	tactgaccgagtctccacca
	q	56.0	122	fw	ggaatgtattctgccttacc
		55.7	222	rv	gtaatctccaaattgtgatgc
PIN1	sq	55.8	474	fw	ttccttacaggtccagctgtt
		55.8	475	rv	agaccaatgtaattggcaaggca
TUB1	sq	60.0	61	fw	cattggtcaagccggttattc
		60.0	62	rv	acccttgaagaccagtacagt

Primers used for quantitative (q) and semiquantitative (sq) PCR. The gene name, annealing temperatures for forward (fw) primer and reverse (rv) primers are given, as well as the stock number of the primers and their nucleotide sequence.

9.1 *PhPDR2* gDNA and cDNA

Genomic DNA sequence of *Petunia hybrida* PDR2, with exons depicted in orange and green.

ATGGAACCAGTAAACTTAGGTAACTTACGAGCGGCTAGTTTGAGAGGAAGTGCAAGGGGAAGTTTAAGTGGAAG
TTTAAGAGCAAATAGTAACTCTATATGGAGAAATGATAATGTTTTCAATCGTTCATCAAGAGATGAAAATGATG
AAGAAGCACTTAAATGGGCAGCTCTTGAAAAACTTCCAACATTTGATCGTTTAAGAAAAGGTTTGTTGTTTGGAT
CTGAAGGTACAGCACCTTCTCAAATTGATATACATGATATTGGTTTTCAAGAAAGACAAGGTTTGCTTGATAGGC
TTGTGAAAGATCCTGATGAAGATAATGAGAAGTTCTTGTTGAAACTCAGAGATAGAATTGACAGGTAAGTAGTA
GAATCTTTTTGTGTGTTAAAAAGAGAGTTCTCGGCTAAAGTGGTCCTTTATGTATTGGATACACTTTATTTTCGG
GAGATTTGGTTCATCGACTTAAAATTAACGGAATTTTCAAAATATCTAGTTAAATTTAACTCCTGTTACGATGTG
CAACTCATGTGCATTTATGTTAGAGGTGCAGCATGAATGCACTTGAGTTGCACATCTTAAGAGTAGTTAAACTTA
ACCAGATTTTTTGAAAGTTCCGTTAGTTTTAGGAGGACCAAATCTCCTAATCTTTTTATATATTTTAAGGACTAT
AGATCTAAAGAGGATACATTAAGGACGAAAATAAAGTATATCCAATACGTTAACAACCATTTTGGCCGAGAACTT
TGTTAAAAGACATAGTTTAACTGAACTTATTGCTTTTGGCTCGAACTATAAATGTTTTAGATGACACTTGTAATA
AAGCCACTGATTTTGGATTGTGAATTTTCCTTATGGTGTGTCTAGGGGTTAATGCACGGTTTAAGCTACGGGTTC
AGCTGAATCTATTAGTTTTGACTTAAATCCTGTTTATTTGTTAAAAAATTTATTAAATATGTACATATATTATTA
AATCTAGAACCAAGAAACTCAAATACTCAGTGAGTTCGATGGTATCCCGAGTTTATAAAGTTCAAATCTTGGATC
GGACTGTTAGTACGTCTTACTTTTGGTATATGTTTTTTTTTAGAGTAGTTGTTATTCATTTAACTATTTAAAATT
TAAGTGTTTTGACAATTGTTCTGTTCTTTTTACAGAGTTGGGCTGGATTTGCCAACAATAGAAGTAAGATATGAG
CATCTACATGTTGTGGCAGATGCATATATAGGAGGCAGAGCTTTGCCTACATTTACAAACTTTGTGACTAATTTT
CTTGAGGTAAGTATAGAAGAAAATTTTGATTTCAAATCTCAATTCTATTTTACTAAAAAGGGTGTTTGTGAATTG
TGACTAACTTTTTTTTTGGTTCGTAGTCATTGTTGACCTCTCTCCATATCCTACCAAGTAAAAAGAGGAAGCTCA
CTATTCTTAATGATGTGAGTGGTATCATTAAGCCTTGCAGACTGACTTTGCTTTTGGGACCTCCTGGTTCTGGCA
AAACTACTTTTTTATTAGCTTTGGCTGGAAAGCTTGATCCTGAACTTAAGGTAAAATTATTTTTTCTTTATACCA
AAAATTTAAGTTATATAATACACTTAATAGACAAATAATTATACTAGTGCAACTCAATTTGTCATGGAAGATTA
GTTACAAGTTTACTAGATTACTAATTAATGTTTATCATCATAGTGCTTTACGTGTAATTTATCTTATAAGTGACA
TGATTGTATAATTATATTTTCAGCTATAATTGCGTAGAACTTAAATTTCAAACCAAACATAAGTAAATGAGCACA
AATAATGAACTAGTTGTAAAACTATGATGAGAACTAAAGTTTTCTGATTCTTTTTTTTTTTTTTTTTTGTGTGT
GTGAAAATCAGGTAACTGGGAAGGTAACCTATAATGGACATGAAATGACTGAATTTGTACCACAAAGAACTGCTG
CTTATATTAGCCAGCATGATTTGCATATTGGAGAAATGACTGTTAGAGAAACCTTGGAATTCTCTGCCAGATGCC
AAGGCATTGGCACTCGTTATGGTTAGCATTTTTTTTCTATAAATGATCTTTTTTCCAGTTAATTCTTCAATAAAT
GTTGAACTTTTATTTACATACATATATTAACTGATGTTTCTTGAAAATATTTACAGAGATGTTGGCTGAACTGTC
AAGAAGAGAGAAAGCAGCTAATATCAAGCCAGACCCTGATATTGATATCTATATGAAGGTAACAACATGTTACAT
GTGAATTATTGAGTTGAACTTGCTTTTATGGTTCTTTATAAATAACCAATAATGTGGACGAAAAAGAATAATAA
GGATCTCCTTGGCTGTAAAGGCGATTTGTCACTTTTGTGAGAAACAAATTAAAGTTTGTTCGATTGAATAGACAC
AGATCGAGAGAAGTAGAAAGTGAAACACATTGAAAAGAGATTGGAGTTGGACACTTGCTTAGTTTCTTCATTTTT
TTAGTGTTCTTTCCTACTACTTGCAATAATAAACATCGACCACTAGTTTTGTGTGGAGTCTGAGAAAGGGCTGGA
CTGCATTTGTCCATCGTGCTACAGTCTTACCTCGCATTTATGCAAGAAGCTGTTTTTATAGTTTCAACATGGATGC
TCTTGGACCTTGGTCACATGACGGGATCCGTCACGCCATGCTCCCTTCCTAAAGAAATGTAGAAATTCCTAACAA
AGAAAATCTAATTAAGAATAACGAGAATCCTTTCTAAAAATAAATAATAAAAGTCAGCTGGTACCCATGGATGC
AATTTGTTAGTGAATAAAAAGCTATTAAACCAAGTAAAAATTTGCAATCTTCAACGTAAATGTTTGTGACCTTCA
TTGTTTGATGACAATGTAGGCATCAGCAACAGAGGGACAAGAAGCAAATGTTGTAACAGATTATGTTCTTAAGGT
AACACTAATTATGTCATATAATTTTTTTAATATTTTGACAATGAGAAGGAAGAAGAAATTTAATAACTAAGAGA
GTTATGAACTCTATCTGCAGATATTGGGACTGGACATTTGTGCAGATACTTTGGTGGGAGATGACATGGTAAGGG
GCATTTCAGGAGGACAAAAGAAGCGTGTGACAACCGGTGAAATGCTTGTTGGACCGTCAAAGGCACTTTTCATGG
ATGAAATCTCAACTGGATTGGATAGTTCCACCACTTACTCTATTGTGAACTCTCTAAGGCAAACTGTGCAAATCT
TGAAGGAAACTGCTGTCATATCTCTCTTGCAGCCAGCACCCGAGACCTACAATTTGTTTGATGACATTATTCTGT
TAACAGATGGTTTAGTTGTCTATCAAGGCCCTCGTGAAGACGTTCTGGCCTTCTTCGAATCCATGGGTTTCAAAT
GCCCTGATAGAAAGGGCGTGGCCGACTTCTTGCAAGAAGTATGTCTTATAATGAACTCCCAATTGTTAAAAATGA
CAAGCATTGATGCATCACTTATTCTAATAGTAGAAATTTATACTTCTTGCAGGTGACATCAAAGAAGGATCAACA
GCAATATTGGGCGAGGAGGGATGAGCCTTACAGGTTTATCACATCAAAAGAATTTGCTGAGGCGTATCAATCATT
CCATGTTGGAAGGAAACAACTGGATGAGCTTGGAGCTCCATTTGACAAGAGCAAAAGCCATCCTGCTGCATTGTC
AAATCAAAAGTACGGTATTGGGAAGAAACAACTCTTAAAGGTCTGCACTGAAAGAGAATACCTGCTAATGAAGA

GGAACTCATTTCTTTTTATATTCAAGTTCTTTCAGGTGACTGCTTTGTCTATTAAAATTATTGGTTCTCTTTTGT
TTTTTCAAATCTGTCTCATCAAATTCCCTTGCAAGTACTAATACCTCTTTTGTTTTGATCTGCTTTCANTGATCCG
TTTTCAGCTTTTAATTATGGCACTCCTGACGATGACCATGTTTCTCCGAACTGAGATGCACCATAATACTGAGGA
GGATGGTGGAACATACGTTGGTGCTCTCTTTTTTGTAATCGTTATGATTATGTTTAATGGAATGACTGAGCTTGG
CATGGTACTTTTTAAGCTTCCTGTCTTCTACAAGCAAAGAGACCTCTTCTTTTACCCCTCATGGGCTTATGCAATT
CCCTCATGGATACTCAAAATCCCTATAACATTTGTTGAAGTTGCTCTTTGGGTGTTCCTCACTTACTATGTCATTG
GATTTGATCCGAACCCAGAAAGGTACGGGAAGAAAAAGTAGATGCAAAGTAAAGATCAGGTTGCCTAATTTCCTT
TTCCCCGAGATTATTAATCAGGAGTCTGATTTTGCAGATTGTTCAAACAGTTCTTCCTACTCATAATAGTAAACC
AGATGGCATCAGCGTTGTTTCGATTCATAGGGGCAGCTGGCAGGACCTTGGGTATTGCTGCTACATTTGGAGCTT
TTGCTCTGCTTTTACAATTTGCATTGGGTGGATTCGTCCTTTCACGAGGTATATTTGGTGATTTATGTGTCTGCA
GAAGCTCTTGGTTTGCTTAAACCAACTAATGTTAGATTGTTAATTATATACTTTGACTAATGGTGCAGATATGAT
GAAGAAATGGTGGATATGGGGTTACTGGACTTCACCGATGATGTATTCTGTGAATGCAATCCTTGTGAATGAATT
TCATGGGAAAAGGTGGAGACGTGTAAGTTTCTCTATCTACTGCTCGTGCAAATAATTAATTTCCTGTATGGATGC
TGAAGCTCAGTCTAATTAATTCAGATTGCACCAAATGGAACTGAGCCACTAGGAGATGCTGTTGTAAGAGGCCGA
GGCTTCTTCCCAGATGCATCCTGGTACTGGATAGGTGTAGGGGCACTTATTGGATTCACAGTCCTCTTTAACATCT
TGTATAGTCTTGCGCTCGCTTATCTCAACCGTGAGTATCTCTCGAGTTTCTCCATTTATTTTTCCCCCAAGGCAAA
TAATTAAATGTTTAGTATGAATACCTACAGCAATTGGTAAGCCGCAAGCTATGATGCCAGAAGACAGTGAAGATG
CCAAAACAACTAGCACTGAGAAAGAAGGTTACAATAGTGAGGGTCAGAATAAGAAAAGGGGAATGGTTCTTCCC
TTTGAACCACATTCCATCACCTTTGATGATGTTATTTACTCTGTTGACATGCCTCAGGTAACTAACCGTTTATTGT
TATTAATCAGAAATTAGCGATTCTAATCCTCCATTTCAACAAACATAGTACTTAAGTTTCTTGACACTTGCAGGA
AATGAAAGATCAGGGTGCCTCTGAAGATAGATTGGTACTTCTGAATGGTGTAAGTGGAGCTTTCAGGCCCGGTGT
TTTGACAGCTTTGATGGGAGTTAGTGGGGCTGGAAAAACAACATTGATGGACGTATTGGCTGGAAGAAAAACAG
GAGGACATATTGAGGGTAGAATCCACATTTCTGGCTATCCCAAGAAGCAAGAAACATTTGCACGTATATCTGGAT
ACTGTGAGCAGAATGATATCCATTCACCTTATGTTACAGTTTATGAGTCATTAGTATACTCCGCTTGGATGCGTT
TACCTCATGATGTTGACGAAAGAACCAGAAAGGTTGGTACTTCTAAAATTCTGTTCTCATAACATGAATTTTGCC
CAAAAATCGGTTAAACACAATAAAGAAGGTAGAACTCATATAACATTTCCTATTATTATCCTGGTGCAGATGTTT
GTTGAGGAAGTTATGGATCTTGTGGAGCTAAGACCATTAAGATCAGCCTTAGTTGGTTTGCCAGGAGTCGACGGT
CTCTCAACTGAGCAACGCAAAAGGTTGACCATTGCAGTGGAACTAGTTGCAAACCCCTCTATCATTTTCATGGAT
GAACCAACATCAGGGCTGGATGCAAGGGCAGCTGCAATTGTCATGAGAGCTGTTAGGAACACAGTTGACACTGGA
AGAACCGTTGTTTGTACCATCCATCAGCCTAGCATCGACATTTTTGAAGCCTTTGATGAGGTAAATTTGATGCAT
TTTGAACTCAATCNAGATACCTTTTGAACTCAATCAAGCTAGTATTTGTTTTTCCTTGTTTCGTCAATGAATACT
AATTGTATAAACACCACTTTCCAGCTATTTCTAATGAAACGAGGAGGACAAGAGATATATGTTGGTCCATTGGGT
CGCAATTCATGCCACTTGATCAAATACTTTGAGGTTAGCTGTCTAAAGGAGAAAGTATTTTCCTTTTTTGAGTTT
ATATGGTTAGATACTAAACTAAGTTTTACATTGTATTCAGTCAATGCCTGGGGTAAGTAAAATAAAAGATGGCT
ACAATCCAGCAACTTGGATGTTAGAAGTCACAACCCCGGGCCAGGAAACGATGTTTGGAGTCGATTTTACTGATT
TATACAAAAAATCAGACCTTTACGGGAGGAACAAAGCGCTGATTACTGAACTGAGTGTGCCTCGCCCTGGTACAA
CAGACCTGCATTTTGATACTCAATACTCACAGCCATTTTGGACCCAATGTATGGCTTGCCTTTGGAAGCAACATT
GGTCATACTGGCGTAATCCTGCTTATACCGCAGTCAGATTTCTGTTCACAGTCATGATATCCTTGGTCTTTGGGAC
AATGTTCTGGGATCTTGGTTCTAAAGTGTAAGTCCAAAGATATGAAGAAAAGCAAAAACAAGTACACAAACTAG
AAAAGACCTTTTAATTCGTAATACTAAAAGCCTATCTTTTTTGGTTACAGGAGTAGGGCCCAAGATCTATCTAAC
GCGATGGGATGCTTGTATGCTGCTGTTCTCTTCATTGGTACACAAAATGCATCATCAGTGCAGCCTGTTGTAGCC
GTTGAGCGTACAGTATTTTACAGAGAAAGAGCTGCTGGAATGTATTCTGCCTTACCCTATGCCTTTGCCCAGGTG
AGCATACAGTTCAACTTCGTATAAGCCTATTTCGAACTTATTTAATGTATGGTACNTATTTCGAGCTTATCTAAT
GTATGGTACTGAATGTTACACACTATAATGTAATATCAAAAAATGTTTTTTGTCTAATTAAAGTAACTAAACTTT
ATCCACTATAACAGTAAAAGTCATAAGACTACTTTGTTTTTTTGGATTAAAGTAACAAAAGGTCAGAAAAATTAC
GAGAATATAGTGATTAAAATTTAGTGGCCTCATTGTTATAGTATATGAGTAAAATTCAGTTAGTTTAAAGTGAG
AAAAAGTAATTTTGTGACTTTATTGTTGTAGTCCGGTAAAGTTCGAAGGCAACATATTAAATTACCTCTCCAGTT
CCAGGTTAATAGACAAAATTACATAGTATAATTTTTCTTCTATCTTGCAGGCTTTCATTGAAATCCCATATATAT
TTGTGCAAGCTACTTTCTGTGGTACCATTATCTATGCTATGATTGGATTTGAATGGACAGTTGAAAAGTACTTTT
GGTACTTGTTCTTCATGTTTTTCACCCTCATGTACTATACCTACTATGGTATGATGACCGTTGCTATTACCCCAAA
CGTGAATGTTGCTCAAGTTGTCTCCGCCTTCTTCTACGGCTTATGGAATCTTTTCTCAGGATTCATTGTTCCACGA
CCTGTAAGTTCTTGAAACACTTGCATTTTTTGTTACATGGAAATTGAGTTTTAGAGCTCGAAAATGACATTTTTT
CTGTTTTATTCCAATGAAAAACAGCGTATGGCCATATGGTGGAGATGGTACTACTGGATTTGTCCTACTGCCTGG
ACCTTATATGGTTTGATTGCATCACAATTTGGAGATTACCAAAATAAACTTACTGATGATGAAACAGTGGAACAA
TACTTGAGACGCTTCTTCGGCTTCAAACATGAATTTCTACCAGTAGTTGGAGTTGTGACTGCTGGATTTACTGTT
CTTTTTGCCTTCACATTTGCTTTTGGTATCAAGGCATTCAACTTCCAGACAAGATAG

9.2 *PhPDR2* promoter sequence

CTATAGGGCACGCGTGGTCGACGGCCCGGGCTGGTCCTGGAACCAAGCTTTGTGTAGGAAAATTTTGCAAACGTT
TTACCACATCCTTGACTGACTATATTTGAGCCAATGATTTGTGCTGGACGACGCTTGTCCCGACATCCATTTAATT
TGGAATAATTCACATTCTAGTAATTACATGAAAATAAGTGTCGAAGGAATAGGCACAAAATTAAATGTTATGAG
ACTTGAAGAAATAGAATGAACATGTGAAATGCTATTACTAGTATCAACTAAGCAAACTTAATTATCTTTCGAAA
ATGGAGTTGAAGTAGTAAAGAGAAAGAAAATTTTCTATAAGAACAAGAATGTACAGAATCTTTTGCTTACGCGT
GATTTCCTTTTTATGTGGATTTAGTGTGCTATTGGATAGTCACAAGGTCCATGAGAATTGGAAGAAATTAAGCCA
GTCAAACAAGGGATGCCTTTCGTAGAAAGACAAATAAGATAGACAACATTGGTATACACTATGTACTCTCCGTCC
ATTTTATTTGTCTCATTTATTTTTACATGCTTTTTATAAAAATATTAATAAAAATGTACTTTTTACTATATTAAT
CCATCTTTATAAAAATATTAATTCTTGTTTCTATTTTTAAAATTAATTAATACTGTGGGCAAATTTAAAAAAAAT
AATTAATTTTATCTTAAACTCTTAAATAAATAAATAATTTGAAACAATTATTTATAATAAGAGACAAATAAATA
GATTGAAGAGTGCATGTAGGACAACTTAATAATGAGGGGGAAAGATACTTGTCTCGAAGGGCAATTGGTAGGGG
CCATCGCTTCTCATAATGCAAGTTCTTTAACATTTTTATATTAACAATAATATTAAGCTAAGTGGGTAGGGGCCA
TCTCTTTCACATTTTTAATATTAACAAGAATCTGTAGCTCAGGATAGGCCATCAAGACTTTTATTTTAACGAGTC
AAACAACGTGGAATTTGAAAAATGAAAAATAAAAAATGAAACGCTTTAATTAGTCTATACAATAGCCCGCCTTT
TTCCTGTACATGTAACATGCTATACATTATATATTATATAATCCCTTGGCCTTTAGAATTATTGCAGCAACTCTT
ACTTTTTCCTTTCATTCTTTTTATTTTCTCTTTCAGATCATTCACTTGAAAAAAACGAAAACCCAAGAACATATT
TCTGAGCTAGAGGGGGTCTGAAAATATAATTTGCATGTTGATTGGTCCATA

SCIENTIFIC WORKING EXPERIENCE

03/2010 – 05/2010	**Scientific assistant** Prof. Dr. Samuel C. Zeeman, Group of Plant Biochemistry ETH Zurich, Institute of Agricultural Sciences
09/2007 – 09/2008	**Scientific assistant / Vice lab manager** Prof. Dr. Yves Barral, ETH Zurich, Institute of Biochemistry
03/2004	Preparation week for International Biology Olympics, Könitz, Switzerland
10/2003	**Student apprentice** Prof. Dr. Beat Keller, Dr. Christof Ringli, University of Zurich, Institute of Plant Biology
07/2003	**Student in summer school** Dr. Bessie F. Lawrence 35th International Summer Science Institute, Rehovot, Israel. Title: "The Effect of LH on the Junctional Communication in Human Choriocarcinoma Cell Line and The Involvement of MAPK Pathway in LH-induced Cx43 Phosphorylation in Rat Ovarian Follicles" Supervisor: Dr. S. Sela-Abramowich

PUBLICATIONS

Sasse, J., Simon S., Gübeli C., Friml J., Martinoia E., Borghi L. (in preparation) The asymmetric and cell-specific localization of Petunia PDR1 regulates the polar transport of the phytohormone strigolactone in plant roots. *Cell Reports*

Sasse, J., Schlegel M., Giner J-L., Bigler, L., Martinoia E., Kretzschmar T. (in preparation) *Petunia hybrida* PDR2 is involved in sterol transport and is crucial for herbivore defense. *The Plant Cell*

Santelia D., Thalmann M., Egloff A., **Sasse J.**, Seung D., Zeeman S.C. (in preparation) Genetic dissection of pathway of starch transitory degradation in *Arabidopsis thaliana.*

Kretzschmar T., **Sasse J.**, Kohlen W., Borghi L., Schlegel M., Bachelier J. B., Reinhardt D., Bours R., Bouwmeester H. J., Martinoia E. (2012) A petunia ABC protein controls strigolactone- dependent symbiotic signalling and branching. *Nature* 483: 341-344

ACKNOWLEDGEMENTS IN PUBLICATIONS

Mendoza M., Norden C., Durrer K., Rauter H., Uhlmann F., Barral Y. (2009) A mechanism for chromosome segregation sensing by the NoCut checkpoint. Nature Cell Biology 11: 477 - 483

Shcheprova Z., Baldi S., Buvelot Frei S., Gonnet G., Barral Y. (2008). A mechanism for asymmetric segregation of age during yeast budding. Nature 454: 728-73

Diet A., Brunner S., Ringli C. (2004) The enl Mutants Enhance the lrx1 Root Hair Mutant Phenotype of Arabidopsis thaliana. Plant & Cell Physiology 45 6: 734-741

TALKS

09/2013	13th World petunia days, Nijmegen, The Netherlands: „*Petunia hybrida* PDR2 confers resistance against a generalist herbivore“
04/2013	Molecular Biology Forum of ETH Zurich and University of Zurich, Zurich, Switzerland: „A petunia transporter involved in herbivory defense“
08/2012	9th Solanaceae Conference, Neuchâtel, Switzerland: „*Petunia hybrida* PDR2 confers resistance against a generalist herbivore“
01/2011	Global Research Lab, Pohang, South Korea: „Petunia as a novel model system to investigate ABC transporters“
09/2010	11th World petunia days, Lyon, France: “PDR1- a putative transporter for a long unknown plant hormone“

CONFERENCE POSTERS

09/2012	1st Molecular Mycorrhiza Meeting, Munich, Germany, „A Petunia ABC protein transports strigolactones and thus regulates axillary branching and initiation of arbuscular mycorrhization “

ATTENDED MEETINGS

08/2011	Syngenta Symposium, Stein Säckingen, Switzerland
01/2011	Plant Winter Conference, Pohang, South Korea